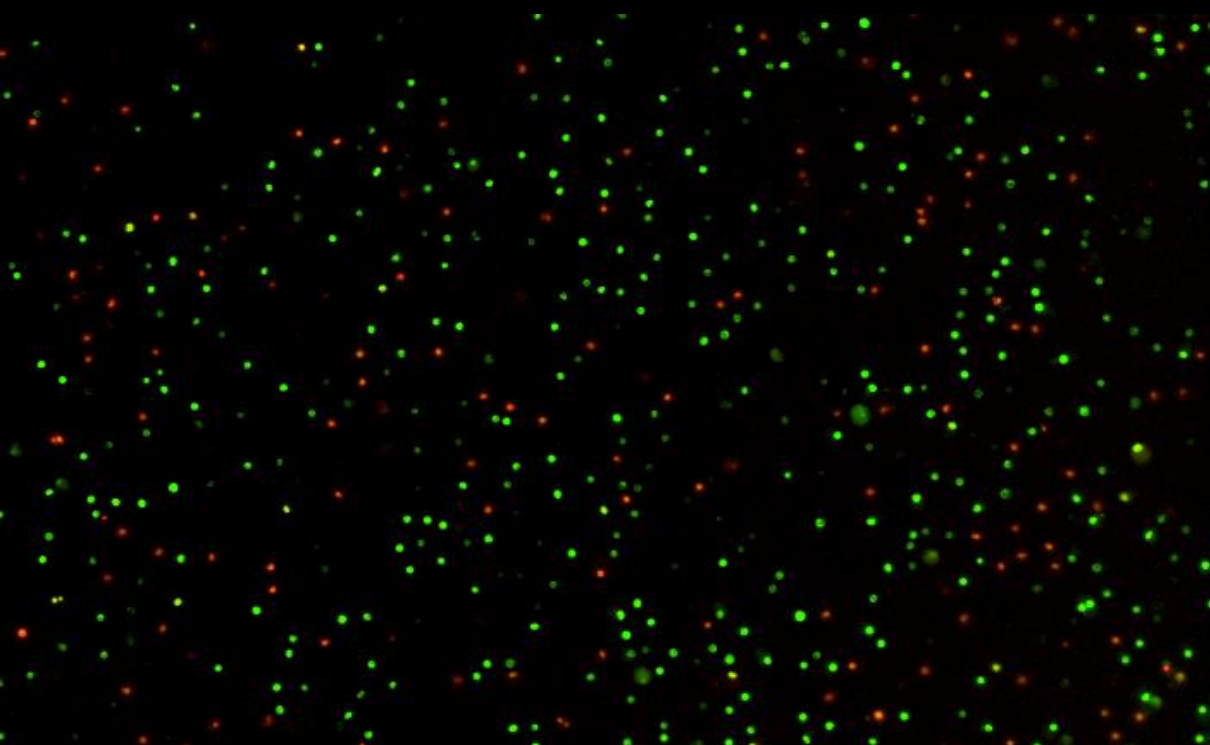


Cell death signaling at the crossroads of inflammasome activation

Nathalia Moraes de Vasconcelos

Promotor: Prof. Dr. Andy Wullaert

Co-Promotor: Prof. Dr. Mohamed Lamkanfi



Cell death signaling at the crossroads of inflammasome activation

Nathalia Moraes de Vasconcelos

Promotor: Prof. Dr. Andy Wullaert

Co-Promotor: Prof. Dr. Mohamed Lamkanfi

Thesis submitted to fulfill the requirements for
achievement of the degree of PhD in Health Sciences

Department of Internal Medicine, Faculty of Medicine and
Health Sciences, Ghent University

Academic year: 2017-2018

Members of the examination committee

Chair

Prof Dr Jan Gettemans, Ghent University

Secretary

Dr Saskia Lippens, Ghent University

Other members

Dr Nozomi Takahashi, Ghent University

Prof Dr Franck Riquet, Ghent University and Lille University

Prof Dr Patrizia Agostinis, KU Leuven

Prof Dr Hamid Kashkar, University of Cologne

Prof Dr Petr Broz, University of Lausanne

Table of contents

Summary.....	ix
Samenvatting.....	xi
List of abbreviations.....	xv
1. Introduction.....	1
1.1. Apoptosis.....	2
1.1.1. Caspases.....	2
1.1.2. Extrinsic pathway.....	5
1.1.3. Intrinsic pathway.....	7
1.1.4. Execution phase of apoptosis and clearance.....	10
1.2. Regulated necrosis.....	13
1.2.1. Necroptosis.....	13
1.2.1.1. Necroptosis in development and immunity.....	15
1.2.2. Emerging pathways of regulated necrosis.....	17
1.3. Cell death and the inflammasomes.....	19
1.3.1. Cell death initiated at the inflammasome complex.....	19
1.3.1.1. Abstract.....	19
1.3.1.2. Canonical and non-canonical inflammasome platforms.....	20

1.3.1.3. Mechanisms of inflammasome-induced pyroptosis	23
1.3.1.4. Pyroptosis in inflammation and anti-microbial host defense.....	27
1.3.1.5. Inflammasome-induced apoptosis and pyronecrosis.....	28
1.3.1.6. Inflammasome-induced cell death in infection and autoinflammation.	30
1.3.1.7. Concluding remarks: inflammasomes as polyvalent cell death controllers.....	32
1.3.2. GSDMD as the pore mediator of pyroptosis.....	34
2. Aims	37
3. Results	39
3.1. A morphological, single cell-based, analysis of pyroptosis	41
3.1.1. Abstract.....	41
3.1.2. Introduction.....	42
3.1.3. Results.....	43
3.1.4. Discussion.....	59
3.1.5. Methods.....	61
3.1.6. Supplementary data.....	64
3.1.7. References.....	76
3.2. A biochemical perspective of pyroptosis.....	79
3.2.1. Abstract.....	79
3.2.2. Main text	80
3.2.3. Methods.....	88
3.2.4. Supplementary data	89
3.2.5. References.....	90
3.3. Effects of the inhibition of serine proteases on cell death induction and inflammasome activation.....	91
3.3.1. PRCP inhibitor Compound 8o activates the NLRP3 inflammasome	91

Table of contents	vii
3.3.1.1. Abstract	91
3.3.1.2. Main text.....	92
3.3.1.3. Methods.....	97
3.3.1.4. References.....	98
3.3.2. DPP8/DPP9 inhibitors as activators of NLRP1b.....	101
3.3.2.1. Abstract	101
3.3.2.2. Introduction	102
3.3.2.3. Results.....	103
3.3.2.4. Discussion.....	110
3.3.2.5. Methods.....	111
3.3.2.6. References.....	112
4. Discussion and Perspectives	117
5. References	123
6. Acknowledgements.....	143
7. Curriculum Vitae.....	145

Summary

Pyroptosis is a form of lytic cell death occurring downstream of inflammasome activation. Pattern recognition receptors from the NOD-like and AIM2-like families and Pypin sense the cytosol of macrophages, monocytes, neutrophils, dendritic cells and other myeloid cell types and epithelial cells for danger- and pathogen-associated molecular patterns. Once activated, these receptors assemble in an ASC-dependent or -independent manner to form the inflammasome platform. Caspase-1 is produced in the cell as a zymogen, and recruitment to the inflammasome allows its proximity-induced autoactivation. Active caspase-1 leads to pyroptotic cell death. Pyroptosis can also be executed by caspase-11, which is activated through the non-canonical inflammasome. Both caspase-1 and caspase-11 pathways converge at cleavage of GSDMD, the executor of cell permeabilization during pyroptosis. However, canonical and non-canonical inflammasomes differentially control cytokine processing. Active caspase-1 also cleaves and activates the pro-cytokines IL1 β and IL18, while caspase-11 relies on downstream activation of caspase-1 to promote cytokine maturation.

Pyroptotic cell death and lysis have been increasingly associated with the release of IL1 β and IL18, while the pyroptotic corpse has been shown to contain intracellular pathogens, facilitating clearance by infiltrating neutrophils. Indeed, pyroptosis has been shown to mediate clearance of a variety of intracellular pathogens, but overt cell death and cytokine release also plays a role in autoinflammatory diseases. While the studies on the execution of cell lysis during pyroptosis have gained track during the past years, the organellar and biochemical mechanisms occurring during cell death execution are still undefined. Therefore, the current thesis aimed at describing the

organellar events happening during pyroptosis and defining the biochemical characteristics of this cell death.

Through a single-cell based, live-cell imaging analysis of pyroptosis induction by the NLRC4, NLRP1b and non-canonical inflammasomes, we defined a set of organellar changes preceding plasma membrane permeabilization. Ionic fluxes, cellular swelling, mitochondrial and lysosomal damage were shared between these inflammasomes, demonstrating they are common pyroptotic-associated events. Furthermore, these observations suggested that a gradual increase in membrane permeabilization is the mechanism behind GSDMD-induced pyroptosis. Our biochemical analysis of NLRC4 and NLRP1b-mediated dying macrophages revealed activation of caspase-3 and -7, with detection of DEVDase activity and cleavage of ROCK1, Bid and p23. These data suggest that pyroptosis comprises a caspase-3/-7 demolition program, previously associated only to apoptosis. In line with this, removal of GSDMD protein or its function after inflammasome triggering caused cell death associated with shrinkage and blebbing, typical of an apoptotic program. This phenotype was independent of the ASC speck, previously described to mediate caspase-8 activation and apoptosis in the absence of caspase-1. In the last part of the thesis, we screened a set pharmacological inhibitors for their ability to promote cell death and inflammasome activation. We demonstrated that inhibition of PRCP by Compound 80 leads to fast cell death. This was accompanied by IL1 β release through the NLRP3 inflammasome. On the other hand, DPP8/DPP9 inhibition by Val-boroPro and 1G244 led to pyroptosis and IL1 β release in mouse macrophages containing the 129-associated allele of *Nlrp1b*. Macrophages lacking this allele still responded to 1G244 and Val-boroPro, albeit with less intensity.

This thesis defined the organellar morphological changes associated to pyroptosis and identified a gradual increase in membrane permeability as the mechanism of cell lysis. We also identified a caspase-3/-7 signature in pyroptotic cells, downstream of caspase-1 activation. Furthermore, we defined two groups of inhibitors for dipeptidases able to induce inflammasome activation and IL1 β release in macrophages.

Samenvatting

Pyroptose is een vorm van lytische celdood die optreedt na activatie van de inflammasoom signalisatie pathway. Receptoren die behoren tot de NOD-like en AIM2-like families alsook Pyrine surveilleren het cytosol van macrofagen en epitheelcellen, om zo signalen te detecteren die wijzen op niet-infectieus gevaar of de aanwezigheid van pathogenen. Eenmaal geactiveerd, assembleren deze receptoren op een ASC-afhankelijke of -onafhankelijke manier om het inflammasoom-platform te vormen. Caspase-1 wordt in de cel geproduceerd als een zymogeen, maar rekrutering door het inflammasoom maakt nabijheid-geïnduceerde autoactivatie mogelijk, waarbij actief caspase-1 leidt tot pyroptotische celdood. Pyroptose kan echter ook worden uitgevoerd door caspase-11, dat geactiveerd wordt door het niet-canonieke inflammasoom. Zowel caspase-1- als caspase-11-gemedieerde signalisatie convergeren bij de verknipping van GSDMD, het eiwit verantwoordelijk voor celpermeabilisatie tijdens pyroptose. Beide caspases divergeren echter op het niveau van cytokine maturatie. Actief caspase-1 verknijpt en activeert de pro-cytokines IL1 β en IL18, terwijl caspase-11 afhankelijk is van downstream activering van caspase-1 om cytokine-maturatie te bevorderen.

Pyroptotische celdood en lyse worden in toenemende mate geassocieerd met vrijstelling van IL1 β en IL18, verder is echter ook aangetoond dat de celresten van pyroptotische cellen intracellulaire pathogenen bevat, wat klaring door infiltrerende neutrofielen vergemakkelijkt. Inderdaad, er is aangetoond dat pyroptose de klaring van een verscheidenheid aan intracellulaire pathogenen medieert, echter massale celdood en cytokine-vrijstelling spelen ook een belangrijke nefaste rol bij auto-inflammatoire aandoeningen. Hoewel er de afgelopen jaren meer en meer studies

zijn gedaan naar de processen die aan de basis liggen van cel lyse tijdens pyroptose, zijn de biochemische mechanismen die plaatsvinden tijdens de uitvoering van celdood nog steeds niet gedefinieerd, alsook over de betrokkenheid van specifieke organellen is er nog veel onduidelijkheid. Daarom was het huidige proefschrift gericht op het beschrijven van de gebeurtenissen die plaatsvinden in specifieke organellen tijdens pyroptose en het definiëren van de biochemische kenmerken van deze pro-inflammatoire vorm van celdood.

Door gebruik te maken van een single-cell benadering, en via live-imaging analyse van pyroptose geïnduceerd door de NLRC4, NLRP1b en niet-canonieke inflammasomen, hebben we een aantal organellaire veranderingen gedefinieerd die voorafgaan aan plasmamembraan permeabilisatie. Fluxen van ionen, cellulaire zwelling, mitochondriale en lysosomale schade werden teruggevonden na activatie van de verschillende inflammasomen, wat aantoont dat dit gebeurtenissen zijn die gelinkt zijn aan pyroptose in het algemeen. Bovendien suggereerden deze waarnemingen dat een geleidelijke toename in membraanpermeabilisatie het mechanisme is achter GSDMD-geïnduceerde pyroptose. Onze biochemische analyse van stervende macrofagen na activatie van het NLRC4 of NLRP1b inflammasoom onthulde een caspase-3/-7-handtekening, met DEVDase-activiteit en verknipping van ROCK1, Bid en p23. Deze bevindingen suggereren dat pyroptose een caspase-3/-7 programma omvat, iets dat normaal gezien geassocieerd wordt met apoptose. In overeenstemming met onze biochemische bevindingen konden we een apoptotisch fenotype waarnemen na het verwijderen van het GSDMD-eiwit of de inactivatie van de functie ervan. Dit fenotype was onafhankelijk van de ASC-speck, een fenomeen dat eerder beschreven werd om caspase-8-activering en apoptose te mediëren in de afwezigheid van caspase-1. Tot slot, in het laatste deel van het proefschrift, screenen we een aantal inhibitoren op hun vermogen om celdood en inflammasoom-activering te bevorderen. We hebben aangetoond dat remming van PRCP door Compound 80 leidt tot snelle celdood. Dit ging gepaard met IL1 β -vrijstelling via het NLRP3-inflammasoom. Aan de andere kant leidde DPP8/DPP9-remming door Val-boroPro en 1G244 tot pyroptose en IL1 β -vrijstelling in muizenmacrofagen die het 129-geassocieerde allel van *Nlrp1b* bevatten. Macrofagen zonder dit allel reageerden nog steeds op 1G244 en Val-boroPro, zij het in beperktere mate.

De huidige thesis definieerde dus specifieke morfologische veranderingen in organellen geassocieerd met pyroptose en identificeerde een geleidelijke toename in membraanpermeabiliteit als het mechanisme van cel lyse. Verder hebben we ook een

caspase-3/-7-handtekening geïdentificeerd in pyroptotische cellen, iets dat plaatsvindt na activering van caspase-1. Verder definieerden we twee groepen inhibitoren van dipeptidasen die in staat zijn om inflammasoom-activering en IL1 β -vrijstelling in macrofagen te induceren.

List of abbreviations

A1	Bcl-2-related protein A1
A20	TNF alpha-induced protein 3
AIM2	Absent in melanoma 2
ALPS	Autoimmune lymphoproliferative syndrome
Apaf-1	Apoptotic protease activating factor 1
ASC	Apoptosis-associated speck-like protein containing CARD
ATP	Adenosine triphosphate
Bcl-2	B-cell lymphoma-2
Bcl-w	Bcl-2-like protein 2
Bcl-xL	Bcl-extra large
BAD	Bcl2-associated agonist of cell death
Bak	Bcl-2 homologous antagonist killer
Bax	Bcl-2-associated X protein
BIR	Baculovirus IAP repeat
BH	Bcl-2-homology
Bid	BH3-interacting domain death agonist
BIM	Bcl2-interacting mediator of cell death
BMDM	Bone marrow-derived macrophage
Bmf	Bcl-2-modifying factor
Bok	Bcl-2 related ovarian killer
CAD	Caspase-activated DNase
CAPS	Cryopyrin-associated periodic syndromes
CARD	Caspase activation and recruitment domains
cFLIP	Cellular FLICE-like inhibitory protein
cGAS	Cyclic GMP-AMP synthase
cIAP	Cellular inhibitor of apoptosis
CYLD	Ubiquitin carboxyl-terminal hydrolase CYLD
CYPD	Cyclophilin D
DAMP	Danger-associated molecular pattern
DC	Dendritic cell
DD	Death Domains
DED	Death effector domain

DFNA5	Deafness associated tumor suppressor
DIABLO	Direct IAP-binding protein with low pi
DISC	Death inducing signalling complex
DPP	Dipeptidyl peptidase
DR	Death receptors
ER	Endoplasmic reticulum
ESCRT	Endosomal sorting complexes required for transport
FADD	Fas-associated protein with death domain
Fas	First apoptosis signal
FasL	Fas ligand
FCAS	Familial cold autoinflammatory syndrome
FMF	Familial Mediterranean Fever
FRET	Fluorescence resonance energy transfer
GBP	Guanylate-binding protein
GSDMA	Gasdermin A
GSDMB	Gasdermin B
GSDMC	Gasdermin C
GSDMD	Gasdermin D
GSDME	Gasdermin E
HMGB1	High mobility group box 1
Htr2	High temperature requirement protein A2
ICAD	Inhibitor of caspase-activated DNase
IFN	Interferon
IL	Interleukin
IMM	Intermembrane Mitochondrial Space
IKK	Inhibitor of nuclear factor kappa-B kinase
LCMV	Lymphocytic choriomeningitis virus
LDH	Lactate dehydrogenase
LeTx	Lethal toxin
LF	Lethal factor
LPS	Lipopolysaccharide
LRR	Leucine-rich repeat
LUBAC	Linear ubiquitin chain assembly complex
MAPK	Mitogen-activated protein kinase
MCL-1	Induced myeloid leukemia cell differentiation protein Mcl-1
MCMV	Murine cytomegalovirus
MK2	MAP kinase-activated protein kinase 2
MKK	MAP kinase kinase
MLC	Myosin light chain
MLKL	Mixed lineage kinase domain-like protein
MOMP	Mitochondrial outer membrane permeabilization
MPO	Myeloperoxidase
MWS	Muckle–Wells syndrome
MyD88	Myeloid differentiation primary response 88
NACHT	Nucleotide-binding NAIP, CIITA, HET-E and TP1
NE	Neutrophil elastase

Nec-1	Necrostatin-1
NEMO	NF- κ B essential modulator
NF- κ B	Nuclear factor kappa-light-chain-enhancer of activated B cells
NLR	Nucleotide-binding oligomerization domain-like receptor
NOMID	Neonatal onset multisystem inflammatory disease
NOS	Nitric oxide species
OMM	Outer mitochondrial membrane
PA	Protective antigen
PAMPs	Pathogen-associated molecular patterns
PARP1	Poly(ADP)ribose polymerase 1
PBMC	Peripheral blood mononuclear cell
PGE2	Prostaglandin E2
PI	Propidium iodide
PRCP	Lysosomal Pro-X carboxypeptidase
PRR	Pattern recognition receptor
PS	Phosphatidylserine
Puma	p53 up-regulated modulator of apoptosis
PYD	Pyrin domain
RAIDD	RIP associated ICH-1/CED-3 homologous protein with a death domain
RAGE	Receptor for advanced glycation endproducts
RHIM	RIP homotypic interaction motif
RIPK	Receptor-interacting serine/threonine-protein kinase
ROCK1	Rho-associated protein kinase 1
ROS	Reactive oxygen species
SMAC	Second mitochondria-derived activator of caspase
STAT1	Signal transducer and activator of transcription 1
STING	Stimulator of interferon genes protein
T3SS	Type III secretion systems
TAB	TAK1-binding protein
TAK1	Transforming growth factor beta-activated kinase 1
TGF β	Transforming growth factor beta
TLR	Toll-like receptor
TNF	Tumor necrosis factor
TNFR	TNF receptor
TRADD	TNFR1-associated death domain protein
TRAF	TNF receptor-associated factor
TRAIL	TNF-related apoptosis-inducing ligand
TRAILR	TRAIL receptor
TRIF	TIR-domain-containing adapter-inducing interferon- β
TRPC1	Transient receptor potential channel 1
TUNEL	Terminal deoxynucleotidyl transferase dUTP nick end labeling
XIAP	X-linked IAP
ZBP1	Z-DNA-binding protein 1

I. Introduction

Studies into regulated forms of cell death started with observations of apoptosis during development. Apoptotic cell death was defined as a highly regulated cellular process through which cells pack their contents into apoptotic bodies for efficient clearance, avoiding spillage of intracellular contents. This concept led to the hypothesis that lysis of a cell was always an uncontrolled mechanism, related to an accidental cell death. However, more recent understanding of the tumor necrosis factor (TNF) receptor signaling pathway, and its ability to induce cell death in the absence of caspase activity, led to the first description of a lytic regulated form of cell death, necroptosis. This allowed the cell death field to recognize that regulated cell death can also be lytic and potentially promote immune activation. The field of regulated necrosis grew and widened the scope of cell death to pathways such as parthanatos, cyclophilin D (CYPD)-regulated cell death, ferroptosis, NETosis and pyroptosis. Cell death plays a significant role during pathogen invasion by a variety of mechanisms. Dying of a cell allows the end of a pathogenic replication niche, while dead cell corpses or their derived molecules can trap pathogens to avoid spread. Furthermore, cell death accounts for the release of signaling molecules. However, cell death can be hijacked by the pathogen in order to aid its replication/life cycle, and extensive cell death accounts for tissue damage and underlies the pathology of some infectious and autoinflammatory diseases. Therefore, a better understanding of the cell death pathways is vital in the generation of new targets for infectious and autoinflammatory disorders. In this line, pyroptosis is unique as it shares features with both apoptosis and necroptosis. Furthermore, its close association to pathogen clearance and cytokine release has boosted the interest of this form of regulated cell death and its potential regulation. The current thesis focuses in the cell death mechanisms occurring downstream of pathogen and danger sensing in macrophages by inflammasomes. This introduction will focus on a

description of the best described forms of regulated cell death, namely apoptosis, necroptosis and netosis, ending with a focus in inflammasome-mediated cell death.

I. I. Apoptosis

Apoptosis is the prototype pathway of regulated cell death. Its name was first coined in 1972, in order to describe a cell dismantling process happening during development, with shrinkage of the cell body and nuclear condensation¹.

Apoptosis plays a role in development and homeostasis of multicellular organisms. Evidence that impairment of the apoptotic signaling alters immune homeostasis is seen in patients with autoimmune lymphoproliferative syndrome (ALPS)². A germline mutation in the *first apoptosis signal* (*Fas*) gene, an apoptosis-inducing receptor, is the cause of 70% of the cases of ALPS, with the most common disease presentations being lymphadenopathy, splenomegaly, and potentially autoimmune complications in non immune organs. This autoimmune phenotype is recapitulated in mice carrying loss of function mutations at *Fas* or at *Bcl2-interacting mediator of cell death* (*BIM*) loci^{3,4}, which encode pro-apoptotic proteins, and the clinical symptoms are associated to a low ability of apoptosis induction in immune cells⁵.

Apoptotic control of the lymphocyte population and maintenance of their homeostasis is done by both induction of apoptosis of auto-reactive T lymphocytes and killing of T and B cells to return to the basal level after clonal expansion⁵. Apoptosis also acts as an effector response of the immune system, performed by cytotoxic T cells and natural killer cells. These rely on the death receptor Fas, together with the perforin system, to clear virus-infected target cells^{6,7}. In addition, most cells of the immune system can be triggered to express the cytokine TNF-related apoptosis-inducing ligand (TRAIL), an apoptosis inducer, as a soluble or membrane-bound protein^{8,9}, in order to aid in clearance of tumor cells. Therefore, many of the immune effector functions can be understood by elucidating apoptotic signaling pathways and their regulation.

I. I. I. Caspases

Early studies on the apoptotic cell death pathway have distinguished a family of cysteine proteases, the caspases, as the responsible effectors for its signaling and execution¹⁰. Homologous caspase genes can be found throughout metazoans, where they regulate cell death and inflammation¹¹. All caspases mediate cleavage of

substrates at an Aspartate and utilize the four amino acids – numbered as P4-P2 – upstream of the cleavage site for substrate recognition¹². Caspases are produced in the cell as zymogens and are molecularly organized as prodomains plus a p20 and p10 subunits, which guard the catalytic activity.

Caspases have been historically subdivided according to their cellular function as either apoptotic or inflammatory caspases¹³. In this context, human caspase-1, -4, -5 and -12 are categorized as inflammatory caspases. Growing evidence supports that both human caspases -4 and -5 perform similar functions as murine caspase-11 and can be considered its homologue¹⁴⁻¹⁸. Human caspase-8, -9, -10, -3, -6 and -7 have been firstly implicated in the induction and execution of apoptosis, hence are referred to as apoptotic caspases¹³. However, recent implication of caspase-8 in the inhibition of necroptosis and, most importantly, in regulation of nuclear factor kappa-light-chain-enhancer of activated B cells (NF- κ B) and inflammatory signaling contests its “apoptotic” classification¹⁹. Therefore, while this classification of caspases describes their most common – or canonical – functions, it poses challenges with the new understandings of caspases signaling cascades and its relationship to inflammation.

In this sense, an alternative method for subdivision of caspases regards the nature of their prodomain²⁰. As the length of the caspase prodomain determines its mode of activation, this classification also reveals the upstream and downstream players in a signaling cascade, and therefore is closely related to a functional role. Initiator caspases comprise the human caspase-1, -2, -4, -5, -8, -9, -10, -12 and -14 and murine caspase-11, which have long prodomains containing an oligomerization domain. These oligomerization domains belong to the superfamily of death domains (DD), and share a six-helical bundle in their structure²¹. DDs are present in many proteins to mediate protein-protein interaction, mostly in a homotypic manner. Caspase-1, -2 -9 and -12 have a caspase activation and recruitment domain (CARD) domain (**Figure 1**). Caspase-1, -2 and -9 interact with a CARD in apoptosis-associated speck-like protein containing CARD (ASC)²², RIP associated ICH-1/CED-3 homologous protein with a death domain (RAIDD)²³ or apoptotic protease activating factor 1 (Apaf-1)²⁴, while an interactor for caspase-12 remains elusive. Interestingly, human caspases -4, -5 and murine caspase-11 also have a CARD domain, but in this scenario the death domain is used for intracellular lipopolysaccharide (LPS) sensing and self oligomerization²⁵. Caspase-8 and -10 have two death effector domain (DED) domains in tandem, which mediates interaction with the DED on Fas-associated protein with death domain (FADD)²⁶⁻²⁸. It is known that oligomerization of initiator caspases in a

higher macromolecule complex, their dimerization, conformational changes and autoprocessing are all steps that play a role for full activation of the protease²⁹⁻³¹. However, the exact molecular requirements for each of these steps in the activation process are still debated. As a general mechanism, caspase autoproteolysis lead by dimerization releases the active p20 and p10 domains which organize themselves into an heterotetramer and locks the caspase in an activated state²⁰. However, for caspase-9, as an example, the catalytic activity of the p20/p10 heterotetramer is several folds higher when associated to the complex with Apaf-1 than when soluble, suggesting the active enzyme remains trapped in the complex³². Furthermore, mutations on caspase-1 hampering its autocleavage demonstrated that full length caspase-1 is able to mediate cell death, but not to efficiently process interleukin(IL)-1 β , its canonical substrate³³. Similarly, caspase-8 bears pro-survival activity while in its unprocessed form³⁴⁻³⁶. For both caspase-1 and caspase-8, their full-length activity seems to be restricted to local or high affinity substrates. Both maintenance of highly active caspases in a complex, as for caspase-9, or of the full-length protein with partial activity, as for caspase-8 and -1, suggests that caspases can have their activity regulated in some instances through local substrate availability.

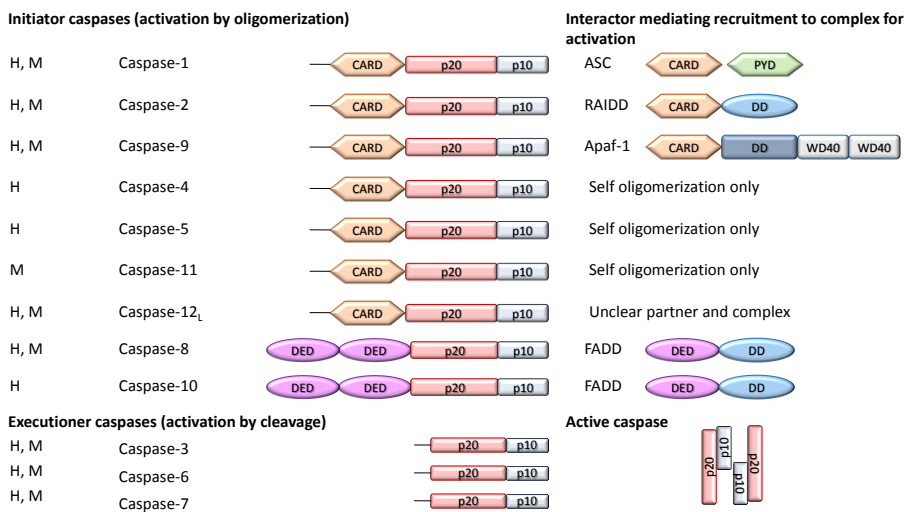


Figure 1. Caspases present in human (H) and mouse (M) systems. Initiator caspases have interacting domains from the DD family, represented by either CARD or DED, used for either sensing and self-oligomerization (hcaspase-4, -5 and mcaspase-11) or for recruitment to macromolecular complexes (caspase-1, -2, -9, -8, -10). An interactor for caspase-12, here shown on its long form (L), is still unknown. Executioner caspases are activated by cleavage. Active caspases organize as heterotetramers containing two p20 and two p10 subunits.

The other group of caspases, the executioners caspase-3, -6 and -7, have a short prodomain and rely on cleavage for activation¹³ (**Figure 1**). Maturation of executioner caspases is done by either an initiator caspase or other protease during a signaling pathway.

Initiation of apoptosis is mostly understood via either an intrinsic pathway, initiated at the mitochondria, or an extrinsic pathway, initiated through death receptors at the plasma membrane. These two signaling mechanisms are further outlined below.

1.1.2. Extrinsic pathway

The extrinsic pathway links extracellular signaling to initiation of apoptosis through engagement of members of the TNF recceptor (TNFR) superfamily located at the plasma membrane³⁷. Within these, the death recceptors (DR) share an extracellular domain rich in cysteines and a cytoplasmic tail containing a DD, essential for recruitment of apoptotic factors and downstream signaling. DR signaling culminates in the formation of a macromolecular complex, the death inducing signalling complex (DISC), through engagement of FADD and caspase-8²¹. FADD recruitment to the DR – or its complex – is mediated by its DD domain³⁸. This homotypic interaction causes conformational changes in FADD, exposing its DED domain for recruitment of procaspase-8. Tandem interactions of procaspase-8 DED domains precipitate the formation of a filament structure, where catalytic domains dimerize and allow proximity-induced autoactivation^{38,39}. The active caspase-8 is released from the DISC as a p18/p10 heterotetramer and cleaves procaspase-3, -7 and -6, activating these procaspases³⁷. Presence or absence of cellular FLICE-like inhibitory protein (cFLIP) at the DISC further regulates caspase-8 activity, dictating if a cell undergoes apoptosis or survives after death receptor engagement^{38,39}.

The DR Fas and TRAIL recceptor (TRAILR)1/2 are normally expressed at the plasma membrane as trimers⁴⁰. Association of these receptors with their cognate ligands, Fas ligand (FasL) and TRAIL respectively, induces conformational changes in their cytoplasmic tail which allows direct recruitment of FADD for DISC formation and downstream apoptotic signaling³⁷.

Activation of caspase-8 through the DR TNFR1, though, involves more steps for DISC formation⁴⁰. Ligation of TNF- α to TNFR1 primarily leads to the formation of a membrane-bound complex, complex I, with the recruitment of TNFR1-associated death domain protein (TRADD), recceptor-interacting serine/threonine-protein kinase (RIPK)1, TNF recceptor-associated factor (TRAF) 2, cellular inhibitor of apoptosis

(cIAP) 1/2 and linear ubiquitin chain assembly complex (LUBAC) complex⁴¹⁻⁴³. Once in complex I, cIAP1/2 and LUBAC attach ubiquitin-chains to (mostly) RIPK1, which serve as scaffold for recruitment of transforming growth factor beta-activated kinase 1 (TAK1)/ TAK1-binding protein (TAB) 2/TAB3 and inhibitor of nuclear factor kappa-B kinase (IKK) α /b/NF- κ B essential modulator (NEMO)⁴³. Therefore, signaling through TNFR1 normally leads to mitogen-activated protein kinase (MAPK) and NF- κ B-dependent survival signaling and cytokine production¹⁹ (**Figure 2**). Nonetheless, several scenarios can deviate from the initial pro-survival effect of TNFR1 stimulation. First, continued signaling on TNFR1 eventually leads to the release of RIPK1 from complex I, which act as a seed to assemble a cytosolic platform, complex IIa or ripoptosome, containing RIPK1, FADD and caspase-8⁴². In presence of a functional NF- κ B response, complex IIa also contains cFLIP, which forms an heterotetramer with caspase-8 to promote cell survival¹⁹. However, under low levels of cFLIP, procaspase-8 homooligomerization at complex IIa drives its activation and initiation of apoptosis. The apoptotic response triggered by complex IIa can also be regulated by RIPK1 ubiquitination status⁴⁴. Deubiquitination of RIPK1 by either ubiquitin carboxyl-terminal hydrolase CYLD (CYLD) or TNF alpha-induced protein 3 (A20) promotes RIPK1 dissociation from complex I, favoring complex IIa assembly^{45,46} (**Figure 2**). Both CYLD and A20 are also transcriptionally regulated by NF- κ B, and therefore represent a negative feedback control to hamper TNFR1-mediated transcription. RIPK1 – and the cell death downstream – can also be regulated by phosphorylation. MAP kinase-activated protein kinase 2 (MK2) activation after TNFR1 signaling leads to phosphorylation of the cytosolic pool of RIPK1 and its incorporation into TNFR1 signaling limits cell death induction^{47,48}. Further, IKK α /b can also phosphorylate RIPK1, preventing its signaling to cell death⁴⁹.

The extrinsic apoptotic pathway is tightly controlled by an efficient NF- κ B response through the means of cFLIP transcription. cFLIP is a homologue of caspase-8, but it is either expressed as a short form (cFLIP_s) bearing only the tandem DED domains, or as a long form (cFLIP_l) with a high homologue sequence to procaspase-8, but harboring mutations which hampers its catalytic activity¹⁹. Both isoforms of cFLIP are recruited to the death receptor signaling complex through interaction with procaspase-8 by means of DED/DED assemblies^{38,39}. cFLIP_s is a well-defined inhibitor of procaspase-8 activation and has been proposed to avoid procaspase-8 homodimerization and autoactivation by preventing procaspase-8 homodimerization at the filament by direct or indirect means³⁹. Furthermore, overexpression studies

have demonstrated that at high concentrations, cFLIPs can act as a cap at the filament, preventing its further elongation³⁸. At high concentrations as in overexpression studies, cFLIP_L can also have an inhibitory function of caspase-8 activity by competing with it for the filament³⁸. However, the physiological role of cFLIP_L seems to be of an activator of procaspase-8³⁴. Heteroligomerization of cFLIP_L and procaspase-8 at the DISC induces conformational changes in caspase-8 which allows its activation without cleavage³⁶. This local active caspase-8 cleaves RIPK1 and RIPK3, also at the complex, preventing these kinases to continue cell death signaling to necroptosis^{35,50}. Active caspase-8 also generates a p43 cFLIP_L form, which regulates NF- κ B and ERK signaling pathways downstream⁵¹. Therefore, low and local caspase-8 activity is associated to survival. Additionally, once cFLIP_L p43 fragment leaves the complex, caspase-8 loses its activity³⁸, further ensuring a survival commitment of the cell.

Finally, absence or low levels of both cFLIPs and cFLIP_L allow homodimerization of procaspase-8 at the DISC filament, self-activation and gain of full activity^{38,39}. The p18/p10 heterotetramer leaves the DISC complex to cleave its cytoplasmic substrates, procaspase-3, -7 and -8. As the survival role for caspase-8 activity is a growing understanding, it would be interesting to understand whether these signaling pathways are a constant mechanism happening inside the cell or whether they are signaling-induced.

1.1.3. Intrinsic pathway

The intrinsic apoptotic pathway unifies a plethora of intracellular stresses into a signaling cascade initiated at the mitochondria. The convergence of signals such as DNA damage, cytoskeleton perturbations, endoplasmic reticulum (ER) stress, mitotic stress and withdrawal of growth hormone to the mitochondria is performed by a group of proteins from the B-cell lymphoma-2 (Bcl-2) family⁵².

Bcl-2 proteins have between one and four Bcl-2-homology (BH) domains, and control apoptosis initiation by promoting or avoiding the release of proapoptotic factors from the intermembrane mitochondrial space (IMM)⁵³. The Bcl-2 family can be further subdivided into three subfamilies, according to their function in the apoptotic cascade. The pro-apoptotic Bcl-2 proteins, Bcl-2 homologous antagonist killer (Bak), Bcl-2-associated X protein (Bax) and Bcl-2 related ovarian killer (Bok) have four BH domains and a transmembrane domain used for integration to organellar membranes²⁰. These three proteins are able to directly cause mitochondrial outer

membrane permeabilization (MOMP) by permeabilizing the outer mitochondrial membrane (OMM) to allow passage of proteins of even 100 kDa⁵³. The other two Bcl-2 subfamilies comprise proteins that regulate the function of Bax, Bak and Bok. In one hand, anti-apoptotic proteins Bcl-extra large (Bcl-xL), induced myeloid leukemia cell differentiation protein Mcl-1 (MCL-1), Bcl-2, Bcl-2-like protein 2 (Bcl-w) and Bcl-2-related protein A1 (A1) hinder Bax/Bak – and potentially Bok – pore formation at the OMM⁵³. On the other hand, Bax/Bak can be activated by BH3-only proteins, the third subfamily, represented by BH3-interacting domain death agonist (Bid), Noxa, p53 up-regulated modulator of apoptosis (Puma), Bcl2-associated agonist of cell death (Bad), Bcl-2-interacting killer (Bik), activator of apoptosis harakiri (Hrk), Bim and Bcl-2-modifying factor (Bmf)⁵².

BH3-only proteins represent the most apical Bcl-2 proteins in a signaling pathway and therefore lie at the crossroads between cellular stress and apoptotic signaling. As such, PUMA and Noxa have their protein levels regulated by p53, thereby linking DNA damage to intrinsic apoptosis⁵⁴. On the other hand, augmented levels of BIM lead to apoptotic initiation after cytokine deprivation or cross-linking of B and T cell receptors⁵². Further, Bid interconnects the extrinsic and intrinsic apoptotic pathways, once it is cleaved by caspase-8, generating its truncated and active version, tBid^{55,56}. These BH3-only proteins can directly engage the pro-apoptotic Bcl-2 proteins, Bax and Bak, to promote conformational changes essential for their activation. However, they also sequester different sets of Bcl-2 anti-apoptotic proteins to sensitize cells to the apoptotic stimuli⁵². Direct interaction between Bcl-2 family members leads to a complex signaling network that dictates cell fate after stress, by finally controlling MOMP occurrence.

Each of the pro-apoptotic Bcl-2 family members, the final controllers of MOMP, is subject to regulation through a specific mechanism, representing their distinct roles in apoptosis initiation. Though a low level of Bak shuttles between the OMM and cytosol, the high hydrophobicity of its tail anchor favors this dynamics towards the OMM⁵⁷, where interaction with the anti-apoptotic Bcl-2 members Bcl-xL and MCL-1 keeps Bak in an inactive state⁵⁸. A transient interaction of Bak with an activating BH3-only protein – and the conformational changes induced thereof –, allows Bak homodimerization through mutual insertion of BH3-domains in the partner's groove⁵⁹. Further oligomerization of these BH3:groove dimers causes reorganization of the OMM and eventually leads to the formation of a proteolipidic pore, responsible for the MOMP⁶⁰.

Bax undergoes a similar activation procedure, with priming by a BH3-only protein causing conformational changes leading to the BH3:groove dimer and pore assembly^{60,61}. However, Bax counts on the control of its intracellular localization as an extra step for activation. Bax is shuttled from the OMM to the cytosol very efficiently by Bcl-xL; thus, it is mainly found in the cytosol^{62,63}. Stress signals cause BH3-only proteins to sequester anti-apoptotic Bcl-2 members, which stops Bax retrotranslocation and allows its accumulation at the OMM⁶². Though this is not enough for activation, accumulation of Bax at the OMM is the first step in apoptotic sensitization.

A similar role for accumulation at the OMM has also been suggested to control the activity of Bok. However, in this case, mere accumulation of Bok protein level could suffice for oligomerization and MOMP, which would be insensitive to regulation by anti-apoptotic Bcl-2 family members⁶⁴. While overt ER-stress was proposed as one of the pathways for building up Bok protein level⁶⁴, ovarian carcinoma cells have been also shown to be prone to Bok-mediated apoptosis through other intrinsic triggers⁶⁵.

Remarkably, though dimers of Bax and Bak can associate for final pore formation, Bok, Bak and Bax can induce MOMP by themselves, and single knockout of these proteins is insufficient to protect cells to intrinsic apoptotic stimuli⁵². However, developmental intrinsic apoptosis has been shown to strongly rely on Bax/Bak, as double knockout mice die prematurely, with accumulation of cells in diverse organs and failure to remove interdigital membranes⁶⁶. So far, a developmental role of Bok has only been shown in clearance of follicles when in a Bax deficient background⁶⁷, though further understanding the role of this Bcl-2 member in apoptosis initiation might highlight other developmental functions.

Finally, MOMP allows the release of several apoptogenic factors in the cytosol, such as cytochrome c, second mitochondria-derived activator of caspase (SMAC)/ direct IAP-binding protein with low pI (DIABLO) and high temperature requirement protein A2 (Htr2)⁶⁸. Cytochrome c normally resides in the IMM, where it participates in the cascade of adenosine triphosphate (ATP) production²¹. Once released in the cytosol, cytochrome c interacts with Apaf-1, allowing its oligomerization dependent on (d)ATP⁶⁹. This macromolecular structure formed by cytochrome c and Apaf-1 is called the Apoptosome²¹. Through CARD-CARD interactions between Apaf-1 and pro-caspase-9, this caspase is recruited to the Apoptosome, where it undergoes dimerization and activation. Active caspase-9, then, cleaves caspase-3/-7/-6 to execute apoptosis. SMAC/DIABLO^{70,71} and Htr2⁷², also released during MOMP, act

downstream on the signaling pathway, inhibiting IAPs to allow efficient caspase activation and apoptosis execution, as commented further below.

1.1.4. Execution phase of apoptosis and clearance

Extrinsic and intrinsic apoptotic signaling pathways converge at the level of activation of the executioners' caspases, by proteolytic cleavage of procaspase-3, -7 and -6 by caspase-8 and caspase-9⁷³. Interestingly, despite efficient cleavage of procaspase-3 and -7 by caspase-8, signaling through the extrinsic apoptotic pathway is not sufficient to promote apoptosis in certain cell types. In the so-called type II cells, distinctively represented by hepatocytes, intrinsic and extrinsic pathways act in a concerted way to determine apoptotic cell death⁷⁴. The connection between the two pathways happens at the level of caspase-8, which cleaves the Bcl-2 protein BID, leading to its active truncated version, tBID^{55,56}. At the mitochondria, tBID sequesters Bcl2 and allows Bax/Bak pore formation⁵⁶. Mitochondrial release of SMAC/DIABLO and its inhibition of X-linked IAP (XIAP) are essential for caspase-3 and -7 to acquire full activity and induce cell death⁷⁵. XIAP is a cytosolic protein, part of the IAP family containing three tandem baculovirus IAP repeat (BIR) domains. XIAP interacts with active caspase-3 and -7, inhibiting their catalytic pocket and downstream apoptosis⁷⁶. Therefore, type II cells are defined by their high levels of XIAP⁷⁵. Interestingly, though cytochrome c, Apaf-1 and caspase-9 aid in the downstream signaling for apoptosis, the mitochondrial signaling to apoptosis after DR engagement in type II cells does not rely on them. In fact, knockout of XIAP in hepatocytes is sufficient to reestablish their ability to undergo DR-induced cell death without mitochondrial signaling⁷⁵. In marked contrast to type II cells, type I cells, such as lymphocytes, are efficient in undergoing DR-dependent cell death in the absence of mitochondrial signaling, given their low level of XIAP. Regulation of apoptosis by type I and type II cells interestingly exemplifies how basal cellular protein regulation determines cell fate.

Finally, cleavage of substrates by caspase-3, -7 and -6 determines the apoptotic phenotypic characteristics of cell demise²⁰. More than 1000 substrates for executioner caspases have been described to this date, demonstrating the complexity of the apoptotic program. Morphologically, shrinkage and cell rounding are some of the *bona fide* features of apoptosis implemented by executioner caspases²⁰. Cleavage of gelsolin by caspase-3 produces an active n-terminal fragment, able to promote polymerized actin to dissociate independently of Ca²⁺⁷⁷. The consequent disruption of

the actin structure causes apoptotic cell rounding. Caspase-3 and -7 also cleave and activate Rho-associated protein kinase 1 (ROCK1) by removal of its auto-inhibitory c-terminal domain⁷⁸⁻⁸⁰. Active ROCK1 phosphorylates myosin light chain (MLC), increasing contraction of the actomyosin system and causing membrane blebbing, another apoptotic defining feature.

Apoptosis is classically defined as a silent form of cell death, since the plasma membrane structure is not compromised during its execution⁷³. Cell rounding, blebbing of the plasma membrane and packaging of the intracellular contents into apoptotic bodies help in a fast clearance by neighboring cells. Furthermore, an important characteristic of apoptotic cells is the early exposure of phosphatidylserine (PS) in the external face of the plasma membrane bilayer⁸¹. In healthy cells, transmembrane proteins called flippases actively keep PS in the inner leaflet of the plasma membrane. However, caspase-3 cleaves and inactivates flippases, while also constitutively activating scramblases, to promote fast and irreversible loss of lipid asymmetry and exposure of PS in early apoptotic cells⁸². PS is an efficient signal for phagocytosis and, in combination with the rounded and packaged cell body, promotes rapid uptake and clearance of apoptotic cells⁸¹, further supporting its immunologically silent role.

Nuclear structure and DNA integrity are also compromised in apoptosis by activity of executioner caspases²⁰. Active caspase-3 and -6 cleave laminins, disrupting the nuclear envelope⁸³, and lead to DNA fragmentation through cleavage of the inhibitor of caspase-activated DNase (ICAD)⁸⁴. Proteasomal degradation of ICAD releases its partner, the caspase-activated DNase (CAD), which translocates to the nucleus where it cleaves the DNA in internucleosomal regions⁸⁴.

The enzyme poly(ADP)ribose polymerase 1 (PARP1) plays important roles in DNA damage repair and its regulation is essential for the progress of programmed cell death⁸⁵. PARP1 is recruited to DNA damage where it catalyses the polymerization of ADP-ribose and bridges the recruitment of DNA-repair factors. However, poly(ADP)ribose synthesis happens at great expense of the intracellular stores of NAD⁺ and ATP. In apoptosis, PARP1 is readily cleaved by caspases -3 and -7, rendering it inactive, in order to maintain intracellular levels of ATP to execute the apoptotic program⁸³.

Caspase-3 seems to be the most efficient executioner caspase in cleavage of apoptotic substrates on the studied mechanisms so far⁸³. This is further confirmed on the severity of phenotype observed in mice lacking caspase-3, which suffer either from

perinatal lethality or mild phenotypic impairments, depending on their genetic background⁸⁶. Contrastingly, Caspase-7^{-/-} and Caspase-6^{-/-} knockout mice develop normally^{87,88}. Further, while the presentation of the apoptotic pathway follows a linear signaling pathway, the physiological pathway might be more complex, with feedback loops and compensatory mechanisms playing a role in the activation of caspases^{88,89}.

Interestingly, in a screening for inhibitors of caspases based on tetrapeptidic sequences, DEVD has been shown to be a major consensus sequence for both caspase-3 and -7⁹⁰, suggesting that these caspases would have overlapping roles. Indeed, absence of both caspases in mice leads to early embryonic lethality⁸⁷. However, while in most systems caspase-3 and caspase-7 seem to indeed overlap, analysis of their substrates suggests that caspase-7 might need the recognition of longer peptide stretches despite the P1-P4 consensus sequence in physiological substrates^{91,92}. Furthermore, attempts to understand the differential roles of executioner caspases have demonstrated that there might be indeed preferentiality in substrate according to the executioner caspase. For example, the cochaperone p23 has been shown to be a preferential substrate of caspase-7, while gelsolin seem to be specifically cleaved by caspase-3⁷⁹. This suggests that the embryonic lethality seen in Caspase-3^{-/-}Caspase-7^{-/-} double knockout mouse could also be related to complementary functions of these caspases in development, possibly affecting different cell types.

In the human body, as millions of cells die each day without triggering a constant immune response⁹³, it confirms that immune suppression is indeed the default mechanism to apoptotic clearance. The activity of caspases seems to be an essential step for eliciting a local immune suppression. First, executioner caspases control PS exposure, which is a potent signal for efferocytosis. Highlighting that PS exposure is a sufficient signal for uptake, liposomes with PS exposed are readily taken up by neighboring cells⁹³. Secondly, caspases may act in a cell intrinsic manner to prevent immune triggering initiated during apoptosis. For example, later stages of Bax/Bak mitochondrial channels allow herniation of inner mitochondrial membrane and release of mitochondrial DNA for intracellular sensing by the cyclic GMP-AMP synthase (cGAS) - stimulator of interferon genes protein (STING) pathway⁹⁴. This response only happens in a caspase-independent setting and promotes interferon(IFN) β secretion and an anti-viral signature on the triggered cell^{95,96}. While it is still unclear how exactly caspases prevent cGAS-signaling and IFN β release, it is tempting to speculate either that their direct cleavage of a mediator is responsible for

dampening inflammation or that their fast activity terminates storages of intracellular signaling platforms. Further, immune silencing during apoptosis is also a cell-extrinsic event. In homeostatic conditions, uptake of apoptotic cells elicits the release of the immunosuppressant cytokines IL10 and transforming growth factor(TGF) β from the phagocyte⁹⁷.

Though immunosuppression is the norm after apoptotic uptake, apoptotic cells can also mediate inflammatory response in conditions of infections. Concomitant stimulation of dendritic cells (DC) with Toll-like receptor (TLR) ligands and apoptotic corpses causes additional secretion of IL6 and IL23 by the DC⁹⁸. The combination of IL6, IL23 and TGF β promotes differentiation and expansion of the highly inflammatory Th17 CD4 T helper cells. As a result, conditioned media from DCs that had been co-stimulated with TLR agonists and apoptotic cells promoted the polarization of naïve CD4 T cells to Th17 profile, while conditioned media of DCs that were fed only apoptotic cells promoted a Treg phenotype⁹⁸. Thus, addressing the role of cell death in the context of pathogen invasion seems imperative to fully understand the immune response elicited.

1.2. Regulated necrosis

Initial descriptions of necrotic cell death focused on the fact that this cell demise terminates on release of intracellular content, as in marked contrast to apoptotic cell death. For 30 years it was largely assumed that apoptotic cell death was the only form of regulated cell death, while necrosis largely represented an accidental death⁹⁹. Studies on the roles of TNF- α have, however, majorly contributed to debunk this concept. Discovered in the 1980s, TNF- α took its name from the necrotic activity it could cause in tumour cells¹⁰⁰. Interestingly, in 2008, Degterev and colleagues described a drug, Necrostatin-1 (Nec-1), which could inhibit TNF- α toxicity, therefore defining that a necrotic death could be regulated¹⁰¹. Soon after, the kinase activity of RIPK1 was described to be the target of Nec-1 inhibition¹⁰², initiating the studies into necroptotic cell death mechanisms and further establishing this as a regulated form of cell death.

1.2.1. Necroptosis

Necroptosis can be defined as a necrotic cell death which relies on mixed lineage kinase domain-like protein (MLKL)¹⁰³. TNFR1, Fas, TRAILR, TLRs, IFN γ R and Z-DNA-binding protein 1 (ZBP1)/DAI were demonstrated to lead to necroptotic

signaling downstream when engaged in absence of caspase activity⁹⁹. Though these lead to similar initiation and regulation of necroptosis, TNFR1 activation is the prototypical necroptotic signaling pathway, and thus the example used herein.

As described earlier, a cell can execute multiple downstream decisions upon engagement of the TNFR1 by TNF α . First, NF- κ B and MAP kinase kinase (MKK)-dependent survival responses are initiated on the establishment of the membrane-bound complex I and RIPK1 ubiquitination^{42,43}. Disengagement of RIPK1 from the membrane-bound complex forms the cytosolic structure called complex II (**Figure 2**). In presence of NF- κ B signaling levels sufficient to upregulate cFLIP_L, this protein is incorporated to complex IIa, and the cFLIP_L/caspase-8 heterotetramer cleaves RIPK1 and RIPK3 also at the complex, maintaining the survival signal¹⁹. Absence of NF- κ B signaling and cFLIP_L upregulation leads to accumulation of caspase-8 at complex IIa and induction of apoptosis. On the opposite side of the spectrum, in absence of caspase-8 on protein level or its catalytic inhibition, RIPK1 and RIPK3 are no longer inhibited, and their association through their RIP homotypic interaction motif (RHIM) domains in complex IIb, or necrosome, promotes their phosphorylation¹⁰⁴. MLKL is recruited to complex IIb and phosphorylated by RIPK3¹⁰⁵, which induces conformational changes that exposes its 4-helical bundle domain, with high affinity for membranes^{106,107}. Oligomerization of MLKL and its association with phosphatidylinositols at the plasma membrane are essential steps for necroptosis¹⁰⁶⁻¹⁰⁸.

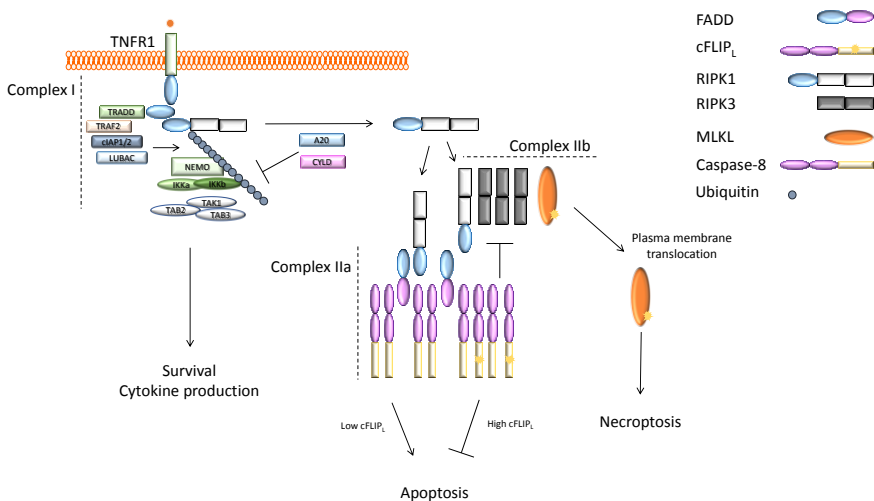


Figure 2. Multiple signaling pathways are possible downstream of TNFR1. Engagement of TNFR1 leads prominently to recruitment of TRADD, RIPK1, cIAP1/2 and LUBAC to complex I. Ubiquitination of RIPK1

allows the recruitment of NEMO/IKK α/β and TAK1/TAB2/TAB3 for a survival signal and cytokine production. Release of RIPK1 from complex I can be modulated by deubiquitination by CYLD and A20, and promotes the formation of a cytosolic complex II. Presence of cFLIP_L at complex IIa determined whether the outcome of its signaling is to maintain survival or induce caspase-8-dependent apoptosis. Absence of caspase-8 or its inhibition allows the formation of complex IIb, where RIPK3 recruits MLKL and phosphorylates it. Phosphorylated MLKL translocates to the plasma membrane and mediates necroptosis.

Whereas the indispensable role of MLKL in necroptosis execution is well defined, the molecular mechanisms responsible for cell lysis are still not fully elucidated. The role of diverse ion influxes have been contested on necroptotic cell death^{107,109-111} and in some cells MLKL seem to rely on plasma membrane-associated channels to terminally execute lysis¹⁰⁸. Conversely, cell rounding has been widely described as a morphological feature of necroptosis in diverse cell lines, happening downstream of MLKL^{111,112}. Furthermore, mitochondrial hyperpolarization and reactive oxygen species (ROS) production have been shown to anticipate plasma membrane lysis during necroptosis of mouse fibroblast cells, L929¹¹². Interestingly, despite canonically being associated to apoptosis, loss of membrane asymmetry and PS translocation to the outer leaflet is an event downstream of MLKL activation; nonetheless it precedes membrane permeabilization^{113,114}. Furthermore, cells undergoing necroptosis shed damaged pieces of membrane as vesicles containing PS at the extracellular side^{113,114}, thereby delaying fatal plasma membrane commitment and promoting uptake by neighbouring cells. This self-repair mechanism relies on the activation of MLKL and its association to proteins of the endosomal sorting complexes required for transport (ESCRT) machinery^{113,115}. Since this phenomenon has been implicated in allowing an efficient NF- κ B response¹¹³, it would be interesting to evaluate the possible consequences of lack of the ESCRT components in *in vivo* disease models.

Fas and TRAILR lead to similar initiation and regulation of necroptosis as in the context of TNFR1⁹⁹. However, IFN γ R seems to rely on signal transducer and activator of transcription 1 (STAT1) for necroptosis induction⁹⁹ and TLR3 and TLR4 recruit RIPK3 based on TIR-domain-containing adapter-inducing interferon- β (TRIF) signaling downstream¹¹⁶.

1.2.1.1. Necroptosis in development and immunity

A developmental role for necroptosis was further pursued in studies with knockout mice for its main players. Of note, the ability to undergo necroptosis is not essential for development, as RIPK3^{-/-} and MLKL^{-/-} single knockouts develop normally and show no spontaneous phenotype^{117,118}. However, absence of RIPK3 rescues the

lethality observed in Caspase-8^{-/-} and allows fully development to adulthood^{119,120}. Caspase-8^{-/-} mice have long been recognized to succumb around embryonic stage E10.5 given their inability to vascularize the yolk sac¹²¹. The survival of RIPK3^{-/-} Caspase-8^{-/-} double knockouts reveals that the ability of this caspase in blocking necroptosis is essential for fully embryonic development. Of note, consistent with the role of caspase-8 in inhibiting RIPK3 when in a heterocomplex with cFLIP, transgenic mice bearing the uncleavable mutant caspase-8 are viable, while their thymocytes are protected from toxicity of Fas injection¹²².

Contrasting RIPK3^{-/-} and MLKL^{-/-} mice, lack of RIPK1 reveals a lethal phenotype and mice die right after birth by an overt systemic inflammation, suggesting RIPK1 has a physiological role of dampening inflammation¹²³. Notably, mice bearing either the D138N or K45A mutations on RIPK1 express catalytic mutant proteins but are viable and survive to adulthood with no reported spontaneous phenotype^{124,125}. Thus, the autoinflammatory phenotype observed in RIPK1^{-/-} mice is due to lack of the scaffold function of RIPK1. Given the requirement for the kinase activity of RIPK1 in necroptosis induction, this further supports that necroptosis is not essential during development.

RIPK1^{-/-} mice die mostly by consequences of skin and intestinal impairments^{123,126}. Each affected compartment on RIPK1^{-/-} mice correlates with the dual role of RIPK1 in controlling caspase-8 and RIPK3, and a full protection is observed in RIPK1^{-/-}RIPK3^{-/-} Caspase-8^{-/-} triple knockout mice^{123,126}.

The intestinal effects of the lack of RIPK1 seem to be associated to overt caspase-8-mediated apoptosis induction of epithelial cells^{127,128}. Commitment of the intestinal barrier, translocation of bacteria, myeloid differentiation primary response 88 (MyD88) and TNFR signaling were all shown to play a role in these mice inability to thrive^{123,127,128}, and absence of RIPK3 could not rescue the absence of RIPK1^{127,128}. On the other hand, the skin abnormalities of RIPK1^{-/-} mice are prevented by lack of RIPK3 or MLKL¹²⁸⁻¹³⁰. While this firmly establishes that necroptosis is the main driver of the skin inflammation observed in these mice, it also surprisingly reveals that RIPK1 can in fact act as an inhibitor of necroptosis. Indeed, absence of RIPK1 seems to unleash the necroptotic ability of ZBP1. While absence of ZBP1 delays the necroptotic phenotype in the skin of the mice, RIPK3 or MLKL completely rescues them, indicating that RIPK1 also prevents other necroptotic signaling from occurring besides ZBP1¹²⁹. In fact, dual deletion of TRIF and ZBP1 phenocopies RIPK3

deletion, indicating both proteins can engage RIPK3-necroptotic signaling in the absence of RIPK1¹³⁰.

ZBP1 contains two DNA/RNA sensing domains in tandem and two RHIM domains, used in the RHIM/RHIM interaction with RIPK3^{130,131}. Besides its role in development, ZBP1 also functions during viral detection, though also in a still elusive mechanism. ZBP1 is required for cell death induction of macrophages during influenza A viral infection¹³². Furthermore, murine cytomegalovirus (MCMV) bypasses host defenses by expressing a RHIM interacting protein, vIRA, which impairs the association between ZBP1 and RIPK3¹³¹. MCMV lacking vIRA induces inflammation in WT animals, in a ZBP1-dependent manner^{131,133}.

Remarkably, an *Escherichia coli* effector, EpsL, was demonstrated to degrade RIPK1, RIPK3, TRIF and ZBP1, thereby preventing necroptotic signaling *in vitro*¹³⁴. Furthermore, *Citrobacter rodentium* lacking the EpsL effector are less efficient in colonizing murine intestines¹³⁴. Thus, targeting the necroptotic pathway might be an evasion mechanism shared between viruses and bacteria. Further suggesting a role for necroptosis in immune response, inhibition of necroptosis during *in vivo* infection by *Staphylococcus aureus* worsens pathology¹³⁵. Necroptotic signaling as an immune response is also indicated by the ability of TLR4 and TLR3 to lead to TRIF-mediated RIPK3 activation and cell death in conditions of caspase inhibition¹¹⁶. It is still to be determined whether caspase inactivation happens physiologically, and in which conditions. Overall, understanding particularly which cells are targeted and what are the immunological consequences of necroptosis induction would aid in the further characterization of the role of necroptosis in infection models.

1.2.2. Emerging pathways of regulated necrosis

Other forms of regulated necrosis which do not rely on RIPK3 and RIPK1 activities have been described. While parthanatos and CYPD-dependent regulated necrosis kill by depletion of the intracellular levels of NAD⁺, ferroptosis is a mechanism in which excessive intracellular iron leads to lipid peroxidation and cell death⁹⁹. Further understanding of their potential participation in immunity and host-pathogen interaction is still to be reached.

Neutrophils, and their cell death by NETosis, though, have a clear role in pathogen clearance¹³⁶. Neutrophils are one of the first immune cells to reach a challenge site, and their effector responses to pathogens relies on release of intracellular granules, phagocytosis, cytokine release and release of neutrophil extracellular traps (NET).

These traps are composed by DNA, histones and neutrophilic proteases¹³⁷. NETs have been demonstrated to selectively trap large pathogens to avoid microbial spread and help clearance¹³⁸. Furthermore, recently they have been shown to also act as scaffold for the neutrophilic proteases cathepsin G and elastase to act on extracellular cytokine processing¹³⁹. NET formation relies mainly in the activity of neutrophil elastase (NE)¹⁴⁰. Once a neutrophil starts to degranulate, its DNA decondenses and is released in the cytoplasm, where it binds to granular proteins. The DNA, together with histones and granular proteins are finally released extracellularly. So far, ROS production is the most upstream player identified in NET formation, and it activates myeloperoxidase (MPO) to induce degranulation¹⁴⁰. MPO then releases NE, which translocates to the nucleus where it degrades histones to promote DNA decondensation. MPO and other granular proteins aid in DNA decondensation but inhibiting NE activity is sufficient to prevent NET formation¹⁴⁰, demonstrating its key role in the process.

While many reports have shown NET occurring during neutrophilic cell death, termed NETosis, there has been descriptions of phagocytic activity of a neutrophil after it has shed a NET¹³⁷. Further, a report has implicated an upstream necroptotic signaling pathway to NET formation¹⁴¹. Further research is needed to uncover whether NET formation lies at the downstream signaling pathway of other lytic forms of cell death, and it might represent a common response of neutrophil to lytic forms of cell death.

I.3. Cell death and the inflammasomes

I.3.1. Cell death initiated at the inflammasome complex

Section 1.3.1. is modified from the review: de Vasconcelos, N.M., Van Opdenbosch, N.; Lamkanfi, M. 2016. Inflammasomes as polyvalent cell death platforms. **Cellular and Molecular Life Sciences**. 73(11-12). p.2335-2347.

I.3.1.1. Abstract

Inflammasomes are multi-protein platforms that are organized in the cytosol to cope with pathogens and cellular stress. The pattern-recognition receptors NLRP1, NLRP3, NLRC4, AIM2 and Pyrin all assemble canonical platforms for caspase-1 activation, while caspase-11-dependent inflammasomes respond to intracellular Gram-negative pathogens. Inflammasomes are chiefly known for their roles in maturation and secretion of the inflammatory cytokines IL1 β and IL18, but they can also induce regulated cell death. Activation of caspases -1 and -11 in myeloid cells can trigger pyroptosis, a lytic and inflammatory cell death mode. Pyroptosis has been implicated in secretion of IL1 β , IL18 and intracellular alarmins. Akin to these factors, it may have beneficial roles in controlling pathogen replication, but become detrimental in the context of chronic autoinflammatory diseases. Inflammasomes are increasingly implicated in induction of additional regulated cell death modes such as pyronecrosis and apoptosis. In this review, we overview recent advances in inflammasome-associated cell death research, illustrating the polyvalent roles of these macromolecular platforms in regulated cell death signaling.

1.3.1.2. Canonical and non-canonical inflammasome platforms

Inflammasomes are cytosolic multiprotein complexes that are assembled when the cell encounters pathogens, toxins, crystals and a diversity of other agents that may harm the host^{142,143}. These potentially cytotoxic agents or the ensuing cellular stress are monitored by a set of intracellular pattern recognition receptors (PRRs) that auto-oligomerize and recruit additional inflammasome components. Similar to the death-inducing signaling complexes that activate the apoptotic initiator caspases -8 and -10¹⁴⁴, and the caspase-9-activating apoptosome¹⁴⁵, oligomerization of inactive procaspase-1 zymogens in inflammasomes results in the proximity-induced autoactivation of the protease¹⁴². The CARD- and pyrin domain (PYD)-containing adaptor protein ASC bridges the recruitment of procaspase-1, although inflammasomes of CARD-containing PRRs may also recruit the inflammatory protease directly^{33,146,147}. Once active, caspase-1 matures and releases the pleiotropic inflammatory cytokines IL1 β and IL18, thereby contributing importantly to inflammatory and immune responses¹⁴⁸. Caspase-1 also induces pyroptosis, a lytic regulated cell death mode of myeloid cells that is emerging as a critical host defense mechanism against microbial pathogens¹⁴⁹. On the other hand, excessive and unwarranted pyroptosis induction is linked to autoinflammatory disease¹⁵⁰⁻¹⁵³. Also, activation of murine caspase-11 and its human orthologs caspases -4 and -5 in the non-canonical inflammasome pathway induces pyroptosis^{14,15,154}. Furthermore, inflammasome-induced cell death responses are increasingly recognized to extend well beyond caspase-1- and -11- induced pyroptosis, and encompass apoptosis and pyronecrosis as discussed in the following paragraphs.

The canonical inflammasomes

By definition, the canonical inflammasomes activate caspase-1. Most canonical inflammasomes are assembled by PRRs that belong to the nucleotide-binding oligomerization domain-like receptor (NLR) family¹⁵⁵, but Pyrin¹⁴³ and HIN200 protein absent in melanoma 2 (AIM2)^{156,157} also engage well-defined inflammasomes. The roles and signaling mechanisms of the different inflammasomes have been reviewed extensively^{142,158-160}, and they will only be briefly discussed here in the context of their roles in regulated cell death signaling.

Akin to other NLRs, NLRP3 possesses a central nucleotide-binding NAIP, CIITA, HET-E and TP1 (NACHT) domain and a number of C-terminal leucine-rich repeat

(LRR) domains that are thought to regulate NLR activation. NLRP3 is a representative member of the NLRP subfamily, which are characterized by a PYD domain in the amino-terminus. The NLRP3 inflammasome is activated in response to a broad variety of pathogen- and danger-related activators that includes Gram-negative bacteria, *Staphylococcus aureus*, RNA viruses, pore-forming toxins, ionophores, crystals, etc.¹⁶¹ (**Figure 3**). As it is unlikely for NLRP3 to physically bind such a diverse set of activators, it is commonly thought that these stimuli may converge on production of a secondary messenger that is monitored by NLRP3. K⁺ efflux, Ca²⁺ signaling, mitochondria-derived ROS, cytosolic release of mitochondrial DNA and cardiolipin, release of lysosomal cathepsins and microtubule-assisted relocation of the NLRP3 inflammasome to mitochondria-ER foci all are mechanisms that may possibly contribute to NLRP3 activation¹⁶²⁻¹⁶⁸, but further research is required to fully understand NLRP3 activation mechanisms.

The human NLRP1 inflammasome has been implicated in Vitiligo-associated autoimmune disease¹⁶⁹, autoimmune Addison's disease¹⁷⁰, type I diabetes^{171,172}, and autoinflammation¹⁷³. Importantly, humans possess only one *Nlrp1* gene, whereas the mouse genome contains *Nlrp1a*, *Nlrp1b* and *Nlrp1c* genes. A number of studies have shown that NLRP1a and NLRP1b assemble inflammasomes that non-redundantly activate caspase-1 in hematopoietic progenitor cells infected with lymphocytic choriomeningitis virus (LCMV)¹⁷⁴, and in macrophages intoxicated with *Bacillus anthracis* lethal toxin (LeTx), respectively¹⁷⁵. LeTx consists of two subunits: the protective antigen (PA) subunit attaches to plasma membrane-bound host receptors and assists in cytosolic translocation of the zinc metalloproteinase subunit lethal factor (LF). In the cytosol, LF protease activity triggers assembly of the NLRP1b inflammasome through mechanisms that are not entirely clear yet^{176,177} (**Figure 3**).

NLRC4 is another NLR protein that assembles a canonical inflammasome¹⁷⁸. Unlike NLRP3, NLRC4 contains an amino-terminal CARD. The NLRC4 inflammasome plays an important role in host defense against *Salmonella enterica* serovar Typhimurium (*S. Typhimurium*), *Legionella pneumophila*, *Pseudomonas aeruginosa*, *Shigella flexneri* and *Burkholderia thailandensis*^{161,179,180}. Members of the NAIP subfamily - which are characterized by amino-terminal BIR motifs - bind flagellin or components of bacterial type III secretion systems (T3SS) of pathogenic bacteria that gain access to the cytosol (**Figure 3**)¹⁸¹⁻¹⁸³. NAIP5-independent phosphorylation of NLRC4 is also required for engagement of flagellin-induced inflammasome signaling^{184,185}. Importantly, while rodents encode multiple NAIP genes, humans

express different isoforms from a single NAIP gene that detect flagellin and T3SS components, respectively¹⁸⁶.

Also the HIN200 family member AIM2 assembles a well-characterized inflammasome. Through its dsDNA-binding HIN200 domain, AIM2 detects the presence of viral and bacterial pathogens in the cytosolic compartment¹⁸⁷⁻¹⁸⁹. AIM2 mediates host defense against cytomegalovirus and influenza virus, but also restricts *Fancisella tularensis*. Guanylate-binding proteins (GBPs) appear dispensable for AIM2 detection of transfected DNA and cytomegalovirus infection, but they are required for responding to AIM2-activating bacterial pathogens^{190,191}. This is explained by the notion that these type I IFN-induced GTPases mediate lysis of bacteria-encapsulating vacuoles or the bacterial cell wall, thereby exposing *F. tularensis* DNA to AIM2 detection.

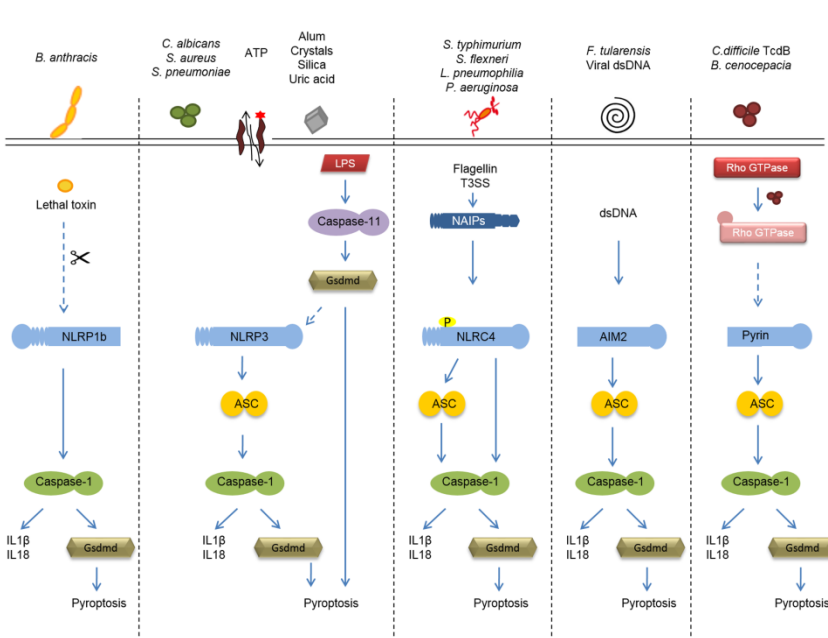


Figure 3. Schematic representation of the inflammasome pathways resulting in pyroptosis. Pyroptosis as a regulated lytic cell death mode of myeloid cells is induced in response to a wide variety of endogenous, environmental and pathogen-derived triggers downstream of inflammasome-associated activation of caspases 1 or 11 in mice, or that of the orthologous caspases -1, -4 and -5 in humans. While the PYD-based NLRP3, AIM2 and Pyrin platforms require the bipartite adaptor protein ASC to recruit and activate caspase-1, the CARD-based NLRP1b and NLRC4 inflammasomes trigger caspase-1-dependent pyroptosis independently of ASC. Both caspases -1 and -11 engage pyroptosis directly by cleaving its substrate GSDMD. The mechanism by which GSDMD triggers pyroptosis is currently unknown.

Pyrin is the latest addition to the list of pattern recognition receptors (PRRs) that engages a canonical inflammasome. Pyrin is mutated in familial Mediterranean Fever

(FMF) patients, and the protein was recently shown to respond to bacterial toxins that post-translationally modify members of the Rho GTPase family^{143,192}. Pathogens such as *Clostridium difficile*, *Clostridium botulinum*, *Vibrio parahaemolyticus*, *Histophilus somni*, and *Burkholderia cenocepacia* express such toxins and induce Pyrin-dependent caspase-1 activation (**Figure 3**). In light of the reported association of Pyrin with the cell cytoskeleton¹⁹³, this suggests that Pyrin may guard disrupted Rho signaling indirectly, possibly by monitoring remodeling of the cytoskeleton downstream of toxin-induced inhibition of the GTPase¹⁴³.

The non-canonical inflammasome

Akin to the role of caspase-1 in canonical inflammasomes, caspase-11 acts as the effector protease of the non-canonical inflammasome¹⁵⁴. Notably, this inflammasome pathway has emerged only recently with the unexpected observation that widely used caspase-1 knockout mice were also deficient in caspase-11 expression¹⁵⁴. The non-canonical inflammasome pathway targets Gram-negative bacteria that gain access to the cytosolic compartment (**Figure 3**). Direct binding of cytosolic LPS was shown to promote caspase-11-mediated pyroptosis as a host defense response that is thought to be important for disposal of macrophages that are infected with *E. coli*, *Citrobacter rodentium*, *Vibrio cholerae* and other Gram-negative pathogens^{25,154}. Akin to their role in lysis of *F. tularensis*-containing vacuoles to license AIM2 inflammasome activation, GBP GTPases act upstream of caspase-11 for inducing pyroptosis of infected macrophages^{194,195}. Caspase-11 cannot mature IL1 β and IL18 directly¹⁹⁶, but it nevertheless promotes secretion of bioactive IL1 β and IL18 indirectly through engagement of the NLRP3 inflammasome¹⁵⁴.

1.3.1.3. Mechanisms of inflammasome-induced pyroptosis

Caspases are well-known for their chief roles in apoptosis signaling³⁷. Unlike their apoptotic counterparts, the inflammatory caspase subset – i.e. human caspases -1, -4 and -5, and murine caspases -1 and -11 - triggers pyroptosis. Maturation of the apoptotic executioner caspases -3 and -7, internucleosomal DNA fragmentation and cleavage of PARP1 are considered hallmarks of apoptosis. However, these events may not be apoptosis-selective biomarkers as terminal deoxynucleotidyl transferase dUTP nick end labeling (TUNEL)-activity is also detected in *S. Typhimurium*-infected macrophages¹⁹⁷⁻¹⁹⁹, and occurs downstream of caspase-1²⁰⁰ (**Figure 4**). Similarly, inflammasome activation promotes caspase-1- dependent maturation of caspase-7, and cleavage of PARP1²⁰⁰⁻²⁰² (**Figure 4**). Unlike caspase-1, however,

deletion of neither caspase-7 nor PARP1 halted pyroptosis by the NLRP3 and NLRC4 inflammasomes^{200,201}, suggesting that caspase-7 and PARP1 may contribute to other inflammasome-linked events. In this regard, caspase-7 activation by the NLRC4 inflammasome was shown to promote endolysosomal destruction of *Legionella pneumophila* in infected macrophages²⁰³, and caspase-7-mediated PARP1 cleavage enhanced transcription of NF- κ B-dependent target genes²⁰². Despite these overlapping molecular characteristics, apoptotic and pyroptotic cells differ markedly in other aspects. Apoptosis features cell body shrinkage (pyknosis) and formation of apoptotic body formation, whereas pyroptotic cells undergo cytoplasmic swelling, consequently leading to opposing immunological outcomes. While apoptosis is an immunologically silent regulated cell death mode in which the plasma membrane integrity of the dying cell is not compromised before cells are phagocytosed, pyroptosis represents a lytic regulated cell death mode that is characterized by early membrane rupture and extracellular release of the intracellular contents. Because these hallmarks do not distinguish pyroptosis from other lytic regulated cell death modes such as necroptosis⁹⁹, pyroptosis is better defined as '*a lytic regulated cell death mode that relies on the enzymatic activity of inflammatory caspases*'. The term '*pyroptosis*' combines the Greek roots '*pyros*' and '*ptosis*' - which respectively stand for '*fire*' and '*falling*' - to highlight the inflammatory nature of this cell death mode²⁰⁴. Although the term pyroptosis was coined only in 2001, reports describing caspase-1-mediated regulated cell death of *S. Typhimurium*- and *S. flexneri*-infected macrophages date back to as early as 1996, even though at the time these events were designated as apoptotic or necrotic cell death²⁰⁵⁻²⁰⁹. In contrast, caspase-11 only recently emerged as a caspase that shares with caspase-1 the ability to induce pyroptosis in Gram-negative-infected macrophages¹⁵⁴.

Though still incompletely understood, understanding of the molecular mechanisms of pyroptosis has gained significant traction lately. The increasingly detailed description of the mechanisms driving caspase-1 and -11 activation in the canonical and non-canonical inflammasome pathways have clarified how pyroptosis is induced by microbial pathogen-associated molecular patterns (PAMPs) and cellular danger signals¹⁶¹. Moreover, the recent discovery that gasdermin D (GSDMD) cleavage is critical for both caspase-1- and -11-induced pyroptosis revealed a shared pyroptosis execution mechanism in the canonical and non-canonical inflammasome arms^{16,210}. Little is currently known about the physiological roles of GSDMD and other gasdermin family members, but cleavage of human GSDMD after Asp275 (corresponding to Asp276 in mouse GSDMD) by caspases-1 and the caspase-11

orthologues caspases -4 and -5 releases an amino-terminal fragment that suffices to induce pyroptosis when overexpressed (**Figure 4**). GSDMD is present in humans, mouse, rat and genomes of other mammals, but absent in birds, insects, amphibians and fish. Notably, the amino-terminal domains of other gasdermin proteins also induce cell death when ectopically expressed, but GSDMD appears the sole family member in which the regulatory carboxy-terminal domain is physically detached from the amino-terminal region by caspase-1/-11 cleavage^{16,210}. It would therefore be interesting to examine whether the cell death-inducing properties of other gasdermins may be exposed by alternative post-translation modifications in the flexible linker region, and whether this contributes to pyroptosis and/or other lytic cell death modes in macrophages and other cell types.

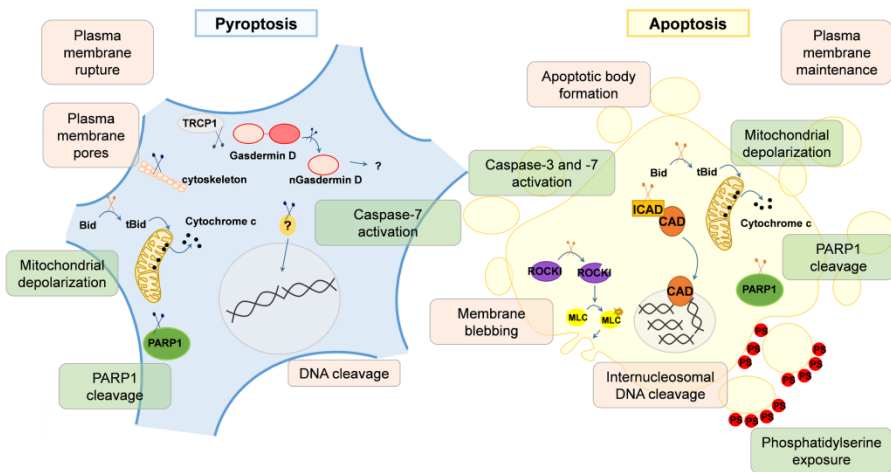


Figure 4. Scheme of the morphological and biochemical features of pyroptosis and apoptosis. These forms of cell death represent two very distinct forms of regulated cell death in terms of their final outcome, but share some important characteristics related to their signalling events (highlighted in green boxes).

Remarkably, while hundreds of caspase cleavage events coordinately orchestrate apoptotic cell death²¹¹⁻²¹³, caspase-11-mediated pyroptosis appears to rely solely on GSDMD cleavage because GSDMD-deficient macrophages are fully protected from caspase-11-induced pyroptosis^{16,210}. Because GSDMD deletion conferred only a temporal protection from caspase-1-induced pyroptosis²¹⁰, it is likely that cleavage of additional substrates contributes to caspase-1-mediated pyroptosis. This also suggests that cleavage events associated with pyroptosis via the canonical and non-canonical inflammasomes may overlap significantly because caspase-11-mediated

GSDMD cleavage indirectly engages caspase-1 downstream of the NLRP3 inflammasome^{16,210}.

A central outstanding question concerns the mechanism(s) by which caspase-1/-11 cleavage of GSDMD engages pyroptosis. Given the early plasma membrane rupture in pyroptotic cells, the amino-terminal GSDMD domain may oligomerize to form a membrane pore akin to how MLKL may act during necroptosis^{106,214}. Alternatively, the pyroptotic GSDMD domain may induce cell lysis indirectly by damaging intracellular organelles that result in disruption of mitochondrial respiration and ATP synthesis. In this regard, activation of the NLRP3 and AIM2 inflammasomes was shown to be associated with caspase-1-mediated mitochondrial damage that was accompanied by cleavage of the pro-apoptotic Bcl-2 family member Bid and cytosolic release of mitochondrial cytochrome *c*²¹⁵ (**Figure 4**). However, transgenic expression of Bcl-2 and deletion of apoptosis-associated mitochondrial outer membrane permeabilization inducers Bid, Bok, Bax and Bak do not alter the course of pyroptosis induced by the NLRP3 or AIM2 inflammasomes^{215,216}, suggesting that mitochondrial destabilization in pyroptotic cells may occur through other mechanisms.

Inflammasome-induced GSDMD cleavage may also induce pyroptosis by modulating ion fluxes from intracellular stores and/or plasma membrane-bound ion channels, which could explain osmosis and the plasma membrane rupture of pyroptotic cells. In this regard, pyroptosis was suggested to be accompanied by caspase-1-induced formation of transmembrane pores of approximately 1.1-2.4 nm prior to cell lysis¹⁹⁷ (**Figure 4**). Unlike caspase-1, caspase-11 was proposed to cleave and degrade the plasma membrane-bound cationic channel subunit transient receptor potential channel 1 (TRPC1) to stimulate unconventional IL1 β secretion²¹⁷, but how this integrates with the essential role of caspase-11-mediated GSDMD cleavage for IL1 β secretion in the context of non-canonical inflammasome activation requires further investigation (**Figure 4**). Without doubt, coming years will provide important progress in understanding the mechanisms driving pyroptosis downstream of caspases -1 and -11, and this is likely to reveal interesting similarities and differences by which the canonical and non-canonical inflammasomes coordinate pyroptotic cell death.

¹ An up to date discussion on GSDMD function is presented in Section 1.3.2.

1.3.1.4. Pyroptosis in inflammation and anti-microbial host defense

Inflammasome activation provides protection against bacterial, viral, fungal and protozoan pathogens, and pyroptosis induction is thought to contribute importantly to anti-microbial host defense^{149,154,218-221}. It is hypothesized that it does so by eliminating intracellular replication niches and by externalizing intracellular pathogens for immune recognition and clearance. In addition, recent reports suggest that pyroptosis may also represent a mechanism for the passive extracellular release of bioactive IL1 β and IL18. Unlike conventional cytokines, IL1 β and the related cytokine IL18 are secreted independently of the ER-Golgi secretory pathway, but instead are synthesized as cytosolic precursors that await their proteolytic cleavage by caspase-1²²¹. IL1 β promotes fever and infiltration of inflammatory cells indirectly through inflammatory mediators such as prostaglandin E₂ (PGE₂), nitric oxide species (NOS) and adhesion molecules. In addition, it modulates T and B cell responses by inducing Th2 and Th17 polarization of naïve CD4 T cells¹⁴⁸. IL18 also regulates T cell maturation by polarizing the response towards Th1 or Th2 patterns in conjunction with IL12¹⁴⁸. By monitoring caspase-1 activity using an engineered fluorescence resonance energy transfer (FRET) sensor in parallel with extracellular IL1 β at the single-cell level, secretion of IL1 β was shown to correlate fully with pyroptosis induction by the NLRP3, NLRC4 and AIM2 inflammasomes²²². Moreover, although a role for GSDMD in active secretion of these cytokines cannot be ruled out, the observation that its deletion delayed pyroptosis induction by the canonical inflammasomes along with extracellular release of mature IL1 β and IL18 suggests a causal link between these inflammasome outcomes^{16,210}.

In addition to IL1 β and IL18, pyroptosis has been associated with externalization of intracellular danger-associated molecular patterns (DAMPs). In particular, release of IL1 β and high mobility group box 1 (HMGB1) have been linked to pyroptosis induction by the canonical and non-canonical inflammasomes^{154,223}. IL1 α is a cytokine highly related to IL1 β , but with the contrasting difference that it does not need to be cleaved to be functional¹⁴⁸. Therefore, release of bioactive IL1 β likely is a common feature of lytic cell death modes, and may account for some of their inflammatory properties. Also, release of HMGB1 has been documented not only during pyroptosis^{154,223}, but also in the context of necroptosis^{224,225}. Intracellular HMGB1 regulates chromosome architecture in the nucleus, and although its intracellular roles confound its analysis as an extracellular DAMP in conditionally-targeted mice²²⁶⁻²²⁸,

studies using antibody-based HMGB1 neutralization have implicated it in a variety of inflammatory disease models. For example, lethality in the caspase-11-dependent LPS-induced endotoxemia model^{154,229} was more effectively prevented by neutralization of HMGB1 than by the combined deletion of IL1 β and IL18^{154,223,230}. It is thought that extracellular HMGB1 may act as a chemokine that engages receptor for advanced glycation endproducts (RAGE) and possibly as a TLR ligand in conjunction with PAMPs²³¹.

In addition to these DAMPs, pyroptotic cells have been suggested to release ASC specks to increase local inflammatory responses or to amplify inflammasome signaling when these aggregates are phagocytosed by neighboring cells^{232,233}. In the extracellular space, ASC specks continue to promote caspase-1 proteolysis of pro-IL1 β , and phagocytosed ASC specks serve as a platform for nucleating inflammasome activation in bystander cells^{232,233}. Thus, by promoting release of ASC specks and DAMPs such as IL1 α , IL1 β , IL18 and HMGB1, pyroptosis is increasingly regarded as a major effector mechanism by which inflammasomes contribute to inflammatory and host defense responses.

1.3.1.5. Inflammasome-induced apoptosis and pyronecrosis

Although inflammasomes have primarily been linked with induction of pyroptosis, mounting evidence suggests that they can elicit additional cell death modes, namely apoptosis and pyronecrosis. Similar to pyroptosis, pyronecrosis is a lytic cell death mode that relies on inflammasome adaptors, namely NLRP3 and ASC, but unlike pyroptosis it proceeds independently of caspase-1 activity^{234,235}. Instead, this inflammatory cell death mode possibly relies on the lysosomal cathepsins to induce cell lysis and HMGB1 release in the context of *Shigella flexneri*- and *Neisseria gonorrhoeae*-infected THP1 cells and human peripheral blood mononuclear cell (PBMC)-derived monocytes^{234,235}.

Current understanding of pyronecrosis is incomplete, but our knowledge on how inflammasomes engage apoptosis is gradually increasing. The first description of apoptosis induction by inflammasomes emerged from studies with ectopically expressed NLRC4 and ASC in HEK293T cells, which lack caspase-1. In this system, NLRC4 and ASC formed a complex that recruited endogenous caspase-8 and induced apoptosis²³⁶. ASC was proposed to engage in direct heterotypic CARD/DED interactions with caspase-8 for apoptosis induction²³⁶⁻²³⁸, although the possibility of a still unidentified component mediating their interaction cannot be ruled out.

Caspase-8 is intimately connected with inflammasome responses, as in addition to its role in mediating inflammasome-associated apoptosis, it mediates transcriptional upregulation of proIL1 β in response to TLR4 engagement, thus also serving as a checkpoint for efficient inflammasome-induced cytokine responses²³⁹. Moreover, caspase-8 is recruited to NLRP3 and NLRC4-engaged ASC specks in the context of pyroptosis signaling²³⁹⁻²⁴¹. Additionally, it was shown to promote IL1 β maturation and secretion from macrophages independently of inflammasomes under conditions of ER stress, fungal infection, death receptor engagement and chemotherapy treatment²⁴²⁻²⁴⁵.

Apoptosis induction with endogenous inflammasome components was more recently demonstrated in caspase-1 and -11-deficient *S. Typhimurium*-infected mouse macrophages²⁴⁶. Using pharmacological caspase-1 inhibition, caspase-1 protease activity was suggested to actively suppress apoptosis in *S. Typhimurium*-infected macrophages, although the mechanism involved remains unknown²⁴⁶. Apoptosis induction in the absence of caspase-1 activity was relayed by the inflammasome adaptors Nlr4 and Nlrp3 in this context²⁴⁶. In a similar manner, caspase-1/11-deficient macrophages that have been exposed to canonical NLRP3 and AIM2 stimuli also responded with delayed induction of apoptosis^{237,238}. Apoptosis was accompanied by caspase-8 recruitment to ASC specks, but caspase-8 could only be fully activated in the absence of caspase-1^{237,238}. It is interesting to note in this respect that ASC was originally cloned as an aggresome-forming protein in retinoic acid- and etoposide-treated apoptotic human promyelocytic leukemia HL-60 cells²⁴⁷, and its expression is suppressed in close to half of primary human breast cancers, suggesting that it may act as a tumor suppressor that induces apoptosis²⁴⁸.

However, formation of ASC specks is not confined to apoptotic cells, but also observed in the context of inflammasome-induced pyroptosis. ASC deletion prevents both pyroptosis and apoptosis induction in the context of the NLRP3 and AIM2 inflammasomes, but it is difficult to establish whether ASC-dependent apoptosis induction emerges from ASC specks or the ASC-containing inflammasome platforms because ASC is critical for bridging the interaction between NLRP3 and AIM2 with caspase-1 in their respective inflammasomes¹⁶¹. Indeed, the formation of the 1-2 micrometer-sized ASC aggregates is considered a hallmark of inflammasome engagement, and their prion-like physicochemical properties are well-documented^{249,250}. ASC specks are also formed in the context of the NLRC4 and NLRP1b inflammasomes, but as both NLRC4 and NLRP1b have a CARD domain, these sensors can directly engage caspase-1 in the absence of ASC utilizing

homotypic CARD interactions^{33,146,147}. Consequently, pyroptosis induction by the NLRC4 and NLRP1b inflammasomes is unhampered in the absence of ASC, whereas ASC is essential for pyroptosis in the context of the PYD-based NLRP3 and AIM2 inflammasomes^{33,146,147}. The observations described above suggest that inflammasome-associated pyroptosis and apoptosis induction may generate profoundly different systemic outcomes, and modulation of these cell death responses may offer novel approaches for treating inflammasome-associated diseases. In conclusion, significant progress was made in recent years in characterizing inflammasome-associated apoptosis, but more work is needed to examine when and how they contribute to inflammasome signaling *in vivo*.

1.3.1.6. Inflammasome-induced cell death in infection and autoinflammation

While understanding the relevance of inflammasome-mediated apoptosis *in vivo* is still in its infancy, a clearer picture on how pyroptosis induction by caspases -1 and -11 contributes to host defense against microbial pathogens, and detrimental inflammation in autoinflammatory diseases is emerging. Pyroptosis has been particularly linked to *in vivo* protection against infection with *Bacillus anthracis* spores, *B. thailandensis*, *B. pseudomalle*, *S. Typhimurium*, *Legionella pneumophila* and *F. tularensis*^{219,251,252}. In *S. Typhimurium* infection, the combined absence of IL1 β and IL18 failed to fully recapitulate the more severe phenotype of caspase-1/-11-deficient mice in agreement with the notion that pyroptosis not only promotes secretion of IL1 β and IL18, but also exposes pathogens to extracellular immune recognition^{219,252}.

However, generalized pyroptosis may also become detrimental to the host. For instance, extensive caspase-1-driven pyroptosis was identified as a major cause of immunodepletion in HIV patients that targets CD4 T cells that have been unproductively infected with the virus^{253,254}. Also, caspase-11-mediated pyroptosis in the absence of caspase-1-dependent cytokine production was suggested to be disadvantageous to the host in terms of efficiently clearing *S. Typhimurium* *in vivo*²⁵⁵. Excessive caspase-11-associated pyroptosis may also be pathogenic during LPS-induced endotoxemia because caspase-11 knockout mice are highly resistant to LPS-induced lethality, while animals lacking IL1 β and IL18 remain largely sensitive^{154,229}. Nevertheless, detailed analysis of the *in vivo* roles of pyroptosis was hampered by the absence of specific biomarkers, but the recent identification of GSDMD cleavage as a

pyroptosis-selective event offers a potentially suitable biomarker for monitoring pyroptosis *in vivo*.

Nevertheless, inflammasome-induced cell death is suspected to contribute to inflammatory pathology in inflammasomopathies, which are hereditary periodic fever syndromes caused by gain-of-function mutations in genes coding for inflammasome components^{151,256}. Cryopyrin-associated periodic syndromes (CAPS) is frequently caused by mutations in and around the central NACHT domain of the inflammasome adaptor NLRP3²⁵⁷. Patients diagnosed with these diseases can be distributed across a spectrum of severity of their clinical outcomes, in which Familial cold autoinflammatory syndrome (FCAS) patients present the mildest form, Muckle-Wells syndrome (MWS) correlates with an intermediate phenotype, while Neonatal onset multisystem inflammatory disease (NOMID) is very severe. CAPS patients exhibit the symptoms of general inflammation, suffering with rash, fever, headache and fatigue that can be triggered by cold exposure, stress or, in its most serious form, even be present in a chronic manner. Severe presentations of CAPS can progress to hearing impairment or even neurological sequelae due to aseptic meningitis²⁵⁷. Some *Nlrp3* SNPs that are associated with CAPS have been shown to render NLRP3 constitutively active, which explains the high levels of inflammation experienced by the patients²⁵⁶. CAPS patients highly benefit from IL1 inhibitors that are already prescribed in the clinic²⁵⁷. However, in mouse models of CAPS, combined blockade of IL1R/IL18R signaling provided less protection from postnatal lethality than caspase-1 deletion, reinforcing the notion that pyroptosis-related DAMPs may contribute to pathology in this autoinflammatory model¹⁵⁰.

Inflammasome-associated cell death may also be an important driver of pathology in recently described autoinflammatory diseases that are caused by activating mutations in NLRC4¹⁵¹⁻¹⁵³. In all studied cases, recurrent fever began early in life, but the other symptoms were variable, including rash and intestinal-commitment. High levels of IL18 in the serum of patients, together with other inflammatory markers, confirmed the correlation of NLRC4-activating mutations with disease onset. In accordance with the clinical presentation, these diseases were termed NLRC4-MAS, SCAN4 and NLRC4-FCAS, respectively¹⁵¹⁻¹⁵³. IL1 β neutralization improved a subset of symptoms in NLRC4-MAS patients and in a mouse model of NLRC4-FCAS, but could not rescue the high levels of circulating IL18. The latter suggests that excessive NLRC4-induced cell death linked with IL18 secretion and macrophage activation syndrome may be an important cause of pathology in NLRC4-associated autoinflammation¹⁵¹⁻¹⁵³. These findings undoubtedly warrant a thorough

investigation of inflammasome-induced cell death responses and its roles in CAPS and NLRC4-associated autoinflammation.

1.3.1.7. Concluding remarks: inflammasomes as polyvalent cell death controllers

We illustrated throughout this review that inflammasomes may regulate several cell death modes and inflammatory mechanisms (**Figure 5**). That a signaling platform would control a variety of downstream cell death pathways is not unprecedented. The death receptor family member TNFR1 can engage at least three different complexes, termed complex I, II and IIb, with each complex promoting a distinct cellular response. Complex I induces NF- κ B- and AP-1-dependent transcription of pro-inflammatory cytokines and the apoptosis inhibitor cFLIP, therefore constituting a pro-survival signal. When complex I-dependent responses are impaired, assembly of complex II activates caspase-8 for induction of apoptosis. When caspase-8 activation fails, complex IIb leads to induction of necroptosis through RIPK1 and 3. Therefore, signaling through TNFR1 is highly regulated, thereby skewing cellular responses to TNF stimulation depending on the cellular context²²⁵. Similarly, inflammasome responses appear to be regulated by an exquisite range of regulatory mechanisms. Although induction of pyroptosis downstream of caspase-1 may be an all-or-none response²²², inflammasome activation itself is tightly controlled at both the transcriptional and post-translational levels. A prime example of transcriptional control is presented by the NF- κ B-dependent induction of NLRP3, proIL1 β and caspase-11 levels in order to license inflammasome assembly, pyroptosis, and the release of mature IL1 β ¹⁶¹. Inflammasome activation is also regulated directly through post-translational modifications, as illustrated by the necessity for NLRP1b autocleavage²⁵⁸, and NLRC4 phosphorylation^{184,185} for inflammasome activation. Primate-specific CARD-only and Pyrin-only proteins represent yet another level of inflammasome regulation²⁵⁹. Overall, tight regulation of inflammasome activation may serve to ensure that cells respond adequately to intracellular pathogen invasion while minimizing as much as possible the collateral damage induced by excessive cell death and inflammatory responses.

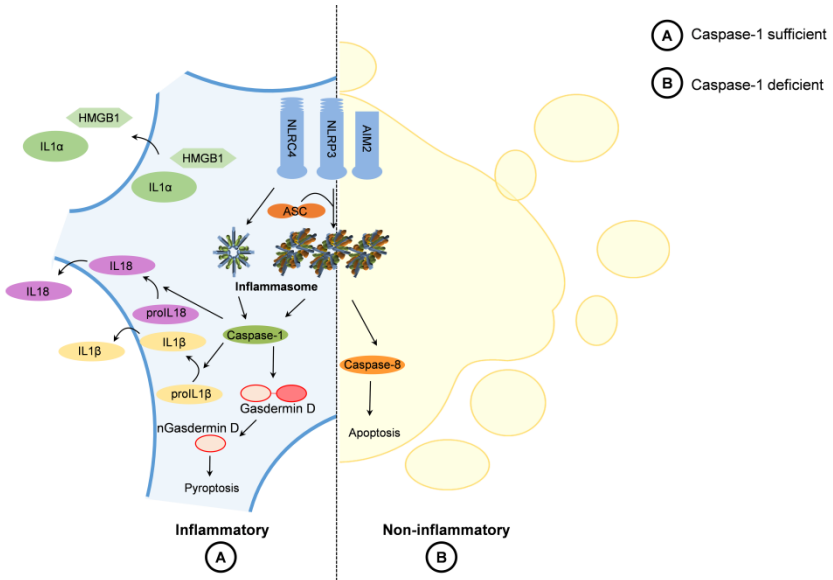


Figure 5. Representation of inflammasomes as cell death switches. While engagement of NLRP3, AIM2 and NLRP4 leads to pyroptosis in the presence of caspase-1, lack of this inflammatory caspase deviates the response towards caspase-8-dependent apoptosis. Importantly, NLRP4 is able to activate caspase-1 in the absence of the adaptor ASC, but the apoptotic phenotype is highly dependent on the adaptor protein. Considering the downstream effects of pyroptosis and apoptosis, inflammasome engagement could potentially play contrasting roles in immune response depending on the expression level of caspase-1.

1.3.2. GSDMD as the pore mediator of pyroptosis

The plasma membrane alterations of pyroptosis have remained so far the most studied feature of this cell death, for its potential to release DAMPs and to cause an immune response in neighboring cells. Through studies with osmoprotectant solutions, caspase-1 was suggested to induce pores between 1.1 to 2.4nm in size at the plasma membrane, with osmotic pressure accounting for total cell lysis¹⁹⁷. Accordingly, further attempts to characterize the pyroptotic pore formation demonstrated that in the presence of glycine as an osmoprotectant, propidium iodide (PI) – a nuclear dye impermeable to intact membranes – can be detected in pyroptotic cells while bigger contents – tracked by lactate dehydrogenase (LDH) – are still retained in the cytoplasm²⁶⁰. However, advance in understanding the pyroptotic lysis only gained traction with the identification of GSDMD as the executor of pyroptosis.

Cleavage of GSDMD by either caspase-1, mouse caspase-11 or human caspase-4 and -5 releases the pore-forming N-terminal domain (GSDMD_N) from its inhibitory C-terminal fragment^{16,261}. GSDMD_N then oligomerizes through intramolecular disulfide bonds and integrates into membranes²⁶²⁻²⁶⁵. In overexpression systems, the GSDMD_N pore has variable sizes, ranging from 10 to 20nm in internal diameter²⁶³⁻²⁶⁵. This pore assembly could potentially allow even large proteins to flux through, which lead to the suggestion that pyroptotic cells do not undergo osmotic pressure during lysis²⁶⁶. However, further physiological characterizations of the GSDMD pore would aid in the understanding of the pyroptotic cell lysis.

While GSDMD_N demonstrates specificity for phospholipids of the cytoplasmic leaflet of the plasma membrane (i.e. Phosphatidylinositol 4-phosphate, Phosphatidylinositol (4,5)-biphosphate and Phosphatidylserine), it can also be found across practically any membrane-bound organelle²⁶²⁻²⁶⁵. This suggests that GSDMD_N mediated killing is programmed to happen from the “inside-out” of cells and might involve pore formation in other organelles besides the plasma membrane.

Interestingly, the toxic activity of the N-terminal fragment of GSDMD is a common feature between the gasdermin family members²⁶³. The gasdermin family had previously been identified in the skin and gastrointestinal tract, hence its naming²⁶⁷. The founder member of the family, GSDMA1, was described as the causative gene of skin anomalies in mice. There are four gasdermin proteins in humans, named gasdermin A (GSDMA), gasdermin B (GSDMB), gasdermin C (GSDMC) and GSDMD²⁶⁸. Mice do not have a homologue for GSDMB, but both GSDMA and

GSDMC are represented by three and four paralogues, respectively. All gasdermin proteins are highly homologous and contain several leucine-rich motifs throughout their structure²⁶⁸. Resolution of the structure of GSDMA3 demonstrated that the previously called Gasdermin-domain is in fact composed by two globular domains, linked by an unstructured loop²⁶³. Three-D structures of the other gasdermin family members are not available yet, though given their high homology, it is assumed that all gasdermin proteins are organized in the same way.

While in one hand the gasdermins gene are highly homologous, they present different spectra of tissue expression. GSDMA1, GSDMA2, GSDMD and GSDMC1-4 have high expression level in the gastrointestinal tract of mice, while absent or low expressed in heart, brain, liver, skeletal muscles and lungs²⁶⁸. Interestingly, throughout the gastrointestinal tract, high mRNA level of each gasdermin family member is found confined to specific locations. GSDMA1 and GSDMA2 are more expressed in the stomach, while GSDMD has higher expression in small intestine and GSDMC's are mostly present in the colon²⁶⁸. In all cases, these GSDMs are expressed in differentiated cells of the epithelial layer²⁶⁹. In contrast to them, human GSDMB shows higher mRNA levels in stem cells of esophagus and stomach²⁶⁹. Considering the gasdermins intrinsic ability to cause cell death, validation of this data on the protein level and further characterization in specific cell types could shed light into which cell death signaling plays a role in the maintenance or immune response of the different tissues.

The gasdermin family members have close proximity of domain to their distant relative deafness associated tumor suppressor (DFNA5)²⁶⁸, initially identified as the gene bearing a mutation causative of nonsyndromic hearing impairment²⁷⁰. In fact, DFNA5 also shares the ability to induce a lytic form of cell death through its N-terminal fragment²⁶³, and a gain of function mutation might be at the foundation of its role in deafness. Despite DFNA5 being initially described as a separate branch in the gasdermin phylogenetic tree²⁶⁸, given its shared ability to induce cell death it was recently proposed that DNFA5 is renamed to gasdermin E (GSDME)²⁷¹.

While the activation of GSDMD is through caspase-1 and -11/-4/-5-mediated cleavage in Aspartate 276/275^{16,261}, it is still unknown how the other gasdermins are activated. Remarkably, the GSDMD cleavage site lies in its unstructured loop, where all gasdermins have lower level of homology²⁶⁸. This suggests that each gasdermin protein is potentially activated by a different mechanism. Indeed, DFNA5/GSDME is cleaved in this same region by caspase-3^{271,272}. Cleavage of DFNA5/GSDME by

caspace-3 has been suggested to lead to secondary necrosis of cells triggered by apoptotic stimuli²⁷². In some systems, however, secondary necrosis was shown to occur normally even in the absence of DFNA5/GSDME²⁷³. This suggests that there might be a stimuli-dependency for DFNA5/GSDME function. Interestingly, cells bearing a high expression level of DFNA5/GSDME were shown to skip the normal features of apoptosis, such as cell shrinkage and blebbing, and to undergo direct lytic cell death after signaling of the apoptotic program²⁷¹. Particularly, the DFNA5/GSDME-mediated lytic cell death would be behind the inflammatory side effects in lungs and intestines after treatment with chemotherapy drugs²⁷¹. An extensive characterization of what constitutes the threshold of DFNA5/GSDME expression level to allow apoptotic blebbing or lysis of the plasma membrane to occur could help understand when homeostatic and pathological cell death follows. Furthermore, understanding tissue and cell type-associated expression of DFNA5/GSDME might shed light into the local roles of this protein in cell death.

In conclusion, despite great recent advance in understanding the function of gasdermins, the field is still left with major fundamental questions. Most of the characterizations done so far have relied on overexpression systems, which might overlook fine-tuned regulations and functions of the gasdermins. Therefore, there should be a focus in establishing *in vivo* physiological roles of gasdermins. Further studies on the regulation and activation mechanisms of the gasdermins will allow a better understanding of cell death regulation and its potential contribution to homeostasis and pathology.

2. Aims

Pyroptosis is a lytic form of regulated cell death happening in myeloid and epithelial cells. Cell death by pyroptosis releases DAMPs such as HMGB1 and IL1 α but is also regarded as a secretion mechanism for the leaderless cytokines IL1 β and IL18. Furthermore, the pyroptotic cell corpse has been shown to contain pathogens to facilitate their clearance by infiltrating immune cells. While pyroptosis aids in innate immunity signaling and clearance in response to bacterial, fungal and viral pathogens, extensive cell death and cytokine release might participate in the pathology of autoinflammatory disorders.

Caspase-1 is a cysteine protease responsible for pyroptotic cell death induction. Further, caspase-1 cleaves and activates the pro-cytokines IL1 β and IL18. While activation of caspase-1 is controlled by the macromolecular structures called canonical inflammasomes, pyroptosis can also be initiated by caspase-11, in a non-canonical inflammasome activation. Caspase-1 and caspase-11 signaling for pyroptosis converge on cleavage of GSDMD. The newly formed N-terminal fragment of GSDMD translocates to the plasma membrane and oligomerizes, forming a pore responsible for cell lysis. To this date, the intracellular mechanisms happening during pyroptosis are not fully understood. In terms of organellar changes, most of the focus on pyroptosis execution has been placed in understanding the alterations at the plasma membrane. However, whether other organelles participate on cell death execution is currently unknown. Furthermore, in addition to GSDMD, IL1 β and IL18, caspase-1 has been shown to cleave several other substrates, whose functions for pyroptosis execution have not been described yet. In fact, lack of GSDMD merely delays cell death after caspase-1 activation. Thus, we hypothesized that cell death on the GSDMD^{-/-} cells after inflammasome trigger could be reminiscent of a more

complex biochemical program already present in the wild type condition, and that an underlying complex pyroptotic program could be happening in addition to the GSDMD pore during cell death execution.

In order to first address the issue of defining the organellar features of pyroptosis, we undertook a live imaging-based analysis to morphologically describe cell death execution. We addressed NLRC4 and NLRP1b-triggered cell death side by side, with the assumption that organellar events happening downstream of caspase-1 activation would be shared between the two inflammasomes. Furthermore, since macrophage cell death after canonical inflammasome triggering could not be rescued by GSDMD ablation, we studied the non-canonical inflammasome, dependent on caspase-11, for questioning the roles of GSDMD in organellar changes observed. In a second stage, we aimed at characterizing the biochemical aspects of pyroptosis execution downstream, utilizing again the NLRC4 and NLRP1b inflammasomes. Particularly for the biochemical studies, these inflammasomes has an extra potential as these receptors contain a CARD domain and engage caspase-1 even in the absence of ASC. Thus, this allowed us to segregate the biochemical events which are ASC-dependent or -independent. Finally, we characterized the ability of inhibitors targeting serine proteases of the prolyl dipeptidase extended family to promote inflammasome activation, IL1 β release and cell death in macrophages.

3. Results

The goal of this doctoral project was to characterize pyroptotic cell death at the morphological and biochemical level. For this end, the canonical inflammasomes NLRP1b and NLRC4 were selected as models for studying downstream cell death induction.

Transgene expression of an NLRP1b allele derived from 129 mice confers macrophages of C57/BL6 mice susceptibility to toxicity by LeTx from *Bacillus anthracis*¹⁷⁵. LeTx is composed of two subunits: PA, which forms a pore for shuttling the metalloprotease, LF, to the cytosol. Cytosolic presence of catalytically active LF triggers the NLRP1b inflammasome²⁷⁴, though through a still undefined mechanism. Furthermore, it is known that proteasomal activity is a requirement for NLRP1b activation²⁷⁴, and that the receptor can promote caspase-1 activation even in the absence of ASC^{146,147}.

The NAIP5/NLRC4 system senses presence of flagellin in the cytosol¹⁸². To accomplish cytosolic delivery of flagellin, a system based on the *B. anthracis* toxin has been devised in which the N-terminal fragment of LF (LFn) was fused at the N-terminal side of flagellin of *Legionella pneumophila*, allowing PA recognition of the chimeric protein (LFn-FlaA) and its shuttling to the cytosol²⁷⁵. Co-treatment of macrophages with PA and LFn-FlaA (called FlaTox) triggers NAIP5, which engages NLRC4 oligomerization and downstream ASC-caspase-1 activation. NLRC4 is also able to directly activate caspase-1 in the absence of ASC through CARD/CARD interactions³³.

To define which intracellular events could be happening before plasma membrane rupture during pyroptotic cell demise, as initial steps we focused on analyzing organellar morphological changes after activation of the NLRP1b and NLRC4

inflammasomes. Given our observation during these studies that GSDMD^{-/-} macrophages die with same kinetics as wild type cells after canonical inflammasome activation, in this section we also studied caspase-11-driven pyroptosis to differentiate GSDMD-dependent and -independent mechanisms. The single cell analyzes used for this purpose are described in Section 3.1 of Results.

While focused on the first part of the project, we observed caspase-3/-7 activity on pyroptotic cells, based on DEVDase reporter, suggestive of a signaling pathway happening in parallel to the GSDMD pore formation. Thus, Section 3.2 of Results comprises the characterization of the molecular events happening in pyroptosis independently of the GSDMD-mediated plasma membrane damage.

Finally, we addressed the role of small compounds targeting the extended dipeptidyl peptidase(DPP)-4 family members on their ability to promote cell death and inflammasome activation. For clarity, these results were separated in two sub-sections: the results on lysosomal Pro-X carboxypeptidase (PRCP) inhibition by Compound 80 are described in Section 3.3.1 of Results; the other DPP inhibitors are combined in Section 3.3.2 of Results.

Each section is in the form of a manuscript, thus containing a specific introduction, description of results and discussion. A combined discussion of all results presented in the thesis is provided in Section 4.

3.1.A morphological, single cell-based, analysis of pyroptosis

Section 3.1. is modified from the research paper: de Vasconcelos, N.M., Van Opdenbosch, N.; Van Gorp, H; Parthoens, E.; Lamkanfi, M.; Single-cell analysis of pyroptosis dynamics reveals conserved GSDMD-mediated subcellular events that precede plasma membrane rupture. *Cell Death and Differentiation*, 2018.

3.1.1. Abstract

Pyroptosis is rapidly emerging as a mechanism of anti-microbial host defense, and of extracellular release of the inflammasome-dependent cytokines IL1 β and IL-18, which contributes to autoinflammatory pathology. Caspases 1, 4, 5 and 11 trigger this regulated form of necrosis by cleaving the pyroptosis effector GSDMD, causing its pore-forming amino-terminal domain to oligomerize and perforate the plasma membrane. However, the subcellular events that precede pyroptotic cell lysis are ill defined. In this study, we triggered primary macrophages to undergo pyroptosis from three inflammasome types and recorded their dynamics and morphology using high-resolution live-cell spinning disk confocal laser microscopy. Based on quantitative analysis of single-cell subcellular events, we propose a model of pyroptotic cell disintegration that is initiated by opening of GSDMD-dependent ion channels or pores that are more restrictive than recently proposed GSDMD pores, followed by osmotic cell swelling, commitment of mitochondria and other membrane-bound organelles prior to sudden rupture of the plasma membrane and full permeability to intracellular proteins. This study provides a dynamic framework for understanding cellular changes that occur during pyroptosis, and charts a chronological sequence of GSDMD-mediated subcellular events that define pyroptotic cell death at the single-cell level.

3.1.2. Introduction

Pyroptosis is a lytic form of regulated cell death that is induced by inflammatory caspases -1, -4, -5 and -11^{1,2}. Various infectious agents, cellular stress conditions and environmental cues may trigger assembly of cytosolic multiprotein platforms termed inflammasomes that recruit caspase-1 and facilitate its proximity-induced autoactivation³. Murine caspase-11 and its human orthologs caspases -4 and -5 are activated by cytosolic LPS, and indirectly promote activation of caspase-1 through the non-canonical inflammasome pathway⁴. Caspase-1 cleaves the biologically inert precursor proteins IL-1 β and IL-18 into the mature, secreted inflammatory cytokines³. Unlike for IL-1 β and IL-18, each of the aforementioned inflammatory caspases can induce pyroptosis directly by cleaving GSDMD at the central linker peptide, which separates the pore-forming amino-terminal domain (GSDMD_N) from the inhibitory carboxy-terminal (GSDMD_C) domain⁵⁻⁸. This cleavage event causes GSDMD_N to oligomerize and insert in the plasma membrane, giving rise to rapid cell lysis. Pyroptosis deprives intracellular pathogens from their replicative niches, and is thought to trap infectious agents in the cellular debris in order to facilitate bacterial clearance by recruited neutrophils⁹. In addition, it is considered an inflammatory form of regulated necrosis because cell rupture promotes the extracellular release of cytosolic proteins such as the leaderless cytokines IL-1 β and IL-18 and the nuclear alarmin HMGB1 that may attract and stimulate secondary innate immune cells^{5,8,10,11}.

Pyroptosis as a cell biological phenomenon was first reported in the context of macrophages that had been infected with the Gram-negative bacterial pathogens *S. flexneri* and *S. Typhimurium*, respectively¹²⁻¹⁴. However, the term pyroptosis was coined only in 2001 to distinguish this inflammatory form of caspase-1-regulated necrosis from accidental necrosis and apoptosis¹⁵. Notably, pyroptosis is thought to share features with both apoptosis and necroptosis, another form of regulated necrosis that relies on RIPK3 and its substrate MLKL for cell death execution¹⁶⁻¹⁸. Akin to apoptosis, pyroptosis is controlled by caspases, and both are thought to be accompanied by fragmentation of nuclear DNA^{12,13,19,20}. Similar to necroptosis, however, pyroptosis is associated with cytosolic swelling, cell rounding, absence of chromatin condensation and early plasma membrane rupture associated with spill out of the cytosolic contents²¹. To the best of our knowledge, there has been no detailed characterization of the morphology and subcellular dynamics that precede pyroptotic cell lysis. Here, we triggered primary macrophages to undergo pyroptosis from two inflammasome types and recorded their dynamics and morphology using

high-resolution live-cell spinning disk confocal laser microscopy. Our findings show that pyroptosis differs from necroptosis, and that it proceeds by a determined sequence of subcellular events for cellular disintegration irrespective of the engaged inflammasome pathway.

3.1.3. Results

Myosin II-independent blebbing and differential cell detachment during pyroptosis and necroptosis

Pyroptosis and necroptosis both are lytic forms of regulated cell death, but it is unclear whether they differ in particular features. C57BL/6J mouse bone marrow-derived macrophages (BMDMs) that express a functional Nlrp1b allele (B6^{NLRP1b+}) can be induced to undergo caspase-1-dependent pyroptosis when stimulated with *B. anthracis* LeTx²². Stimulation with TNF+BV6+zVAD-fmk (TBz) induces necroptosis in macrophages and other cell types²³. We used these cytotoxic agents to compare the morphological features of B6^{NLRP1b+} BMDMs undergoing necroptosis and pyroptosis. As previously reported in necroptotic L929sAhFas cells²⁴, TBz-treated B6^{NLRP1b+} macrophages readily detached from the adherent surface and rounded up prior to losing plasma membrane integrity and becoming Sytox Green-positive (**Fig. 1a and Supplemental Movie 1**). The membrane appeared smooth during this process, and formation of balloon-like protrusions of the plasma membrane that were reminiscent of blebs were seen concomitant with the loss of plasma membrane integrity (**Fig. 1a**). Unlike necroptotic cells, pyroptotic macrophages remained attached to the adherent surface until they became Sytox Green-positive (**Fig. 1b and Supplemental Movie 2**). As during necroptosis, however, plasma membrane rupture was accompanied by the formation of blebs (**Fig. 1b**). The ROCK-I inhibitor Y27632 and the selective inhibitor of non-muscle myosin II ATPases (-)-blebbistatin inhibited blebbing in apoptotic cells (data not shown). However, inhibition of ROCK-I and myosin-II had no effect on pyroptotic and necroptotic blebbing (**Fig. 1c, d**).

Phosphatidylserine exposure is closely associated with plasma membrane rupture during pyroptosis

Early PS exposure is a hallmark of apoptosis that attracts engulfing cells²⁵. Recent studies showed that also mammalian cell lines undergoing necroptosis, as well as necrotic cells in the nematode *Caenorhabditis elegans* actively present PS on their outer surfaces prior to cell lysis in order to recruit phagocytes^{26,27}. To study the kinetics of

PS exposure relative to plasma membrane rupture during pyroptosis, LeTx-treated B6^{NLRP1b+} BMDMs were quantified for Annexin-V-FITC and PI positivity over time.

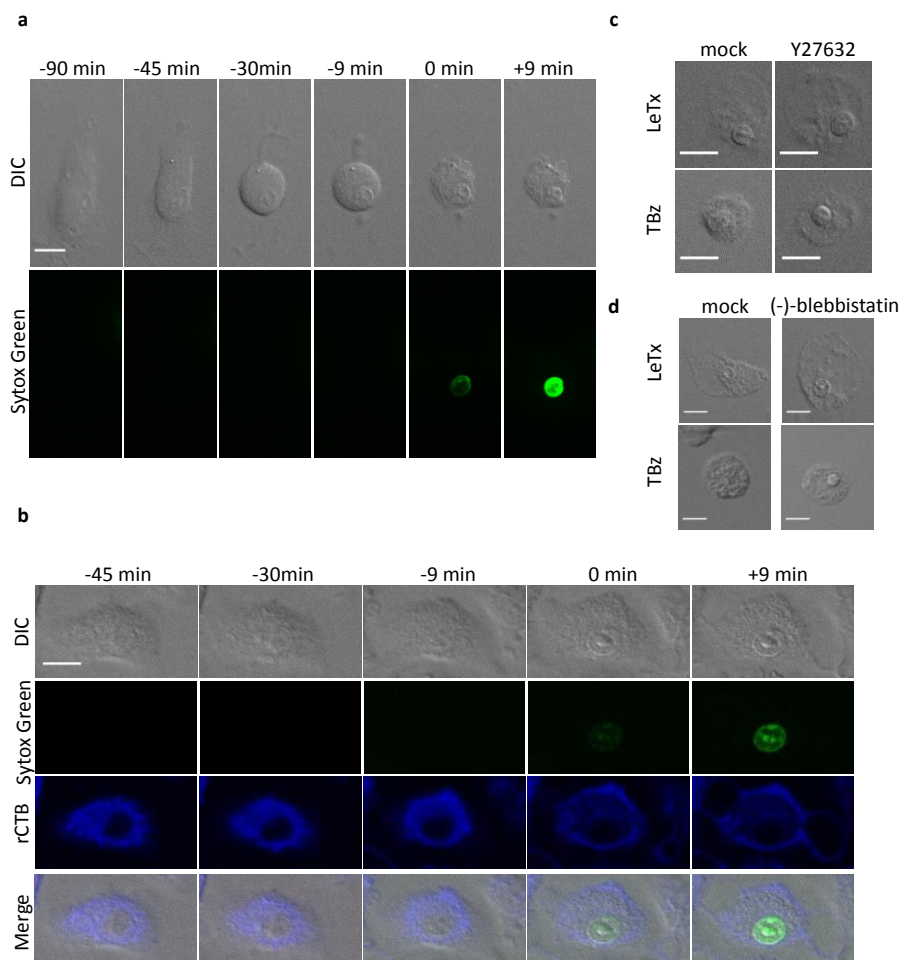
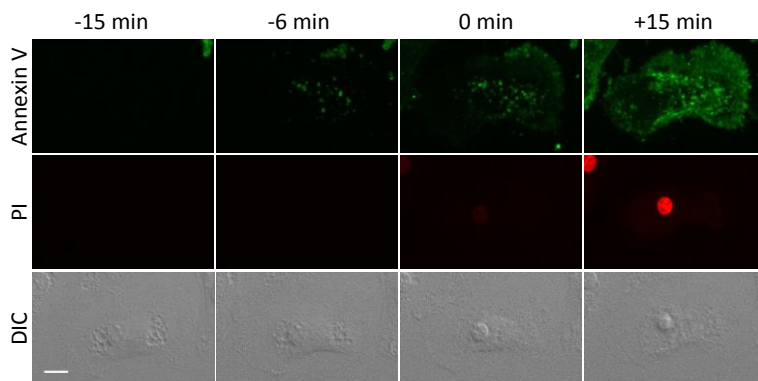


Figure 1. Cell detachment and blebbing during necroptosis and pyroptosis. **a**, BMDMs were stimulated with TNF+BV6+zVAD-fmk (TBz) and imaged in culture media containing Sytox Green. **b**, rCTB stained BMDMs were stimulated with LeTx and imaged as in (a). **a**, **b**, Confocal images were acquired every three minutes. **c**, **d**, BMDMs pretreated with Y27632 (10 μ M) (**c**) or (-)-blebbistatin (10 μ M) (**d**) were stimulated with LeTx or TBz and imaged. Fluorescent micrographs show the maximum intensity projection (Sytox Green) or the single plane (rCTB) of a representative cell from three independent experiments (TBz n=30; LeTx n=30; LeTx+Y27632 n=25; TBz+Y27632 n=23; LeTx+(-)-blebbistatin n=19; TBz+(-)-blebbistatin n=20). In all panels time point zero indicates the first detection of Sytox Green. All scale bars, 10 μ m.

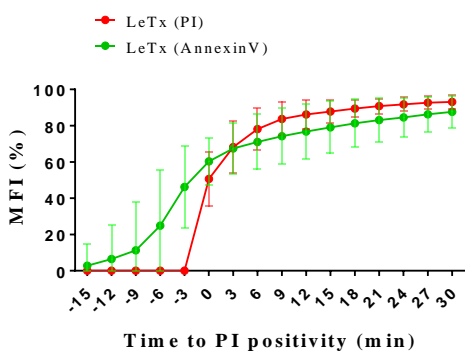
This analysis indicated that Annexin-V positivity preceded plasma membrane rupture with approximately 9-12 minutes during LeTx-induced pyroptosis (**Fig. 2a, b, Supplemental Figure 1a and Supplemental Movie 3**). Exposure of untreated

B6^{NLRP1b+} BMDMs failed to yield signals for Annexin-V and PI during this time interval, demonstrating specificity of these findings (**Supplemental Movie 4**).

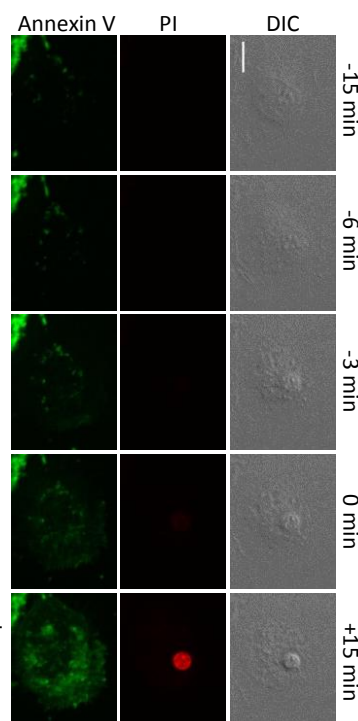
a



b



c



d

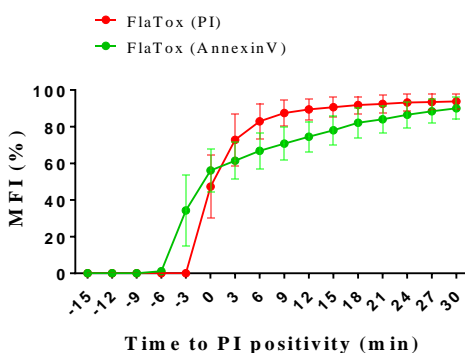


Figure 2. PS exposure happens during pyroptosis. a-d, BMDMs were stimulated with LeTx (a, b) or FlaTox (c, d) and imaged in culture media containing Annexin-V-FITC and PI. Confocal images were acquired every 3 minutes. Graphs show the percentage of mean fluorescence intensity (MFI) calculated as described in *Online Methods*, and values represent the mean \pm SD of all individual cells that were imaged in three independent

experiments (LeTx n=18; FlaTox n=21). Single cell plots are shown in Supplemental Figure 1. Fluorescent micrographs show the maximum intensity projection of a representative. In all panels time point zero indicates the first detection of PI. All scale bars, 10 μ m.

To understand whether Annexin-V staining prior to cell lysis is a shared feature of pyroptosis when routed through other inflammasomes, we repeated the analysis for LFn-FlaA-treated B6^{NLRP1b+} BMDMs. LFn-FlaA selectively triggers NAIP5/NLRC4 inflammasome-dependent pyroptosis and consists of *Legionella pneumophila* flagellin (FlaA) fused to the N-terminal domain of *B. anthracis* lethal factor (LFn) to enable *B. anthracis* protective antigen (PA)-assisted cytosolic delivery of the fusion protein²⁸. Quantification of data from 21 cells from several independent experiments showed that Annexin-V staining was observed in B6^{NLRP1b+} BMDMs treated with PA + LFn-FlaA (here called FlaTox) approximately 3 minutes before cells became PI-positive (**Fig. 2c, d, Supplemental Figure 1b and Supplemental Movie 5**). Future studies will need to confirm that this corresponds to active PS exposure to the outer leaflet of the plasma membrane, given that the confocal micrographs do not allow enough resolution to differentiate between inner or outer staining of PS. However, we favour the latter hypothesis given that Annexin-V staining could be observed while the plasma membrane was still impermeable to PI (**Fig. 2b, d**). We conclude from these studies that PS exposure happens in pyroptosis, and is closely associated with plasma membrane rupture.

Mitochondrial commitment independently of the apoptotic Bax/Bak pore

Mitochondria play a central role during apoptosis with the release of cytochrome c and other molecules that reside in the mitochondrial intermembrane space promoting assembly of the apoptosome and caspase-mediated cellular dismantling²⁹. In contrast, the role of mitochondria in inflammasome signalling is contentious. Mitochondrial damage has been proposed to occur downstream of the NLRP3 and AIM2 inflammasomes, with caspase-1 activation and IL-1 β secretion proceeding independently of the Bcl2-regulated Bax/Bak pore, Parkin-mediated mitophagy, and the Cyclophilin D-dependent mitochondrial permeability transition pore³⁰. Mitochondrial damage and dismantling of the organelle have also been suggested to occur upstream of the NLRP3 inflammasome because blockade of mitochondrial voltage-dependent anion channels (VDAC) and Bcl2 overexpression in macrophages selectively inhibited caspase-1 activation and IL-1 β secretion by the NLRP3 inflammasome³¹. We performed a longitudinal live cell analysis of mitochondrial

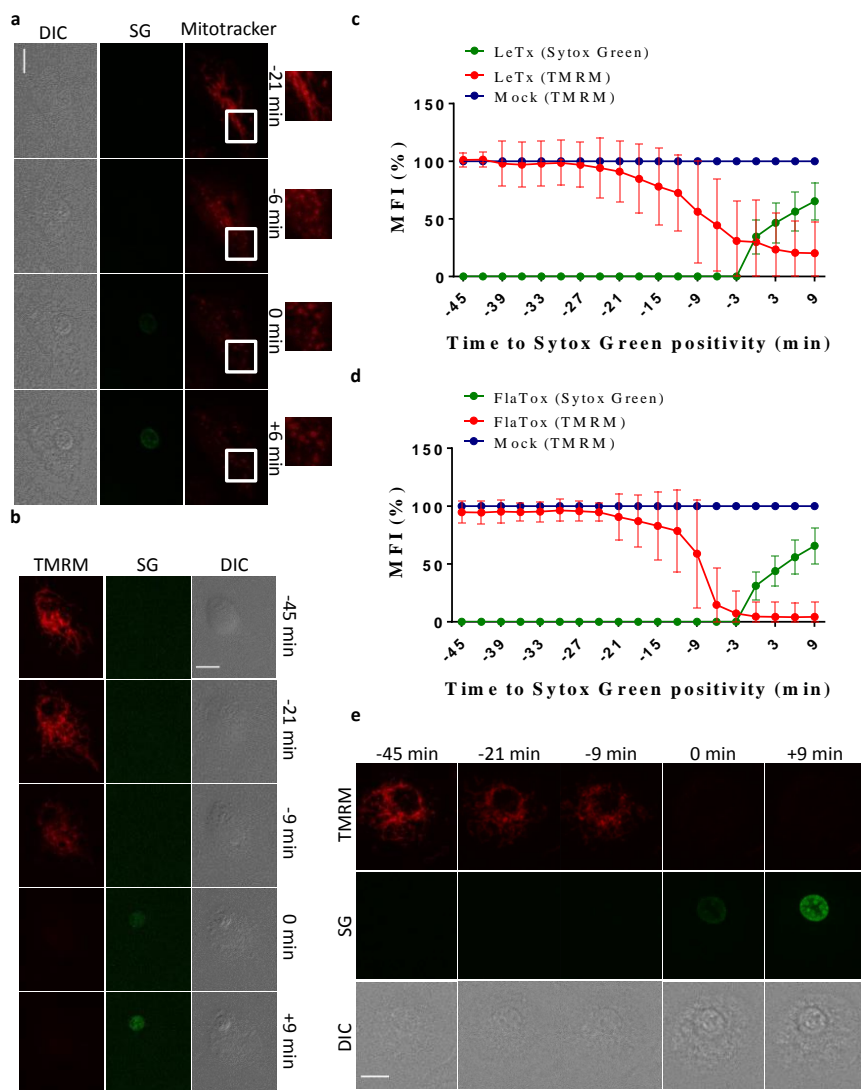


Figure 3. Mitochondria are damaged during pyroptosis. **a**, BMDMs were preloaded with Mitotracker Red CMXRos and stimulated with LeTx in culture media containing Sytox Green (n=50). Confocal images were acquired every 3 minutes. **b-e**, BMDMs were preloaded with TMRM and stimulated with either LeTx (**b**, **c**) or FlaTox (**d**, **e**) and imaged as in (**a**). Graphs show the percentage of mean fluorescence intensity (MFI) calculated as described in *Online Methods*, and values represent the mean \pm SD of all individual cells that were imaged in five independent experiments (LeTx, n=28; FlaTox n=28). Single cell plots are shown in Supplemental Figure 3. Fluorescent micrographs show the maximum intensity projection (TMRM and Sytox Green) or the single plane (Mitotracker) of a representative cell. In all panels time point zero indicates the first detection of Sytox Green. All scale bars, 10 μ m.

dynamics to better understand the role of this organelle in pyroptosis. Active mitochondria of B6^{NLRP1b+} macrophages were labelled with the membrane potential

($\Delta\Psi_m$)-insensitive dye MitoTracker Red CMXRos. Consistent with mitochondrial commitment during pyroptosis, the tubular mitochondrial network seen in mock-treated cells (**Supplemental Fig. 2**) was lost following LeTx challenge (**Fig. 3a and Supplemental Movie 6**). Notably, mitochondria appeared rounded and fragmented before cell rupture, marked by Sytox Green internalization, was evident (**Fig. 3a**). A quantitative analysis of TMRM fluorescence, a mitochondrial membrane potential ($\Delta\Psi_m$)-sensitive dye, confirmed that LeTx-induced mitochondrial membrane depolarization occurred approximately 18-21 minutes before plasma membrane rupture (**Fig. 3b, c, Supplemental Figure 3a and Supplemental Movie 7**). As reported for the AIM2 and NLRP3 inflammasomes³², the pro-apoptotic Bcl2 family member BID was cleaved when pyroptosis was induced in LeTx-intoxicated B6^{NLRP1b+} macrophages (**Supplemental Fig. 4a**). However, LeTx-induced caspase-1 maturation and LDH release were unaffected in BMDMs from transgenic mice that overexpress the Bax/Bak pore antagonist Bcl2 under control of the H2K promoter (**Supplemental Fig. 4b, c**).

Bcl2-transgenic BMDMs were also shown to induce normal caspase-1 activation and IL-1 β secretion in response to NLRP3-activating stimuli³⁰. Moreover, we found that the kinetics of LeTx-induced TMRM signal decay in Bcl2-overexpressing B6^{NLRP1b+} macrophages was comparable to that of B6^{NLRP1b+} macrophages, consistent with mitochondrial outer membrane permeabilization during pyroptosis occurring independently of the Bax/Bak pore (**Supplemental Fig. 4d, e**). Notably, the kinetics of mitochondrial decay induced by the NLRC4 inflammasome was remarkably consistent with that of LeTx-treated macrophages, both featuring a loss of TMRM signal approximately 20 minutes before plasma membrane rupture (**Fig. 3d, e, Supplemental Figure 3b and Supplemental Movie 8**). Thus, Bcl2-insensitive mitochondrial damage is a conserved feature of pyroptotic cell dismantling.

Lysosome decay precedes pyroptotic plasma membrane rupture

To document the fate of lysosomes during pyroptosis, we stained B6^{NLRP1b+} macrophages with LysoTracker, a fluorescent probe that is highly selective for acidic organelles, and imaged the lysosomal fluorescence over time. Lysosome staining remained relatively stable following LeTx stimulation until LysoTracker fluorescence declined gradually 6-9 minutes before the plasma membrane ruptured (**Fig. 4a, b, Supplemental Figure 5a and Supplemental Movie 9**). These results are in line with a previous report demonstrating that LeTx induced a loss of lysosomal acidity which depended on expression of a LeTx-responsive NLRP1b allele³³. Lysosome decay was

not restricted to LeTx because we also observed a decrease in LysoTracker staining when pyroptosis was induced through the NLRC4 inflammasome (Fig. 4c, d, Supplemental Figure 5b and Supplemental Movie 10). The kinetics of lysosome destabilization in FlaTox-treated macrophages was closely aligned with that of LeTx-intoxicated cells, with LysoTracker signal decay occurring around 6-9 minutes before cells became Sytox Green-positive (Fig. 4c, d). Together, these results demonstrate that lysosome decay is a conserved feature of pyroptosis that precedes plasma membrane damage by about 10 minutes.

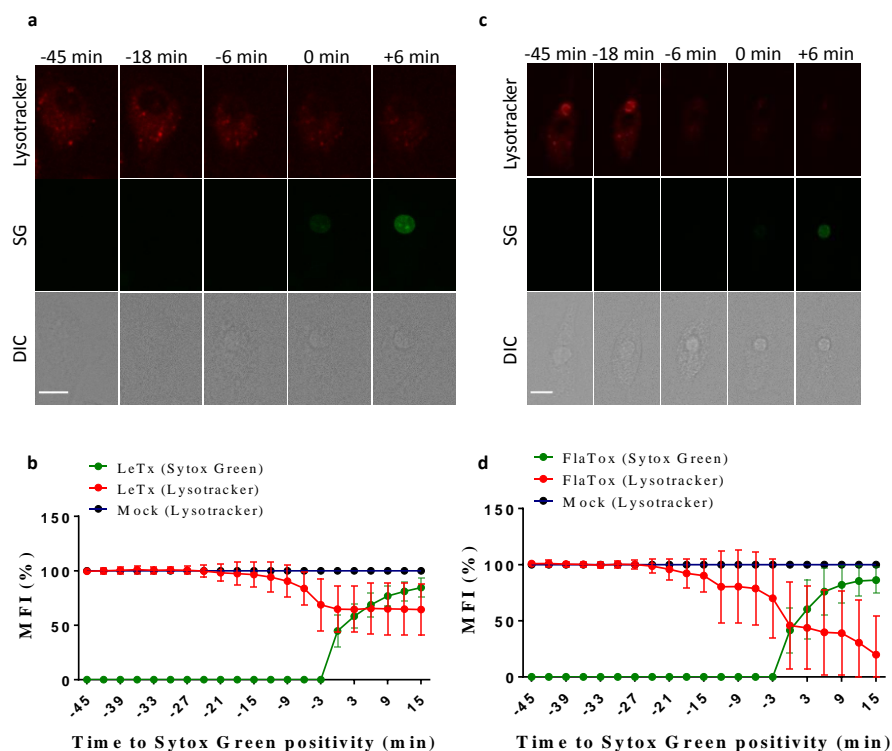


Figure 4. Lysosomes decay prior to pyroptotic cell lysis. a-d, BMDMs preloaded with LysoTracker and stimulated with LeTx (a, b) or FlaTox (c, d) were imaged throughout cell death in culture media containing Sytox Green. Confocal images were taken every 3 minutes. Graphs show the percentage of mean fluorescence intensity (MFI) calculated as described in *Online Methods*, and values represent the mean \pm SD of all individual cells that were imaged in three independent experiments (LeTx, n=27; FlaTox n=19). Single cell plots are shown in Supplemental Figure 5. Fluorescent micrographs show the maximum intensity projection of a representative cell out of at least 19 imaged cells. In all panels time point zero indicates the first detection of Sytox Green. All scale bars, 10 μ m.

Nuclear rounding and condensation are late-stage pyroptotic events

Nuclear condensation and internucleosomal DNA fragmentation are hallmark features of apoptosis. Early studies of pyroptosis suggested that caspase-1 activation in *S. Typhimurium*-infected macrophages triggers a diffuse pattern of DNA fragmentation in the absence of nuclear condensation^{12,19}. In agreement, several reports documented terminal deoxynucleotidyl transferase-mediated dUTP-biotin nick end-label (TUNEL) activity in *S. Typhimurium*-infected macrophages^{12,19,20,34}. However, little is known about the dynamics of early and late-stage nuclear events during pyroptosis.

We stained nuclear DNA of B6^{NLRP1b+} macrophages with Hoechst 33342 (Hoechst) stain, and imaged cells to track the shape and size of the nucleus following LeTx challenge. Pyroptotic macrophages retained an ellipsoid-shaped nucleus until they became Sytox Green-positive (**Fig. 5a and Supplemental Movie 11**). In agreement, examination of sphericity – a measure of how close the shape of an object is to a perfect sphere – using the Imaris microscopy image analysis platform confirmed that the macrophage nucleus rounded up concurrently to the loss of plasma membrane integrity (**Fig. 5b and Supplemental Figure 6a**). From these analyses, we also noted that the nucleus appeared more condensed following plasma membrane rupture.

Consistently, a kinetic analysis of the nucleus' Feret diameter - a measure of an object size along a specified direction – showed that nuclear condensation is a late-stage pyroptotic event that occurs together with plasma membrane rupture (**Fig. 5c and Supplemental Figure 6b**). Similarly, pyroptosis induction in FlaTox-treated

macrophages was accompanied by nuclear rounding and condensation around the time when cells turned Sytox Green-positive (**Fig 5d-f, Supplemental Figure 6c, d and Supplemental Movie 12**). These results demonstrate that nuclear rounding and condensation are late-stage pyroptotic events.

Cell swelling during pyroptosis

Cell volume depends on the osmotic movement of water across the plasma membrane, which is fundamentally regulated by ion and voltage gradients and balanced by active ion transport across membranes³⁵. Dissipation of cellular ionic gradients increases intracellular osmotic pressure, leading to water influx, cell swelling and sudden bursting of the cell membrane. Pyroptotic cells have long been recognized to swell²⁰, but the current model that pyroptosis is induced by the insertion in the plasma membrane of large pre-assembled non-selective GSDMD pores suggests that simultaneous exchange of ions and proteins across the plasma

membrane should maintain osmolarity during pyroptosis³⁶. To gain more insight in this process, we studied the cell volume dynamics of primary macrophages undergoing pyroptotic cell death.

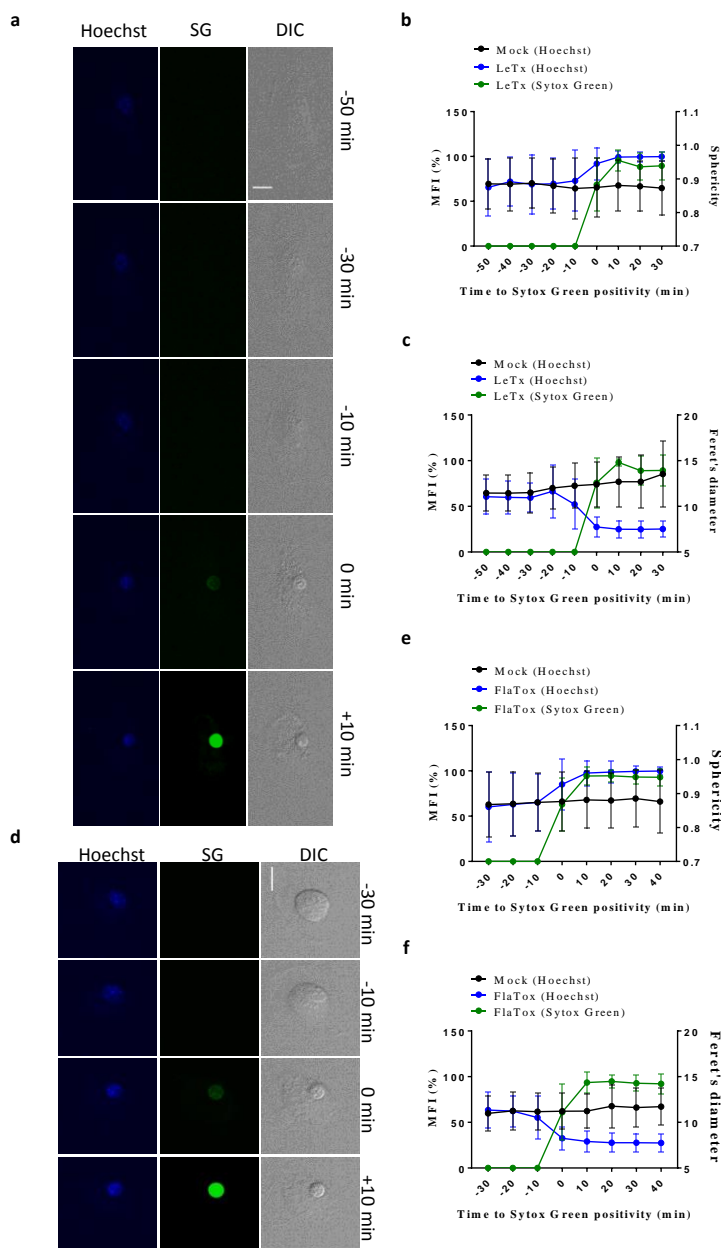


Figure 5. Nuclei round up and condense during pyroptosis. a-e, BMDMs were preloaded with Hoechst dye and stimulated with LeTx (a, b, c) or FlaTox (c, d, e) before imaging in culture media containing Sytox Green. Confocal images were acquired every 10 minutes. Graphs show the percentage of mean fluorescence intensity

(MFI) of Sytox Green and nuclear sphericity or the Feret's diameter based on Hoechst staining, all calculated as described in *Online Methods*. Values represent the mean \pm SD of individual cells imaged in three independent experiments (LeTx: Sphericity n=24, Feret's diameter n= 18; FlaTox: Sphericity n=26, Feret's diameter n=20). Single cell plots are shown in Supplemental Figure 6. Fluorescent micrographs show the maximum intensity projection of a representative cell. In all panels time point zero indicates the first detection of Sytox Green. All scale bars, 10 μ m.

The plasma membrane of B6^{NLRP1b+} macrophages was stained with Cholera Toxin Subunit B (rCTB) coupled to the fluorescent dye Alexa594. Cells were subsequently stimulated with LeTx to induce pyroptosis by the NLRP1b inflammasome, and we recorded single-cell volume changes in real-time until cell lysis was evident by Sytox Green staining. Contrary to mock-treated macrophages, LeTx induced a gradual increase in cell volume starting approximately 13 minutes before cell rupture (**Fig. 6a, b, Supplemental Fig. 7a and Supplemental Movie 13**). The cell volume increased by up to 50% before contracting again after cell lysis (**Fig. 6a, b**). Pyroptosis following FlaTox-induced activation of the NLRC4 inflammasome also was associated with cell swelling before cellular internalization of Sytox Green was observed (**Fig. 6c, d, Supplemental Fig. 7b and Supplemental Movie 14**). Under these conditions, cells swelled up to 30% (**Fig. 6d**). A recent study proposed the pomegranate-derived polyphenolic compound punicalagin to inhibit NLRP3 and AIM2 inflammasome-induced IL-1 β secretion by preventing plasma membrane permeability downstream of inflammasome activation³⁷. Punicalagin inhibited release of LDH in the culture medium and PI internalization by LeTx-intoxicated B6^{NLRP1b+} macrophages (**Supplemental Fig. 8a, f**), but in our hands was associated with upstream blockade of caspase-1 maturation, calcium influx and cell swelling (**Supplemental Fig. 8**). Punicalagin also interfered with FlaTox-induced caspase-1 maturation and LDH release in a dose-dependent manner (**Supplemental Fig. 9a-e**), suggesting that this compound interferes with pyroptosis and IL-1 β secretion by upstream blockage of inflammasome activation. Although these findings undermined punicalagin's further use for probing pyroptosis execution mechanisms, our results demonstrate that osmotic swelling occurs in advance of cell lysis.

Pyroptosis features ion fluxing prior to cell lysis

An early report estimated pyroptotic membrane pores in *S. Typhimurium*-infected macrophages to be 1.1-2.4 nm in diameter based on the size range of osmoprotectant molecules that prevented cell lysis²⁰. More recent studies showed that GSDMD_N

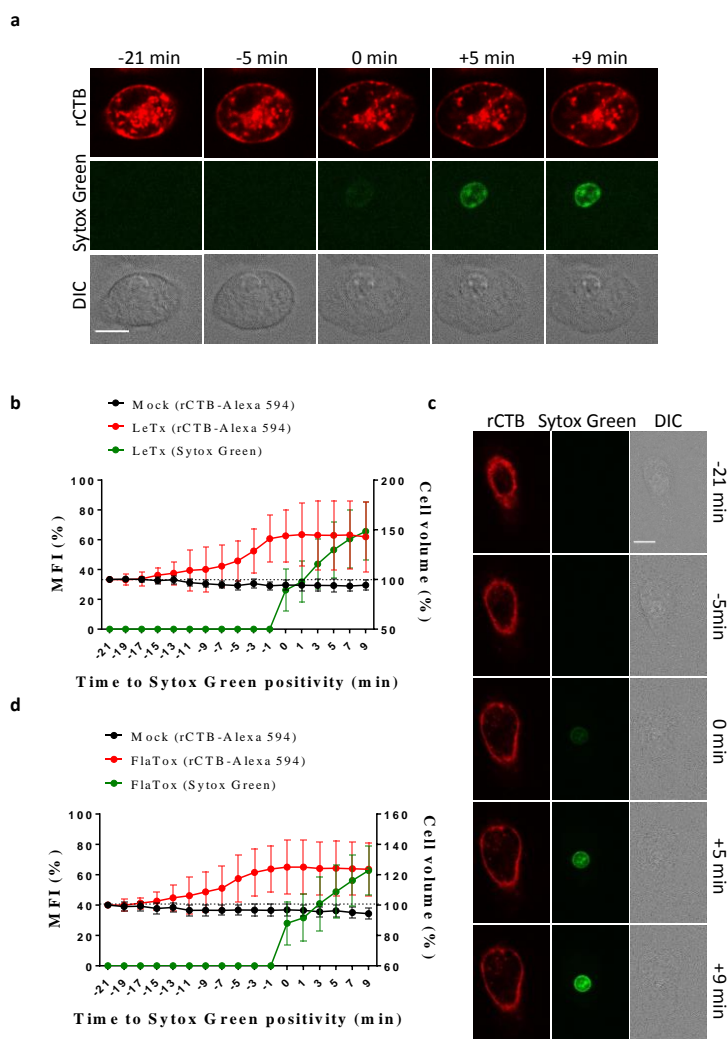


Figure 6. Cell swelling precedes pyroptotic cell rupture. a-d, BMDMs stained with Cholera Toxin subunit B-Alexa 594 (rCTB) were stimulated with LeTx (**a, b**) or FlaTox (**c, d**) and imaged in culture media containing Sytox Green. Confocal images were acquired every 1.5 minutes. Graphs show the percentage of mean fluorescence intensity (MFI) of Sytox Green and cell volume quantifications based on rCTB-Alexa 594 staining, both calculated as described in *Online Methods*. Values represent the mean \pm SD of individual cells imaged in three independent experiments (LeTx, $n=26$; FlaTox $n=16$). Fluorescent micrographs show the maximum intensity projection (Sytox Green) or the single plane (rCTB) of a representative cell. Single cell plots are shown in Supplemental Figure 7. In all panels time point zero indicates the first detection of Sytox Green. All scale bars, 10 μ m.

pores with inner diameters of 10-20 nm formed in liposomes, suggesting that pyroptosis may be associated with assembly of pyroptotic pores that are sufficiently large to theoretically allow passage of IL-1 β , IL-18 and other cytosolic proteins^{6,7,38,39}.

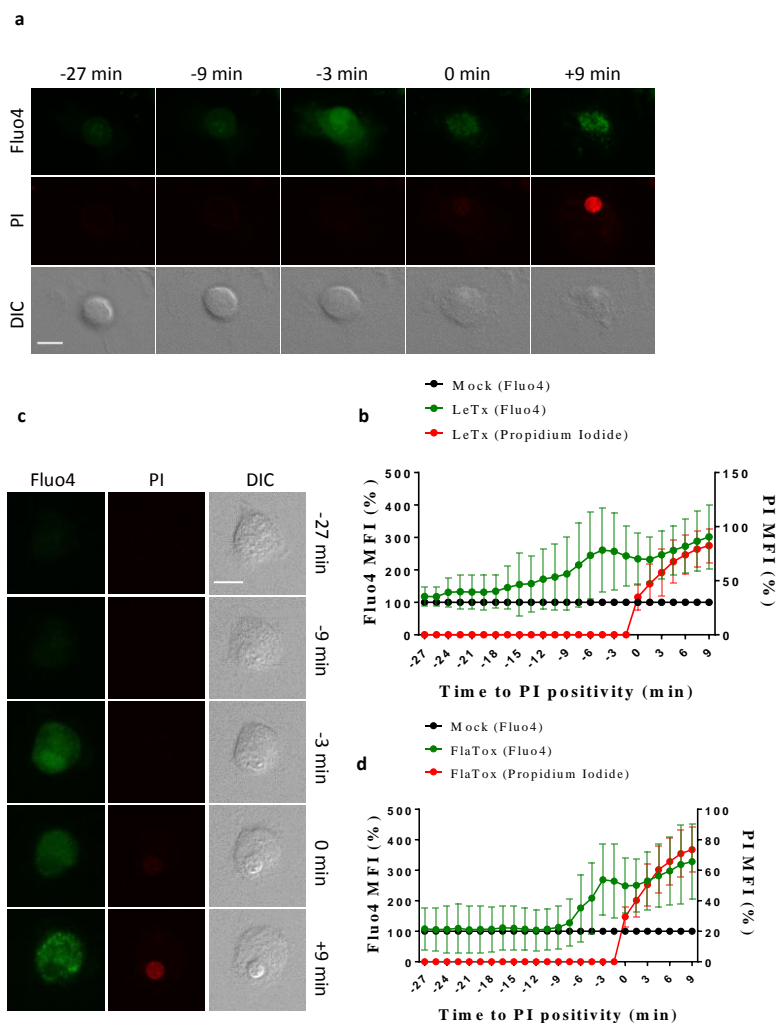


Figure 7. Ca^{2+} influx occurs prior to total membrane permeabilization in pyroptosis. a-d, BMDMs preloaded with the cell-permeant Ca^{2+} indicator Fluo4 were imaged after stimulation with LeTx (a, b) or FlaTox (c, d) in culture media containing PI. Confocal images were acquired every 1.5 minutes. Graphs show the percentage of mean fluorescence intensity (MFI) calculated as described in *Online Methods*, and values represent the mean \pm SD of individual cells imaged in four independent experiments (LeTx, n=24; FlaTox n=23). Single cell plots are shown in Supplemental Figure 10. Fluorescent micrographs show the maximum intensity projection of a representative cell. In all panels time point zero indicates the first detection of PI. All scale bars, 10 μm .

However, GSDMD_N oligomers formed in 293T cells overexpressing GSDMD_N appeared more heterogeneous in size³⁹. Our observation that pyroptotic cells undergo cell volume increase up to 10 minutes before total lysis (Fig. 6), suggested pyroptotic cells have permeability of their plasma membrane prior to total lysis, as marked by Sytox Green. We therefore hypothesized that pyroptosis may proceed in a sequential manner with defined ion-restrictive pores or channels opening prior to

assembly of large, non-selective GSDMD_N pores that lead to catastrophic cell lysis. To probe the size dynamics of pyroptotic pores under physiological conditions, LeTx-stimulated B6^{NLRP1b+} macrophages were pre-loaded with Fluo4, a cell-permeant fluorogenic probe that fluoresces strongly upon Ca²⁺ binding, and tracked for internalization of Ca²⁺ (M_w = 40 Da; van der waals radius = 0,23 nm) relative to uptake of the DNA intercalating agent PI (M_w = 668 Da). In agreement with our hypothesis, we observed an increase in Fluo4 staining that preceded PI incorporation by approximately 12-15 minutes (**Fig. 7a, b, Supplemental Fig. 10a and Supplemental Movie 15**). Echoing these results, induction of pyroptosis through the NLRC4 inflammasome in FlaTox-treated BMDMs also was associated with Ca²⁺ entry prior to PI-positivity. Under these conditions, an increased Fluo4 signal was noted 6-9 minutes before cells became PI-positive (**Fig. 7c, d, Supplemental Fig. 10b and Supplemental Movie 16**), in line with FlaTox-induced cell volume increase being slightly delayed relative to LeTx-treated cells (**Fig. 6**). Notably, internalization of the DNA-intercalating agent ethidium bromide (M_w = 394 Da) occurred only slightly ahead of Sytox Green (M_w = 609 Da) uptake (**Supplemental Fig. 11 and Supplemental Movie 17**), suggesting that pyroptotic ion fluxing was mediated by a channel or pore that excludes molecules sized 400 Da and more, and that DNA-intercalating dyes enter pyroptotic cells sequentially according to their molecular weight.

GSDMD mediates early ionic flux and mitochondrial decay in pyroptotic cells

GSDMD_N pores were recently reported to have inner diameters of 10-20 nm when assembled *in vitro* in liposomes^{6,7,38,39}. However, our observations demonstrate that pyroptotic Ca²⁺ influx precedes plasma membrane rupture and involves a pore or channel that excludes entry of DNA-intercalating agents with M_w of 394-609 Da. We hypothesized that early ionic flux and cell swelling during pyroptosis is mediated by GSDMD pores of lower stoichiometry while the larger structures that form in liposomes may represent a terminal steady-state phase of GSDMD pore assembly associated with catastrophic cell lysis. Empirical analysis of the hypothesis that GSDMD pores mediated early pyroptotic Ca²⁺ influx was vitiated by the observation that LeTx and FlaTox treatment of *GSDMD*^{-/-} macrophages induced apoptosis with kinetics matching those of pyroptosis induction in GSDMD-sufficient B6^{NLRP1b+} and C57BL/6J (B6) macrophages, respectively (**Supplemental Fig. 12a, b**). Apoptosis has previously also been documented in *GSDMD*^{-/-} macrophages following stimulation

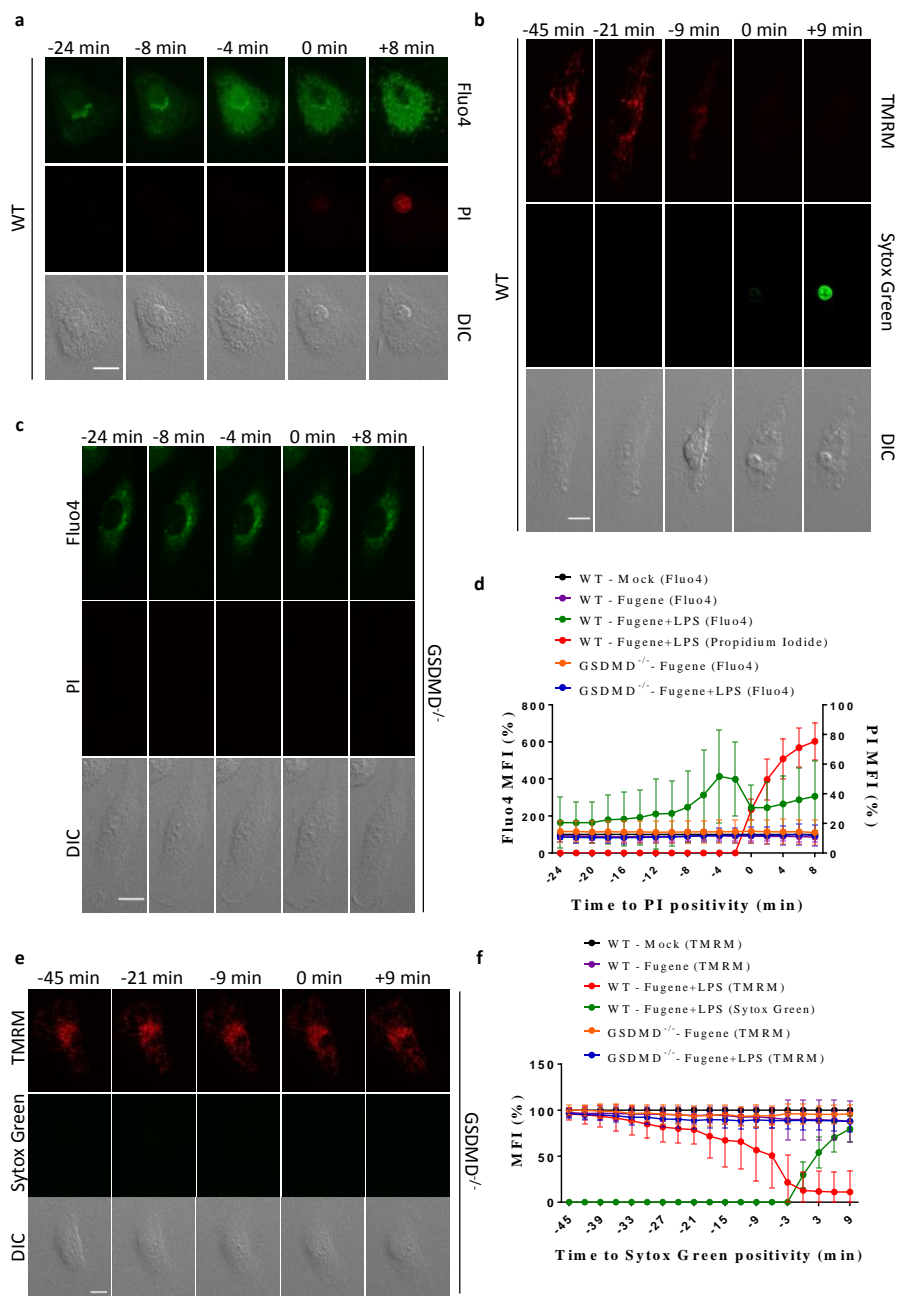


Figure 8. GSDMD-deficiency prevents LPS transfection-induced early Ca^{2+} influx and mitochondrial decay. **a, c**, Pam3csk4-primed BMDMs of the indicated genotypes were preloaded with the cell-permeant Ca^{2+} indicator Fluo4 and imaged after transfection with LPS (Fugene+LPS), treated with Fugene alone, or “mock”-treated in culture media containing PI. Confocal images were acquired every 2 minutes. Fluorescent micrographs show the maximum intensity projection of a representative cell. **b, e**, BMDMs of the indicated genotypes were preloaded with TMRM and imaged after transfection with LPS (Fugene+LPS), treated with

Fugene alone, or “mock”-treated in culture media containing Sytox Green. Confocal images were acquired every 3 minutes. Fluorescent micrographs show the maximum intensity projection of a representative cell. **d, f**, Graphs show the percentage of mean fluorescence intensity (MFI) calculated as described in *Online Methods*, and values represent the mean \pm SD of individual cells imaged in three or four independent experiments (Fluo4: WT n=18, GSDMD^{-/-} n=28; TMRM: WT n=18, GSDMD^{-/-} n=29). Single cell plots are shown in Supplemental Figure 14. In all panels time point zero indicates the first detection of PI/Sytox Green. All scale bars, 10 μ m.

with LPS + nigericin and upon infection with *S. Typhimurium*⁴⁰. Therefore, the kinetics of apoptosis induction in GSDMD^{-/-} macrophages that align with pyroptosis timelines impeded examination of the role of GSDMD pores in early pyroptotic ion fluxing following treatment with the above canonical inflammasome agonists.

LPS transfection is a non-canonical inflammasome stimulus that triggers caspase-11- and GSDMD-mediated pyroptosis^{5,8}. LPS transfection-induced pyroptosis was associated with a robust Fluo4 signal in wildtype macrophages, indicating that early Ca²⁺ influx is a shared commonality of pyroptosis induction by the non-canonical and canonical inflammasome pathways (**Fig. 8a**). LPS transfection also resulted in a loss of TMRM signal and mitochondrial decay prior to cell lysis (**Fig. 8b**), akin to our observations with the canonical inflammasome agonists LeTx and FlaTox (**Fig. 3**). Having established that pyroptosis induction by the non-canonical inflammasome shares Ca²⁺ influx and mitochondrial decay as early features with pyroptosis induced through canonical inflammasome pathways, we next addressed the role of GSDMD in these processes. Contrary to canonical inflammasome agonists (LeTx and FlaTox) that triggered fast induction of apoptosis in GSDMD^{-/-} macrophages (**Supplemental Fig. 12**), incorporation of PI by LPS-transfected GSDMD^{-/-} macrophages was delayed by approximately 5 hours relative to pyroptotic wildtype macrophages (**Supplemental Fig. 13**), thus providing a suitable time window for examining the potential role of GSDMD in pyroptosis-associated early Ca²⁺ influx and mitochondrial decay. Notably, GSDMD-deficiency not only protected against pyroptotic plasma membrane rupture during the timeframe of imaging, but also abolished the early Ca²⁺ influx seen in LPS-transfected wildtype macrophages (**Fig. 8a, c, d, Supplemental Fig. 14a and Supplemental Movie 18**). LPS-transfected GSDMD^{-/-} macrophages also maintained their mitochondrial polarization during the imaging timeframe, unlike LPS-transfected wildtype macrophages that lost their mitochondrial membrane potential during pyroptosis induction (**Fig. 8b, e, f, Supplemental Fig. 14b and Supplemental Movie 19**). To conclude, we show that both early Ca²⁺ influx and mitochondrial decay are conserved mechanisms of

pyroptotic cell demise that are mediated by GSDMD and precede plasma membrane rupture.

Pyroptosis causes non-selective extracellular release of cytosolic and organellar proteins

The extracellular release of host-derived DAMPs that are normally kept in the intracellular milieu is considered a major mechanism by which necrotic cell death promotes inflammation. In addition to IL1 β and IL18, pyroptotic cells are known to release the cytosolic protein LDH – the enzymatic activity of which in culture media is often used as a surrogate marker of plasma membrane rupture – and the nuclear DAMPs HMGB1 and IL1 α ^{4,10}. Pyroptotic cells were recently shown to contain organelles and microbial pathogens inside the ‘pore-induced intracellular trap’⁹, but whether proteins that reside in membrane-bound organelles are spilled extracellularly is unclear. To address this question, we stimulated macrophages with LeTx or FlaTox for the indicated durations (**Fig. 9a, b**) before the extracellular medium and total cell lysates were analysed by Western blotting for a suite of organellar proteins. In parallel, the extracellular medium was analysed for LDH

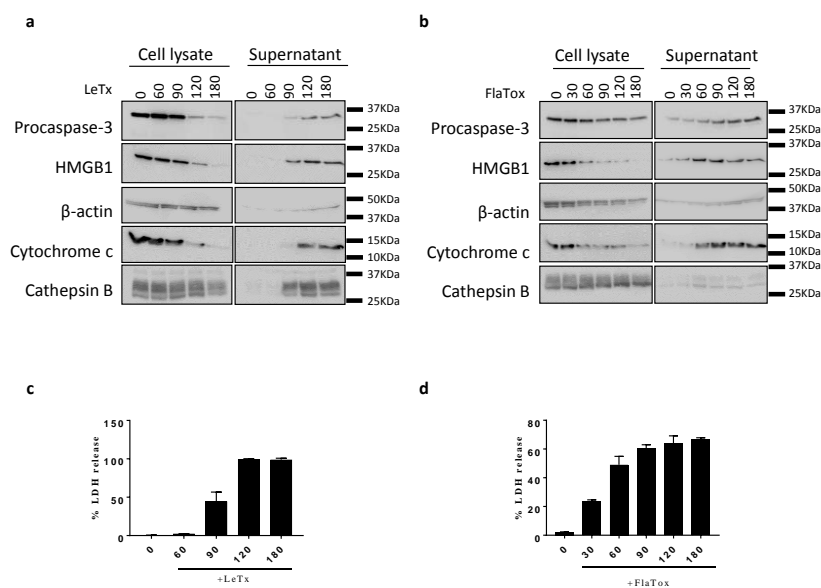


Figure 9. Pyroptosis triggers non-selective release of cytosolic and organellar proteins. Culture supernatants and cell lysates of BMDMs stimulated with LeTx (**a**) or FlaTox (**b**) for the depicted durations were analysed by Western blotting for the indicated proteins. (**c**, **d**) Culture supernatants used in (**a**, **b**) were assayed for LDH activity. Data are representative of three independent experiments.

activity, near-maximal values of which were reached 120 and 90 minutes post-treatment for LeTx- and FlaTox-stimulated cells, respectively (**Fig. 9c, d**). The

extracellular levels of procaspase-3 raised concurrent herewith, whereas the cellular pool of this cytosolic protein diminished accordingly over time (Fig. 9c, d). β -actin and the nuclear DAMP HMGB1 were also retrieved in supernatants of both LeTx- and FlaTox-stimulated cells. Moreover, mitochondrial cytochrome c and lysosomal cathepsin B were spilled with comparable kinetics in the extracellular space (Fig. 9a, b), consistent with our observation that both mitochondria and lysosomes are damaged during pyroptosis. Together, these results highlight that a broad set of proteins and potential DAMPs originating from damaged organelles and the cytosol alike are targeted for non-selective extracellular release during pyroptosis.

3.1.4. Discussion

The requirement for the proteolytic activity of inflammatory caspases fundamentally distinguishes pyroptosis from apoptosis, necroptosis and accidental necrosis. It has long been recognized that the induction of pyroptosis in parallel to caspase-1-mediated maturation of IL-1 β and IL-18 may constitute a powerful defense mechanism of the host against microbial pathogens¹⁵. Pyroptosis is now thought to not only remove the replicative niche of intracellular pathogens, but was also shown to promote the passive release of IL-1 β , IL-18 and DAMP molecules that attract neutrophils and contribute to a pro-inflammatory environment that contribute to pathogen clearance^{5,11,40}. In addition, engulfed bacteria were recently demonstrated to get trapped in the pyroptotic cell corpse, which has been coined the 'pyroptotic intracellular trap', as a mechanism to counter pathogen spreading and to facilitate efferocytosis by infiltrating neutrophils⁹.

Despite its evident role in anti-microbial host defense and the recent identification of GSDMD as a key pyroptosis effector molecule, the distinguishing features and subcellular dynamics of pyroptotic cells have remained largely unmapped. Comparing necroptotic and pyroptotic macrophage cell death, we found that contrary to necroptosis, cells that undergo pyroptosis remain attached to the adherent surface throughout the entire cell death process. This suggests that cell adhesion molecules such as integrins, selectins, syndecans and cadherins may be disrupted during necroptosis, but not in pyroptosis. It would also be interesting in this respect to investigate whether this differential feature of pyroptotic and necroptotic cell death leads to distinct consequences to the surrounding tissue in an *in vivo* context. We also showed that myosin-II and ROCK-I activity are dispensable for pyroptotic and necroptotic blebbing, whereas they are known to be essential for

blebbing during apoptosis. Future studies should explore whether pyroptotic and necroptotic blebbing are passively induced by osmotic pressure, or actively regulated processes that involve specific enzymes.

Our single-cell analysis of pyroptosis kinetics revealed that pyroptosis is characterized by ionic fluxing and cell swelling that is accompanied by mitochondrial depolarization and lysosome leakage well before cells ultimately lost their plasma membrane integrity concomitant with evidence of late-stage nuclear condensation. We thus observed a conserved sequence of subcellular events that preceded plasma membrane rupture by up to 20 minutes, challenging the current model that pyroptosis is induced by the insertion in the plasma membrane of pre-assembled large non-selective GSDMD pores with inner diameters of 10-20 nm. Pores of this size would likely maintain osmolarity by allowing the simultaneous passage of ions, small molecules and proteins, and thus would not be able to account for the early cell swelling we observed. Important in this regard is our demonstration that Ca^{2+} influx could precede the uptake of cell-impermeant fluorescent dye molecules (sized 400 Da or more) and plasma membrane rupture by 12-15 minutes, arguing that pyroptosis is executed by an increasing permeability of the plasma membrane and that formation of large non-selective GSDMD pores is a late-stage pyroptotic event that is associated with the breakdown of the plasma membrane. Consistently, an early estimate of the pyroptotic membrane pore diameter in *S. Typhimurium*-infected macrophages suggested it to be 1.1-2.4 nm in diameter, although the identity of such pores have not been defined²⁰. Considering our demonstration that GSDMD is required for early Ca^{2+} influx and mitochondrial membrane depolarization of LPS-transfected macrophages, it is tempting to speculate that GSDMD_N monomers insert in membranes individually or as small oligomers that further assemble into higher order oligomers, reminiscent of the mechanism used by Bax in the mitochondrial outer membrane and cation-selective actinoporin pores⁴¹. Such 'non-concerted' membrane insertion model for GSDMD_N pore assembly would account for both early ion-selective fluxing and late-stage non-selective GSDMD_N pore formation. Moreover, GSDMD_N oligomers formed in GSDMD_N-overexpressing 293T cells were reported to be heterogeneous in size³⁹.

We further observed that pyroptotic plasma membrane rupture is kinetically closely associated with Annexin-V-positivity. Considering that phosphatidylserine is an 'eat-me' signal for phagocytes, it will be interesting to determine the timeframe by which extracellular release of IL1 β and IL18 precedes efferocytosis of the pyroptotic corpse,

and to study the role of PS in this process. We also showed that pyroptosis is associated with an apparently non-discriminatory extracellular spilling of proteins from both the cytosolic and organellar compartments. The latter suggests that enzymes and DAMPs that normally reside in membrane-bound organelles such as the nucleus, mitochondria and lysosomes might potentially exert specific roles and contribute to an inflammatory milieu following their release from pyroptotic cells. In conclusion, this study charted a chronological sequence of subcellular events that define pyroptotic cell death at the single-cell level, and provides a dynamic framework for understanding cellular changes that occur during pyroptosis.

3.1.5. Methods

Mice. B6^{NLRP1b⁺ 22}, H2K-Bcl2^{Tg 42} and GSDMD^{-/- 5} mice have been reported. C57BL/6J mice were originally bought from the Jackson Laboratories and bred in-house. Mice were housed in individually ventilated cages and kept under pathogen-free conditions at the animal facilities of Ghent University. All animal experiments were conducted with permission of the ethics committee on laboratory animal welfare of Ghent University.

Reagents. Recombinant expression and purification of LFn-FlaA was performed as described²⁸. *B. anthracis* protective antigen (PA) and lethal factor (LF) were acquired from List Biologicals. Tetramethylrhodamine (TMRM, T668), LysoTracker (L7528), Sytox Green (S7020), Mitotracker (M7512), Fluo4 (F14217), Pluronic F-127 (P6867), Hoechst 33342 Trihydrochloride Trihydrate (H1399), Propidium Iodide (P3566) and Cholera Toxin Subunit B (CTB) coupled to Alexa 594 (C22842) or 647 (C34778) were purchased from Thermo Scientific. Propidium Iodide (PI) solution (556463) and Annexin-V-FITC (556419) were from BD Biosciences. The antibodies used in the study were anti-caspase-1 (AG-20B-0042-C10, Adipogen), anti-Cathepsin B (31718S, Cell Signaling Technology), anti-Cytochrome c (11940S, Cell Signaling Technology), anti-HMGB1 (ab18256, Abcam), anti-caspase-3 (9662S, Cell Signaling Technology), anti- β -Actin-HRP (sc-47778, Santa Cruz Biotechnology), anti-BID (AF860, R&D systems). HRP-conjugated secondary antibodies were acquired from Jackson ImmunoResearch Laboratories and enhanced chemiluminescence solution was from Thermo Scientific. Punicalagin (P0023) was from Sigma Aldrich and the CytoTox 96 Non-Radioactive Cytotoxicity Assay (G1780) and FugeneHD Transfection Reagent were purchased from Promega. Y27632 and (-)-blebbistatin were acquired from

Selleckchem. Pam3-csk4 (tlrl-pms) and LPS-SM (tlrl-smlps) were acquired from Invivogen.

Macrophage differentiation and stimulation. Macrophages were differentiated by culturing bone marrow progenitor cells in Iscove's modified Dulbecco's medium (IMDM; Lonza) containing 10% (v/v) heat-inactivated FBS, 30% (v/v) L929 cell-conditioned medium, 1% (v/v) non-essential amino acids (Lonza), 100 U/ml penicillin and 100 mg/ml streptomycin at 37 °C in a humidified atmosphere containing 5% CO₂ for six days. Bone marrow-derived macrophages (BMDMs) were then seeded into 8-well μ -slides (Ibidi) or in multiple wells plates as needed, in IMDM containing 10% FBS, 1% non-essential amino acids and antibiotics. For NLRP1b inflammasome activation, cells were stimulated with LeTx (1 μ g/ml PA combined with 0,5 or 1 μ g/ml LF). The NLRC4 inflammasome was activated in BMDMs treated with FlaTox (1 μ g/ml PA combined with 1 μ g/ml LFn-FlaA). Necroptosis was induced with mTNF α (20 ng/ml), BV6 (2 μ M) and zVAD-fmk (50 μ M). In some experiments, BMDMs were treated with Y27632 (10 μ M), (-)-blebbistatin (10 μ M) or punicalagin (25 or 50 μ M) before inflammasome stimuli. For the non-canonical inflammasome activation, BMDMs were primed with Pam3-csk4 (1 μ g/ml) for 6h in Opti-MEM medium. Then, cells were either mock treated or stimulated with 0,25% (v/v) Fugene with or without LPS (2 μ g/ml).

Live cell imaging. BMDMs were incubated with TMRM (400 nM), LysoTracker (50 nM), Mitotracker (25 nM) and Hoechst (20 ng/ml) for 30 min at 37°C, after which they were washed to fresh culture media. For plasma membrane labelling, cells were incubated with CTB Alexa 594 or CTB Alexa 647 (10 μ g/ml) for 30 min at 4°C and then washed with fresh media. In other experiments, Fluo4 (5 μ M) was mixed in a 1:1 (v/v) ratio with Pluronic F-127 (20% w/v in DMSO) before adding the mixture to cells in HBSS. Cells were incubated with Fluo4 solution for 30 min at room temperature and washed to fresh media containing Fluo4 (2.5 μ M). Imaging was performed in culture media containing Sytox Green (10 nM) or PI (0.5 μ g/ml).

Image acquisition and processing. In each experiment, 2-3 fields/condition were selected for time-lapse imaging using an observer Z.1 spinning disk microscope (Zeiss, Zaventem, Belgium) equipped with a Yokogawa disk CSU-X1. Cells were incubated in a chamber with a 5% CO₂ atmosphere at 37°C throughout the experiment. DIC and fluorescence images were acquired at regular intervals ranging from 1 to 10 minutes apart, with the use of a pln Apo 40x/1.4 oil DIC III objective and a Rolera em-c2 camera. Image acquisition started at the moment of stimulation with

LeTx, FlaTox and TBz; and after 2h of LPS transfection for pyroptosis induction by the non-canonical inflammasome pathway. Cells were imaged at least until they became positive for Sytox Green or PI. Z-stacks consisted of 5 or 8 planes with a Z-interval of 2 μ m. Mock-treated cells were imaged in parallel to ensure that imaging and staining procedures were not cytotoxic.

Representative images and movies were extracted and edited in Fiji software. Image quantifications were performed on the 3D images through voxel-based quantification of the mean fluorescence intensity (MFI), volume and sphericity in Imaris x64 7.7.2 (Bitplane) software package. Obtained fluorescence data were normalized for bleaching against the corresponding time points of mock-treated cells that were imaged in parallel. Cell volume and MFI percentages were plotted relative to each cell's initial value, except for Annexin-V, Sytox Green and PI percentages, which were plotted against the maximum noted values. The Feret diameter of Hoechst-stained nuclei was determined for each Z-slice using Fiji software, and the highest value obtained for each time point was retained and shown. All graph data on main figures depict the mean of multiple cells that were quantified in each independent experiment \pm SD. All graph data on supplementary figures depict the individual values obtained for each cell after normalization. The time indication in presented graphs and image panels is relative to the moment when cells became positive for Sytox Green or PI. Time zero in movie stills refers to the start of imaging.

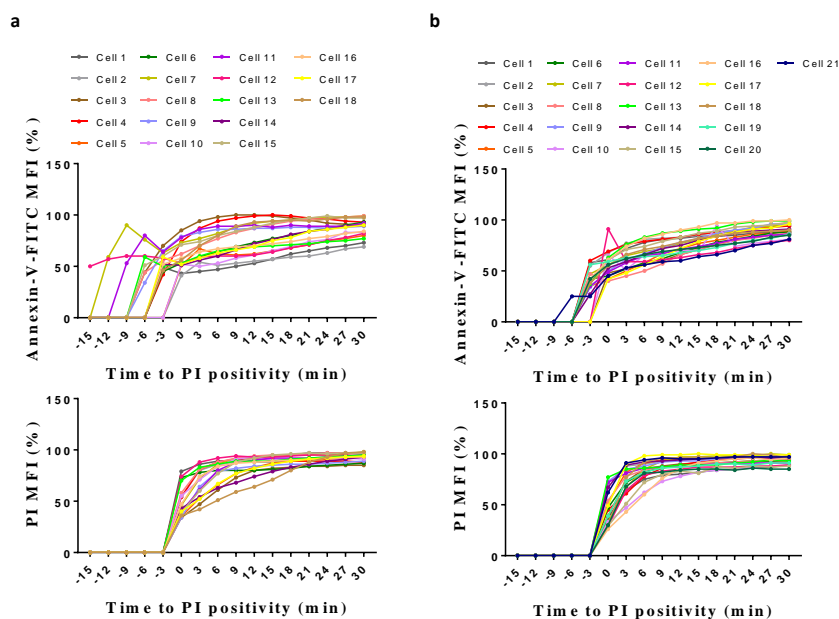
Western Blotting. Unless otherwise stated, cell lysates and culture supernatants were combined for Western blotting. Protein samples were denatured in Laemmli buffer, boiled at 95 °C for 10 min, separated by SDS-PAGE and transferred to PVDF membranes. PBS supplemented with 0.05% Tween-20 (v/v) and 3% nonfat dry milk (w/v) was used for blocking and washing of membranes. Immunoblots were incubated overnight with primary antibodies against cathepsin B and cytochrome c (1:1000 in TBS, 0,1% Tween-20, 5% BSA), HMGB1 or caspase-3 (1:1000 in PBS, 0,1% Tween-20, 5% nonfat dry milk), caspase-1 or BID (1:1000 in PBS, 0,05% Tween-20, 3% nonfat dry milk), followed by HRP-conjugated secondary antibodies raised against mouse, goat or rabbit (1:5000). The β -Actin-HRP antibody was used at 1:5000 in PBS 0,1% Tween-20, 5% nonfat dry milk. All proteins were detected by enhanced chemiluminescence.

Kinetic of LDH release. The supernatant of cells stimulated at various time points was collected and centrifuged at 300xg for 5min to remove cellular debris. LDH measurement was performed with the CytoTox 96 Non-Radioactive Cytotoxicity

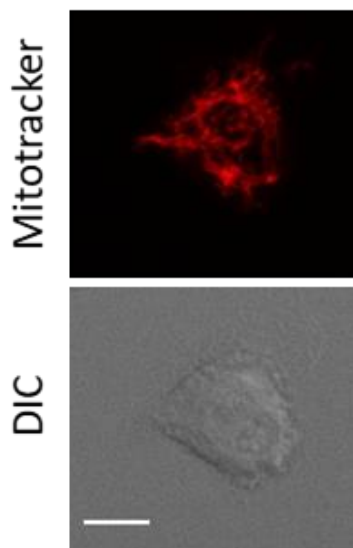
Assay kit according to the manufacturers' instructions, in samples diluted 1:5 in PBS. Data was plotted considering the O.D. value obtained in a well treated with Triton-x100 as 100%.

Cell permeabilization kinetics (Incucyte). BMDMs were plated and stimulated in a 96-well plate in media containing PI (0,1 ug/ml) and data was acquired with a 10x objective using the Incucyte Zoom system (Essen BioScience) in a CO₂ and temperature controlled environment. Each condition was run in (technical) duplicates. The number of fluorescent objects was counted with Incucyte ZOOM (Essen BioScience) software and was plotted considering as 100% the highest value obtained in a well treated with Triton-x100.

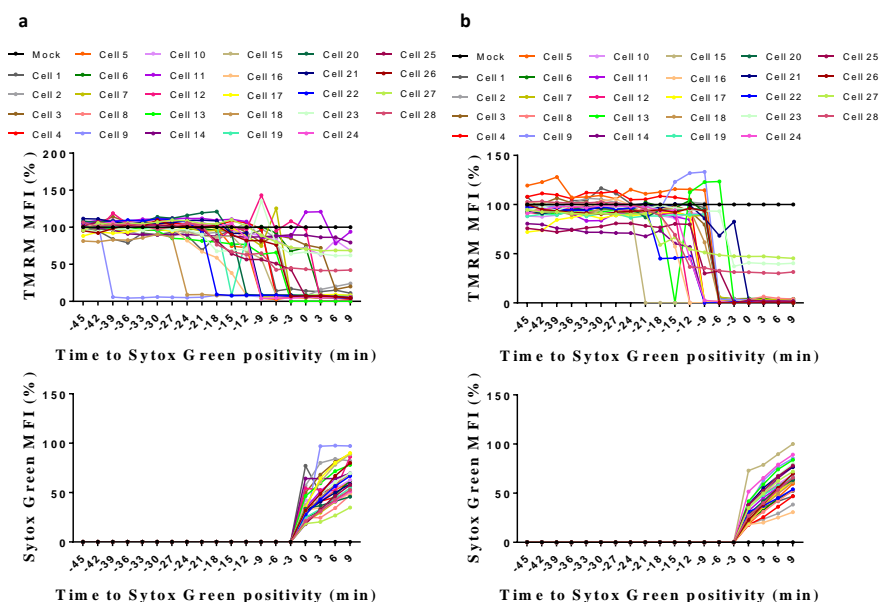
3.1.6. Supplementary data



Supplemental Figure 1. PS exposure during pyroptosis. a, b B6^{Nlrp1b} BMDMs were stimulated with LeTx (a) or FlaTox (b) and imaged in culture media containing Annexin-V-FITC and PI. Confocal images were acquired every 3 minutes. Graphs show the percentage of mean fluorescence intensity (MFI) of single cells (LeTx n=18; FlaTox n=21), calculated as described in *Methods*, of Annexin-V (upper panel) or PI (lower panel) signals. In all panels time point zero indicates the first detection of PI. Relates to Figure 2b, d.

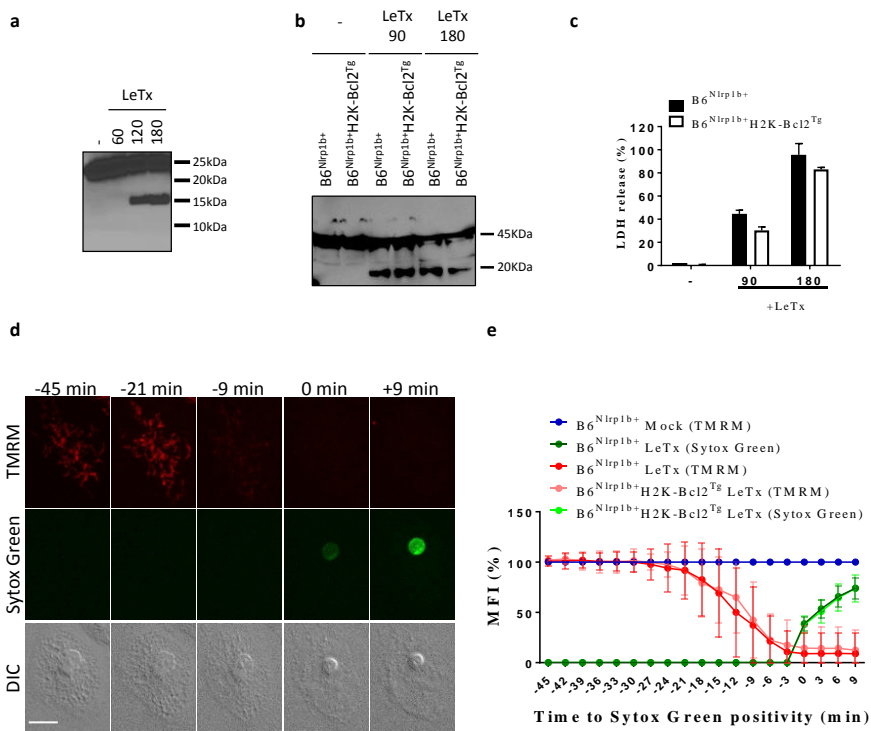


Supplemental Figure 2. Mitochondrial morphology of mock-treated BMDMs. B6^{Nlrp1b} BMDMs preloaded with Mitotracker Red CMXRos were imaged in culture media containing Sytox Green (n=50). A single plane of a representative cell is shown. Scale bars, 10 μ m.

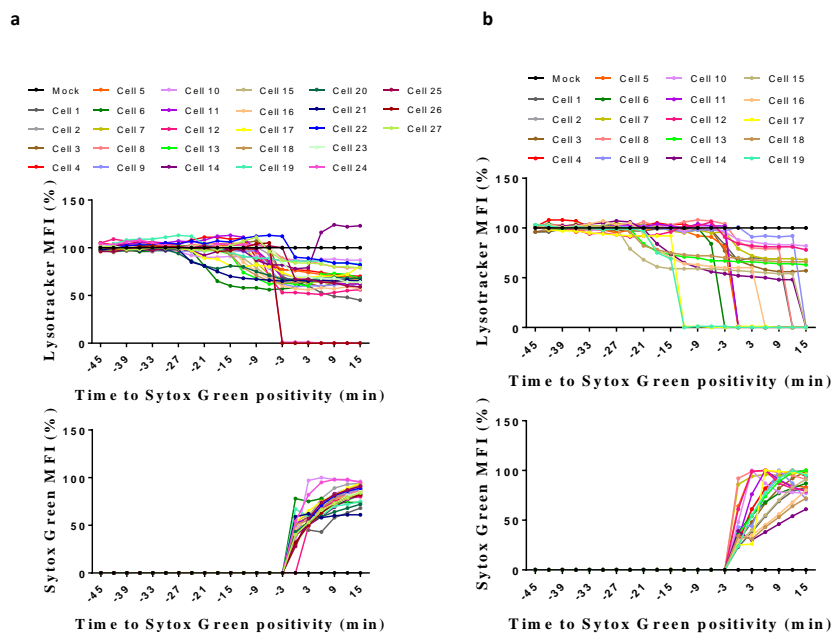


Supplemental Figure 3. Mitochondrial damage during pyroptosis. a, b B6^{Nlrp1b} BMDMs were preloaded with TMRM and stimulated with either LeTx (a) or FlaTox (b) and imaged in culture media containing Sytox Green. Confocal images were acquired every 3 minutes. Graphs show the percentage of mean fluorescence intensity (MFI) of single cells (LeTx, n=28; FlaTox n=28), calculated as described in *Methods*, of TMRM (upper panel) or Sytox Green (lower panel) signals. “Mock” lines represent the average of the values obtained in

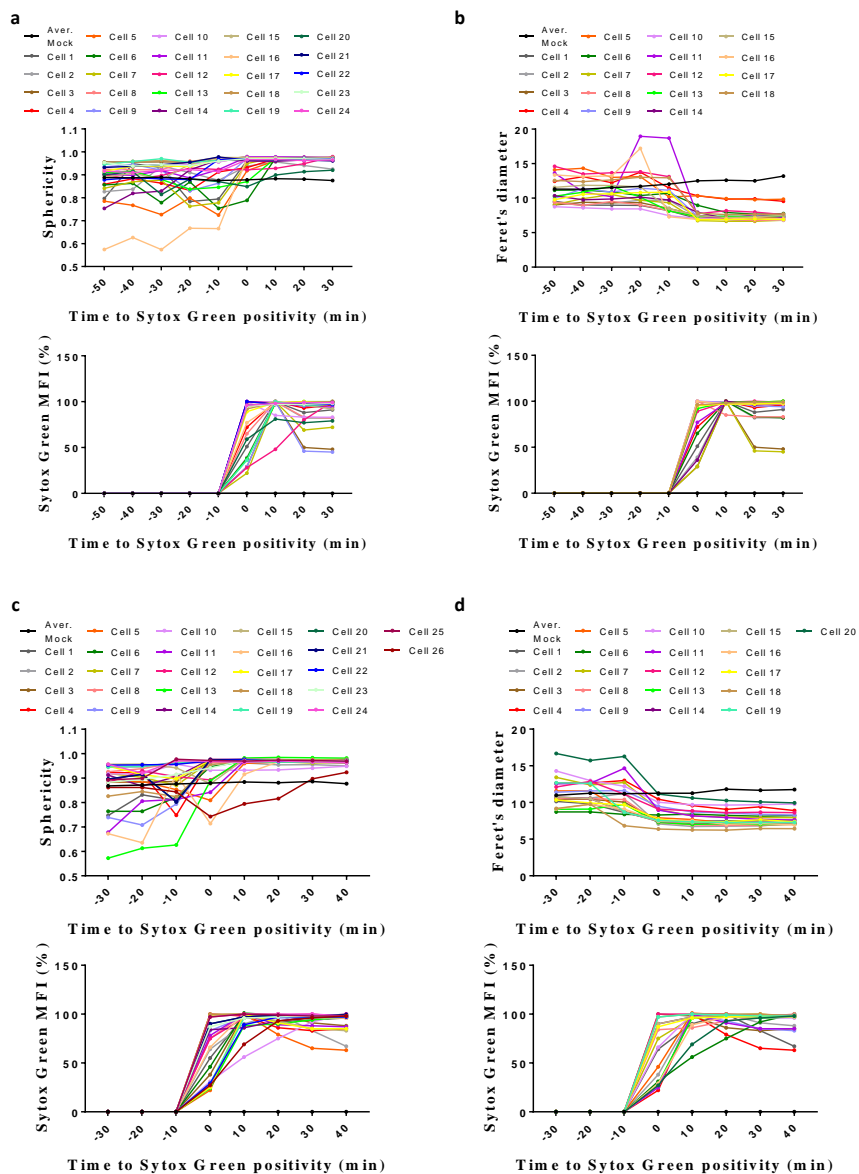
unstimulated cells, imaged in parallel. In all panels time point zero indicates the first detection of Sytox Green. Relates to Figure 3c, e.



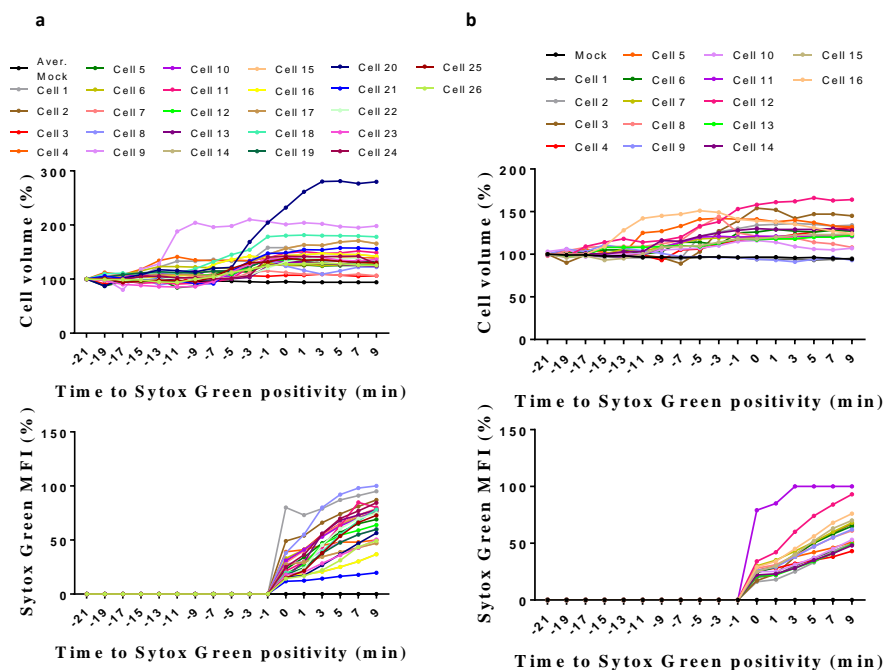
Supplemental Figure 4. Bax/Bak pores are dispensable for pyroptosis-associated mitochondrial damage. Protein lysates of B6^{Nlrp1b+} BMDMs stimulated with LeTx for 60, 120 or 180 minutes were analysed by Western blotting for BID. **a-c**, Protein lysate of B6^{Nlrp1b+} and B6^{Nlrp1b+}H2K-Bcl2^{Tg} BMDMs that have been stimulated with LeTx for 90 or 180 minutes were assayed by Western blotting for caspase-1 maturation (**b**), and their culture supernatants were assayed for LDH activity (**c**). **d, e** B6^{Nlrp1b+} and B6^{Nlrp1b+}H2K-Bcl2^{Tg} BMDMs were loaded with TMRM and stimulated with LeTx in culture media containing Sytox Green. Confocal images were acquired every 3 minutes. Graphs show the percentage of mean fluorescence intensity (MFI) calculated as described in *Methods*, and values represent the mean \pm SD of individual cells imaged in 3 independent experiments (B6^{Nlrp1b+} n=26; B6^{Nlrp1b+}H2K-Bcl2^{Tg} n=21). Fluorescent micrographs show the maximum intensity projection of a representative cell. In panels **d, e** time point zero indicates the first detection of Sytox Green. All scale bars, 10 <



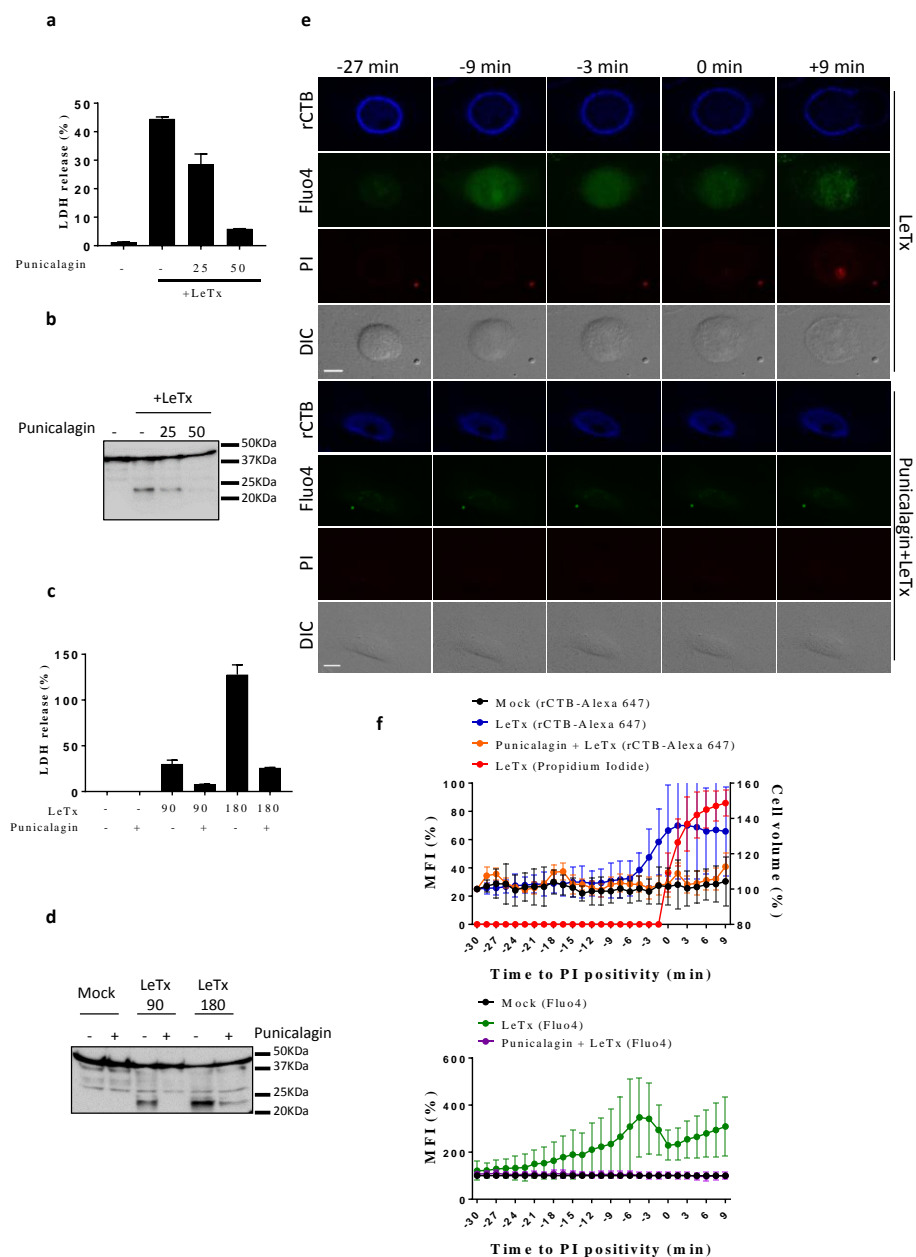
Supplemental Figure 5. Lysosomes decay prior to pyroptotic cell lysis. **a, b** B6^{Nlrp1b+} or B6 BMDMs preloaded with Lysotracker and stimulated with LeTx (**a**) or FlaTox (**b**), respectively, were imaged throughout cell death in culture media containing Sytox Green. Confocal images were taken every 3 minutes. Graphs show the percentage of mean fluorescence intensity (MFI) of single cells (LeTx, n=27; FlaTox n=19), calculated as described in *Methods*, of Lysotracker (upper panel) or Sytox Green (lower panel) signals. “Mock” lines represent the average of the values obtained in unstimulated cells, imaged in parallel. In all panels time point zero indicates the first detection of Sytox Green. Relates to Figure 4b, d.



Supplemental Figure 6. Nuclei round up and condense during pyroptosis. a-d B6^{Nlrp1b+} BMDMs were preloaded with Hoechst dye and stimulated with LeTx (a, b) or FlaTox (c, d) before imaging in culture media containing Sytox Green. Confocal images were acquired every 10 minutes. Graphs show values for nuclear sphericity (a, c, upper panels) or Feret's diameter (b, d, upper panels) based on Hoechst staining or the percentage of mean fluorescence intensity (MFI) of Sytox Green signal (lower panels) of single cells (LeTx: Sphericity n=24, Feret's diameter n= 18; FlaTox: Sphericity n=26, Feret's diameter n=20), calculated as described in *Methods*. "Mock" lines represent the average of the values obtained in unstimulated cells, imaged in parallel. In all panels time point zero indicates the first detection of Sytox Green. Relates to Figure 5b, c, d, e.

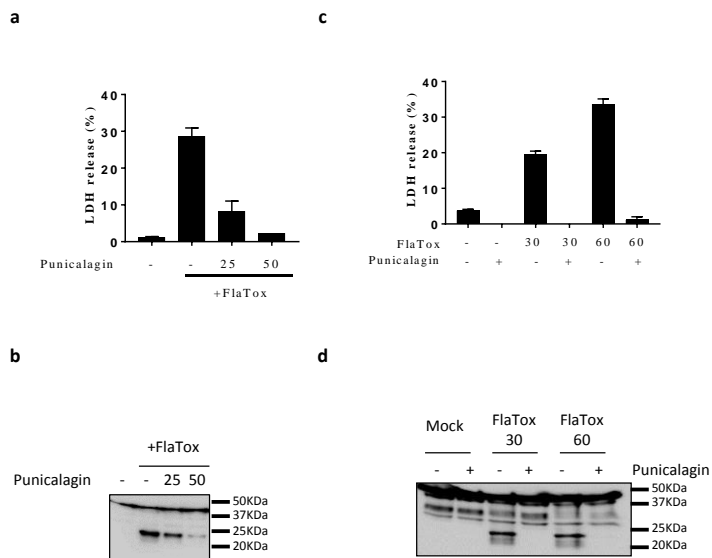


Supplemental Figure 7. Cell swelling precedes pyroptotic cell rupture. **a, b** B6^{Nlrp1b⁺} or B6 BMDMs stained with Cholera Toxin subunit B-Alexa 594 (rCTB) were stimulated with LeTx (**a**) or FlaTox (**b**), respectively, and imaged in culture media containing Sytox Green. Confocal images were acquired every 1.5 minutes. Graphs show the percentage of cell volume quantifications based on rCTB-Alexa 594 staining (upper panel) or the mean fluorescence intensity (MFI) of Sytox Green signal (lower panels) of single cells (LeTx, n=26; FlaTox n=16), calculated as described in *Methods*. “Mock” lines represent the average of the values obtained in unstimulated cells, imaged in parallel. In all panels time point zero indicates the first detection of Sytox Green. Relates to Figure 6b, d.

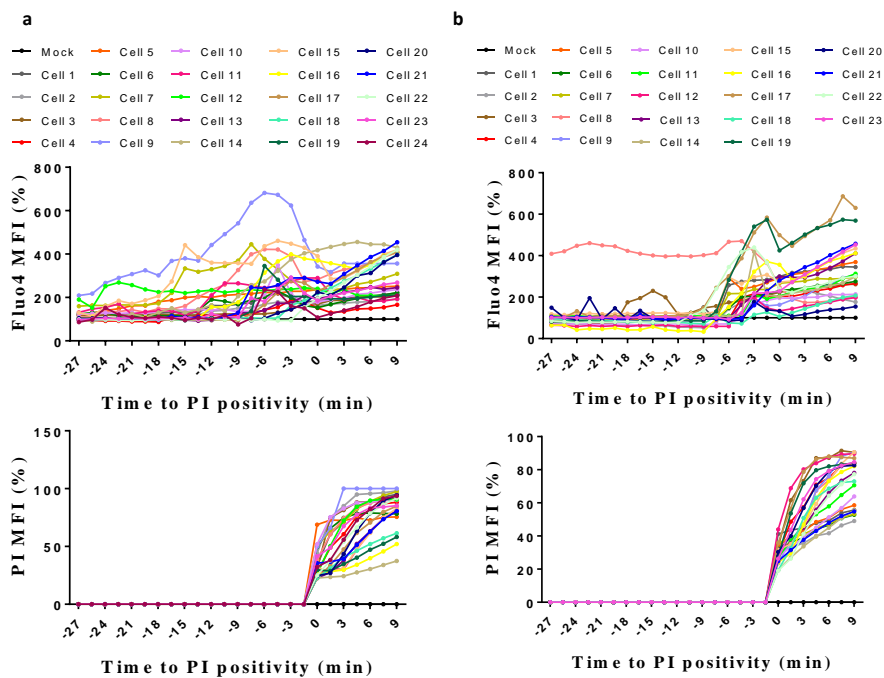


Supplemental Figure 8. Punicalagin inhibits LeTx-induced pyroptosis caspase-1 activation. **a, b** $B6^{Nlrp1b+}$ BMDMs were pretreated with Punicalagin at the indicated concentrations (μM) and stimulated with LeTx for 90 min. Culture supernatants were assayed for LDH (**a**), and protein lysates for caspase-1 by Western blotting (**b**). **(c, d)** BMDMs were pretreated with Punicalagin ($50 \mu\text{M}$) and stimulated with LeTx for 90 or 180 minutes. Culture supernatants were assayed for LDH (**c**), and protein lysates for caspase-1 by Western blotting (**d**). **(e, f)** $B6^{Nlrp1b+}$ BMDMs that had been preloaded with the Ca^{2+} indicator Fluo4 and stained with CTB-Alexa 647 (rCTB) were incubated with Punicalagin ($50 \mu\text{M}$) or vehicle control before cells were stimulated with LeTx and imaged in culture media containing PI. Confocal images were acquired every 1.5 minutes. Graphs show

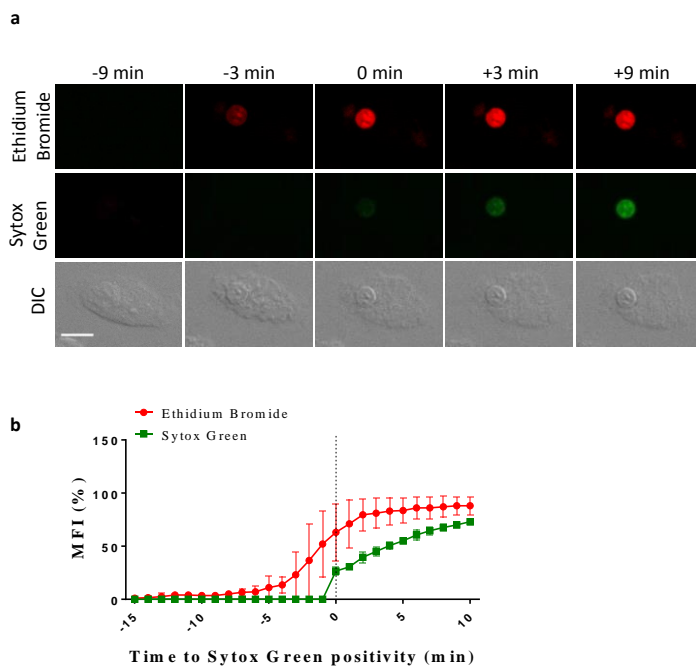
the percentage of mean fluorescence intensity (MFI) of PI (upper panel, left axis) and Fluo4 (lower panel) and cell volume quantifications based on rCTB-Alexa 647 staining (upper panel, right axis), all calculated as described in *Methods*. Values represent the mean \pm SD of 2 independent experiments (LeTx n=11; Punicalagin+LeTx n=9). Fluorescent micrographs show the maximum intensity projection (PI and Fluo4) or the single plane (rCTB) of a representative cell. All scale bars, 10 μ m.



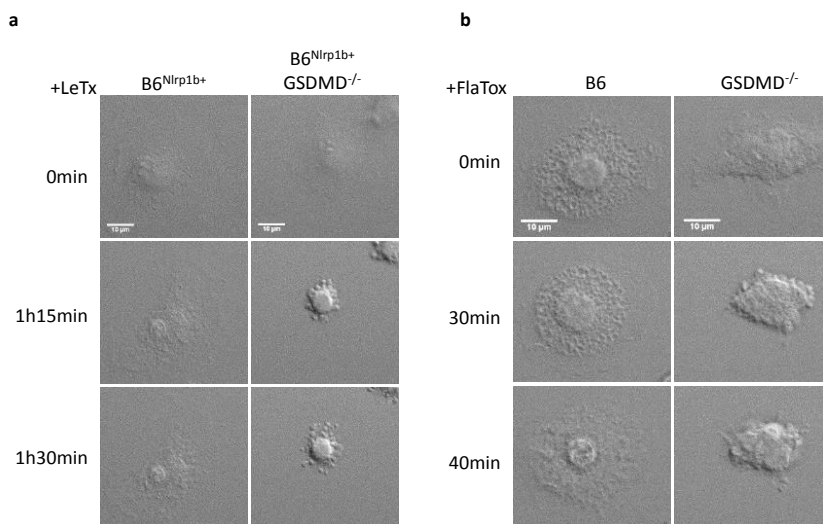
Supplemental Figure 9. Punicalagin inhibits FlaTox-induced caspase-1 activation. **a, b** B6^{Nlrp1b+} BMDMs were pretreated with Punicalagin at the indicated concentrations (μ M) and stimulated with FlaTox for 30 min. Culture supernatants were assayed for LDH (**a**), and protein lysates for caspase-1 by Western blotting (**b**). BMDMs were pretreated with Punicalagin (50 μ M) and stimulated with FlaTox for 30 or 60 minutes. Culture supernatants were assayed for LDH (**c**), and protein lysates for caspase-1 by Western blotting (**d**). Data are representative of 2 independent experiments.



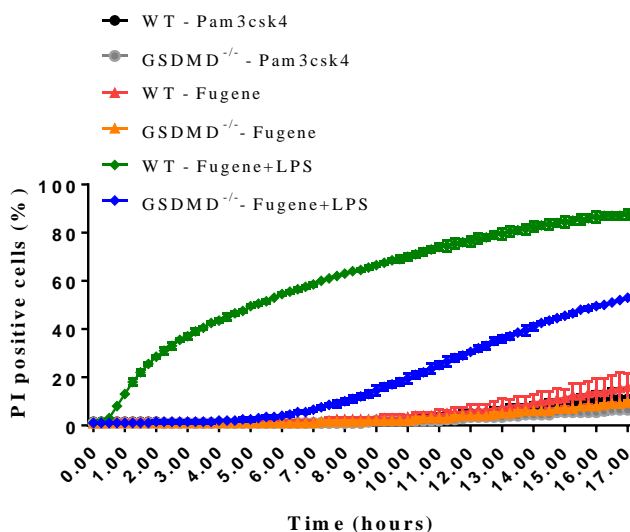
Supplemental Figure 10. Pyroptotic Ca^{2+} influx occurs prior to total membrane permeabilization. a-d B6^{Nlrp1b} BMDMs preloaded with the cell-permeant Ca^{2+} indicator Fluo4 were imaged after stimulation with LeTx (a) or FlaTox (b) in culture media containing PI. Confocal images were acquired every 1.5 minutes. Graphs show the percentage of mean fluorescence intensity (MFI) of single cells (LeTx, n=24; FlaTox n=23), calculated as described in *Methods*, of Fluo4 (upper panel) or PI (lower panel) signals. “Mock” lines represent the average of the values obtained in unstimulated cells, imaged in parallel. In all panels time point zero indicates the first detection of PI. Relates to Figure 7b, d.



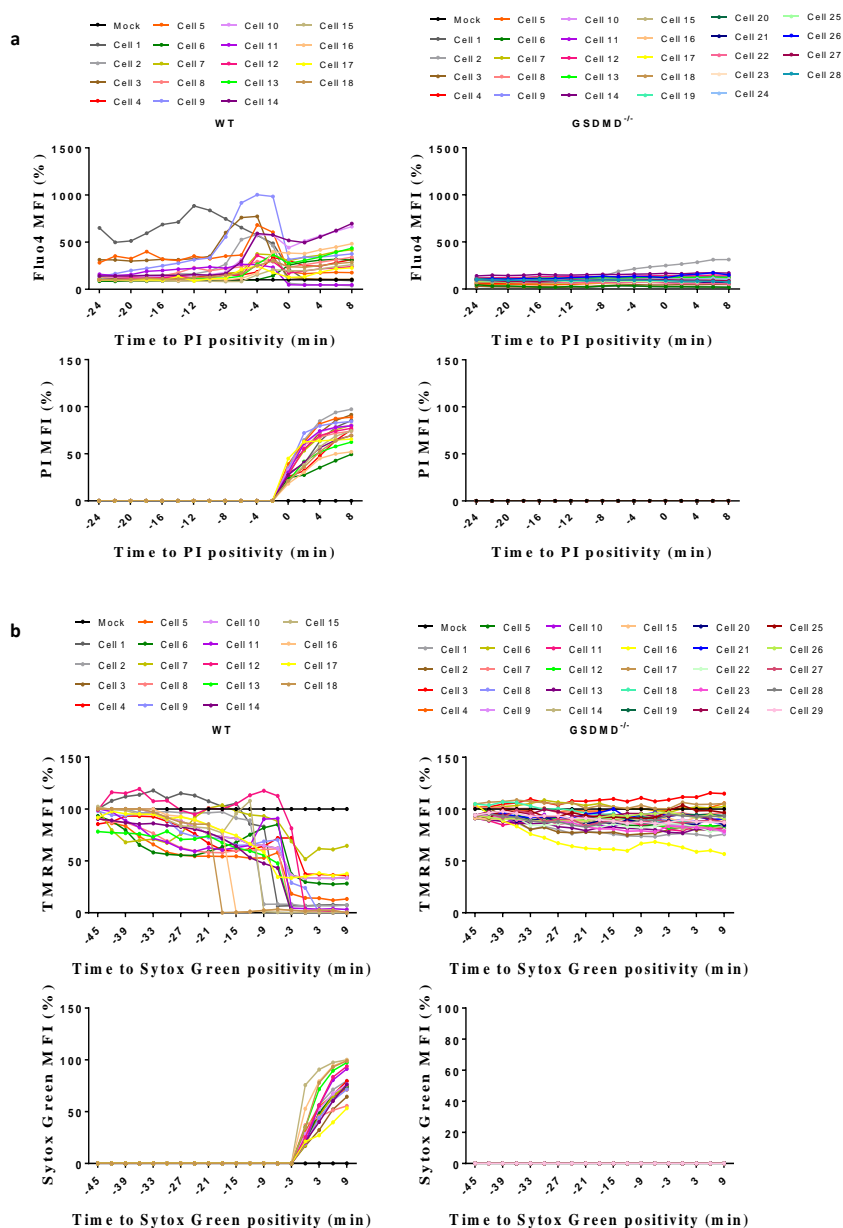
Supplemental Figure 11. Pyroptotic cells provide sequential permeability to Ethidium Bromide and Sytox Green. **a, b** $B6^{Nlrp1b+}$ BMDMs were stimulated with LeTx and imaged in culture media containing Ethidium Bromide and Sytox Green. Confocal images were acquired every 1 minute. Graph shows the percentage of mean fluorescence intensity (MFI) calculated as described in *Methods*, and values represent the mean \pm SD of individual cells imaged in 3 independent experiments ($n=50$). Fluorescent micrographs show the maximum intensity projection of a representative cell. In all panels time point zero indicates the first detection of Sytox Green. All scale bars, 10 μ m.



Supplemental Figure 12. Canonical inflammasome stimuli induce apoptosis in GSDMD-deficient macrophages with kinetics similar to pyroptosis induction in WT cells. **a, b** BMDMs of indicated genotypes were stimulated with LeTx (**a**) or FlaTox (**b**). Images show the bright field of representative cells (LeTx n=20; FlaTox n=18). All scale bars, 10 μ m.



Supplemental Figure 13. Delayed membrane permeabilization following non-canonical inflammasome activation in GSDMD-deficient macrophages. Pam3csk4-primed GSDMD-deficient and -sufficient B6 BMDMs were transfected with LPS (2 μ g/ml, Fugene+LPS), treated with Fugene alone or kept without treatment and imaged in media containing PI. The number of positive cells was quantified relative to a Triton-x100-treated well (considered 100%) of each genotype. Values represent mean \pm SD of technical duplicates of a representative experiment out of 3 independent experiments.



Supplemental Figure 14. GSDMD deficiency rescues Ca²⁺ influx and mitochondrial decay associated with activation of the non-canonical inflammasome. **a, b** Pam3csk4-primed BMDMs of WT (**a**) and GSDMD^{-/-} (**b**) mice were preloaded with the cell-permeant Ca²⁺ indicator Fluo4 and imaged after transfection with LPS (2 μg/ml, Fugene+LPS), Fugene alone or mock-treated in culture media containing PI. Confocal images were acquired every 2 minutes. **c, d** BMDMs of WT (**c**) and GSDMD^{-/-} (**d**) mice were preloaded with TMRM and imaged after transfection with LPS (2 μg/ml, Fugene+LPS), Fugene alone or mock-treated in culture media containing Sytox Green. Confocal images were acquired every 3 minutes. Graphs show the percentage of mean fluorescence intensity (MFI) of single cells (Fluo4: WT n=18, GSDMD^{-/-} n=28; TMRM: WT n=18, GSDMD^{-/-} n=29), calculated as described in *Methods*, of Fluo4 and TMRM (upper panels) or PI and Sytox Green (lower

panels) signals. "Mock" lines represent the average of the values obtained in unstimulated cells that were imaged in parallel. In all panels time point zero indicates the first detection of PI. Relates to Figure 8d, f.

3.1.7. References

- 1 Vande Walle, L. & Lamkanfi, M. Pyroptosis. *Curr Biol* **26**, R568-572, doi:10.1016/j.cub.2016.02.019 (2016).
- 2 Jorgensen, I. & Miao, E. A. Pyroptotic cell death defends against intracellular pathogens. *Immunol Rev* **265**, 130-142, doi:10.1111/imr.12287 (2015).
- 3 Lamkanfi, M. & Dixit, V. M. Mechanisms and functions of inflammasomes. *Cell* **157**, 1013-1022, doi:10.1016/j.cell.2014.04.007 (2014).
- 4 Kayagaki, N. *et al.* Non-canonical inflammasome activation targets caspase-11. *Nature* **479**, 117-121, doi:10.1038/nature10558 (2011).
- 5 Kayagaki, N. *et al.* Caspase-11 cleaves gasdermin D for non-canonical inflammasome signalling. *Nature* **526**, 666-671, doi:10.1038/nature15541 (2015).
- 6 Ding, J. *et al.* Pore-forming activity and structural autoinhibition of the gasdermin family. *Nature* **535**, 111-116, doi:10.1038/nature18590 (2016).
- 7 Aglietti, R. A. *et al.* GsdmD p30 elicited by caspase-11 during pyroptosis forms pores in membranes. *Proc Natl Acad Sci U S A* **113**, 7858-7863, doi:10.1073/pnas.1607769113 (2016).
- 8 Shi, J. *et al.* Cleavage of GSDMD by inflammatory caspases determines pyroptotic cell death. *Nature* **526**, 660-665, doi:10.1038/nature15514 (2015).
- 9 Jorgensen, I., Zhang, Y., Krantz, B. A. & Miao, E. A. Pyroptosis triggers pore-induced intracellular traps (PITs) that capture bacteria and lead to their clearance by efferocytosis. *J Exp Med* **213**, 2113-2128, doi:10.1084/jem.20151613 (2016).
- 10 Lamkanfi, M. *et al.* Inflammasome-dependent release of the alarmin HMGB1 in endotoxemia. *J Immunol* **185**, 4385-4392, doi:10.4049/jimmunol.1000803 (2010).
- 11 Liu, T. *et al.* Single-cell imaging of caspase-1 dynamics reveals an all-or-none inflammasome signaling response. *Cell Rep* **8**, 974-982, doi:10.1016/j.celrep.2014.07.012 (2014).
- 12 Monack, D. M., Raupach, B., Hromockyj, A. E. & Falkow, S. Salmonella typhimurium invasion induces apoptosis in infected macrophages. *Proc Natl Acad Sci U S A* **93**, 9833-9838 (1996).
- 13 Chen, Y., Smith, M. R., Thirumalai, K. & Zychlinsky, A. A bacterial invasin induces macrophage apoptosis by binding directly to ICE. *EMBO J* **15**, 3853-3860 (1996).
- 14 Hersh, D. *et al.* The Salmonella invasin SipB induces macrophage apoptosis by binding to caspase-1. *Proc Natl Acad Sci U S A* **96**, 2396-2401 (1999).
- 15 Cookson, B. T. & Brennan, M. A. Pro-inflammatory programmed cell death. *Trends Microbiol* **9**, 113-114 (2001).
- 16 Newton, K. & Manning, G. Necroptosis and Inflammation. *Annu Rev Biochem* **85**, 743-763, doi:10.1146/annurev-biochem-060815-014830 (2016).
- 17 Pasparakis, M. & Vandenabeele, P. Necroptosis and its role in inflammation. *Nature* **517**, 311-320, doi:10.1038/nature14191 (2015).
- 18 Rickard, N. A., Heidtke, U. J. & O'Beirne, G. A. Assessment of auditory processing disorder in children using an adaptive filtered speech test. *Int J Audiol* **52**, 687-697, doi:10.3109/14992027.2013.802380 (2013).

-
- 19 Brennan, M. A. & Cookson, B. T. Salmonella induces macrophage death by caspase-1-dependent necrosis. *Mol Microbiol* **38**, 31-40 (2000).
- 20 Fink, S. L. & Cookson, B. T. Caspase-1-dependent pore formation during pyroptosis leads to osmotic lysis of infected host macrophages. *Cell Microbiol* **8**, 1812-1825, doi:10.1111/j.1462-5822.2006.00751.x (2006).
- 21 Lamkanfi, M. & Dixit, V. M. Manipulation of host cell death pathways during microbial infections. *Cell Host Microbe* **8**, 44-54, doi:10.1016/j.chom.2010.06.007 (2010).
- 22 Van Opdenbosch, N. *et al.* Activation of the NLRP1b inflammasome independently of ASC-mediated caspase-1 autoproteolysis and speck formation. *Nat Commun* **5**, 3209, doi:10.1038/ncomms4209 (2014).
- 23 Newton, K. *et al.* Is SIRT2 required for necroptosis? *Nature* **506**, E4-6, doi:10.1038/nature13024 (2014).
- 24 Vanden Berghe, T. *et al.* Necroptosis, necrosis and secondary necrosis converge on similar cellular disintegration features. *Cell Death Differ* **17**, 922-930, doi:10.1038/cdd.2009.184 (2010).
- 25 Taylor, R. C., Cullen, S. P. & Martin, S. J. Apoptosis: controlled demolition at the cellular level. *Nat Rev Mol Cell Biol* **9**, 231-241, doi:10.1038/nrm2312 (2008).
- 26 Li, Z. *et al.* Necrotic Cells Actively Attract Phagocytes through the Collaborative Action of Two Distinct PS-Exposure Mechanisms. *PLoS Genet* **11**, e1005285, doi:10.1371/journal.pgen.1005285 (2015).
- 27 Gong, Y. N. *et al.* ESCRT-III Acts Downstream of MLKL to Regulate Necroptotic Cell Death and Its Consequences. *Cell* **169**, 286-300 e216, doi:10.1016/j.cell.2017.03.020 (2017).
- 28 von Moltke, J. *et al.* Rapid induction of inflammatory lipid mediators by the inflammasome in vivo. *Nature* **490**, 107-111, doi:10.1038/nature11351 (2012).
- 29 Wang, C. & Youle, R. J. The role of mitochondria in apoptosis*. *Annu Rev Genet* **43**, 95-118, doi:10.1146/annurev-genet-102108-134850 (2009).
- 30 Allam, R. *et al.* Mitochondrial apoptosis is dispensable for NLRP3 inflammasome activation but non-apoptotic caspase-8 is required for inflammasome priming. *EMBO Rep* **15**, 982-990, doi:10.15252/embr.201438463 (2014).
- 31 Zhou, R., Yazdi, A. S., Menu, P. & Tschopp, J. A role for mitochondria in NLRP3 inflammasome activation. *Nature* **469**, 221-225, doi:10.1038/nature09663 (2011).
- 32 Yu, J. *et al.* Inflammasome activation leads to Caspase-1-dependent mitochondrial damage and block of mitophagy. *Proc Natl Acad Sci U S A* **111**, 15514-15519, doi:10.1073/pnas.1414859111 (2014).
- 33 Averette, K. M. *et al.* Anthrax lethal toxin induced lysosomal membrane permeabilization and cytosolic cathepsin release is Nlrp1b/Nalp1b-dependent. *PLoS One* **4**, e7913, doi:10.1371/journal.pone.0007913 (2009).
- 34 Lamkanfi, M. *et al.* Targeted peptide-centric proteomics reveals caspase-7 as a substrate of the caspase-1 inflammasomes. *Mol Cell Proteomics* **7**, 2350-2363, doi:10.1074/mcp.M800132-MCP200 (2008).
- 35 Kay, A. R. How Cells Can Control Their Size by Pumping Ions. *Front Cell Dev Biol* **5**, 41, doi:10.3389/fcell.2017.00041 (2017).
- 36 Chen, X. *et al.* Pyroptosis is driven by non-selective gasdermin-D pore and its morphology is different from MLKL channel-mediated necroptosis. *Cell Res* **26**, 1007-1020, doi:10.1038/cr.2016.100 (2016).

-
- 37 Martin-Sanchez, F. *et al.* Inflammasome-dependent IL-1beta release depends upon membrane permeabilisation. *Cell Death Differ* **23**, 1219-1231, doi:10.1038/cdd.2015.176 (2016).
- 38 Sborgi, L. *et al.* GSDMD membrane pore formation constitutes the mechanism of pyroptotic cell death. *EMBO J* **35**, 1766-1778, doi:10.15252/embj.201694696 (2016).
- 39 Liu, X. *et al.* Inflammasome-activated gasdermin D causes pyroptosis by forming membrane pores. *Nature* **535**, 153-158, doi:10.1038/nature18629 (2016).
- 40 He, W. T. *et al.* Gasdermin D is an executor of pyroptosis and required for interleukin-1beta secretion. *Cell Res* **25**, 1285-1298, doi:10.1038/cr.2015.139 (2015).
- 41 Cosentino, K., Ros, U. & Garcia-Saez, A. J. Assembling the puzzle: Oligomerization of alpha-pore forming proteins in membranes. *Biochim Biophys Acta* **1858**, 457-466, doi:10.1016/j.bbamem.2015.09.013 (2016).
- 42 Domen, J., Gandy, K. L. & Weissman, I. L. Systemic overexpression of BCL-2 in the hematopoietic system protects transgenic mice from the consequences of lethal irradiation. *Blood* **91**, 2272-2282 (1998).

3.2. A biochemical perspective of pyroptosis

Section 3.2. is structured as the manuscript: de Vasconcelos, N.M.* and Van Opendenbosch, N.*; Van Gorp, H; Lamkanfi, M. Caspase-1-dependent pyroptosis comprises an apoptotic program. In preparation.

**contributed equally to the work*

3.2.1. Abstract

Inflammasomes are key elements of the innate immune response to bacterial and viral pathogens¹. However, uncontrolled inflammasome activation can also be the causing mechanism of hereditary inflammatory disorders². Canonical inflammasome-activated cells still undergo cell death in the absence of GSDMD³, and previous studies have shown caspase-7 to be a substrate of caspase-1⁴. Here we show that caspase-1 activates a caspase-3 and -7-mediated apoptotic program during the execution of pyroptosis downstream of the NLRC4 and NLRP1b inflammasomes. DEVDase activity, considered a hallmark of apoptosis, was present in pyroptotic bone marrow-derived macrophages, and pyroptosis was accompanied by cleavage of typical apoptotic markers ROCK1, p23, PARP1 and Bid. Absence of GSDMD revealed an apoptotic phenotype, which was insensitive to the ablation of ASC or to TLR-priming. Double deficiency for caspase-3 and -7 rescued the observed DEVDase activity and delayed plasma membrane permeabilization for 4h. Overall, we conclude that both caspase-1 and caspase-8 can mediate an apoptotic program downstream of the inflammasome. We propose a model in which inflammasome activation leads to several parallel death programs: caspase-8 and -1-mediated apoptosis and caspase-1-induced pore formation through GSDMD. All these pathways act in a concerted manner in WT macrophages, and therefore are key molecular constituents of pyroptosis. The existence of these parallel cell death pathways suggests redundancy in cell death induction mechanisms of an infected macrophage to ensure pathogenic disease resolution.

3.2.2. Main text

Anthrax lethal toxin (LeTx) elicits NLRP1b inflammasome activation and pyroptosis in B6 BMDMs containing the LeTx-sensitive *Nlrp1b* allele of 129 mice⁵. Analysis of the caspase maturation profile in B6^{Nlrp1b+} BMDMs treated for 2h with LeTx demonstrated caspase-1 conversion into its mature p20 form (**Fig. 1a**). Confirming what has been observed with NLRP3 and NLRC4 inflammasomes⁴, caspase-3 and -7 were cleaved to their active form after LeTx triggering of B6^{Nlrp1b+} macrophages. Activation of the NLRC4 inflammasome can be accomplished by a system employing the N-terminal fragment of *B. anthracis* Lethal Factor fused to Flagellin from *Legionella pneumophila* for its cytoplasmic delivery through combination with Protective Antigen (FlaTox)⁸. After 2h of FlaTox treatment, we could detect caspase-1 maturation in BMDMs (**Fig. 1a**). Interestingly, in the context of NLRC4 activation, the p43 and p18 forms of caspase-8 was detected 2h post treatment. Further confirming the published data, caspase-3 and caspase-7 were matured after FlaTox treatment.

To probe whether caspase-3 and -7 cleavages in pyroptotic macrophages correlated to their activation, we employed a time-kinetics analysis with a fluorogenic probe containing the caspase-3 and caspase-7-target substrate sequence, DEVD, using the imaging-based Incucyte system. Treatment of B6^{Nlrp1b+} BMDMs with LeTx led to PI staining, indicative of the pyroptosis-induced permeabilization of the plasma membrane, after only 1h30 (**Fig. 1b**). The DEVD-based probe stained LeTx-triggered cells with similar kinetics and at comparable level as PI. Similarly, intoxication of BMDMs with FlaTox lead to DEVDase activity, which was concomitant to membrane permeabilization, detected through PI staining. Both the extrinsic and intrinsic apoptotic pathways converge into activation of caspase-3 and -7, and therefore DEVDase activity is considered a hallmark of apoptosis. NLRP1b and NLRC4-induced pyroptosis generated DEVD-activity at comparable levels to the well described apoptotic trigger, Staurosporine (**Fig. 1b**). DEVD activity was specific for downstream activation of inflammasomes, because triggering BMDMs lacking the *Nlrp1b* transgene with LeTx did not induce any DEVD signal in the cells (**Fig. 1c**). Similarly, NLRC4^{-/-} BMDMs were unable to induce DEVD signal after FlaTox treatment (**Fig. 1d**). During the extrinsic apoptotic pathway, activation of caspase-8 at the death receptor complex leads to downstream activation of caspase-3 and -7 and apoptotic dismantling of the cell. Ablation of ASC has been shown to impair caspase-8 activation in the speck downstream of NLRP1b and NLRC4 inflammasomes, while caspase-1 continued to induce pyroptosis^{6,7}. Indeed, B6^{Nlrp1b+}ASC^{-/-} BMDMs

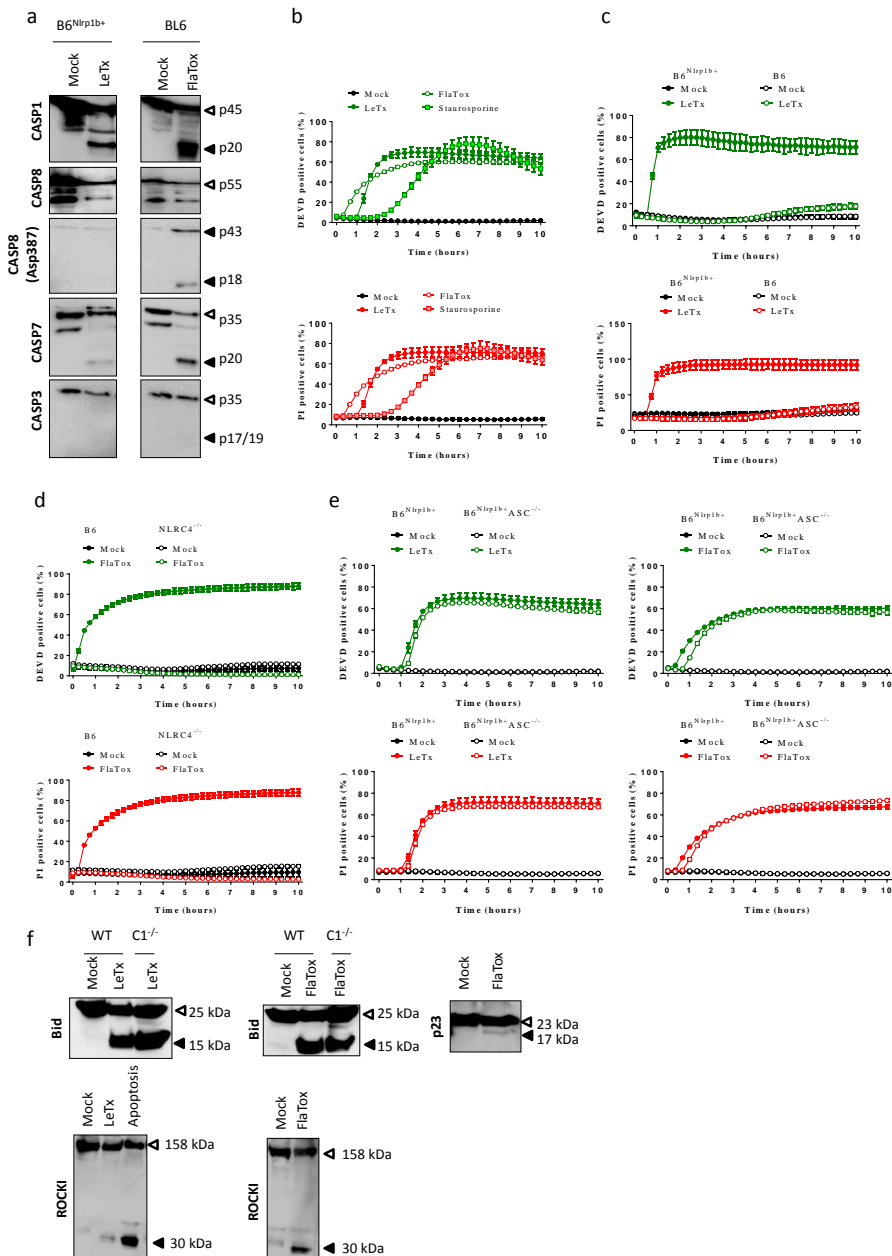


Figure 1. NLRP1b and NLR4-induced pyroptosis is associated to a Caspase-3/7 signature. **a, f**, B6^{Nlrp1b+} or B6 macrophages were treated with LeTx and FlaTox, respectively, for 2h and lysates run on WB for detection of the indicated proteins. **b**, B6^{Nlrp1b+} macrophages treated with either LeTx, FlaTox or Staurosporine in media containing DEVD-probe and PI were imaged on an Incucyte platform. **c**, B6^{Nlrp1b+} and B6 macrophages were treated with LeTx and assayed as in **(b)**. **d**, B6 and NLR4^{-/-} macrophages were treated with FlaTox and assayed as in **(b)**. **e**, B6^{Nlrp1b+} and B6^{Nlrp1b+}ASC^{-/-} macrophages were treated with LeTx or FlaTox and assayed as in **(b)**. In all conditions, the number of positive cells was quantified relative to a PI stained, Triton-x100-

treated well (considered 100%). Values represent mean \pm SD of technical duplicates of a representative experiment from three biological repeats.

underwent plasma membrane permeabilization with same kinetics as B6^{Nlrp1b+} after LeTx or FlaTox triggering (**Fig. 1e**). Similarly, ablation of ASC in BMDMs did not hamper DEVDase activity or its kinetics after both NLRP1b and NLRC4 inflammasomes, suggesting this event is not mediated by caspase-8 activation at the ASC speck (**Fig. 1e**).

To confirm the DEVDase activity in pyroptotic cells was not an off-target effect of other active caspases, we analyzed lysates of either LeTx or FlaTox-triggered cells for substrates normally cleaved during the execution phase of apoptosis. ROCK1, p23 and Bid were cleaved in BMDMs triggered with LeTx and FlaTox (**Fig. 1f**) into similar cleavage fragments than reported during apoptosis. These data establish that caspase-3 and -7 are activated during pyroptosis in an ASC-independent manner and contribute to biochemical aspects of this form of cell death.

We hypothesized that the rapid lysis of the plasma membrane mediated by GSDMD would stop intracellular signaling and decided to use GSDMD^{-/-} BMDMs to examine the caspase-3 and -7 cleavage events in more detail. B6^{Nlrp1b+}GSDMD^{-/-} BMDMs were hampered in LDH release after stimulation of the NLRP1b inflammasome with LeTx (**Fig. 2a**). However, further microscopic evaluation of B6^{Nlrp1b+}GSDMD^{-/-} macrophages demonstrated these not to be protected from cell death, as the cells appeared shrunken and displayed blebbing, consistent with apoptosis induction (**Fig. 2b**). Previous reports have shown that lack of GSDMD after engagement of a caspase-1-dependent inflammasome does not protect from cell death, as macrophages undergo apoptosis^{3,9}. Flow cytometry of B6^{Nlrp1b+}GSDMD^{-/-} macrophages triggered with LeTx demonstrated a population positive for Annexin-V while impermeable to PI (AnnexinV⁺/PI) (**Fig. 2c**), consistent with apoptosis. Activation of the NLRP1b inflammasome was not altered by lack of GSDMD, and the total populations of dead cells were comparable between GSDMD-deficient and sufficient cells. NLRC4 engagement in the absence of GSDMD lead to a similar pattern, with lack of LDH being associated to an apoptotic phenotype and cells staining as AnnexinV⁺/PI (**Fig. 2d-f**).

Analysis of the profile of caspase maturation in GSDMD^{-/-} cells demonstrated that caspase-8 is strongly matured into its p18 forms in the presence of LeTx or FlaTox (**Fig. 2g**). Similarly, caspase-3 was robustly matured into the active p17 fragment. Interestingly, the level of caspase-7 maturation in apoptotic cells was comparable to

those of pyroptotic cells. We had previously shown that morphological changes in GSDMD^{-/-} BMDMs proceed with a kinetic similar to pyroptotic changes. Analysis of

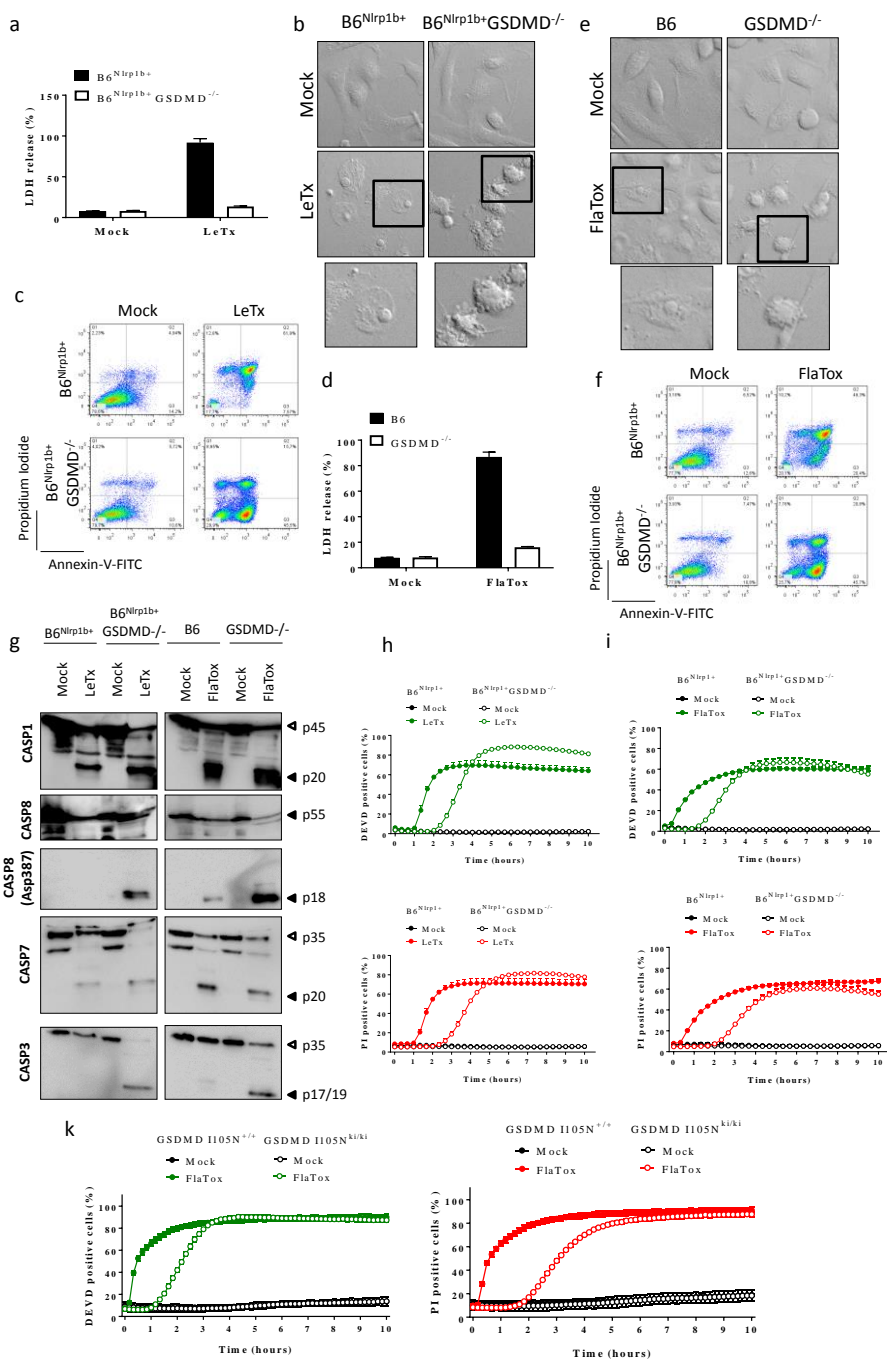


Figure 2. Lack of GSDMD reveals an apoptotic phenotype after NRLP1b and NLR4 inflammasome activation. **a-g**, B6^{Nlrp1b+} or B6 macrophages with or without GSDMD were treated with either LeTx or FlaTox,

respectively, for 2h and their supernatants probed for LDH activity (**a, d**), imaged under a confocal microscope (**b, e**), cells collected for FACS analysis of Annexin V/PI positivity (**c, f**), and lysates run on WB for detection of the indicated proteins (**g**). **h**, B6^{Nlrp1b+} or B6 macrophages with or without GSDMD were treated with either LeTx or FlaTox, respectively, in media containing DEVD-probe and PI were imaged on an Incucyte platform. **i**, GSDMD^{I105N} knock-in homozygous (GSDMDI105N^{ki/ki}) or WT (GSDMDI105N^{+/+}) macrophages were treated with FlaTox in media containing DEVD-probe and PI were imaged on an Incucyte platform. The number of positive cells was quantified relative to a PI stained, Triton-x100-treated well (considered 100%) for each genotype. Values represent mean \pm SD of technical duplicates of a representative experiment from three biological repeats.

DEVDase activity on GSDMD^{-/-} macrophages showed similar levels to their WT counterparts when stimulated with either LeTx or FlaTox, though GSDMD^{-/-} BMDMs had a delay in comparison to GSDMD sufficient cells (**Fig. 2h**). Kinetics of DEVDase activity on GSDMD^{-/-} macrophages followed the same as PI internalization, an indication of secondary necrosis in this case. A possible explanation for the delayed DEVDase activity versus the observation of comparable caspase-7 maturation levels is that the substrate is not efficient in entering cells with an intact plasma membrane. Therefore, the rapid lysis of pyroptotic cells causes a faster accumulation of the dye than in apoptotic ones. However, together with the ROCK1, PARP1 and Bid cleavage, we conclude that the probe displays specificity for caspase-3 and -7 activities.

In order to understand whether it was the lack of GSDMD or of its function that allowed the apoptotic phenotype to appear in GSDMD^{-/-} cells, we have made use of the ENU-generated mouse knockin GSDMD^{I105N}, in which GSDMD is expressed but unable to cause cell lysis³. Activation of GSDMD^{ki/ki} BMDMs with FlaTox led to apoptosis with similar kinetics than GSDMD^{-/-} BMDMs (**Fig. 2i**), establishing that the lack of function of GSDMD is sufficient to reveal the apoptotic phenotype. Of note, also on the GSDMD^{-/-} background, inflammasome signaling through NLRP1b was essential for activation of caspase-1, -3, -7 and -8 plus the detection of DEVDase activity, after LeTx stimulation (**Sup. Fig. 1**).

Caspase-8 activation during inflammasome triggering of caspase-1-deficient macrophages has been shown to occur in the ASC speck⁷. Given that cells lacking GSDMD contained active caspase-1, we analyzed whether the apoptotic phenotype observed in the absence of GSDMD expression was related to the described caspase-8 arm. Surprisingly, lack of ASC could also not protect from LeTx or FlaTox induced apoptosis, and allowed blebbing and cell shrinkage, concomitant to the appearance of an AnnexinV⁺/PI⁺ population similar to B6^{Nlrp1b+}GSDMD^{-/-} dying macrophages (**Fig. 3a, b**). Kinetics of DEVDase activity and PI incorporation of B6^{Nlrp1b+}ASC^{-/-}GSDMD^{-/-}

triggered with LeTx led, however, to a 20% decay in the maximum number of stained cells (Fig. 3d). FlaTox-intoxicated BMDMs showed a 50% reduction in their

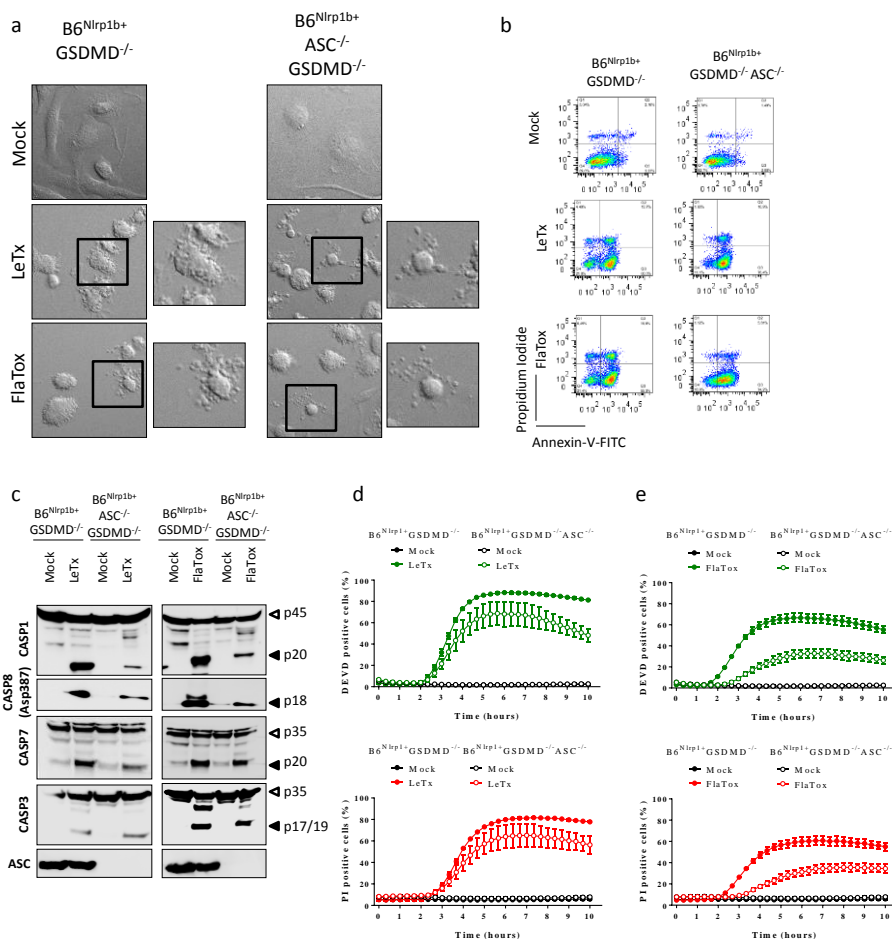


Figure 3. Lack of ASC does not impair apoptosis in the GSDMD-deficient genotype after NLRP1b and NLRC4 inflammasome activation. a-c, $B6^{Nlrp1b+} GSDMD^{-/-}$ or $B6^{Nlrp1b+} GSDMD^{-/-} ASC^{-/-}$ macrophages were treated with either LeTx or FlaTox for 2h and imaged under a confocal microscope (a), cells collected for FACS analysis of Annexin V/PI positivity (b), and lysates run on WB for detection of the indicated proteins (c). d, e, $B6^{Nlrp1b+} GSDMD^{-/-}$ or $B6^{Nlrp1b+} GSDMD^{-/-} ASC^{-/-}$ macrophages were treated with either LeTx (d) or FlaTox (e) in media containing DEVD-probe and PI were imaged on an Incucyte platform. The number of positive cells was quantified relative to a PI stained, Triton-x100-treated well (considered 100%) for each genotype. Values represent mean \pm SD of technical duplicates of a representative experiment from three biological repeats.

DEVDase maximum activity and PI incorporation (Fig. 3e). While caspase-1 is activated in the absence of ASC after NLRP1b and NLRC4 inflammasomes, its p20 form is no longer detectable^{5,10}. However, ablation of ASC in the $GSDMD^{-/-}$ background restored the maturation of caspase-1 into its p20 (Fig. 3c). Further, while

caspace-8 was still processed in $B6^{Nlrp1b+}ASC^{-}/GSDMD^{-/}$ triggered for NLRP1b inflammasome activation, lack of ASC lead to a significant reduction of caspace-8 maturation after FlaTox triggering (Fig. 3c), confirming the more pronounced need of the NLRC4 inflammasome for ASC. Interestingly, we could not detect any reduction on the cleavage pattern of caspace-3 and caspace-7 in the absence of ASC. Overall, the data indicate that in the GSDMD-deficient background, caspace-8 can be activated outside of the ASC speck after inflammasome triggers.

To address the role for caspace-3 and -7 in the apoptotic phenotype observed, we made immortalized $B6^{Nlrp1b+}GSDMD^{-/}Casp3^{flox/flox}Casp7^{flox/flox}LysM-Cre^{+}$ myeloid progenitor cells and differentiated them to BMDMs (iBMDMs). DEVDase activity was abolished and the signal was diminished below threshold levels in $B6^{Nlrp1b+}GSDMD^{-/}Casp3^{flox/flox}Casp7^{flox/flox}LysM-Cre^{+}$ immortalized macrophages stimulated with LeTx, while control $B6^{Nlrp1b+}GSDMD^{-/}$ showed DEVDase staining when undergoing pyroptosis, further proving the specificity of the probe in our system (Fig. 4a). Remarkably, there was a delay of 4h in PI incorporation by these cells when compared to $B6^{Nlrp1b+}GSDMD^{-/}$. FlaTox-intoxication of iBMDMs showed a similar pattern, demonstrating the importance of caspace-3 and -7 for the apoptotic phenotype in GSDMD-deficient macrophages (Fig. 4b). Despite a significant reduction of DEVDase activity, Western blot analysis demonstrated that caspace-3 and -7 excisions were not complete in $LysM-Cre^{+}$ cells (Fig. 4c). Interestingly, caspace-1 and caspace-8 were activated at similar levels in caspace-3 and -7-deficient and sufficient cells, following treatment with LeTx and FlaTox.

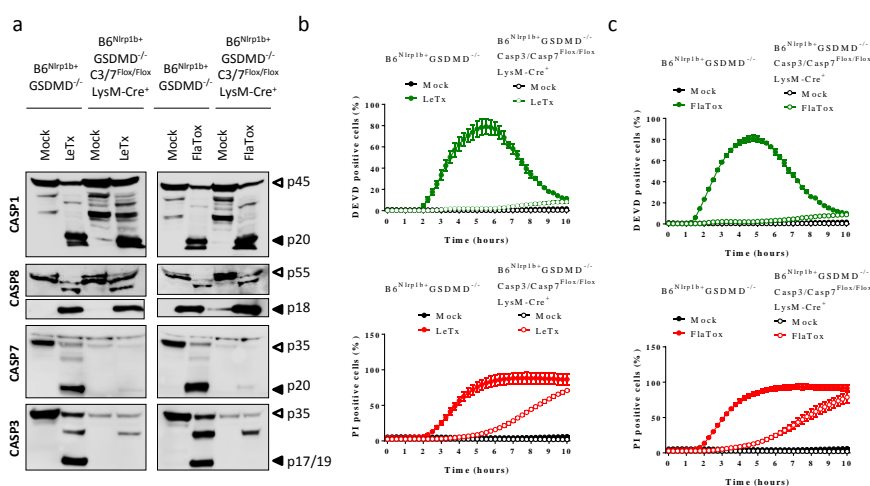


Figure 4. Caspace-3/-7 control apoptosis downstream of NLRP1b and NLRC4 inflammasomes in the GSDMD-deficient genotype. a, $B6^{Nlrp1b+}GSDMD^{-/}$ or $B6^{Nlrp1b+}GSDMD^{-/}Casp3^{flox/flox}Casp7^{flox/flox}LysM-Cre^{+}$

immortalized macrophages were treated with either LeTx or FlaTox for 2h and lysates run on WB for detection of the indicated proteins. **b, c**, B6^{Nlrp1b}GSDMD^{-/-} or B6^{Nlrp1b}GSDMD^{-/-}Casp3^{Flox/Flox}Casp7^{Flox/Flox}LysM-Cre⁺ immortalized macrophages were treated with either LeTx (**b**) or FlaTox (**c**) in media containing DEVD-probe and PI were imaged on an Incucyte platform. The number of positive cells was quantified relative to a PI stained, Triton-x100-treated well (considered 100%) for each genotype. Values represent mean \pm SD of technical duplicates of a representative experiment from three biological repeats.

In conclusion, in this work we have shown that NLRP1b and NLRP4 inflammasome activation leads to a signature of caspase-3 and -7 activity in pyroptotic cells, and lack of GSDMD reveals this apoptotic program. In the GSDMD^{-/-} background, caspase-8 maturation was not prevented by lack of ASC, suggesting a caspase feedback loop could be responsible for activating caspase-8. Thus, inflammasome-dependent apoptosis in GSDMD deficient cells is a distinct mechanism than apoptosis happening in the absence of caspase-1 (**Figure 5**). The data presented here demonstrates that pyroptosis comprises a concerted coordination of a caspase cascade, in parallel to the pore formation by GSDMD. Defining the role of this apoptotic cascade happening during inflammasome activation may highlight alternative targets for treatment of inflammasome-mediated diseases.

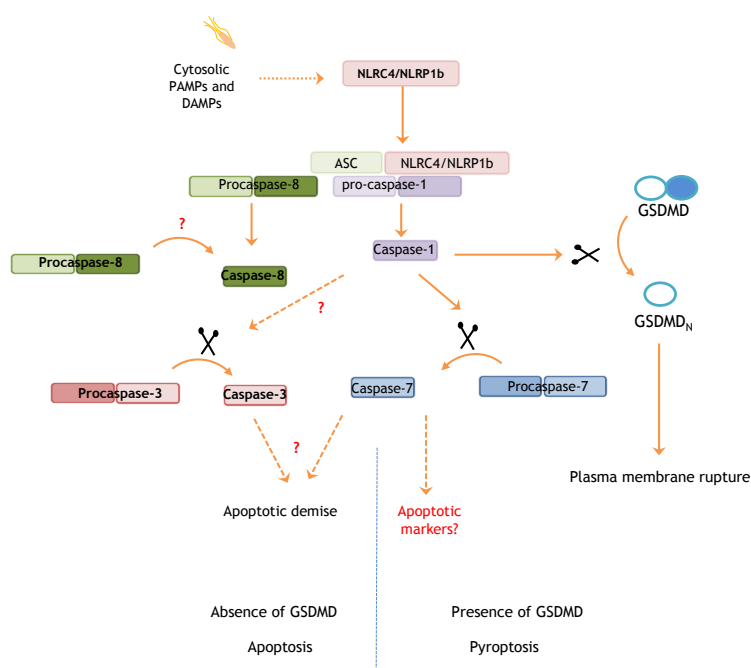


Figure 5. A model for the molecular pathways downstream of the inflammasome. Engagement of the inflammasome by cytosolic recognition of PAMPs or DAMPs activates caspase-1. Caspase-1 cleaves GSDMD for pore membrane formation, but also activates executioner caspases downstream, mainly caspase-7, accounting for an apoptotic substrate signature. The contribution of each executioner caspase to the DEVDase profile in WT cells remains to be determined, but given the high levels of caspase-7 activation it is tempting to speculate this is the responsible caspase. Absence of GSDMD reveals an apoptotic phenotype which is

unimpaired by absence of ASC, suggesting caspase-8 activation at the ASC speck is not the driver of apoptosis. However, both caspase-3 and caspase-7 participate on the apoptotic phenotype of GSDMD-deficient cells.

3.2.3. Methods

Mice. B6^{Nlrp1b+11}, GSDMD^{-/-12} and ASC^{-/-13} mice have been described before. C57BL/6J mice were originally purchased from Charles River, and bred in-house. Animals were housed in individually ventilated cages under specific pathogen-free conditions, and studies were conducted under protocols approved by Ghent University Committee on Use and Care of Animals.

Macrophage differentiation and stimulation. BMDMs were generated by culturing mouse bone marrow cells in L-cell-conditioned IMDM supplemented with 10% FBS, 1% non-essential amino acids and 1% penicillin-streptomycin for 6 days in a humidified atmosphere containing 5% CO₂. BMDMs were seeded in 12-well plates, and the next day either left untreated or stimulated with anthrax protective antigen (PA, 1 µg/ml, Quadragech) and lethal factor (LF, 500 ng/ml, Quadragech) or LFn-Flag¹⁴ (1 µg/ml). Alternatively, BMDMs were treated with the proteasome inhibitor MG132 (10 µM, Calbiochem) for 30 minutes prior to LeTx incubation.

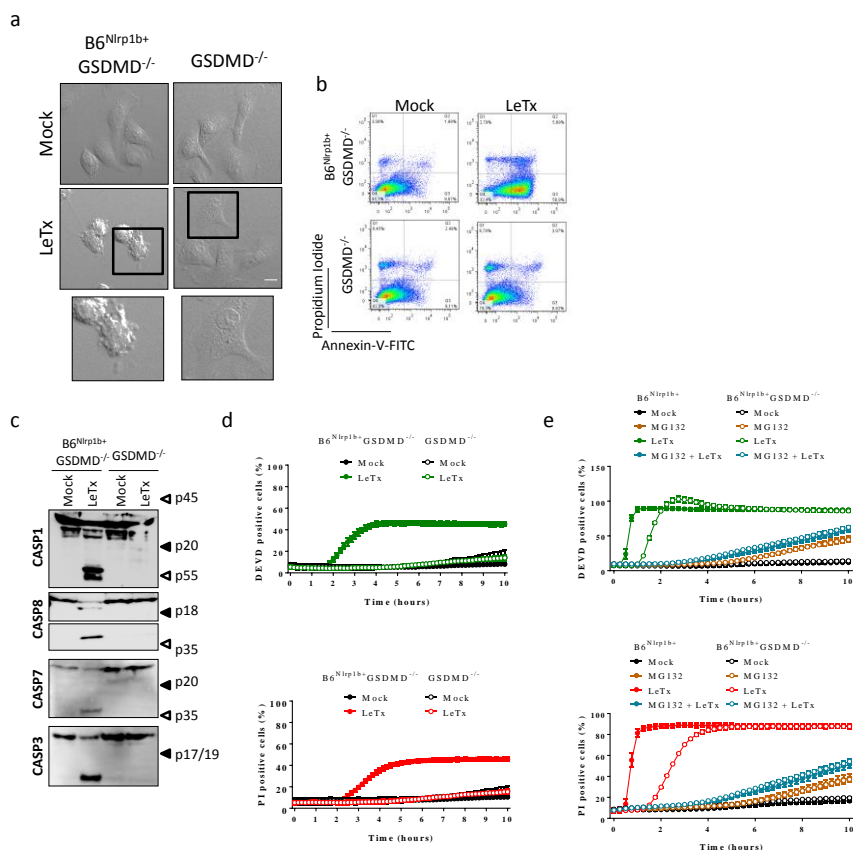
Western blotting. Cell lysates were incubated with cell lysis buffer (20 mM Tris HCl pH 7.4, 200 mM NaCl, 1% NP-40) and denatured in laemmli buffer. For detection of caspase-1, ASC, caspase-3 and caspase-7, p23, ROCK1 and Bid a part of the supernatant was kept with the cell lysates. Subsequently the protein samples were boiled at 95°C for 10 min and separated by SDS-PAGE. Separated proteins were transferred to nitrocellulose membranes. Blocking, incubation with antibody and washing of the membrane were done in PBS supplemented with 0.05% or 0.2% Tween-20 (v/v) and 3% non-fat dry milk. Immunoblots were incubated overnight with primary antibodies against caspase-1 (AG-20B-0042-C100, Adipogen), caspase-8 (ALX-804-447-C100, 1G12, Enzo Life Sciences; 8592S, D5B2, Cell signaling), caspase-3 (9662, Cell Signaling; 9664S, 5A1E, Cell signaling), ASC (AG-25B-0006, Adipogen), caspase-7 (9491, Cell Signaling; 9492, Cell Signaling), ROCK1 (ab45171, Abcam), p23 (MA3-414, Thermo Scientific) and Bid (AF860, R&D systems). Horseradish peroxidase-conjugated goat anti-mouse (115-035-146, Jackson Immunoresearch Laboratories), anti-rabbit (111-035-144, Jackson Immunoresearch Laboratories) or anti-rat (112-035-143, Jackson Immunoresearch Laboratories) secondary antibodies were used to detect proteins by enhanced chemiluminescence (Thermo Scientific).

Cell death kinetic measurements. A plate-based fluorescent assay (Incucyte, Essenbio) was used to quantify cell permeabilization with PI incorporation (Propidium Iodide, Thermo Scientific, final concentration 0,1 $\mu\text{g/ml}$) and caspase-3/7 activation (CellEvent Caspase3/7 Green substrate, Invitrogen) according to the manufacturers' instructions. Data were acquired and analyzed using the Incucyte Zoom system (Essenbio). Briefly, cells were stimulated in a 96-well plate and incubated in a CO_2 and temperature-controlled environment that allowed measurement of fluorescent signals over a time span of 10 hrs.

FACS Annexin V measurements

Annexin V (BD Pharmingen) staining on cells was performed according to the manufacturer's instructions. Flow cytometry was used to measure stained cells and data were analyzed with FlowJo Software.

3.2.4. Supplementary data



of GSDMD-deficient BMDMs. **a-c**, B6^{Nlrp1b}GSDMD^{-/-} or GSDMD^{-/-} macrophages were treated with either LeTx for 2h and imaged under a confocal microscope (**a**), cells collected for FACS analysis of Annexin V/PI positivity (**b**), and lysates run on WB for detection of the indicated proteins (**c**). **d**, B6^{Nlrp1b} or B6 macrophages treated with LeTx in media containing DEVD-probe and PI were imaged on an Incucyte platform. **e**, B6^{Nlrp1b} macrophages pretreated or not with MG132 were triggered with LeTx in media containing DEVD-probe and PI and imaged on an Incucyte platform. The number of positive cells was quantified relative to a PI stained, Triton-x100-treated well (considered 100%) for each genotype. Values represent mean \pm SD of technical duplicates of a representative experiment from three biological repeats.

3.2.5. References

- 1 Broz, P. & Dixit, V. M. Inflammasomes: mechanism of assembly, regulation and signalling. *Nature reviews. Immunology* **16**, 407-420, doi:10.1038/nri.2016.58 (2016).
- 2 Lamkanfi, M. & Dixit, V. M. Mechanisms and functions of inflammasomes. *Cell* **157**, 1013-1022, doi:10.1016/j.cell.2014.04.007 (2014).
- 3 Kayagaki, N. *et al.* Caspase-11 cleaves gasdermin D for non-canonical inflammasome signalling. *Nature* **526**, 666-671, doi:10.1038/nature15541 (2015).
- 4 Lamkanfi, M. *et al.* Targeted peptidocentric proteomics reveals caspase-7 as a substrate of the caspase-1 inflammasomes. *Molecular & cellular proteomics : MCP* **7**, 2350-2363, doi:10.1074/mcp.M800132-MCP200 (2008).
- 5 Van Opdenbosch, N. *et al.* Activation of the NLRP1b inflammasome independently of ASC-mediated caspase-1 autoproteolysis and speck formation. *Nature communications* **5**, 3209, doi:10.1038/ncomms4209 (2014).
- 6 Schneider, K. S. *et al.* The Inflammasome Drives GSDMD-Independent Secondary Pyroptosis and IL-1 Release in the Absence of Caspase-1 Protease Activity. *Cell reports* **21**, 3846-3859, doi:10.1016/j.celrep.2017.12.018 (2017).
- 7 Van Opdenbosch, N. *et al.* Caspase-1 Engagement and TLR-Induced c-FLIP Expression Suppress ASC/Caspase-8-Dependent Apoptosis by Inflammasome Sensors NLRP1b and NLRC4. *Cell reports* **21**, 3427-3444, doi:10.1016/j.celrep.2017.11.088 (2017).
- 8 von Moltke, J. *et al.* Rapid induction of inflammatory lipid mediators by the inflammasome in vivo. *Nature* **490**, 107-111, doi:10.1038/nature11351 (2012).
- 9 He, W. T. *et al.* Gasdermin D is an executor of pyroptosis and required for interleukin-1beta secretion. *Cell research* **25**, 1285-1298, doi:10.1038/cr.2015.139 (2015).
- 10 Broz, P., von Moltke, J., Jones, J. W., Vance, R. E. & Monack, D. M. Differential requirement for Caspase-1 autoproteolysis in pathogen-induced cell death and cytokine processing. *Cell host & microbe* **8**, 471-483, doi:10.1016/j.chom.2010.11.007 (2010).
- 11 Boyden, E. D. & Dietrich, W. F. Nalp1b controls mouse macrophage susceptibility to anthrax lethal toxin. *Nature genetics* **38**, 240-244, doi:10.1038/ng1724 (2006).
- 12 Kayagaki, N. *et al.* Caspase-11 cleaves gasdermin D for non-canonical inflammasome signalling. *Nature* **526**, 666-671, doi:10.1038/nature15541 (2015).
- 13 Mariathasan, S. *et al.* Differential activation of the inflammasome by caspase-1 adaptors ASC and Ipaf. *Nature* **430**, 213-218, doi:10.1038/nature02664 (2004).
- 14 von Moltke, J. *et al.* Rapid induction of inflammatory lipid mediators by the inflammasome in vivo. *Nature* **490**, 107-111, doi:10.1038/nature11351 (2012).

3.3. Effects of the inhibition of serine proteases on cell death induction and inflammasome activation

3.3.1. PRCP inhibitor Compound 8o activates the NLRP3 inflammasome

Section 3.3.1. is structured as the manuscript: de Vasconcelos, N.M.; Van Opdenbosch, N.; Vliegen, G.; Van Der Veken, P.; De Meester, I.; Lamkanfi, M. Lysosomal Prolyl carboxypeptidase antagonist Compound 8o induces macrophage cell death and NLRP3 inflammasome-dependent IL1 β release. In preparation.

3.3.1.1. Abstract

Despite the suggested role for Prolyl carboxypeptidase (PRCP) in inflammation, its function in macrophage biology has not been addressed yet. Here we made use of a PRCP antagonist, Compound 8o, to profile the response of bone marrow-derived macrophages. We found that Compound 8o induced high toxicity of macrophages and IL1 β secretion. Cell death occurred independently of necroptosis, extrinsic apoptosis and pyroptosis, while IL1 β release was rescued in the absence of the NLRP3 inflammasome components. Thus, inhibition of PRCP by Compound 8o triggers cell death and NLRP3-dependent IL1 β release.

3.3.1.2. Main text

Prolyl carboxypeptidase (PRCP) is a lysosomal serine protease that cleaves off the most carboxy-terminal amino acid of its substrates (proteins and peptides) when this is preceded by Proline residue¹. Angiotensin II and III and prekallikrein are established substrates of PRCP, linking this carboxypeptidase to regulation of blood pressure and cardiovascular functions². Notably, polymorphisms in the gene encoding PRCP were shown to significantly increase the risk for preeclampsia in patients with a history of hypertension³. Furthermore, PRCP has been detected in the synovial fluids of atherosclerotic lesions, although its impact on the disease has not been fully elucidated⁴. Because of its clinical association with cardiovascular disease, understanding of PRCP biology has focused primarily on its roles in endothelial cells. However, PRCP-like protease activity has also been reported in macrophages^{4,5}. Considering that PRCP has been implicated in initiation of inflammatory responses, and given the central role macrophages play in inflammatory responses, we set out to investigate the role of PRCP in macrophage biology using pharmacological tool agents.

To inhibit the carboxypeptidase activity of PRCP in macrophages, we took advantage of Compound 80, a previously discovered small molecule that reversibly antagonizes PRCP protease activity with high specificity and efficacy⁶. BMDMs were treated with Compound 80 and then analyzed microscopically to observe morphological changes. Interestingly, we found that BMDMs treated with Compound 80 displayed extensively swollen cytoplasmic vacuoles within 3h post-treatment (**Fig. 1a**). To probe whether inhibition of PRCP in macrophages lead to cytotoxicity, we tracked the incorporation of Sytox Green over time using the IncuCyte platform. Sytox Green is a cell-impermeant dye that enters cells and stains nuclear DNA only when the plasma membrane is permeabilized, a defining feature of necrotic cell death. Notably, treatment of BMDMs with Compound 80 led to a rapid cell death response that proceeded in a concentration-dependent manner. Compound 80 killed close to 100% of BMDMs after 6h of incubation with 25 μ M, while 10 μ M of Compound 80 triggered about 50% of BMDMs to undergo cell death by 24h (**Fig. 1b**). A component of the extracellular wall of bacteria, LPS, can act as a survival signal in macrophages by signaling through TLR4 to induce expression of NF- κ B-dependent anti-apoptotic proteins. However, priming BMDMs for 2h with LPS prior to Compound 80 stimulation did not alter the level or kinetics of cell death induction by Compound 80

at neither 25 μM and 10 μM of the inhibitor (**Fig. 1c**), suggesting that Compound 8o induces a cell death pathway that is insensitive to TLR4-induced survival signaling.

Several forms of regulated lytic cell death have recently been uncovered, with different effects on immune stimulation. Necroptosis is regulated by two members of the RIP kinase family, RIPK1 and RIPK3. Activation of these kinases downstream of death receptors and intracellular sensor proteins leads to phosphorylation of pseudokinase MLKL, the translocation of which to the plasma membrane triggers lysis of the cell⁷. To address whether PRCP inhibition with Compound 8o was mediated by the necroptosis machinery, we treated macrophages from RIPK1 D138N (RIPK1 KD) mutant macrophages, which lack RIPK1 kinase activity, with Compound 8o. Abrogation of the kinase activity of RIPK1 has been demonstrated to impair its functions for necroptosis induction, while allowing NF- κB signaling to occur⁸. Interestingly, RIPK1 kinase deficiency was unable to stop cell death from LPS-primed BMDMs treated with Compound 8o (**Fig. 2a**), suggesting that necroptosis is dispensable for Compound 8o-induced cytotoxicity. Consistent herewith, we found that MLKL-deficient BMDMs underwent plasma membrane permeabilization with unchanged kinetics relative to wildtype macrophages that had been treated with Compound 8o (**Fig. 2a**).

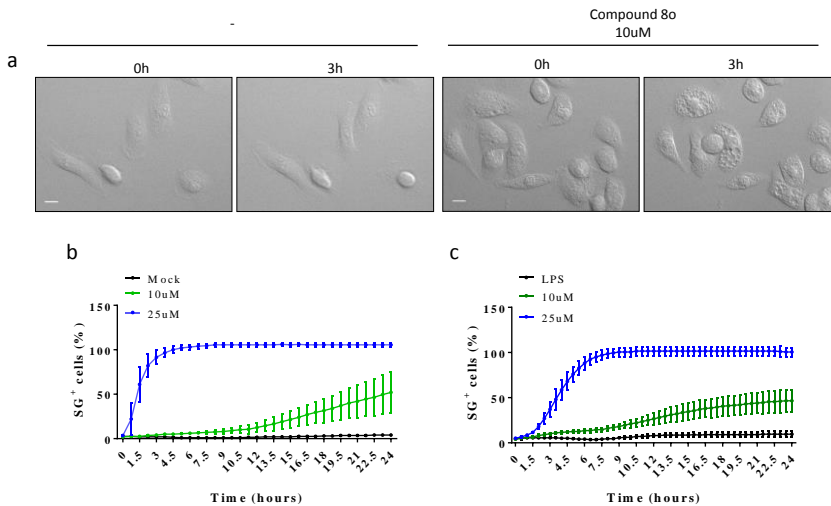


Figure 1. Compound 8o leads to toxicity of bone marrow-derived macrophages. **a**, BMDMs were treated with 10uM of Compound 8o or kept without treatment. DIC images were acquired at the beginning of the experiment and after 3h. **b**, BMDMs were treated with 10 μM or 25 μM of Compound 8o or mock-treated and imaged on an INCUCYTE in media containing Sytox Green. **c**, BMDMs were initially primed with LPS (100ng/ml) for 3h and then treated as in (**b**). The number of positive cells was quantified relative to a Triton-

x100-treated well (considered 100%). Values represent mean \pm SD of technical duplicates of a representative experiment from three biological repeats.

Activation of death receptors can also lead to caspase-8-dependent apoptosis⁹. Apoptotic cells typically pack their contents into apoptotic bodies and undergo cell death without spill out of cytoplasmic material. Nonetheless, failure in clearance of apoptotic cells, as occurs in cell culture models and patients with functional defects in the phagocytic machinery, eventually leads to a process called secondary necrosis, in which the plasma membrane of the apoptotic cell is compromised, and its intracellular cargo is released¹⁰. To examine the role of extrinsic apoptosis in the plasma membrane permeabilization observed after Compound 80 treatment, we studied whether caspase-8 deletion interferes with Compound 80-induced cell death in macrophages. Importantly, lack of caspase-8 is perinatally lethal, but mice are rescued from lethality by a RIPK3-deficient background¹¹. However, we found that combined deficiency in caspase-8 and RIPK3 failed to protect BMDMs from Compound 80-induced cytotoxicity (**Fig. 2b**), indicating that simultaneous blockade of both extrinsic apoptosis as well as necroptosis did not prevent cell death induction downstream of PRCP inhibition.

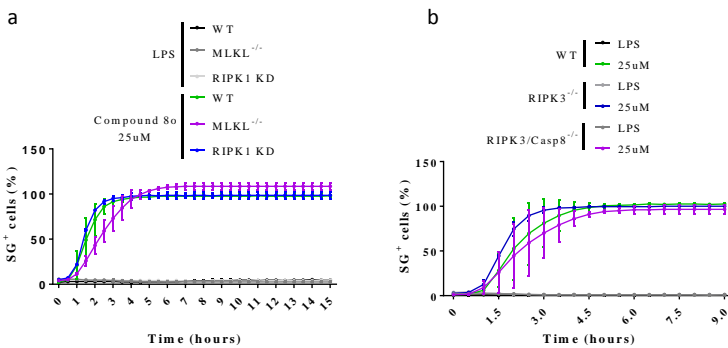


Figure 2. Compound 80 toxicity is not mediated by necroptosis. a, b, WT, RIPK1 D138N (RIPK1 KD), MLKL^{-/-} (a), RIPK3^{-/-} and RIPK3/Casp8^{-/-} (b) BMDMs were initially primed with LPS (100ng/ml) and treated with 25 μ M of Compound 80 or kept without treatment and imaged on an INCUCYTE in media containing Sytox Green. The number of positive cells was quantified relative to a Triton-x100-treated well (considered 100%) for each genotype. Values represent mean \pm SD of technical duplicates of a representative experiment from three biological repeats.

Pyroptosis is a distinct mechanism of lytic cell death that proceeds downstream of inflammasome activation. Inflammasomes are a set of cytosolic protein complexes that induce activation of caspase-1 in myeloid cells and epithelial cells. Caspase-1 subsequently cleaves its high affinity substrate, GSDMD^{12,13}. The free N-terminal GSDMD_N fragment then translocates to the plasma membrane and its oligomerization leads to highly structured GSDMD_N pores which are responsible for

lysis of the cell¹⁴⁻¹⁷. Active caspase-1 also cleaves the inactive precursor forms of cytokines pro-IL1 β and pro-IL18. Both cytokines lack an ER-Golgi targeting sequence, and therefore are not secreted through the classical ER-Golgi secretory system¹⁸. Instead, several reports suggest a role for cell death in secretion of these active cytokines^{13,19,20}. To understand whether Compound 80 triggers inflammasome activation in macrophages, we analyzed supernatants of Compound 80-treated BMDMs for IL1 β release. Notably, IL1 β was readily detected in the supernatants of BMDMs that had been stimulated with Compound 80 for 4h (Fig. 3a). Longer treatments of 8h and 24h with Compound 80 did not increase the level of IL1 β release, consistent with the high toxicity of the compound. Considering these results, we next addressed whether pyroptosis plays a role in the cell lysis observed with Compound 80. We made use of Caspase-1^{-/-}/Caspase-11^{-/-} BMDMs to prevent downstream inflammasome activation. Following treatment with Compound 80, however, these cells underwent cell death with similar kinetics and at similar levels relative to wildtype macrophages (Fig. 3b). Yet, lack of caspase-1 and caspase-11 completely abrogated IL1 β release, demonstrating that PRCP inhibition with Compound 80 induces inflammasome-dependent IL1 β release parallelly to inflammasome-independent cell death (Fig. 3c).

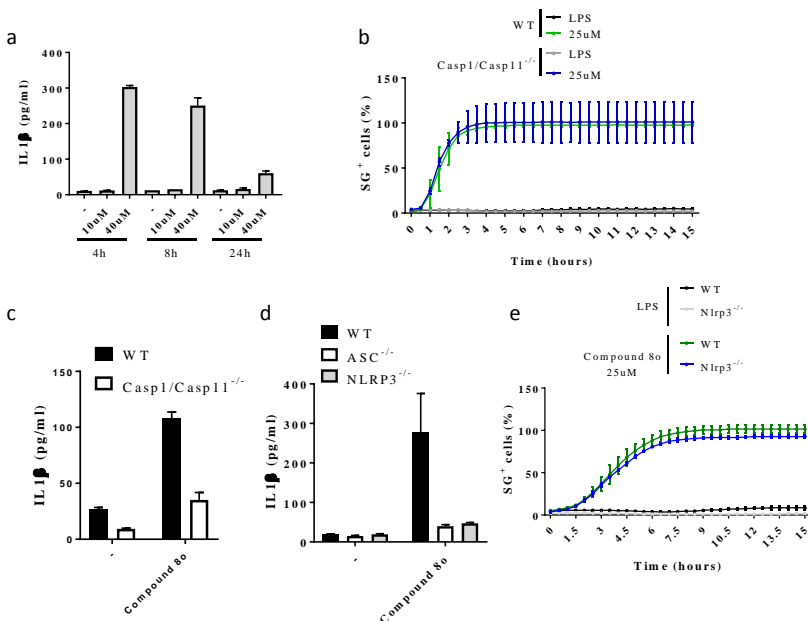


Figure 3. Compound 80 activates the NLRP3 inflammasome in macrophages. **a**, BMDMs were initially primed with LPS (100ng/ml) for 3h, then treated with 10 μ M or 40 μ M Compound 80 for either 4h, 8h and 24h, and their supernatants were assayed for IL1 β . **b**, **e**, WT and Caspase1/11^{-/-} (**b**), NLRP3^{-/-} and ASC^{-/-} (**e**)

BMDMs were initially primed with LPS (100ng/ml) and treated with 25 μ M of Compound 80 or kept without treatment and imaged on an INCUCYTE in media containing Sytox Green. The number of positive cells was quantified relative to a Triton-x100-treated well (considered 100%) for each genotype. **c, d**, WT, Caspase1/11^{-/-} (**c**), NLRP3^{-/-} and ASC^{-/-} (**d**) BMDMs were initially primed with LPS (100ng/ml) for 3h, then treated with 40uM Compound 80 for 4h, and their supernatants were assayed for IL1 β release. Values represent mean \pm SD of technical duplicates of a representative experiment from three biological repeats.

Caspase-1 activation can be elicited from several intracellular inflammasome receptors, with NLRP3 sensing a diverse variety of stimuli, including pore forming toxins, ATP, particulate matter and lysosomal damage¹⁸. NLRP3 associates with the bipartite protein ASC to form a cytosolic speck to which caspase-1 is recruited. NLRP3 activation has been shown to also occur downstream of lytic forms of cell death, such as caspase-11-triggered pyroptosis²¹ and MLKL-mediated necroptosis²⁰. In these systems, abrogation of either NLRP3, its binding partner ASC or caspase-1 stops IL1 β release but does not influence the cell death program elicited. To understand if NLRP3 could be responsible for the IL1 β release after PRCP inhibition, we probed WT, ASC^{-/-} and NLRP3^{-/-} BMDMs with Compound 80. Interestingly, in the absence of ASC or NLRP3 we could no longer detect IL1 β in the supernatant of Compound 80-treated BMDMs (**Fig. 3d**), establishing that the NLRP3 inflammasome is responsible for IL1 β release in Compound 80-treated macrophages. However, NLRP3 deletion did not alter toxicity of Compound 80 in macrophages supporting the notion that inflammasome activation is not responsible for the cell death elicited by this PRCP antagonist (**Fig. 3d**).

In conclusion, we have shown that use of a PRCP inhibitor, Compound 80, leads to a fast and lytic form of cell death in macrophages. This cell death was independent of RIPK1 kinase function, MLKL and RIPK3, discarding necroptosis as its mechanism. Furthermore, lack of caspase-8 and caspase-1/caspase-11 could not rescue BMDMs from Compound 80-induced cytotoxicity, demonstrating that extrinsic apoptosis and pyroptosis are dispensable for the cell death observed. Importantly, in the context of inflammasome signaling, lack of caspase-1 has been demonstrated to allow a shift to a caspase-8-dependent pathway, merely delaying death of triggered macrophages^{22,23}. However, in this scenario, caspase-8 and the cell death induced are under control of NF- κ B signaling for survival, and thus can be prevented by TLR stimulation^{23,24}. In our experimental settings, macrophages were primed with LPS before triggering cell death with Compound 80. Therefore, we believe the lack of effect is not due to a rapid cell death switch, but rather reflects that caspase-1 is not essential for the cell death program triggered by PRCP inhibition.

Interestingly, macrophages treated with Compound 80 matured and secreted IL1 β in a NLRP3, ASC and caspase-1/-11-dependent manner. *In vivo*, IL1 β has been shown to be able to promote neutrophilia in the context of a bacterial infection in order to promote pathogen clearance but can also contribute to overt local inflammation¹⁸. Our finding that IL1 β is released from macrophages treated with Compound 80 suggests that PRCP inhibition can have inflammatory effects *in vivo*. Furthermore, the NLRP3 response observed after PRCP inhibition occurred either downstream or independently of the cell death program. Further understanding of the cell death mechanism triggered after PRCP inhibition could answer its relationship to NLRP3 activation. Overall, to our knowledge, our research for the first time investigated the role of PRCP inhibition in macrophages and interrogated the contribution of the well described cell death pathways (i.e. necroptosis, pyroptosis and extrinsic apoptosis) to its toxicity. The high toxicity observed suggests that PRCP may regulate important physiological pathways, and its inhibition might have detrimental effects *in vivo*. Indeed, previous reports have suggested that downregulation of PRCP is related to reduction in cell proliferation and increased cell death, though this was considered to be independent on PRCP activity²⁵. Future research into PRCP targeting for clinical applications should take into consideration the possible toxic effects of Compound 80 in macrophages.

3.3.1.3. Methods

Mice. Casp8/RIPK3^{-/-}²⁶, RIPK1 D138N (RIPK1 KD)²⁷, RIPK3^{-/-}²⁸, MLKL^{-/-}²⁹, NLRP3^{-/-}³⁰, ASC^{-/-}³¹, Casp1/11^{-/-}³² mice have been reported. C57BL/6J mice were originally bought from the Jackson Laboratories and bred in-house. Mice were housed in individually ventilated cages and kept under pathogen-free conditions at the animal facilities of Ghent University. All animal experiments were conducted with permission of the ethics committee on laboratory animal welfare of Ghent University.

Primary macrophage differentiation and stimulation. Macrophages were differentiated by culturing bone marrow progenitor cells in Iscove's modified Dulbecco's medium (IMDM; Lonza) containing 10% (v/v) heat-inactivated FBS, 30% (v/v) L929 cell-conditioned medium, 1% (v/v) non-essential amino acids (Lonza), 100 U/ml penicillin and 100 mg/ml streptomycin at 37 °C in a humidified atmosphere containing 5% CO₂ for six days. Bone marrow-derived macrophages (BMDMs) were then seeded into 96 or 24 well plates as needed, in IMDM containing 10% FBS, 1% non-essential amino acids and antibiotics. On the next day, cells were changed to

fresh media and either primed or not with LPS (100ng/ml) for 3h prior to treatment with Compound 8o (water) at either 10, 25 or 40 μ M.

Imaging of macrophages. BMDMs grown on 8-well μ -slide chambers (Ibidi) were either left untreated or received 10 μ M of Compound 8o. DIC images were acquired using an observer Z.1 spinning disk microscope (Zeiss, Zaventem, Belgium) equipped with a Yokogawa disk CSU-X1.

Cell death kinetics (Incucyte). Analysis of cell death was performed through incorporation of 500 nM of Sytox Green dye (S7020, Thermo Scientific) in a 96-well format assay. Data was acquired with a 10x objective using the IncuCyte Zoom system (Essen BioScience) in a CO₂ and temperature-controlled environment. Each condition was run in (technical) duplicates. The number of fluorescent objects was counted with Incucyte ZOOM (Essen BioScience) software and was plotted considering as 100% the highest value obtained in a well treated with Triton-x100.

Cytokine analysis. Unless otherwise stated, cell supernatant was collected after 4h of stimulation, and the culture medium was measured by magnetic bead-based multiplex assay using Luminex technology (Bio-Rad) according to the manufacturer's instructions.

3.3.1.4. References

- 1 Soisson, S. M. *et al.* Structural definition and substrate specificity of the S28 protease family: the crystal structure of human prolylcarboxypeptidase. *BMC Struct Biol* **10**, 16, doi:10.1186/1472-6807-10-16 (2010).
- 2 Jeong, J. K. & Diano, S. Prolyl carboxypeptidase and its inhibitors in metabolism. *Trends Endocrinol Metab* **24**, 61-67, doi:10.1016/j.tem.2012.11.001 (2013).
- 3 Wang, L. *et al.* Prolylcarboxypeptidase gene, chronic hypertension, and risk of preeclampsia. *Am J Obstet Gynecol* **195**, 162-171, doi:10.1016/j.ajog.2006.01.079 (2006).
- 4 Kumamoto, K., Stewart, T. A., Johnson, A. R. & Erdos, E. G. Prolylcarboxypeptidase (angiotensinase C) in human lung and cultured cells. *The Journal of clinical investigation* **67**, 210-215, doi:10.1172/JCI110015 (1981).
- 5 Jackman, H. L. *et al.* Plasma membrane-bound and lysosomal peptidases in human alveolar macrophages. *Am J Respir Cell Mol Biol* **13**, 196-204, doi:10.1165/ajrcmb.13.2.7626287 (1995).
- 6 Zhou, C. *et al.* Design and synthesis of prolylcarboxypeptidase (PrCP) inhibitors to validate PrCP as a potential target for obesity. *J Med Chem* **53**, 7251-7263, doi:10.1021/jm101013m (2010).
- 7 Weinlich, R., Oberst, A., Beere, H. M. & Green, D. R. Necroptosis in development, inflammation and disease. *Nature reviews. Molecular cell biology* **18**, 127-136, doi:10.1038/nrm.2016.149 (2017).

- 8 Berger, S. B. *et al.* Cutting Edge: RIP1 kinase activity is dispensable for normal development but is a key regulator of inflammation in SHARPIN-deficient mice. *Journal of immunology* **192**, 5476-5480, doi:10.4049/jimmunol.1400499 (2014).
- 9 Ashkenazi, A. & Salvesen, G. Regulated cell death: signaling and mechanisms. *Annual review of cell and developmental biology* **30**, 337-356, doi:10.1146/annurev-cellbio-100913-013226 (2014).
- 10 Wickman, G., Julian, L. & Olson, M. F. How apoptotic cells aid in the removal of their own cold dead bodies. *Cell death and differentiation* **19**, 735-742, doi:10.1038/cdd.2012.25 (2012).
- 11 Kaiser, W. J. *et al.* RIP3 mediates the embryonic lethality of caspase-8-deficient mice. *Nature* **471**, 368-372, doi:10.1038/nature09857 (2011).
- 12 He, W. T. *et al.* Gasdermin D is an executor of pyroptosis and required for interleukin-1beta secretion. *Cell research* **25**, 1285-1298, doi:10.1038/cr.2015.139 (2015).
- 13 Kayagaki, N. *et al.* Caspase-11 cleaves gasdermin D for non-canonical inflammasome signalling. *Nature* **526**, 666-671, doi:10.1038/nature15541 (2015).
- 14 Aglietti, R. A. *et al.* GsdmD p30 elicited by caspase-11 during pyroptosis forms pores in membranes. *Proceedings of the National Academy of Sciences of the United States of America* **113**, 7858-7863, doi:10.1073/pnas.1607769113 (2016).
- 15 Ding, J. *et al.* Pore-forming activity and structural autoinhibition of the gasdermin family. *Nature* **535**, 111-116, doi:10.1038/nature18590 (2016).
- 16 Liu, X. *et al.* Inflammasome-activated gasdermin D causes pyroptosis by forming membrane pores. *Nature* **535**, 153-158, doi:10.1038/nature18629 (2016).
- 17 Sborgi, L. *et al.* GSDMD membrane pore formation constitutes the mechanism of pyroptotic cell death. *The EMBO journal* **35**, 1766-1778, doi:10.15252/embj.201694696 (2016).
- 18 Lamkanfi, M. & Dixit, V. M. Mechanisms and functions of inflammasomes. *Cell* **157**, 1013-1022, doi:10.1016/j.cell.2014.04.007 (2014).
- 19 Shi, J. *et al.* Cleavage of GSDMD by inflammatory caspases determines pyroptotic cell death. *Nature*, doi:10.1038/nature15514 (2015).
- 20 Conos, S. A. *et al.* Active MLKL triggers the NLRP3 inflammasome in a cell-intrinsic manner. *Proceedings of the National Academy of Sciences of the United States of America* **114**, E961-E969, doi:10.1073/pnas.1613305114 (2017).
- 21 Kayagaki, N. *et al.* Non-canonical inflammasome activation targets caspase-11. *Nature* **479**, 117-121, doi:10.1038/nature10558 (2011).
- 22 Rauch, I. *et al.* NAIP-NLRC4 Inflammasomes Coordinate Intestinal Epithelial Cell Expulsion with Eicosanoid and IL-18 Release via Activation of Caspase-1 and -8. *Immunity* **46**, 649-659, doi:10.1016/j.immuni.2017.03.016 (2017).
- 23 Van Opdenbosch, N. *et al.* Caspase-1 Engagement and TLR-Induced c-FLIP Expression Suppress ASC/Caspase-8-Dependent Apoptosis by Inflammasome Sensors NLRP1b and NLRC4. *Cell reports* **21**, 3427-3444, doi:10.1016/j.celrep.2017.11.088 (2017).
- 24 Lee, B. L. *et al.* ASC- and caspase-8-dependent apoptotic pathway diverges from the NLRC4 inflammasome in macrophages. *Scientific reports* **8**, 3788, doi:10.1038/s41598-018-21998-3 (2018).
- 25 Adams, G. N. *et al.* Prolylcarboxypeptidase promotes angiogenesis and vascular repair. *Blood* **122**, 1522-1531, doi:10.1182/blood-2012-10-460360 (2013).

- 26 Newton, K. *et al.* Activity of protein kinase RIPK3 determines whether cells die by necroptosis or apoptosis. *Science* **343**, 1357-1360, doi:10.1126/science.1249361 (2014).
- 27 Berger, S. B. *et al.* Cutting Edge: RIP1 kinase activity is dispensable for normal development but is a key regulator of inflammation in SHARPIN-deficient mice. *Journal of immunology* **192**, 5476-5480, doi:10.4049/jimmunol.1400499 (2014).
- 28 Newton, K., Sun, X. & Dixit, V. M. Kinase RIP3 is dispensable for normal NF-kappa Bs, signaling by the B-cell and T-cell receptors, tumor necrosis factor receptor 1, and Toll-like receptors 2 and 4. *Molecular and cellular biology* **24**, 1464-1469 (2004).
- 29 Murphy, J. M. *et al.* The pseudokinase MLKL mediates necroptosis via a molecular switch mechanism. *Immunity* **39**, 443-453, doi:10.1016/j.immuni.2013.06.018 (2013).
- 30 Mariathasan, S. *et al.* Cryopyrin activates the inflammasome in response to toxins and ATP. *Nature* **440**, 228-232, doi:10.1038/nature04515 (2006).
- 31 Mariathasan, S. *et al.* Differential activation of the inflammasome by caspase-1 adaptors ASC and Ipaf. *Nature* **430**, 213-218, doi:10.1038/nature02664 (2004).
- 32 Kuida, K. *et al.* Altered cytokine export and apoptosis in mice deficient in interleukin-1 beta converting enzyme. *Science* **267**, 2000-2003 (1995).

3.3.2. DPP8/DPP9 inhibitors as activators of NLRP1b

Section 3.3.2. is structured as the manuscript: de Vasconcelos, N.M.; Van Opdenbosch, N.; Vliegen, G.; Van Der Veken, P.; De Meester, I.; Lamkanfi, M. Inhibition of DPP8/DPP9 elicits an NLRP1b-dependent inflammasome activation. In preparation.

3.3.2.1. Abstract

The dipeptidases DPP8 and DPP9 have been implicated in a number of inflammatory pathologies, but their role remains elusive. Recently, pharmacological inhibition of DPP8/DPP9 was suggested to trigger inflammasome-dependent cytokine release, although the mechanism involved is ill-defined. Here we demonstrate that transgenic expression of the 129S-allele of *Nlrp1b* in C57/BL6 (B6^{Nlrp1b+}) sensitizes mouse macrophages to cell death after inhibition of DPP8/DPP9 by Val-boroPro or 1G244. The cytotoxic effects observed are accompanied by enhanced IL1 β and IL18 release, consistent with an inflammasome-dependent response. 1G244 triggered cell death and cytokine release in B6^{Nlrp1b+} macrophages were partially hampered by pre-treatment with the proteasomal inhibitor, MG132. Further, ablation of ASC in a B6^{Nlrp1b+} background still allowed cell death to proceed after either Val-boroPro or 1G244 treatments, while lack of caspase-1 delayed cell death and prevented IL1 β and IL18 release. Therefore, inhibition of DPP8/DPP9 activates the Nlrp1b inflammasome.

3.3.2.2. Introduction

Serine proteases from the prolyl oligopeptidases family cleave dipeptides after a Proline located, mostly, at the N-terminal site of a protein sequence. DPPIV, FAP, DPP8, DPP9, DPP2 and PREP can be broadly considered within the same family, given their shared substrate specificity and high level of homology¹. These proteases have been shown to play distinct roles in inflammation and immune responses, acting in the regulation of T cell activation, bioavailability of chemokines and tissue remodelling². Inhibition of prolyl oligopeptidases are a promising target given their roles in disease pathologies with inflammatory components such as atherosclerosis. Nevertheless, inhibitor specificity within the family has been a challenging issue¹.

While the substrates and roles of DPP2 and PREP are still elusive¹, the prototypical member of the family DPPIV is used as a target in the clinic for control of type 2 diabetes^{3,4}. FAP, on the other hand, has collagenase activity and plays roles in wound healing and tumorigenesis². Clinical trials have been undertaken with a FAP inhibitor, Val-boroPro (VBP), for therapy of advanced non-small cell lung carcinoma and melanoma^{5,6}. While there was a therapeutic response with VBP administration, concerns on its safety lead to termination of the study². Indeed, VBP is also a potent inhibitor of DPP8, DPP9 and DPP4.

DPP8 and DPP9 are the most homologous proteases in the family. Control of protein turnover, antigen presentation and inflammation are some of the functions associated to DPP9 activity^{7,8}. However defining DPP8/DPP9 roles in physiological conditions is a challenging endeavour².

Inflammasomes play important roles during inflammatory responses against pathogenic invasion⁹. These cytosolic platforms rely on the sensing of a variety of intracellular danger or pathogen associated molecules by pattern recognition receptors of the Nod-like receptors and AIM2-like receptors families and Pyrin¹⁰. Once triggered, they assemble with the bipartite molecule ASC to form the inflammasome platform. Caspase-1 is a serine protease produced as a zymogen in the cytosol and relies on the recruitment to inflammasomes for proximity-induced autoactivation⁹. Active caspase-1 cleaves and activates the pro-form cytokines pro-IL1 β and pro-IL18⁹. Further, caspase-1 cleaves GSDMD^{11,12}, releasing an N-terminal fragment which translocates to the plasma membrane and perforates it during pyroptotic cell death¹³⁻¹⁶. Therefore, caspase-1 acts to both activate IL1 β and IL18 and to promote their release through GSDMD-mediated pyroptotic cell death.

Remarkably, Val-boroPro (VBP) and its activity in DPP8 and DPP9 inhibition has been suggested to induce procaspase-1-dependent cell death in the human monocytic-like cell THP1, seemingly in the absence of an upstream inflammasome receptor¹⁷. While caspase-1 can be activated in the absence of cleavage, this mechanistically is associated to the lack of ASC after engagement of CARD-containing receptors¹⁸⁻²⁰. Therefore, it remained unclear how VBP engaged caspase-1 independently of inflammasome sensors and how it activates caspase-1 without induced autocleavage in THP1 cells.

A further publication suggested a role for the NLRP1b inflammasome in VBP activity²¹. Most of the data on VBP activity is done in RAW cells, a macrophage cell line originated from Balb/c mice. However, *in vivo* studies and analysis of primary macrophages are in cells derived from C57BL/6J mice, which express a *Nlrp1b* allele that is considered inactive²². While humans only have one *Nlrp1* gene, mice have three orthologues: *Nlrp1a*, *Nlrp1b* and *Nlrp1c*. *Nlrp1c* is regarded as a pseudogene, whereas an activating mutation on *Nlrp1a* has been shown to be linked to inflammasome assembly and pyroptosis in hematopoietic progenitor cells²³. The best characterized mouse Nlrp1 orthologue is Nlrp1b, whose activation and inflammasome assembly have been shown to occur after *Bacillus anthracis* derived LeTx triggering^{22,24}. Furthermore, five different alleles of *Nlrp1b* are encoded in various mice strains²². Allele 1, found in 129S and Balb/c mice, and allele 5, found in the CAST/EiJ line, promote susceptibility of their macrophages to LeTx intoxication. On the other hand, allele 2, found in A/J and C57BL/6J mice together with alleles 3 and 4 in other inbred strains, confer resistance of macrophages from these mouse strains to LeTx.

Cleavage of the allele 1 of NLRP1b (for clarity, here called NLRP1b1) at its FIIND domain, LeTx catalytic activity and proteasome function are the determinants of NLRP1b1 inflammasome activation^{25,26}, though it is still not understood how these events relate to one another. Therefore, the current work aimed at clarifying the ability of DPP8/DPP9 inhibition to activate an inflammasome, to determine the inflammasome receptor responsible for the IL1 β and IL18 release and the mechanism of cell death induction.

3.3.2.3. Results

DPP8/DPP9 inhibitors induce macrophage cell death and IL1 β and IL18 release

To validate the ability of VBP to induce toxicity in murine primary macrophages, bone marrow-derived macrophages (BMDMs) were treated with increasing concentrations of VBP, and the kinetics of cell death was tracked on an Incucyte platform. Staining by Sytox Green, a membrane-impermeable dye, was used as a marker for lytic cell death. When analysed for 24h for incorporation of Sytox Green, VBP induced a low, but consistent levels of BMDM cell death, accounting for at most 30% of toxicity at 24h at all concentrations tested (**Fig. 1a**). A modification at the n-terminal end of VBP has been shown to hamper its inhibitory activity. Interestingly, N-acetyl-VBP (NacVBP) failed to induce toxicity in BMDMs (**Fig. 1b**), suggesting VBP toxic effects are due to its inhibition of the catalytic activity of DPP proteases. However, an alteration to a cyclic form shown to improve VBP (CyclicVBP) stability also failed to induce BMDM toxicity up to 24h (**Fig. 1c**).

VBP has been shown to not specifically inhibit DPP8 and DPP9, also acting on DPP4 and FAP with similar affinity. To understand whether the effect we observed was specific to any of these dipeptidases, we made use of inhibitors with a more confined selectivity profile and analysed BMDM cell death. Sitagliptin, UAMC0039, UAMC01110, KYP-2047/UAMC0714 have been shown to specifically inhibit DPP4, DPP2, FAP and PREP, respectively. However, none of these inhibitors were able to induce BMDM cell death when used in similar concentrations than VBP (**Fig. 1d-g**). This suggests that the toxicity observed with VBP treatment is related to its inhibition of DPP8/DPP9. Confirming this hypothesis, 1G244, which is regarded as a specific DPP8/DPP9 inhibitor, induced cell death in BMDMs more efficiently than VBP (**Fig. 1h**). Therefore, DPP8/DPP9 inhibition is toxic to BMDMs.

Inhibition of DPP8 and DPP9 leads to IL1 β release in NLRP1b1-dependent and independent pathways

Macrophage cell death is often regarded as a mechanism of cytokine secretion, particularly for IL1 β and IL18 through activation of inflammasomes. Furthermore, VBP has been shown to induce IL1 β and IL18 secretion in human macrophages, though through a still ill-defined mechanism. Therefore, to validate VBP activities in BMDMs, we primed macrophages with LPS and subsequently treated them with VBP. VBP treatment led to a low, but consistent secretion of IL1 β and IL18 in the supernatant of BMDMs, particularly at 24h post stimulation (**Fig. 2a, b**). NacVBP was unable to induce IL1 β secretion up to 24h post-treatment (**Fig. 2c**), suggesting VBP needs to inhibit a catalytic activity to activate an inflammasome. Correlating with our previous cell death data, CyclicVBP also did not induce any IL1 β release, but IL1 β

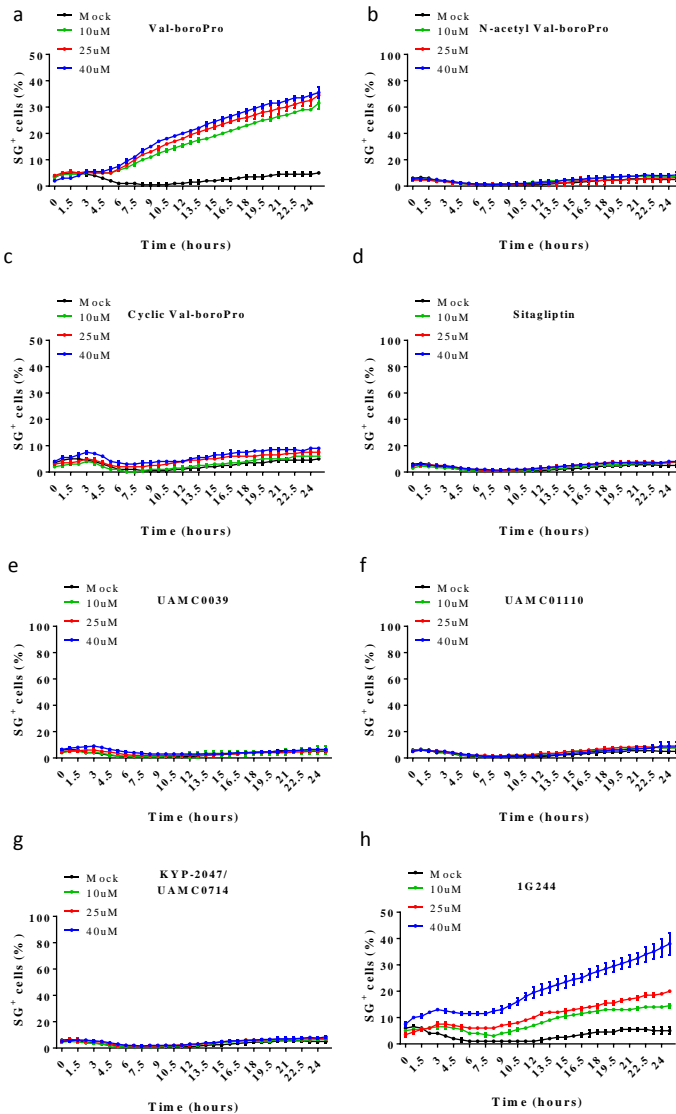


Figure 1. Inhibition of DPP8/DPP9 by Val-boroPro and 1G244 is toxic to primary BMDMs. a-h, B6 BMDMs were treated with 10, 25 or 40 μM of Val-boroPro (a), N-acetyl-Val-boroPro (b), Cyclic-Val-boroPro (c), Sitagliptin (d), UAMC0039 (e), UAMC01110 (f), KYP-2047/UAMC0714 (g) or 1G244 (h) or mock-treated and imaged on an INCUCYTE platform in media containing Sytox Green. The number of positive cells was quantified relative to a Triton-x100-treated well (considered 100%). Values represent mean ± SD of technical duplicates of a representative experiment from three biological repeats.

could be readily detected in the supernatant of 1G244-treated macrophages from 8h post-stimulation (Fig. 2d, e). IL18 could not be detected in the supernatant of NacVBP, CyclicVBP and 1G244 treated BMDMs (data not shown).

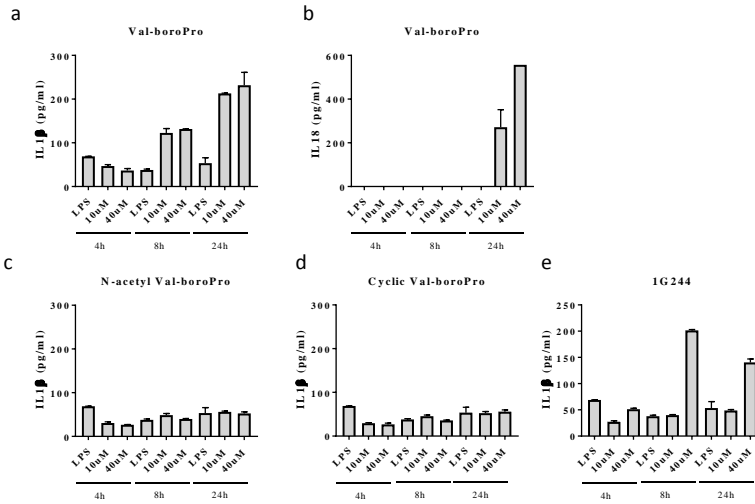


Figure 2. BMDMs treated with Val-boroPro or 1G244 release IL1 β and IL18. **a, c-e**, B6 BMDMs were initially primed with LPS (100ng/ml) for 3h, then treated with 10 μ M or 40 μ M of Val-boroPro (**a, b**), N-acetyl-Val-boroPro (**c**), Cyclic-Val-boroPro (**d**) or 1G244 (**e**). Collected supernatants after 4h, 8h and 24h were assayed for IL1 β (**a, c-e**) or IL18 (**b**). Values represent mean \pm SD of technical duplicates of a representative experiment from three biological repeats.

While we could detect low levels of IL1 β after VBP treatment, these were not in line with previous reports of DPP8/DPP9 inhibition on THP1 human cells. All inflammasome receptors are similarly represented in human and mouse macrophages, except for the NLRP1 family members. Humans have only one *Nlrp1* gene, but mice have three orthologues *Nlrp1a*, *Nlrp1b* and *Nlrp1c*. Furthermore, from the five *Nlrp1b* alleles existing throughout mice strains, the allele 1 found in 129S mice confers susceptibility to *B. anthracis*-derived LeTx, while allele 2 present in C57BL/6J hinders their response to LeTx. To compare the role of NLRP1b in C57BL/6J macrophages, we made use of transgene expression of the 129S-derived *Nlrp1b* allele (*Nlrp1b1*) in B6 macrophages which has been shown to render these sensitive to LeTx intoxication. Similarly, B6^{Nlrp1b1+} macrophages were sensitized to DPP8/DPP9 inhibition by VBP, CyclicVBP and 1G244 (**Fig. 3a, c, d**). Furthermore, NacVBP still had no effects on B6^{Nlrp1b1+} BMDMs (**Fig. 3b**), confirming that the effects observed are due to catalytic inhibition of DPP8/DPP9. Cytokine analysis detected IL1 β and IL18 on supernatant of B6^{Nlrp1b1+} BMDMs 4h after treatment by VBP and 1G244 (**Fig. 3 e, f, j, k**), which accumulated up to 24h. Furthermore, CyclicVBP induced IL1 β and IL18 release in B6^{Nlrp1b1+} BMDMs, while NacVBP failed to do so (**Fig. 3g-i**). Therefore,

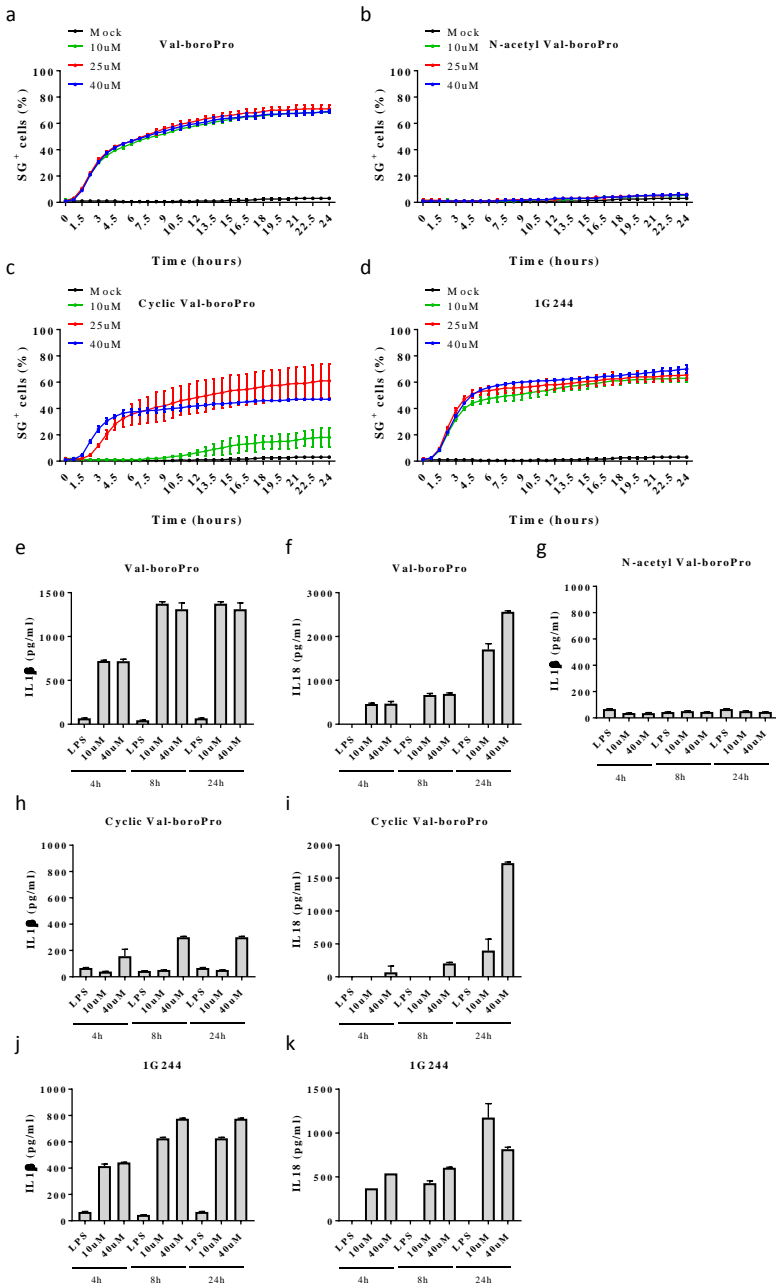


Figure 3. Presence of 129-derived allele of *Nlrp1b* sensitises macrophages to DPP8/DPP9 inhibition. a-d, B6^{Nlrp1b1+} BMDMs were treated with 10, 25 or 40 μM of Val-boroPro (a), N-acetyl-Val-boroPro (b), Cyclic-Val-boroPro (c) or 1G244 (d) or mock-treated and imaged on an INCUCYTE platform in media containing Sytox Green. The number of positive cells was quantified relative to a Triton-x100-treated well (considered 100%). Values represent mean ± SD of technical duplicates of a representative experiment from three biological repeats. e-k, B6^{Nlrp1b1+} BMDMs were initially primed with LPS (100ng/ml) for 3h, then treated with 10 μM or 40

μM of Val-boroPro (e, f), N-acetyl-Val-boroPro (g), Cyclic-Val-boroPro (h, i) or 1G244 (j, k). Supernatants collected after 4h, 8h and 24h were assayed for IL1 β (e, g, h, j) or IL18 (f, i, k). Values represent mean \pm SD of technical duplicates of a representative experiment from three biological repeats.

inhibition of DPP8/DPP9 by VBP or 1G244 leads to NLRP1b inflammasome activation, when in presence of *Nlrp1b* allele 1.

DPP8/DPP9-mediated Nlrp1b1 activation is not hampered by absence of ASC but partially requires proteasomal activity for activation

Inhibition of the proteasome by MG132 hampers activation of the NLRP1b inflammasome by its canonical trigger LeTx. To understand if the proteasome requirement was a shared event after DPP8/DPP9 inhibition, we pre-treated B6^{Nlrp1b1+} BMDMs with MG132 prior to 1G244 stimulation. Interestingly, MG132 delayed cell death after 1G244 treatment in B6^{Nlrp1b1+} BMDMs, but was unable to fully protect cells (Fig. 4a). Release of IL1 β and IL18 cytokines, on the other hand, was reduced to background levels when cells were treated with MG132 prior to 1G244 (Fig. 4b, c), suggesting a conserved upstream pathway of the NLRP1b inflammasome activation.

NLRP1b and NLRC4 proteins contain CARD domains. Therefore, these receptors are unique as they do not fully depend on the adaptor molecule ASC to bridge their interaction with caspase-1. As it was shown after LeTx-triggering, B6^{Nlrp1b1+ASC-/-} BMDMs still underwent cell death after both VBP and 1G244 stimulation, though at diminished levels (Fig. 4d, e). Thus, our results so far established that the upstream requirements for NLRP1b activation, namely the need for proteasomal activity but not ASC, are shared between LeTx intoxication and DPP8/DPP9 inhibition.

DPP8/DPP9 inhibition leads to pyroptosis in Nlrp1b1 sufficient cells

Inflammasomes act as platforms for caspase-1 activation, which cleave its high affinity substrate GSDMD for pyroptotic cell death. Treatment with VBP and 1G244 led to a lytic form of cell death which was mostly NLRP1b-dependent (Fig. 1 and Fig. 2). Therefore, we hypothesized that DPP8/DPP9 inhibition could promote caspase-1-dependent pyroptosis. Indeed, B6^{Nlrp1b1+} BMDMs deficient for caspase-1/-11 were protected from cell death after both VBP and 1G244 treatments (Fig. 4d, e). Lack of caspase-1/-11 in the B6^{Nlrp1b1+} background also prevented release of IL1 β and IL18 in the supernatant of BMDMs treated with 1G244 (Fig. 4f, g). Interestingly, triggering NLRP1b inflammasome with LeTx in the absence of caspase-1/-11 has been shown to only delay cell death, promoting a switch to a caspase-8-dependent apoptosis. In this scenario, either lack of both ASC and caspase-1/-11 or TLR-stimulation abrogates cell

death by impairing caspase-8 activation. However, after VBP and 1G244 treatment, ablation of caspase-1/-11 was sufficient to protect BMDMs from cell death during the time analysed, demonstrating a toxicity curve similar to the ASC/Caspase-1/Caspase-11^{-/-} cells (Fig. 4d, e). Therefore, DPP8/DPP9 inhibition by VBP and 1G244 represents a canonical NLRP1b inflammasome trigger, causing downstream caspase-1-dependent pyroptosis and IL1 β and IL18 release.

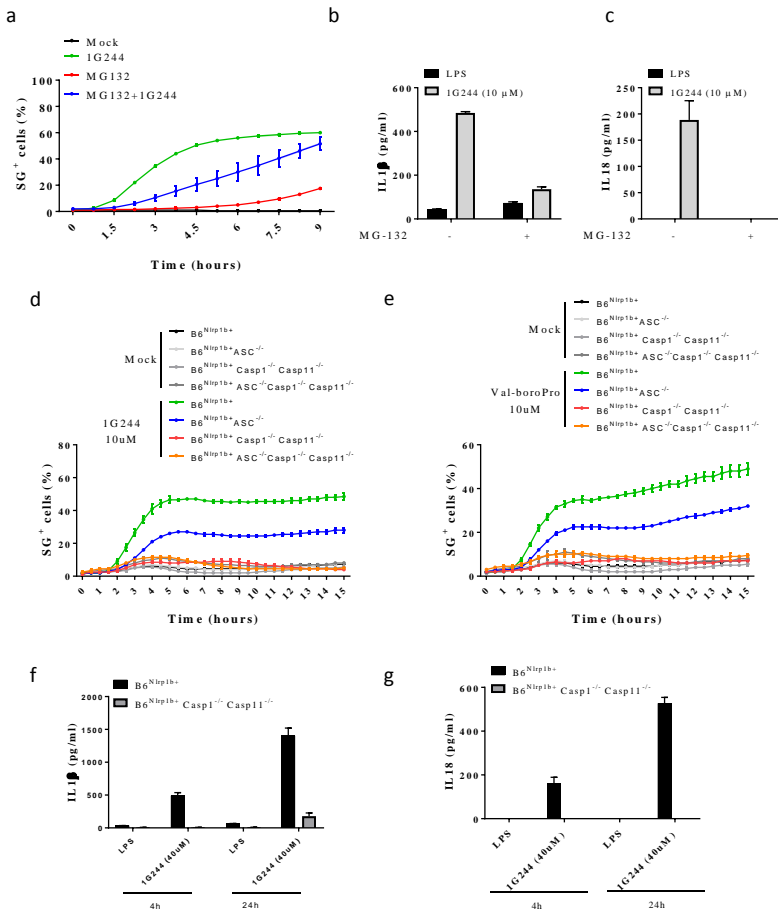


Figure 4. DPP8/DPP9 inhibition leads to MG-132-mediated, ASC independent and caspase-1/11-dependent activation of the NLRP1b inflammasome. **a**, B6^{Nlrp1b}^{+/+} BMDMs were triggered with 10 μ M 1G244 or mock-treated in presence or absence of MG132 and imaged on an INCUCYTE platform in media containing Sytox Green. The number of positive cells was quantified relative to a Triton-x100-treated well (considered 100%). Values represent mean \pm SD of technical duplicates of a representative experiment from two biological repeats. **b**, **c**, LPS-primed B6^{Nlrp1b}^{+/+} BMDMs were treated as in (a) and supernatants collected after 4h for IL1 β (b) or IL18 (c) measurement in the supernatant. Values represent mean \pm SD of technical duplicates of a representative experiment from two biological repeats. **d**, **e**, B6^{Nlrp1b}^{+/+}, B6^{Nlrp1b}^{+/+} ASC^{-/-}, B6^{Nlrp1b}^{+/+} Casp1^{-/-}, B6^{Nlrp1b}^{+/+} ASC^{-/-} Casp1^{-/-}, B6^{Nlrp1b}^{+/+} ASC^{-/-} Casp1^{-/-} Casp11^{-/-} BMDMs were treated with 10 μ M of either 1G244 (d) or Val-boroPro (e) or mock-treated and imaged on an INCUCYTE platform in media containing Sytox Green. The number of positive cells was quantified relative to a Triton-x100-treated well (considered 100%) for each genotype.

Values represent mean \pm SD of technical duplicates of one biological repeat. **f, g**, LPS-primed B6^{Nlrp1b1+} and B6^{Nlrp1b1+}Caspase-1/-11^{-/-} BMDMs were treated as in **(d)** and supernatants collected after 24h for IL1 β (**f**) or IL18 (**g**) measurement in the supernatant. Values represent mean \pm SD of technical triplicates of one biological repeat.

3.3.2.4. Discussion

In the current study, we have demonstrated that DPP8 and DPP9 inhibition is a trigger for inflammasome activation. In NLRP1b1⁺ cells, containing the 129 allele 1, treatment with VBP and 1G244 led to fast cell death and IL1 β and IL18 release, both events being controlled by caspase-1. Furthermore, ASC deficiency was unable to hamper cell death after 1G244 and VBP treatment, while proteasome inhibition by MG132 partially impaired cell death and cytokine release. Therefore, in NLRP1b competent cells, inhibition of DPP8 and DPP9 leads to a canonical NLRP1b inflammasome activation and pyroptosis, sharing conserved regulatory mechanisms with the LeTx trigger. These results suggest that the NLRP1b inflammasome is a sensor of DPP8/DPP9 activity. Whether the activity of DPP8/DPP9 in the NLRP1b protein is direct or indirect is still to be determined. Our results also demonstrated that absence of NLRP1b delayed cell death and cytokine production, but both effects were still present at 24h post treatment. Further studies will be needed to delineate the contribution of other inflammasome receptors in B6 cells after DPP8/DPP9 inhibition.

While DPP8 function is still elusive, DPP9 activity has been implicated in cell viability of T lymphocytes and human skin cells^{27,28}. In line with our results in which primary macrophages derived from either B6^{Nlrp1b1+} or pure B6 have differential responses after DPP8/DPP9 inhibition, toxicity of DPP8/DPP9 inhibition has been demonstrated to be more prominent in the J774.A macrophage cell line, originated from Balb/c mice, than in C57BL/6J primary macrophages²⁹. Furthermore, a S739A point mutation hampers DPP9 proteolytic activity and prevents mice from developing passed neonatal stage³⁰. Remarkably, DPP9^{S739A/S739A} mice were developed in C57BL/6J background. Our observation that B6 macrophages die upon DPP8/DPP9 inhibition and release IL1 β suggests that the lethality observed in DPP9^{S739A/S739A} mice might be related to an overt cell death and immune overactivation. A more in-depth analysis of the immune compartments of DPP9^{S739A/S739A} mutant mice would be needed to understand the physiological functions for DPP9 activity.

In conclusion, DPP8/DPP9 proteases control inflammasome-dependent responses, which are enhanced in an NLRP1b-dependent manner. Characterization of

pathogens able to inhibit DPP8/DPP9 could shed light on the physiological roles of the NLRP1b inflammasome. Further studies on the role of DPP8/DPP9 in the B6 background could aid in understanding its developmental role.

3.3.2.5. Methods

Mice. ASC^{-/-} ³¹, Casp1/11^{-/-} ³² and B6^{Nlrp1b1+} ³³ mice have been reported, and the genotypes thereof obtained by breeding. C57BL/6J mice were originally bought from the Jackson Laboratories and bred in-house. Mice were housed in individually ventilated cages and kept under pathogen-free conditions at the animal facilities of Ghent University. All animal experiments were conducted with permission of the ethics committee on laboratory animal welfare of Ghent University.

Reagents. Recombinant expression and purification of *B. anthracis* protective antigen (PA) was performed as described. *B. anthracis* lethal factor (LF) was acquired from List Biologicals. Sytox Green (S7020) was purchased from Thermo Scientific. The antibody for caspase-1 (AG-20B-0042-C10) was acquired from Adipogen. HRP-conjugated secondary antibody was acquired from Jackson Immunoresearch Laboratories and enhanced chemiluminescence solution was from Thermo Scientific. LPS-SM (tlrl-smlps) was acquired from Invivogen.

Primary macrophage differentiation and stimulation. Macrophages were differentiated by culturing bone marrow progenitor cells in Iscove's modified Dulbecco's medium (IMDM; Lonza) containing 10% (v/v) heat-inactivated FBS, 30% (v/v) L929 cell-conditioned medium, 1% (v/v) non-essential amino acids (Lonza), 100 U/ml penicillin and 100 mg/ml streptomycin at 37 °C in a humidified atmosphere containing 5% CO₂ for six days. Bone marrow-derived macrophages (BMDMs) were then seeded into 96 or 24 well plates as needed, in IMDM containing 10% FBS, 1% non-essential amino acids and antibiotics. On the next day, cells were changed to fresh media and either primed or not with LPS (100ng/ml) for 3h prior to treatment with Sitagliptin (water), 1G244 (DMSO), UAMC0039 (water), UAMC01110 (DMSO), Val-boroPro (0,1%TFA in DMSO), N-acetyl Val-boroPro (DMSO), Cyclic Val-boroPro (0,1%TFA in DMSO) or KYP-2047/UAMC0714 (DMSO) at either 10, 25 or 40uM (**Table 1**). For NLRP1b inflammasome activation, cells were stimulated with LeTx (1 µg/ml PA combined with 0,5 µg/ml LF).

Table 1. Summary of the inhibitors used in the study and their IC₅₀ values for DPPIV family members. Values represent IC₅₀ (nM).

	DPP-IV	DPP8	DPP9	FAP	PREP	DPP-II	Ref
Val-boroPro	4	11	560	390	>100,000	n/a	34
1G244	>100,000	14	53	>100,000	n/a	n/a	35
Sitagliptin	10	48000	>100000	>100000	n/a	n/a	36
UAMC01110	>100000	>100000	>100000	11	>50000	n/a	37
UAMC00039	165000	142 000	78600	n/a	n/a	0.48	38
KYP-2047	>100000	n/a	>100000	>100000	6	>100000	39

Cell death kinetics (Incucyte). Analysis of cell death was performed through incorporation of 500 nM of Sytox Green dye in a 96-well format assay. Data was acquired with a 10x objective using the Incucyte Zoom system (Essen BioScience) in a CO₂ and temperature-controlled environment. Each condition was run in (technical) duplicates. The number of fluorescent objects was counted with Incucyte ZOOM (Essen BioScience) software and was plotted considering as 100% the highest value obtained in a well treated with Triton-x100.

Cytokine analysis. Cell culture supernatant was collected after 4h, 8h and 24h of stimulation, and the culture medium was measured by magnetic bead-based multiplex assay using Luminex technology (Bio-Rad) according to the manufacturer's instructions.

3.3.2.6. References

- 1 Waumans, Y., Baerts, L., Kehoe, K., Lambeir, A. M. & De Meester, I. The Dipeptidyl Peptidase Family, Prolyl Oligopeptidase, and Prolyl Carboxypeptidase in the Immune System and Inflammatory Disease, Including Atherosclerosis. *Frontiers in immunology* **6**, 387, doi:10.3389/fimmu.2015.00387 (2015).
- 2 Wagner, L., Klemann, C., Stephan, M. & von Horsten, S. Unravelling the immunological roles of dipeptidyl peptidase 4 (DPP4) activity and/or structure homologue (DASH) proteins. *Clinical and experimental immunology* **184**, 265-283, doi:10.1111/cei.12757 (2016).
- 3 Deacon, C. F. Dipeptidyl peptidase-4 inhibitors in the treatment of type 2 diabetes: a comparative review. *Diabetes Obes Metab* **13**, 7-18, doi:10.1111/j.1463-1326.2010.01306.x (2011).

- 4 Drucker, D. J. & Nauck, M. A. The incretin system: glucagon-like peptide-1 receptor agonists and dipeptidyl peptidase-4 inhibitors in type 2 diabetes. *Lancet* **368**, 1696-1705, doi:10.1016/S0140-6736(06)69705-5 (2006).
- 5 Eager, R. M. *et al.* Phase II trial of talabostat and docetaxel in advanced non-small cell lung cancer. *Clin Oncol (R Coll Radiol)* **21**, 464-472, doi:10.1016/j.clon.2009.04.007 (2009).
- 6 Eager, R. M. *et al.* Phase II assessment of talabostat and cisplatin in second-line stage IV melanoma. *BMC Cancer* **9**, 263, doi:10.1186/1471-2407-9-263 (2009).
- 7 Geiss-Friedlander, R. *et al.* The cytoplasmic peptidase DPP9 is rate-limiting for degradation of proline-containing peptides. *The Journal of biological chemistry* **284**, 27211-27219, doi:10.1074/jbc.M109.041871 (2009).
- 8 Zhang, H. *et al.* Identification of novel dipeptidyl peptidase 9 substrates by two-dimensional differential in-gel electrophoresis. *The FEBS journal* **282**, 3737-3757, doi:10.1111/febs.13371 (2015).
- 9 Lamkanfi, M. & Dixit, V. M. Mechanisms and functions of inflammasomes. *Cell* **157**, 1013-1022, doi:10.1016/j.cell.2014.04.007 (2014).
- 10 Broz, P. & Dixit, V. M. Inflammasomes: mechanism of assembly, regulation and signalling. *Nature reviews. Immunology* **16**, 407-420, doi:10.1038/nri.2016.58 (2016).
- 11 Shi, J. *et al.* Cleavage of GSDMD by inflammatory caspases determines pyroptotic cell death. *Nature*, doi:10.1038/nature15514 (2015).
- 12 Kayagaki, N. *et al.* Caspase-11 cleaves gasdermin D for non-canonical inflammasome signalling. *Nature* **526**, 666-671, doi:10.1038/nature15541 (2015).
- 13 Aglietti, R. A. *et al.* GsdmD p30 elicited by caspase-11 during pyroptosis forms pores in membranes. *Proceedings of the National Academy of Sciences of the United States of America* **113**, 7858-7863, doi:10.1073/pnas.1607769113 (2016).
- 14 Ding, J. *et al.* Pore-forming activity and structural autoinhibition of the gasdermin family. *Nature* **535**, 111-116, doi:10.1038/nature18590 (2016).
- 15 Liu, X. *et al.* Inflammasome-activated gasdermin D causes pyroptosis by forming membrane pores. *Nature* **535**, 153-158, doi:10.1038/nature18629 (2016).
- 16 Sborgi, L. *et al.* GSDMD membrane pore formation constitutes the mechanism of pyroptotic cell death. *The EMBO journal* **35**, 1766-1778, doi:10.15252/embj.201694696 (2016).
- 17 Okondo, M. C. *et al.* DPP8 and DPP9 inhibition induces pro-caspase-1-dependent monocyte and macrophage pyroptosis. *Nature chemical biology* **13**, 46-53, doi:10.1038/nchembio.2229 (2017).
- 18 Van Opendenbosch, N. *et al.* Activation of the NLRP1b inflammasome independently of ASC-mediated caspase-1 autoproteolysis and speck formation. *Nature communications* **5**, 3209, doi:10.1038/ncomms4209 (2014).
- 19 Guey, B., Bodnar, M., Manie, S. N., Tardivel, A. & Petrilli, V. Caspase-1 autoproteolysis is differentially required for NLRP1b and NLRP3 inflammasome function. *Proceedings of the National Academy of Sciences of the United States of America* **111**, 17254-17259, doi:10.1073/pnas.1415756111 (2014).
- 20 Broz, P., von Moltke, J., Jones, J. W., Vance, R. E. & Monack, D. M. Differential requirement for Caspase-1 autoproteolysis in pathogen-induced cell death and cytokine processing. *Cell host & microbe* **8**, 471-483, doi:10.1016/j.chom.2010.11.007 (2010).

- 21 Okondo, M. C. *et al.* Inhibition of Dpp8/9 Activates the Nlrp1b Inflammasome. *Cell Chem Biol* **25**, 262-267 e265, doi:10.1016/j.chembiol.2017.12.013 (2018).
- 22 Boyden, E. D. & Dietrich, W. F. Nalp1b controls mouse macrophage susceptibility to anthrax lethal toxin. *Nature genetics* **38**, 240-244, doi:10.1038/ng1724 (2006).
- 23 Masters, S. L. *et al.* NLRP1 inflammasome activation induces pyroptosis of hematopoietic progenitor cells. *Immunity* **37**, 1009-1023, doi:10.1016/j.immuni.2012.08.027 (2012).
- 24 Moayeri, M. *et al.* Inflammasome sensor Nlrp1b-dependent resistance to anthrax is mediated by caspase-1, IL-1 signaling and neutrophil recruitment. *PLoS pathogens* **6**, e1001222, doi:10.1371/journal.ppat.1001222 (2010).
- 25 Frew, B. C., Joag, V. R. & Mogridge, J. Proteolytic processing of Nlrp1b is required for inflammasome activity. *PLoS pathogens* **8**, e1002659, doi:10.1371/journal.ppat.1002659 (2012).
- 26 Chavarria-Smith, J. & Vance, R. E. Direct proteolytic cleavage of NLRP1B is necessary and sufficient for inflammasome activation by anthrax lethal factor. *PLoS pathogens* **9**, e1003452, doi:10.1371/journal.ppat.1003452 (2013).
- 27 Gabrilovac, J., Cupic, B., Zapletal, E., Kraus, O. & Jakic-Razumovic, J. Dipeptidyl peptidase 9 (DPP9) in human skin cells. *Immunobiology* **222**, 327-342, doi:10.1016/j.imbio.2016.09.007 (2017).
- 28 Chowdhury, S. *et al.* Regulation of dipeptidyl peptidase 8 and 9 expression in activated lymphocytes and injured liver. *World journal of gastroenterology : WJG* **19**, 2883-2893, doi:10.3748/wjg.v19.i19.2883 (2013).
- 29 Waumans, Y. *et al.* The Dipeptidyl Peptidases 4, 8, and 9 in Mouse Monocytes and Macrophages: DPP8/9 Inhibition Attenuates M1 Macrophage Activation in Mice. *Inflammation* **39**, 413-424, doi:10.1007/s10753-015-0263-5 (2016).
- 30 Gall, M. G. *et al.* Targeted inactivation of dipeptidyl peptidase 9 enzymatic activity causes mouse neonate lethality. *PloS one* **8**, e78378, doi:10.1371/journal.pone.0078378 (2013).
- 31 Mariathasan, S. *et al.* Differential activation of the inflammasome by caspase-1 adaptors ASC and Ipaf. *Nature* **430**, 213-218, doi:10.1038/nature02664 (2004).
- 32 Kuida, K. *et al.* Altered cytokine export and apoptosis in mice deficient in interleukin-1 beta converting enzyme. *Science* **267**, 2000-2003 (1995).
- 33 Boyden, E. D. & Dietrich, W. F. Nalp1b controls mouse macrophage susceptibility to anthrax lethal toxin. *Nature genetics* **38**, 240-244, doi:10.1038/ng1724 (2006).
- 34 Lankas, G. R. *et al.* Dipeptidyl peptidase IV inhibition for the treatment of type 2 diabetes - Potential importance of selectivity over dipeptidyl peptidases 8 and 9. *Diabetes* **54**, 2988-2994, doi:DOI 10.2337/diabetes.54.10.2988 (2005).
- 35 Wu, J. J. *et al.* Biochemistry, pharmacokinetics, and toxicology of a potent and selective DPP8/9 inhibitor. *Biochem Pharmacol* **78**, 203-210, doi:10.1016/j.bcp.2009.03.032 (2009).
- 36 Kim, D. *et al.* (2R)-4-oxo-4-[3-(trifluoromethyl)-5,6-dihydro[1,2,4]triazolo[4,3-a]pyrazin-7(8H)-yl]-1-(2,4,5-trifluorophenyl)butan-2-amine: a potent, orally active dipeptidyl peptidase IV inhibitor for the treatment of type 2 diabetes. *J Med Chem* **48**, 141-151, doi:10.1021/jm0493156 (2005).

37 Jansen, K. et al. Selective Inhibitors of Fibroblast Activation Protein (FAP) with a (4-Quinolinoyl)-glycyl-2-cyanopyrrolidine Scaffold. *ACS Med Chem Lett* 4, 491-496, doi:10.1021/ml300410d (2013).

38 Van Goethem, S. et al. Structure-activity relationship studies on isoindoline inhibitors of dipeptidyl peptidases 8 and 9 (DPP8, DPP9): is DPP8-selectivity an attainable goal? *J Med Chem* 54, 5737-5746, doi:10.1021/jm200383j (2011).

39 Ryabtsova, O. et al. Acylated Gly-(2-cyano)pyrrolidines as inhibitors of fibroblast activation protein (FAP) and the issue of FAP/prolyl oligopeptidase (PREP)-selectivity. *Bioorg Med Chem Lett* 22, 3412-3417, doi:10.1016/j.bmcl.2012.03.107 (2012).

4. Discussion and Perspectives

Pyroptosis is a form of regulated cell death happening in macrophages and epithelial cells linked to inflammasome activation²⁷⁶. Cytosolic receptors belonging to the families of the Nod-like receptors, AIM2-like receptors and Pypin sense intracellular damage or pathogen associated patterns. Their activation and assembly to the bipartite protein ASC forms the inflammasome platform. Procaspase-1 is recruited to this platform for proximity-induced autoactivation¹⁶¹. Furthermore, a non-canonical inflammasome directed by caspase-11 can independently execute pyroptotic cell death¹⁵⁴. Remarkably, both caspase-1 and caspase-11 converge on activation of the same substrate, GSDMD, to mediate plasma membrane rupture during pyroptosis^{16,261}. While in the last 15 years there has been much advance in understanding the upstream inflammasome players, the mechanisms governing cell death are still elusive.

In the presented organellar analysis of pyroptosis (Section 3.1), we defined a conserved set of organellar changes associated to pyroptotic cell death execution. Ionic fluxing, cellular swelling, mitochondrial depolarization and lysosomal leakage all preceded final plasma membrane lysis, as reported by Sytox Green or PI uptake. These events anticipated membrane rupture after both NLRP1b and NLRC4 inflammasome activation. Furthermore, non-canonical inflammasome activation directed a similar demise program, with mitochondrial depolarization and ionic fluxes happening prior to membrane commitment, in a GSDMD-dependent way. Hence, these represent pyroptotic shared events.

In combining these data, we propose a model in which pyroptosis undergoes through a gradual increase in plasma membrane permeability in a GSDMD-dependent manner. This effect could be accomplished by insertion of GSDMD_N in the plasma membrane as either single molecules or oligomers of low orders of magnitude, which would account for early alterations in cellular permeability (Figure 1). Further oligomerization of GSDMD_N at the plasma membrane and formation of the highly organized pore of 10-20 nm in diameter²⁶²⁻²⁶⁵ would account for final stages of pyroptotic permeability and release of intracellular contents.

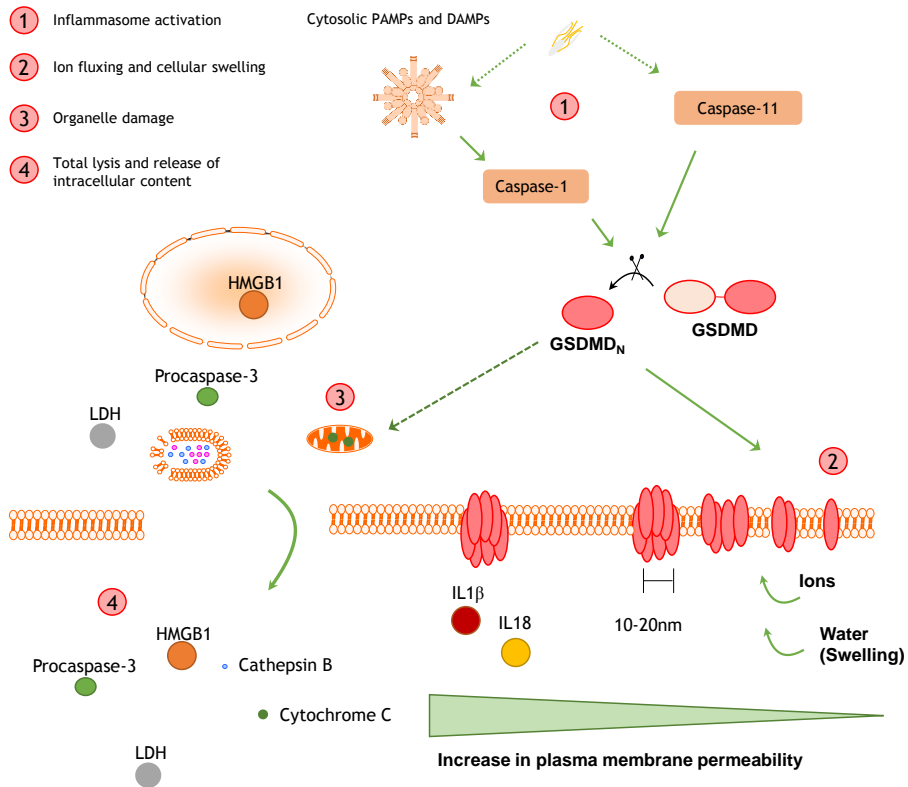


Figure 1. A schematic overview of the morphological changes associated to pyroptosis induction after NLRP1b and NLR4 inflammasome activation. Caspase-1 activation after canonical triggers leads to pyroptosis comprising mitochondrial depolarization and fragmentation, lysosomal decay and nuclear rounding. At the plasma membrane, cell death downstream of the inflammasome is accompanied by a gradual increase in permeability, demonstrated by ionic fluxing and cellular swelling which preceded incorporation of nuclear dyes PI or Sytox Green. Furthermore, caspase-11 and the non-canonical inflammasome activation converge at the level of GSDMD cleavage. Non-canonical inflammasome-mediated cell death was similarly accompanied by ionic fluxing and mitochondrial decay, which were dependent on the presence of GSDMD. At final cell lysis (4), intracellular contents are released with no specificity.

The close temporal associations between phosphatidylserine exposure in pyroptotic cells and plasma membrane rupture could guarantee rapid and efficient uptake of the cell corpse, avoiding pathogen spread. Pyroptotic cell corpses have been shown to contain intracellular pathogens to facilitate removal by infiltrating neutrophils in structures called PITs²⁷⁷. It is tempting to speculate that PS exposure on the pyroptotic cell corpse helps in the uptake of the PITs and pathogen removal, and it would be interesting to address what are the potential pathological consequences of lack of PS exposure in pyroptotic cells during an infection *in vivo*. On our analysis of intracellular components that are released after NLRP1b and NLRC4 inflammasome activation, we found that there is no selectivity towards which intracellular proteins are released during pyroptotic cell rupture. This reinforces the concept that the maintenance of pathogens in the PITs is probably a reflection of their size, as organelles are also maintained in the cellular corpse. However, it suggests that pathogen-derived proteins could also be released in the extracellular milieu and activate neighboring cells.

Presence of cathepsin B, cytochrome c and HMGB1 in the supernatants of pyroptotic macrophages suggests that organellar damage is a marked feature of pyroptosis, and accounts for release of proteins without selectivity during cell death. Interestingly, GSDMD_N has been found to be present across most intracellular membranes^{262,263,265}, consistent with our observed dependency for GSDMD_N in mitochondrial damage. However, GSDMD_N damage of the plasma membrane could also account for damage on mitochondria and lysosomes, by unbalancing electrochemical gradients imposed by the plasma membrane. A temporal analysis of intracellular localization of GSDMD_N during cell death could aid in answering whether pyroptotic organellar damage is directly mediated by GSDMD_N or reflects the plasma membrane damage cause by GSDMD_N.

Further, through our analysis of biochemical events downstream of NLRC4 and NLRP1b inflammasome activation, we demonstrated that DEVDase activity can be detected in pyroptotic cells, which is accompanied by cleavage of substrates typically associated to apoptosis, namely ROCK1, Bid and p23 (Section 3.2). This suggests that pyroptotic cell death happening downstream of the canonical inflammasome is a combination of an apoptotic signature (DEVDase) and pore formation at the plasma membrane, executed by GSDMD. Interestingly, caspase-7 was chiefly activated in pyroptotic cells, as it has previously been reported²⁰⁰. Thus, it is tempting to speculate that caspase-7 is the executioner caspase responsible for the pyroptotic

DEVDase signature. GSDMD^{-/-} cells triggered for the NLRC4 and NLRP1b inflammasomes undergo apoptosis with same kinetics as WT cells undergo pyroptosis (Section 3.1). Furthermore, GSDMD^{-/-} macrophages triggered with FlaTox and LeTx demonstrated similar levels of DEVDase activity than WT cells. This suggests that the apoptotic phenotype observed in GSDMD^{-/-} cells relies on caspase-1 and represents the program of executioner caspases happening in WT cells during pyroptosis. Indeed, ablation of ASC, known to mediate caspase-8 recruitment to the inflammasome and its activation in conditions of lack of caspase-1^{278,279}, could not rescue GSDMD^{-/-} macrophages from apoptosis after LeTx and FlaTox. Of note, caspase-3 was found to be weakly activated in NLRP1b and NLRC4-triggered pyroptotic cells, but was markedly matured in GSDMD^{-/-} cells after the same stimuli. This suggests that caspase-3 and caspase-7 are either matured at different moments or by a different mechanism upstream, which would be more markedly present in GSDMD^{-/-}-triggered macrophages. It remains to be determined whether each of the executioner caspases has a prominent role in the DEVDase activity of NLRP1b and NLRC4-triggered pyroptotic cells and whether both executioner caspases are needed for the apoptotic phenotype in NLRP1b and NLRC4-triggered GSDMD^{-/-} macrophages.

In conclusion, activation of the inflammasome leads to a complex network of caspase activation downstream. Activation of caspase-1 at the ASC speck, leads to processing of several substrates such as IL1 β , IL18, GSDMD and executioner caspases, in either a direct or indirect way. Caspase-8 recruitment to the ASC speck also happens, though in a slower manner, being more obvious in conditions of delayed cell rupture, as in absence of caspase-1 or its catalytic activity^{278,279}. Therefore, engagement of a canonical inflammasome would account for three parallel signaling pathways to cell death: a caspase-1-dependent membrane rupture by GSDMD; a caspase-1-dependent apoptotic program, through cleavage of executioner caspases; and a slower ASC-dependent recruitment of caspase-8 and apoptosis.

Interestingly, some of the morphological events observed in pyroptosis are reminiscent of apoptosis (**Table 1**), namely mitochondrial fragmentation and depolarization, phosphatidylserine exposure on the outer leaflet of the plasma membrane and DNA degradation. We have shown that, during non-canonical inflammasome activation, mitochondrial depolarization depends on GSDMD (Section 3.1). Considering caspase-11 also activates NLRP3 and caspase-1 downstream, and that lack of GSDMD after caspase-11 activation not only impairs

pyroptosis, but also prevents caspase-1 activation downstream of NLRP3²⁶¹, it remains unclear whether the mitochondrial depolarization is dependent on caspase-11 or caspase-1. Next steps on pyroptosis research could address which of the pyroptotic morphological events which are shared with apoptosis are dependent on caspase-7 and caspase-3 activation downstream of the canonical inflammasome.

Table 1. Comparison of morphological alterations in pyroptotic and apoptotic cells.

Morphological Feature	Pyroptosis	Apoptosis
Mitochondrial fragmentation	Yes	Yes ²⁰
Mitochondrial membrane potential	Depolarization	Depolarization ²⁰
Lysosomal membrane permeabilization	Yes	Yes ²⁸⁰
DNA fragmentation	Yes, as a diffuse TUNEL staining ²⁰⁷	Yes, condensed TUNEL staining ²⁰⁷
Nuclear morphology	Condensation (late onset)	Condensation and fragmentation ²⁰
Annexin-V staining	Yes (late onset)	Yes ²⁰
Cellular morphology	Swelling and rupture, while attached	Contraction of cell body and blebbing ²⁰
Vesicle shedding/apoptotic bodies	To be determined	Apoptotic bodies ²⁰
Release of intracellular contents	Yes, including organellar proteins	No ²⁰

Contrary to pyroptosis, apoptosis is regarded as a silent form of cell death, not accounting for the induction of an inflammatory signaling in the local tissue⁷³. Interestingly, mutations in genes of inflammasome receptors can cause genetic autoinflammatory diseases, commonly named as inflammasomopathies, due to an overt inflammasome activation. One of the most common presentations of inflammasomopathies are recurrent fever attacks, and patients normally experience a health improve when treated with IL1 antagonists²⁵⁷. This suggests that IL1 β , and potentially IL1 α , signaling is one of the most detrimental effects of the excessive inflammasome activation in these patients. For example, mutations in *MEFV*, the gene encoding the inflammasome receptor Pyrin, is the causative agent of FMF, and patients also benefit from IL1 inhibition²⁸¹. An FMF-knock-in mouse engineered to contain a human domain of the *MEFV* gene and its autoactivation mutation is

completely protected when in an IL1 β -null background²⁸². Remarkably, lack of GSDMD in these MEFV mice also completely protects from pathology²⁸³. This suggests that targeting GSDMD in the clinic might be an efficient alternative approach for treating patients with inflammasomopathies. However, given our knowledge that GSDMD^{-/-} macrophages still undergo cell death after inflammasome activation, it would be interesting to address the long-term effects of absence of GSDMD in inflammasomopathies models.

While inflammasome-mediated responses have been shown to be protective to a number of bacterial infections¹⁴², it is still unclear how absence of GSDMD in macrophages could alter their response to infections *in vivo*. Furthermore, future research could address whether pathogens could differentially regulate each of the cell death pathways downstream of inflammasome activation.

Finally, in the last part of the current thesis, we characterized how inhibition of two proteases from the extended prolyl dipeptidases family could cause inflammasome activation (Section 3.3). PRCP inhibition by Compound 80 led to a lytic form of cell death with fast kinetics, independently from the major cell death players of necroptosis, extrinsic apoptosis and pyroptosis. In addition, Compound 80 elicited NLRP3 inflammasome activation and release of IL1 β in treated BMDMs. Description of the cell death mediator could elucidate whether NLRP3 activation is downstream of parallel to PRCP inhibition.

DPP8/DPP9 inhibition also led to cell death induction and IL1 β release, more pronounced in BMDMs containing the 129-associated allele of *Nlrp1b*. NLRP1b-sufficient cells relied on caspase-1 for cell death and IL1 β released, establishing ValboroPro and 1G244 as NLRP1b inflammasome activators and pyroptosis inducing agents. It remains to be analyzed how human cells, which possess only one *Nlrp1* locus, behave as. Overall, these results demonstrate that use of PRCP or DPP8/DPP9 inhibitors can in fact have inflammatory roles *in vivo*. This should be taken into consideration when assessing their potential for clinical use.

5. References

- 1 Kerr, J. F., Wyllie, A. H. & Currie, A. R. Apoptosis: a basic biological phenomenon with wide-ranging implications in tissue kinetics. *Br J Cancer* **26**, 239-257 (1972).
- 2 Shah, S., Wu, E., Rao, V. K. & Tarrant, T. K. Autoimmune lymphoproliferative syndrome: an update and review of the literature. *Current allergy and asthma reports* **14**, 462, doi:10.1007/s11882-014-0462-4 (2014).
- 3 Bouillet, P. *et al.* Proapoptotic Bcl-2 relative Bim required for certain apoptotic responses, leukocyte homeostasis, and to preclude autoimmunity. *Science* **286**, 1735-1738 (1999).
- 4 Watanabe-Fukunaga, R., Brannan, C. I., Copeland, N. G., Jenkins, N. A. & Nagata, S. Lymphoproliferation disorder in mice explained by defects in Fas antigen that mediates apoptosis. *Nature* **356**, 314-317, doi:10.1038/356314a0 (1992).
- 5 Nagata, S. & Tanaka, M. Programmed cell death and the immune system. *Nature reviews. Immunology* **17**, 333-340, doi:10.1038/nri.2016.153 (2017).
- 6 Kagi, D. *et al.* Fas and perforin pathways as major mechanisms of T cell-mediated cytotoxicity. *Science* **265**, 528-530 (1994).
- 7 Lowin, B., Hahne, M., Mattmann, C. & Tschopp, J. Cytolytic T-cell cytotoxicity is mediated through perforin and Fas lytic pathways. *Nature* **370**, 650-652, doi:10.1038/370650a0 (1994).
- 8 Halaas, O., Vik, R., Ashkenazi, A. & Espevik, T. Lipopolysaccharide induces expression of APO2 ligand/TRAIL in human monocytes and macrophages. *Scand J Immunol* **51**, 244-250 (2000).
- 9 Ehrlich, S., Infante-Duarte, C., Seeger, B. & Zipp, F. Regulation of soluble and surface-bound TRAIL in human T cells, B cells, and monocytes. *Cytokine* **24**, 244-253 (2003).
- 10 Nicholson, D. W. Caspase structure, proteolytic substrates, and function during apoptotic cell death. *Cell death and differentiation* **6**, 1028-1042, doi:10.1038/sj.cdd.4400598 (1999).

- 11 Lamkanfi, M., Declercq, W., Kalai, M., Saelens, X. & Vandenabeele, P. Alice in caspase land. A phylogenetic analysis of caspases from worm to man. *Cell death and differentiation* **9**, 358-361, doi:10.1038/sj/cdd/4400989 (2002).
- 12 Strasser, A., O'Connor, L. & Dixit, V. M. Apoptosis signaling. *Annual review of biochemistry* **69**, 217-245, doi:10.1146/annurev.biochem.69.1.217 (2000).
- 13 Creagh, E. M. Caspase crosstalk: integration of apoptotic and innate immune signalling pathways. *Trends in immunology* **35**, 631-640, doi:10.1016/j.it.2014.10.004 (2014).
- 14 Baker, P. J. *et al.* NLRP3 inflammasome activation downstream of cytoplasmic LPS recognition by both caspase-4 and caspase-5. *European journal of immunology* **45**, 2918-2926, doi:10.1002/eji.201545655 (2015).
- 15 Schmid-Burgk, J. L. *et al.* Caspase-4 mediates non-canonical activation of the NLRP3 inflammasome in human myeloid cells. *European journal of immunology* **45**, 2911-2917, doi:10.1002/eji.201545523 (2015).
- 16 Shi, J. *et al.* Cleavage of GSDMD by inflammatory caspases determines pyroptotic cell death. *Nature*, doi:10.1038/nature15514 (2015).
- 17 Vigano, E. *et al.* Human caspase-4 and caspase-5 regulate the one-step non-canonical inflammasome activation in monocytes. *Nature communications* **6**, 8761, doi:10.1038/ncomms9761 (2015).
- 18 Lagrange, B. *et al.* Human caspase-4 detects tetra-acylated LPS and cytosolic Francisella and functions differently from murine caspase-11. *Nature communications* **9**, 242, doi:10.1038/s41467-017-02682-y (2018).
- 19 Tummers, B. & Green, D. R. Caspase-8: regulating life and death. *Immunological reviews* **277**, 76-89, doi:10.1111/imr.12541 (2017).
- 20 Taylor, R. C., Cullen, S. P. & Martin, S. J. Apoptosis: controlled demolition at the cellular level. *Nature reviews. Molecular cell biology* **9**, 231-241, doi:10.1038/nrm2312 (2008).
- 21 Park, H. H. *et al.* The death domain superfamily in intracellular signaling of apoptosis and inflammation. *Annual review of immunology* **25**, 561-586, doi:10.1146/annurev.immunol.25.022106.141656 (2007).
- 22 Martinon, F., Burns, K. & Tschopp, J. The inflammasome: a molecular platform triggering activation of inflammatory caspases and processing of proIL-beta. *Molecular cell* **10**, 417-426 (2002).
- 23 Tinel, A. & Tschopp, J. The PIDDosome, a protein complex implicated in activation of caspase-2 in response to genotoxic stress. *Science* **304**, 843-846, doi:10.1126/science.1095432 (2004).
- 24 Li, P. *et al.* Cytochrome c and dATP-dependent formation of Apaf-1/caspase-9 complex initiates an apoptotic protease cascade. *Cell* **91**, 479-489 (1997).
- 25 Shi, J. *et al.* Inflammatory caspases are innate immune receptors for intracellular LPS. *Nature* **514**, 187-192, doi:10.1038/nature13683 (2014).
- 26 Muzio, M. *et al.* FLICE, a novel FADD-homologous ICE/CED-3-like protease, is recruited to the CD95 (Fas/APO-1) death-inducing signaling complex. *Cell* **85**, 817-827 (1996).
- 27 Vincenz, C. & Dixit, V. M. Fas-associated death domain protein interleukin-1beta-converting enzyme 2 (FLICE2), an ICE/Ced-3 homologue, is

- proximally involved in CD95- and p55-mediated death signaling. *The Journal of biological chemistry* **272**, 6578-6583 (1997).
- 28 Fernandes-Alnemri, T. *et al.* In vitro activation of CPP32 and Mch3 by Mch4, a novel human apoptotic cysteine protease containing two FADD-like domains. *Proceedings of the National Academy of Sciences of the United States of America* **93**, 7464-7469 (1996).
- 29 Hu, Q. *et al.* Molecular determinants of caspase-9 activation by the Apaf-1 apoptosome. *Proceedings of the National Academy of Sciences of the United States of America* **111**, 16254-16261, doi:10.1073/pnas.1418000111 (2014).
- 30 Hu, Q., Wu, D., Chen, W., Yan, Z. & Shi, Y. Proteolytic processing of the caspase-9 zymogen is required for apoptosome-mediated activation of caspase-9. *The Journal of biological chemistry* **288**, 15142-15147, doi:10.1074/jbc.M112.441568 (2013).
- 31 Salvesen, G. S. & Dixit, V. M. Caspase activation: the induced-proximity model. *Proceedings of the National Academy of Sciences of the United States of America* **96**, 10964-10967 (1999).
- 32 Rodriguez, J. & Lazebnik, Y. Caspase-9 and APAF-1 form an active holoenzyme. *Genes & development* **13**, 3179-3184 (1999).
- 33 Broz, P., von Moltke, J., Jones, J. W., Vance, R. E. & Monack, D. M. Differential requirement for Caspase-1 autoproteolysis in pathogen-induced cell death and cytokine processing. *Cell host & microbe* **8**, 471-483, doi:10.1016/j.chom.2010.11.007 (2010).
- 34 Micheau, O. *et al.* The long form of FLIP is an activator of caspase-8 at the Fas death-inducing signaling complex. *The Journal of biological chemistry* **277**, 45162-45171, doi:10.1074/jbc.M206882200 (2002).
- 35 Feng, S. *et al.* Cleavage of RIP3 inactivates its caspase-independent apoptosis pathway by removal of kinase domain. *Cellular signalling* **19**, 2056-2067, doi:10.1016/j.cellsig.2007.05.016 (2007).
- 36 Pop, C. *et al.* FLIP(L) induces caspase 8 activity in the absence of interdomain caspase 8 cleavage and alters substrate specificity. *The Biochemical journal* **433**, 447-457, doi:10.1042/BJ20101738 (2011).
- 37 Ashkenazi, A. & Salvesen, G. Regulated cell death: signaling and mechanisms. *Annual review of cell and developmental biology* **30**, 337-356, doi:10.1146/annurev-cellbio-100913-013226 (2014).
- 38 Hughes, M. A. *et al.* Co-operative and Hierarchical Binding of c-FLIP and Caspase-8: A Unified Model Defines How c-FLIP Isoforms Differentially Control Cell Fate. *Molecular cell* **61**, 834-849, doi:10.1016/j.molcel.2016.02.023 (2016).
- 39 Fu, T. M. *et al.* Cryo-EM Structure of Caspase-8 Tandem DED Filament Reveals Assembly and Regulation Mechanisms of the Death-Inducing Signaling Complex. *Molecular cell* **64**, 236-250, doi:10.1016/j.molcel.2016.09.009 (2016).
- 40 Lavrik, I., Golks, A. & Krammer, P. H. Death receptor signaling. *J Cell Sci* **118**, 265-267, doi:10.1242/jcs.01610 (2005).
- 41 Mahoney, D. J. *et al.* Both cIAP1 and cIAP2 regulate TNFalpha-mediated NF-kappaB activation. *Proceedings of the National Academy of Sciences of the*

- United States of America* **105**, 11778-11783, doi:10.1073/pnas.0711122105 (2008).
- 42 Micheau, O. & Tschopp, J. Induction of TNF receptor I-mediated apoptosis via two sequential signaling complexes. *Cell* **114**, 181-190 (2003).
- 43 Haas, T. L. *et al.* Recruitment of the linear ubiquitin chain assembly complex stabilizes the TNF-R1 signaling complex and is required for TNF-mediated gene induction. *Molecular cell* **36**, 831-844, doi:10.1016/j.molcel.2009.10.013 (2009).
- 44 Annibaldi, A. & Meier, P. Checkpoints in TNF-Induced Cell Death: Implications in Inflammation and Cancer. *Trends in molecular medicine* **24**, 49-65, doi:10.1016/j.molmed.2017.11.002 (2018).
- 45 Lu, T. T. *et al.* Dimerization and ubiquitin mediated recruitment of A20, a complex deubiquitinating enzyme. *Immunity* **38**, 896-905, doi:10.1016/j.immuni.2013.03.008 (2013).
- 46 Wang, L., Du, F. & Wang, X. TNF-alpha induces two distinct caspase-8 activation pathways. *Cell* **133**, 693-703, doi:10.1016/j.cell.2008.03.036 (2008).
- 47 Dondelinger, Y. *et al.* MK2 phosphorylation of RIPK1 regulates TNF-mediated cell death. *Nature cell biology*, doi:10.1038/ncb3608 (2017).
- 48 Jaco, I. *et al.* MK2 Phosphorylates RIPK1 to Prevent TNF-Induced Cell Death. *Molecular cell* **66**, 698-710 e695, doi:10.1016/j.molcel.2017.05.003 (2017).
- 49 Dondelinger, Y. *et al.* NF-kappaB-Independent Role of IKKalpha/IKKbeta in Preventing RIPK1 Kinase-Dependent Apoptotic and Necroptotic Cell Death during TNF Signaling. *Molecular cell* **60**, 63-76, doi:10.1016/j.molcel.2015.07.032 (2015).
- 50 Lin, Y., Devin, A., Rodriguez, Y. & Liu, Z. G. Cleavage of the death domain kinase RIP by caspase-8 prompts TNF-induced apoptosis. *Genes & development* **13**, 2514-2526 (1999).
- 51 Koenig, A. *et al.* The c-FLIPL cleavage product p43FLIP promotes activation of extracellular signal-regulated kinase (ERK), nuclear factor kappaB (NF-kappaB), and caspase-8 and T cell survival. *The Journal of biological chemistry* **289**, 1183-1191, doi:10.1074/jbc.M113.506428 (2014).
- 52 Strasser, A. The role of BH3-only proteins in the immune system. *Nature reviews. Immunology* **5**, 189-200, doi:10.1038/nri1568 (2005).
- 53 Kalkavan, H. & Green, D. R. MOMP, cell suicide as a BCL-2 family business. *Cell death and differentiation* **25**, 46-55, doi:10.1038/cdd.2017.179 (2018).
- 54 Villunger, A. *et al.* p53- and drug-induced apoptotic responses mediated by BH3-only proteins puma and noxa. *Science* **302**, 1036-1038, doi:10.1126/science.1090072 (2003).
- 55 Li, H., Zhu, H., Xu, C. J. & Yuan, J. Cleavage of BID by caspase 8 mediates the mitochondrial damage in the Fas pathway of apoptosis. *Cell* **94**, 491-501 (1998).
- 56 Luo, X., Budihardjo, I., Zou, H., Slaughter, C. & Wang, X. Bid, a Bcl2 interacting protein, mediates cytochrome c release from mitochondria in response to activation of cell surface death receptors. *Cell* **94**, 481-490 (1998).

- 57 Todt, F. *et al.* Differential retrotranslocation of mitochondrial Bax and Bak. *The EMBO journal* **34**, 67-80, doi:10.15252/embj.201488806 (2015).
- 58 Willis, S. N. *et al.* Proapoptotic Bak is sequestered by Mcl-1 and Bcl-xL, but not Bcl-2, until displaced by BH3-only proteins. *Genes & development* **19**, 1294-1305, doi:10.1101/gad.1304105 (2005).
- 59 Brouwer, J. M. *et al.* Bak core and latch domains separate during activation, and freed core domains form symmetric homodimers. *Molecular cell* **55**, 938-946, doi:10.1016/j.molcel.2014.07.016 (2014).
- 60 Bleicken, S., Landeta, O., Landajueta, A., Basanez, G. & Garcia-Saez, A. J. Proapoptotic Bax and Bak proteins form stable protein-permeable pores of tunable size. *The Journal of biological chemistry* **288**, 33241-33252, doi:10.1074/jbc.M113.512087 (2013).
- 61 Dewson, G. *et al.* Bax dimerizes via a symmetric BH3:groove interface during apoptosis. *Cell death and differentiation* **19**, 661-670, doi:10.1038/cdd.2011.138 (2012).
- 62 Schellenberg, B. *et al.* Bax exists in a dynamic equilibrium between the cytosol and mitochondria to control apoptotic priming. *Molecular cell* **49**, 959-971, doi:10.1016/j.molcel.2012.12.022 (2013).
- 63 Edlich, F. *et al.* Bcl-x(L) retrotranslocates Bax from the mitochondria into the cytosol. *Cell* **145**, 104-116, doi:10.1016/j.cell.2011.02.034 (2011).
- 64 Llambi, F. *et al.* BOK Is a Non-canonical BCL-2 Family Effector of Apoptosis Regulated by ER-Associated Degradation. *Cell* **165**, 421-433, doi:10.1016/j.cell.2016.02.026 (2016).
- 65 Einsele-Scholz, S. *et al.* Bok is a genuine multi-BH-domain protein that triggers apoptosis in the absence of Bax and Bak. *J Cell Sci* **129**, 3054, doi:10.1242/jcs.193946 (2016).
- 66 Lindsten, T. *et al.* The combined functions of proapoptotic Bcl-2 family members bak and bax are essential for normal development of multiple tissues. *Molecular cell* **6**, 1389-1399 (2000).
- 67 Ke, F. *et al.* Consequences of the combined loss of BOK and BAK or BOK and BAX. *Cell death & disease* **4**, e650, doi:10.1038/cddis.2013.176 (2013).
- 68 Dewson, G. & Kluck, R. M. Mechanisms by which Bak and Bax permeabilise mitochondria during apoptosis. *J Cell Sci* **122**, 2801-2808 (2009).
- 69 Zou, H., Henzel, W. J., Liu, X., Lutschg, A. & Wang, X. Apaf-1, a human protein homologous to *C. elegans* CED-4, participates in cytochrome c-dependent activation of caspase-3. *Cell* **90**, 405-413 (1997).
- 70 Du, C., Fang, M., Li, Y., Li, L. & Wang, X. Smac, a mitochondrial protein that promotes cytochrome c-dependent caspase activation by eliminating IAP inhibition. *Cell* **102**, 33-42 (2000).
- 71 Verhagen, A. M. *et al.* Identification of DIABLO, a mammalian protein that promotes apoptosis by binding to and antagonizing IAP proteins. *Cell* **102**, 43-53 (2000).
- 72 van Loo, G. *et al.* The serine protease Omi/HtrA2 is released from mitochondria during apoptosis. Omi interacts with caspase-inhibitor XIAP and induces enhanced caspase activity. *Cell death and differentiation* **9**, 20-26, doi:10.1038/sj.cdd.4400970 (2002).

- 73 Elmore, S. Apoptosis: a review of programmed cell death. *Toxicologic pathology* **35**, 495-516, doi:10.1080/01926230701320337 (2007).
- 74 Yin, X. M. *et al.* Bid-deficient mice are resistant to Fas-induced hepatocellular apoptosis. *Nature* **400**, 886-891, doi:10.1038/23730 (1999).
- 75 Jost, P. J. *et al.* XIAP discriminates between type I and type II FAS-induced apoptosis. *Nature* **460**, 1035-1039, doi:10.1038/nature08229 (2009).
- 76 Scott, F. L. *et al.* XIAP inhibits caspase-3 and -7 using two binding sites: evolutionarily conserved mechanism of IAPs. *The EMBO journal* **24**, 645-655, doi:10.1038/sj.emboj.7600544 (2005).
- 77 Kothakota, S. *et al.* Caspase-3-generated fragment of gelsolin: effector of morphological change in apoptosis. *Science* **278**, 294-298 (1997).
- 78 Sebbagh, M. *et al.* Caspase-3-mediated cleavage of ROCK I induces MLC phosphorylation and apoptotic membrane blebbing. *Nature cell biology* **3**, 346-352, doi:10.1038/35070019 (2001).
- 79 Walsh, J. G. *et al.* Executioner caspase-3 and caspase-7 are functionally distinct proteases. *Proceedings of the National Academy of Sciences of the United States of America* **105**, 12815-12819, doi:10.1073/pnas.0707715105 (2008).
- 80 Coleman, M. L. *et al.* Membrane blebbing during apoptosis results from caspase-mediated activation of ROCK I. *Nature cell biology* **3**, 339-345, doi:10.1038/35070009 (2001).
- 81 Wickman, G., Julian, L. & Olson, M. F. How apoptotic cells aid in the removal of their own cold dead bodies. *Cell death and differentiation* **19**, 735-742, doi:10.1038/cdd.2012.25 (2012).
- 82 Segawa, K. & Nagata, S. An Apoptotic 'Eat Me' Signal: Phosphatidylserine Exposure. *Trends in cell biology* **25**, 639-650, doi:10.1016/j.tcb.2015.08.003 (2015).
- 83 Slee, E. A., Adrain, C. & Martin, S. J. Executioner caspase-3, -6, and -7 perform distinct, non-redundant roles during the demolition phase of apoptosis. *The Journal of biological chemistry* **276**, 7320-7326, doi:10.1074/jbc.M008363200 (2001).
- 84 Enari, M. *et al.* A caspase-activated DNase that degrades DNA during apoptosis, and its inhibitor ICAD. *Nature* **391**, 43-50, doi:10.1038/34112 (1998).
- 85 Kim, M. Y., Zhang, T. & Kraus, W. L. Poly(ADP-ribosyl)ation by PARP-1: 'PAR-laying' NAD⁺ into a nuclear signal. *Genes & development* **19**, 1951-1967, doi:10.1101/gad.1331805 (2005).
- 86 Leonard, J. R., Klocke, B. J., D'Sa, C., Flavell, R. A. & Roth, K. A. Strain-dependent neurodevelopmental abnormalities in caspase-3-deficient mice. *J Neuropathol Exp Neurol* **61**, 673-677 (2002).
- 87 Lakhani, S. A. *et al.* Caspases 3 and 7: key mediators of mitochondrial events of apoptosis. *Science* **311**, 847-851, doi:10.1126/science.1115035 (2006).
- 88 Zheng, T. S. *et al.* Deficiency in caspase-9 or caspase-3 induces compensatory caspase activation. *Nat Med* **6**, 1241-1247, doi:10.1038/81343 (2000).
- 89 Van de Craen, M., Declercq, W., Van den brande, I., Fiers, W. & Vandenabeele, P. The proteolytic procaspase activation network: an in vitro

- analysis. *Cell death and differentiation* **6**, 1117-1124, doi:10.1038/sj.cdd.4400589 (1999).
- 90 Thornberry, N. A. *et al.* A combinatorial approach defines specificities of members of the caspase family and granzyme B. Functional relationships established for key mediators of apoptosis. *The Journal of biological chemistry* **272**, 17907-17911 (1997).
- 91 Demon, D. *et al.* Proteome-wide substrate analysis indicates substrate exclusion as a mechanism to generate caspase-7 versus caspase-3 specificity. *Molecular & cellular proteomics : MCP* **8**, 2700-2714, doi:10.1074/mcp.M900310-MCP200 (2009).
- 92 Boucher, D., Blais, V. & Denault, J. B. Caspase-7 uses an exosite to promote poly(ADP ribose) polymerase 1 proteolysis. *Proceedings of the National Academy of Sciences of the United States of America* **109**, 5669-5674, doi:10.1073/pnas.1200934109 (2012).
- 93 Ravichandran, K. S. Find-me and eat-me signals in apoptotic cell clearance: progress and conundrums. *The Journal of experimental medicine* **207**, 1807-1817, doi:10.1084/jem.20101157 (2010).
- 94 McArthur, K. *et al.* BAK/BAX macropores facilitate mitochondrial herniation and mtDNA efflux during apoptosis. *Science* **359**, doi:10.1126/science.aao6047 (2018).
- 95 White, M. J. *et al.* Apoptotic caspases suppress mtDNA-induced STING-mediated type I IFN production. *Cell* **159**, 1549-1562, doi:10.1016/j.cell.2014.11.036 (2014).
- 96 Rongvaux, A. *et al.* Apoptotic caspases prevent the induction of type I interferons by mitochondrial DNA. *Cell* **159**, 1563-1577, doi:10.1016/j.cell.2014.11.037 (2014).
- 97 Voll, R. E. *et al.* Immunosuppressive effects of apoptotic cells. *Nature* **390**, 350-351, doi:10.1038/37022 (1997).
- 98 Torchinsky, M. B., Garaude, J., Martin, A. P. & Blander, J. M. Innate immune recognition of infected apoptotic cells directs T(H)17 cell differentiation. *Nature* **458**, 78-82, doi:10.1038/nature07781 (2009).
- 99 Vanden Berghe, T., Linkermann, A., Jouan-Lanhouet, S., Walczak, H. & Vandennebeele, P. Regulated necrosis: the expanding network of non-apoptotic cell death pathways. *Nature reviews. Molecular cell biology* **15**, 135-147, doi:10.1038/nrm3737 (2014).
- 100 Mannel, D. N., Moore, R. N. & Mergenhagen, S. E. Macrophages as a source of tumoricidal activity (tumor-necrotizing factor). *Infection and immunity* **30**, 523-530 (1980).
- 101 Degtarev, A. *et al.* Chemical inhibitor of nonapoptotic cell death with therapeutic potential for ischemic brain injury. *Nature chemical biology* **1**, 112-119, doi:10.1038/nchembio711 (2005).
- 102 Degtarev, A. *et al.* Identification of RIP1 kinase as a specific cellular target of necrostatins. *Nature chemical biology* **4**, 313-321, doi:10.1038/nchembio.83 (2008).

- 103 Galluzzi, L. *et al.* Molecular mechanisms of cell death: recommendations of the Nomenclature Committee on Cell Death 2018. *Cell death and differentiation*, doi:10.1038/s41418-017-0012-4 (2018).
- 104 Cho, Y. S. *et al.* Phosphorylation-driven assembly of the RIP1-RIP3 complex regulates programmed necrosis and virus-induced inflammation. *Cell* **137**, 1112-1123, doi:10.1016/j.cell.2009.05.037 (2009).
- 105 Sun, L. *et al.* Mixed lineage kinase domain-like protein mediates necrosis signaling downstream of RIP3 kinase. *Cell* **148**, 213-227, doi:10.1016/j.cell.2011.11.031 (2012).
- 106 Dondelinger, Y. *et al.* MLKL compromises plasma membrane integrity by binding to phosphatidylinositol phosphates. *Cell reports* **7**, 971-981, doi:10.1016/j.celrep.2014.04.026 (2014).
- 107 Chen, X. *et al.* Translocation of mixed lineage kinase domain-like protein to plasma membrane leads to necrotic cell death. *Cell research* **24**, 105-121, doi:10.1038/cr.2013.171 (2014).
- 108 Cai, Z. *et al.* Plasma membrane translocation of trimerized MLKL protein is required for TNF-induced necroptosis. *Nature cell biology* **16**, 55-65, doi:10.1038/ncb2883 (2014).
- 109 Gong, Y. N., Guy, C., Crawford, J. C. & Green, D. R. Biological events and molecular signaling following MLKL activation during necroptosis. *Cell cycle* **16**, 1748-1760, doi:10.1080/15384101.2017.1371889 (2017).
- 110 Xia, B. *et al.* MLKL forms cation channels. *Cell research* **26**, 517-528, doi:10.1038/cr.2016.26 (2016).
- 111 Ros, U. *et al.* Necroptosis Execution Is Mediated by Plasma Membrane Nanopores Independent of Calcium. *Cell reports* **19**, 175-187, doi:10.1016/j.celrep.2017.03.024 (2017).
- 112 Vanden Berghe, T. *et al.* Necroptosis, necrosis and secondary necrosis converge on similar cellular disintegration features. *Cell death and differentiation* **17**, 922-930, doi:10.1038/cdd.2009.184 (2010).
- 113 Gong, Y. N. *et al.* ESCRT-III Acts Downstream of MLKL to Regulate Necroptotic Cell Death and Its Consequences. *Cell* **169**, 286-300 e216, doi:10.1016/j.cell.2017.03.020 (2017).
- 114 Zargarian, S. *et al.* Phosphatidylserine externalization, "necroptotic bodies" release, and phagocytosis during necroptosis. *PLoS Biol* **15**, e2002711, doi:10.1371/journal.pbio.2002711 (2017).
- 115 Yoon, S., Kovalenko, A., Bogdanov, K. & Wallach, D. MLKL, the Protein that Mediates Necroptosis, Also Regulates Endosomal Trafficking and Extracellular Vesicle Generation. *Immunity* **47**, 51-65 e57, doi:10.1016/j.immuni.2017.06.001 (2017).
- 116 Kaiser, W. J. *et al.* Toll-like receptor 3-mediated necrosis via TRIF, RIP3, and MLKL. *The Journal of biological chemistry* **288**, 31268-31279, doi:10.1074/jbc.M113.462341 (2013).
- 117 Newton, K., Sun, X. & Dixit, V. M. Kinase RIP3 is dispensable for normal NF-kappa Bs, signaling by the B-cell and T-cell receptors, tumor necrosis factor receptor 1, and Toll-like receptors 2 and 4. *Molecular and cellular biology* **24**, 1464-1469 (2004).

- 118 Wu, J. *et al.* Mkl knockout mice demonstrate the indispensable role of Mkl
in necroptosis. *Cell research* **23**, 994-1006, doi:10.1038/cr.2013.91 (2013).
- 119 Oberst, A. *et al.* Catalytic activity of the caspase-8-FLIP(L) complex inhibits
RIPK3-dependent necrosis. *Nature* **471**, 363-367, doi:10.1038/nature09852
(2011).
- 120 Kaiser, W. J. *et al.* RIP3 mediates the embryonic lethality of caspase-8-
deficient mice. *Nature* **471**, 368-372, doi:10.1038/nature09857 (2011).
- 121 Sakamaki, K. *et al.* Ex vivo whole-embryo culture of caspase-8-deficient
embryos normalize their aberrant phenotypes in the developing neural tube
and heart. *Cell death and differentiation* **9**, 1196-1206,
doi:10.1038/sj.cdd.4401090 (2002).
- 122 Kang, T. B. *et al.* Mutation of a self-processing site in caspase-8 compromises
its apoptotic but not its nonapoptotic functions in bacterial artificial
chromosome-transgenic mice. *Journal of immunology* **181**, 2522-2532 (2008).
- 123 Rickard, J. A. *et al.* RIPK1 regulates RIPK3-MLKL-driven systemic
inflammation and emergency hematopoiesis. *Cell* **157**, 1175-1188,
doi:10.1016/j.cell.2014.04.019 (2014).
- 124 Newton, K. *et al.* Activity of protein kinase RIPK3 determines whether cells
die by necroptosis or apoptosis. *Science* **343**, 1357-1360,
doi:10.1126/science.1249361 (2014).
- 125 Berger, S. B. *et al.* Cutting Edge: RIP1 kinase activity is dispensable for
normal development but is a key regulator of inflammation in SHARPIN-
deficient mice. *Journal of immunology* **192**, 5476-5480,
doi:10.4049/jimmunol.1400499 (2014).
- 126 Dillon, C. P. *et al.* RIPK1 blocks early postnatal lethality mediated by
caspase-8 and RIPK3. *Cell* **157**, 1189-1202, doi:10.1016/j.cell.2014.04.018
(2014).
- 127 Takahashi, N. *et al.* RIPK1 ensures intestinal homeostasis by protecting the
epithelium against apoptosis. *Nature* **513**, 95-99, doi:10.1038/nature13706
(2014).
- 128 Dannappel, M. *et al.* RIPK1 maintains epithelial homeostasis by inhibiting
apoptosis and necroptosis. *Nature* **513**, 90-94, doi:10.1038/nature13608
(2014).
- 129 Lin, J. *et al.* RIPK1 counteracts ZBP1-mediated necroptosis to inhibit
inflammation. *Nature* **540**, 124-128, doi:10.1038/nature20558 (2016).
- 130 Newton, K. *et al.* RIPK1 inhibits ZBP1-driven necroptosis during
development. *Nature* **540**, 129-133, doi:10.1038/nature20559 (2016).
- 131 Upton, J. W., Kaiser, W. J. & Mocarski, E. S. DAI/ZBP1/DLM-1 complexes
with RIP3 to mediate virus-induced programmed necrosis that is targeted
by murine cytomegalovirus vIRA. *Cell host & microbe* **11**, 290-297,
doi:10.1016/j.chom.2012.01.016 (2012).
- 132 Kuriakose, T. *et al.* ZBP1/DAI is an innate sensor of influenza virus
triggering the NLRP3 inflammasome and programmed cell death pathways.
Sci Immunol **1**, doi:10.1126/sciimmunol.aag2045 (2016).

- 133 Maelfait, J. *et al.* Sensing of viral and endogenous RNA by ZBP1/DAI induces necroptosis. *The EMBO journal* **36**, 2529-2543, doi:10.15252/embj.201796476 (2017).
- 134 Pearson, J. S. *et al.* EspL is a bacterial cysteine protease effector that cleaves RHIM proteins to block necroptosis and inflammation. *Nat Microbiol* **2**, 16258, doi:10.1038/nmicrobiol.2016.258 (2017).
- 135 Kitur, K. *et al.* Necroptosis Promotes Staphylococcus aureus Clearance by Inhibiting Excessive Inflammatory Signaling. *Cell reports* **16**, 2219-2230, doi:10.1016/j.celrep.2016.07.039 (2016).
- 136 Sollberger, G., Tilley, D. O. & Zychlinsky, A. Neutrophil Extracellular Traps: The Biology of Chromatin Externalization. *Dev Cell* **44**, 542-553, doi:10.1016/j.devcel.2018.01.019 (2018).
- 137 Papayannopoulos, V. Neutrophil extracellular traps in immunity and disease. *Nature reviews. Immunology* **18**, 134-147, doi:10.1038/nri.2017.105 (2018).
- 138 Branzk, N. *et al.* Neutrophils sense microbe size and selectively release neutrophil extracellular traps in response to large pathogens. *Nature immunology* **15**, 1017-1025, doi:10.1038/ni.2987 (2014).
- 139 Clancy, D. M., Henry, C. M., Sullivan, G. P. & Martin, S. J. Neutrophil extracellular traps can serve as platforms for processing and activation of IL-1 family cytokines. *The FEBS journal* **284**, 1712-1725, doi:10.1111/febs.14075 (2017).
- 140 Papayannopoulos, V., Metzler, K. D., Hakkim, A. & Zychlinsky, A. Neutrophil elastase and myeloperoxidase regulate the formation of neutrophil extracellular traps. *The Journal of cell biology* **191**, 677-691, doi:10.1083/jcb.201006052 (2010).
- 141 Schreiber, A. *et al.* Necroptosis controls NET generation and mediates complement activation, endothelial damage, and autoimmune vasculitis. *Proceedings of the National Academy of Sciences of the United States of America* **114**, E9618-E9625, doi:10.1073/pnas.1708247114 (2017).
- 142 Lamkanfi, M. & Dixit, V. M. Inflammasomes and their roles in health and disease. *Annual review of cell and developmental biology* **28**, 137-161, doi:10.1146/annurev-cellbio-101011-155745 (2012).
- 143 Xu, H. *et al.* Innate immune sensing of bacterial modifications of Rho GTPases by the Pylrin inflammasome. *Nature* **513**, 237-241, doi:10.1038/nature13449 (2014).
- 144 Medema, J. P. *et al.* FLICE is activated by association with the CD95 death-inducing signaling complex (DISC). *The EMBO journal* **16**, 2794-2804, doi:10.1093/emboj/16.10.2794 (1997).
- 145 Renucci, M., Stennicke, H. R., Scott, F. L., Liddington, R. C. & Salvesen, G. S. Dimer formation drives the activation of the cell death protease caspase 9. *Proceedings of the National Academy of Sciences of the United States of America* **98**, 14250-14255, doi:10.1073/pnas.231465798 (2001).
- 146 Guey, B., Bodnar, M., Manie, S. N., Tardivel, A. & Petrilli, V. Caspase-1 autoproteolysis is differentially required for NLRP1b and NLRP3 inflammasome function. *Proceedings of the National Academy of Sciences of the*

- United States of America* **111**, 17254-17259, doi:10.1073/pnas.1415756111 (2014).
- 147 Van Opdenbosch, N. *et al.* Activation of the NLRP1b inflammasome independently of ASC-mediated caspase-1 autoproteolysis and speck formation. *Nature communications* **5**, 3209, doi:10.1038/ncomms4209 (2014).
- 148 Dinarello, C. A. Immunological and inflammatory functions of the interleukin-1 family. *Annual review of immunology* **27**, 519-550, doi:10.1146/annurev.immunol.021908.132612 (2009).
- 149 Jorgensen, I. & Miao, E. A. Pyroptotic cell death defends against intracellular pathogens. *Immunological reviews* **265**, 130-142, doi:10.1111/imr.12287 (2015).
- 150 Brydges, S. D. *et al.* Divergence of IL-1, IL-18, and cell death in NLRP3 inflammasomopathies. *The Journal of clinical investigation* **123**, 4695-4705, doi:10.1172/JCI71543 (2013).
- 151 Canna, S. W. *et al.* An activating NLRC4 inflammasome mutation causes autoinflammation with recurrent macrophage activation syndrome. *Nature genetics* **46**, 1140-1146, doi:10.1038/ng.3089 (2014).
- 152 Kitamura, A., Sasaki, Y., Abe, T., Kano, H. & Yasutomo, K. An inherited mutation in NLRC4 causes autoinflammation in human and mice. *The Journal of experimental medicine* **211**, 2385-2396, doi:10.1084/jem.20141091 (2014).
- 153 Romberg, N. *et al.* Mutation of NLRC4 causes a syndrome of enterocolitis and autoinflammation. *Nature genetics* **46**, 1135-1139, doi:10.1038/ng.3066 (2014).
- 154 Kayagaki, N. *et al.* Non-canonical inflammasome activation targets caspase-11. *Nature* **479**, 117-121, doi:10.1038/nature10558 (2011).
- 155 Kanneganti, T. D., Lamkanfi, M. & Nunez, G. Intracellular NOD-like receptors in host defense and disease. *Immunity* **27**, 549-559, doi:10.1016/j.immuni.2007.10.002 (2007).
- 156 Burckstummer, T. *et al.* An orthogonal proteomic-genomic screen identifies AIM2 as a cytoplasmic DNA sensor for the inflammasome. *Nature immunology* **10**, 266-272, doi:10.1038/ni.1702 (2009).
- 157 Fernandes-Alnemri, T., Yu, J. W., Datta, P., Wu, J. & Alnemri, E. S. AIM2 activates the inflammasome and cell death in response to cytoplasmic DNA. *Nature* **458**, 509-513, doi:10.1038/nature07710 (2009).
- 158 Latz, E., Xiao, T. S. & Stutz, A. Activation and regulation of the inflammasomes. *Nature reviews. Immunology* **13**, 397-411, doi:10.1038/nri3452 (2013).
- 159 Horvath, G. L., Schrum, J. E., De Nardo, C. M. & Latz, E. Intracellular sensing of microbes and danger signals by the inflammasomes. *Immunological reviews* **243**, 119-135, doi:10.1111/j.1600-065X.2011.01050.x (2011).
- 160 Saavedra, P. H., Demon, D., Van Gorp, H. & Lamkanfi, M. Protective and detrimental roles of inflammasomes in disease. *Seminars in immunopathology*, doi:10.1007/s00281-015-0485-5 (2015).

- 161 Lamkanfi, M. & Dixit, V. M. Mechanisms and functions of inflammasomes. *Cell* **157**, 1013-1022, doi:10.1016/j.cell.2014.04.007 (2014).
- 162 Hornung, V. *et al.* Silica crystals and aluminum salts activate the NALP3 inflammasome through phagosomal destabilization. *Nature immunology* **9**, 847-856, doi:10.1038/ni.1631 (2008).
- 163 Shimada, K. *et al.* Oxidized mitochondrial DNA activates the NLRP3 inflammasome during apoptosis. *Immunity* **36**, 401-414, doi:10.1016/j.immuni.2012.01.009 (2012).
- 164 Heid, M. E. *et al.* Mitochondrial reactive oxygen species induces NLRP3-dependent lysosomal damage and inflammasome activation. *Journal of immunology* **191**, 5230-5238, doi:10.4049/jimmunol.1301490 (2013).
- 165 Iyer, S. S. *et al.* Mitochondrial cardiolipin is required for Nlrp3 inflammasome activation. *Immunity* **39**, 311-323, doi:10.1016/j.immuni.2013.08.001 (2013).
- 166 Misawa, T. *et al.* Microtubule-driven spatial arrangement of mitochondria promotes activation of the NLRP3 inflammasome. *Nature immunology* **14**, 454-460, doi:10.1038/ni.2550 (2013).
- 167 Munoz-Planillo, R. *et al.* K(+) efflux is the common trigger of NLRP3 inflammasome activation by bacterial toxins and particulate matter. *Immunity* **38**, 1142-1153, doi:10.1016/j.immuni.2013.05.016 (2013).
- 168 Horng, T. Calcium signaling and mitochondrial destabilization in the triggering of the NLRP3 inflammasome. *Trends in immunology* **35**, 253-261, doi:10.1016/j.it.2014.02.007 (2014).
- 169 Jin, Y. *et al.* NALP1 in vitiligo-associated multiple autoimmune disease. *The New England journal of medicine* **356**, 1216-1225, doi:10.1056/NEJMoa061592 (2007).
- 170 Jin, Y., Birlea, S. A., Fain, P. R. & Spritz, R. A. Genetic variations in NALP1 are associated with generalized vitiligo in a Romanian population. *The Journal of investigative dermatology* **127**, 2558-2562, doi:10.1038/sj.jid.5700953 (2007).
- 171 Magitta, N. F. *et al.* A coding polymorphism in NALP1 confers risk for autoimmune Addison's disease and type 1 diabetes. *Genes and immunity* **10**, 120-124, doi:10.1038/gene.2008.85 (2009).
- 172 Motta, V. N. *et al.* Identification of the inflammasome Nlrp1b as the candidate gene conferring diabetes risk at the Idd4.1 locus in the nonobese diabetic mouse. *Journal of immunology* **194**, 5663-5673, doi:10.4049/jimmunol.1400913 (2015).
- 173 Grandemange, S. *et al.* NLRP1 mutations cause autoinflammatory diseases in human. *Pediatric Rheumatology* **13**, O22 (2015).
- 174 Masters, S. L. *et al.* NLRP1 inflammasome activation induces pyroptosis of hematopoietic progenitor cells. *Immunity* **37**, 1009-1023, doi:10.1016/j.immuni.2012.08.027 (2012).
- 175 Boyden, E. D. & Dietrich, W. F. Nalp1b controls mouse macrophage susceptibility to anthrax lethal toxin. *Nature genetics* **38**, 240-244, doi:10.1038/ng1724 (2006).

- 176 Chavarria-Smith, J. & Vance, R. E. Direct proteolytic cleavage of NLRP1B is necessary and sufficient for inflammasome activation by anthrax lethal factor. *PLoS pathogens* **9**, e1003452, doi:10.1371/journal.ppat.1003452 (2013).
- 177 Wickliffe, K. E., Leppla, S. H. & Moayeri, M. Killing of macrophages by anthrax lethal toxin: involvement of the N-end rule pathway. *Cellular microbiology* **10**, 1352-1362, doi:10.1111/j.1462-5822.2008.01131.x (2008).
- 178 Mariathasan, S. *et al.* Differential activation of the inflammasome by caspase-1 adaptors ASC and Ipaf. *Nature* **430**, 213-218, doi:10.1038/nature02664 (2004).
- 179 Franchi, L. *et al.* Cytosolic flagellin requires Ipaf for activation of caspase-1 and interleukin 1beta in salmonella-infected macrophages. *Nature immunology* **7**, 576-582, doi:10.1038/ni1346 (2006).
- 180 Miao, E. A. *et al.* Innate immune detection of the type III secretion apparatus through the NLRC4 inflammasome. *Proceedings of the National Academy of Sciences of the United States of America* **107**, 3076-3080, doi:10.1073/pnas.0913087107 (2010).
- 181 Lightfield, K. L. *et al.* Critical function for Naip5 in inflammasome activation by a conserved carboxy-terminal domain of flagellin. *Nature immunology* **9**, 1171-1178, doi:10.1038/ni.1646 (2008).
- 182 Zhao, Y. *et al.* The NLRC4 inflammasome receptors for bacterial flagellin and type III secretion apparatus. *Nature* **477**, 596-600, doi:10.1038/nature10510 (2011).
- 183 Yang, J., Zhao, Y., Shi, J. & Shao, F. Human NAIP and mouse NAIP1 recognize bacterial type III secretion needle protein for inflammasome activation. *Proceedings of the National Academy of Sciences of the United States of America* **110**, 14408-14413, doi:10.1073/pnas.1306376110 (2013).
- 184 Qu, Y. *et al.* Phosphorylation of NLRC4 is critical for inflammasome activation. *Nature* **490**, 539-542, doi:10.1038/nature11429 (2012).
- 185 Matusiak, M. *et al.* Flagellin-induced NLRC4 phosphorylation primes the inflammasome for activation by NAIP5. *Proceedings of the National Academy of Sciences of the United States of America* **112**, 1541-1546, doi:10.1073/pnas.1417945112 (2015).
- 186 Kortmann, J., Brubaker, S. W. & Monack, D. M. Cutting Edge: Inflammasome Activation in Primary Human Macrophages Is Dependent on Flagellin. *Journal of immunology* **195**, 815-819, doi:10.4049/jimmunol.1403100 (2015).
- 187 Fernandes-Alnemri, T. *et al.* The AIM2 inflammasome is critical for innate immunity to *Francisella tularensis*. *Nature immunology* **11**, 385-393, doi:10.1038/ni.1859 (2010).
- 188 Jones, J. W. *et al.* Absent in melanoma 2 is required for innate immune recognition of *Francisella tularensis*. *Proceedings of the National Academy of Sciences of the United States of America* **107**, 9771-9776, doi:10.1073/pnas.1003738107 (2010).
- 189 Rathinam, V. A. *et al.* The AIM2 inflammasome is essential for host defense against cytosolic bacteria and DNA viruses. *Nature immunology* **11**, 395-402, doi:10.1038/ni.1864 (2010).

- 190 Meunier, E. *et al.* Guanylate-binding proteins promote activation of the AIM2 inflammasome during infection with *Francisella novicida*. *Nature immunology* **16**, 476-484, doi:10.1038/ni.3119 (2015).
- 191 Man, S. M. *et al.* The transcription factor IRF1 and guanylate-binding proteins target activation of the AIM2 inflammasome by *Francisella* infection. *Nature immunology* **16**, 467-475, doi:10.1038/ni.3118 (2015).
- 192 Gavrilin, M. A. *et al.* Activation of the pyrin inflammasome by intracellular *Burkholderia cenocepacia*. *Journal of immunology* **188**, 3469-3477, doi:10.4049/jimmunol.1102272 (2012).
- 193 Mansfield, E. *et al.* The familial Mediterranean fever protein, pyrin, associates with microtubules and colocalizes with actin filaments. *Blood* **98**, 851-859 (2001).
- 194 Pilla, D. M. *et al.* Guanylate binding proteins promote caspase-11-dependent pyroptosis in response to cytoplasmic LPS. *Proceedings of the National Academy of Sciences of the United States of America* **111**, 6046-6051, doi:10.1073/pnas.1321700111 (2014).
- 195 Meunier, E. *et al.* Caspase-11 activation requires lysis of pathogen-containing vacuoles by IFN-induced GTPases. *Nature* **509**, 366-370, doi:10.1038/nature13157 (2014).
- 196 Wang, S. *et al.* Identification and characterization of Ich-3, a member of the interleukin-1beta converting enzyme (ICE)/Ced-3 family and an upstream regulator of ICE. *The Journal of biological chemistry* **271**, 20580-20587 (1996).
- 197 Fink, S. L. & Cookson, B. T. Caspase-1-dependent pore formation during pyroptosis leads to osmotic lysis of infected host macrophages. *Cellular microbiology* **8**, 1812-1825, doi:10.1111/j.1462-5822.2006.00751.x (2006).
- 198 Monack, D. M., Raupach, B., Hromockyj, A. E. & Falkow, S. *Salmonella typhimurium* invasion induces apoptosis in infected macrophages. *Proceedings of the National Academy of Sciences of the United States of America* **93**, 9833-9838 (1996).
- 199 Chen, L. M., Kaniga, K. & Galan, J. E. *Salmonella* spp. are cytotoxic for cultured macrophages. *Molecular microbiology* **21**, 1101-1115 (1996).
- 200 Lamkanfi, M. *et al.* Targeted peptidecentric proteomics reveals caspase-7 as a substrate of the caspase-1 inflammasomes. *Molecular & cellular proteomics : MCP* **7**, 2350-2363, doi:10.1074/mcp.M800132-MCP200 (2008).
- 201 Malireddi, R. K., Ippagunta, S., Lamkanfi, M. & Kanneganti, T. D. Cutting edge: proteolytic inactivation of poly(ADP-ribose) polymerase 1 by the Nlrp3 and Nlrc4 inflammasomes. *Journal of immunology* **185**, 3127-3130, doi:10.4049/jimmunol.1001512 (2010).
- 202 Erener, S. *et al.* Inflammasome-activated caspase 7 cleaves PARP1 to enhance the expression of a subset of NF-kappaB target genes. *Molecular cell* **46**, 200-211, doi:10.1016/j.molcel.2012.02.016 (2012).
- 203 Akhter, A. *et al.* Caspase-7 activation by the Nlrc4/Ipaf inflammasome restricts *Legionella pneumophila* infection. *PLoS pathogens* **5**, e1000361, doi:10.1371/journal.ppat.1000361 (2009).
- 204 Cookson, B. T. & Brennan, M. A. Pro-inflammatory programmed cell death. *Trends in microbiology* **9**, 113-114 (2001).

- 205 Chen, Y., Smith, M. R., Thirumalai, K. & Zychlinsky, A. A bacterial invasin induces macrophage apoptosis by binding directly to ICE. *The EMBO journal* **15**, 3853-3860 (1996).
- 206 Hersh, D. *et al.* The Salmonella invasin SipB induces macrophage apoptosis by binding to caspase-1. *Proceedings of the National Academy of Sciences of the United States of America* **96**, 2396-2401 (1999).
- 207 Brennan, M. A. & Cookson, B. T. Salmonella induces macrophage death by caspase-1-dependent necrosis. *Molecular microbiology* **38**, 31-40 (2000).
- 208 Jesenberger, V., Procyk, K. J., Yuan, J., Reipert, S. & Baccarini, M. Salmonella-induced caspase-2 activation in macrophages: a novel mechanism in pathogen-mediated apoptosis. *The Journal of experimental medicine* **192**, 1035-1046 (2000).
- 209 Hilbi, H. *et al.* Shigella-induced apoptosis is dependent on caspase-1 which binds to IpaB. *The Journal of biological chemistry* **273**, 32895-32900 (1998).
- 210 Kayagaki, N. *et al.* Caspase-11 cleaves gasdermin D for non-canonical inflammasome signaling. *Nature*, doi:10.1038/nature15541 (2015).
- 211 Fischer, U., Janicke, R. U. & Schulze-Osthoff, K. Many cuts to ruin: a comprehensive update of caspase substrates. *Cell death and differentiation* **10**, 76-100, doi:10.1038/sj.cdd.4401160 (2003).
- 212 Van Damme, P. *et al.* Caspase-specific and nonspecific in vivo protein processing during Fas-induced apoptosis. *Nature methods* **2**, 771-777, doi:10.1038/nmeth792 (2005).
- 213 Dix, M. M., Simon, G. M. & Cravatt, B. F. Global mapping of the topography and magnitude of proteolytic events in apoptosis. *Cell* **134**, 679-691, doi:10.1016/j.cell.2008.06.038 (2008).
- 214 Su, L. *et al.* A plug release mechanism for membrane permeation by MLKL. *Structure* **22**, 1489-1500, doi:10.1016/j.str.2014.07.014 (2014).
- 215 Yu, J. *et al.* Inflammasome activation leads to Caspase-1-dependent mitochondrial damage and block of mitophagy. *Proceedings of the National Academy of Sciences of the United States of America* **111**, 15514-15519, doi:10.1073/pnas.1414859111 (2014).
- 216 Allam, R. *et al.* Mitochondrial apoptosis is dispensable for NLRP3 inflammasome activation but non-apoptotic caspase-8 is required for inflammasome priming. *EMBO reports* **15**, 982-990, doi:10.15252/embr.201438463 (2014).
- 217 Py, B. F. *et al.* Caspase-11 controls interleukin-1beta release through degradation of TRPC1. *Cell reports* **6**, 1122-1128, doi:10.1016/j.celrep.2014.02.015 (2014).
- 218 Lamkanfi, M. & Dixit, V. M. Manipulation of host cell death pathways during microbial infections. *Cell host & microbe* **8**, 44-54, doi:10.1016/j.chom.2010.06.007 (2010).
- 219 Aachoui, Y. *et al.* Caspase-11 protects against bacteria that escape the vacuole. *Science* **339**, 975-978, doi:10.1126/science.1230751 (2013).
- 220 Kayagaki, N. *et al.* Noncanonical inflammasome activation by intracellular LPS independent of TLR4. *Science* **341**, 1246-1249, doi:10.1126/science.1240248 (2013).

- 221 Lamkanfi, M. Emerging inflammasome effector mechanisms. *Nature reviews. Immunology* **11**, 213-220, doi:10.1038/nri2936 (2011).
- 222 Liu, T. *et al.* Single-cell imaging of caspase-1 dynamics reveals an all-or-none inflammasome signaling response. *Cell reports* **8**, 974-982, doi:10.1016/j.celrep.2014.07.012 (2014).
- 223 Lamkanfi, M. *et al.* Inflammasome-dependent release of the alarmin HMGB1 in endotoxemia. *Journal of immunology* **185**, 4385-4392, doi:10.4049/jimmunol.1000803 (2010).
- 224 Kaczmarek, A., Vandenabeele, P. & Krysko, D. V. Necroptosis: the release of damage-associated molecular patterns and its physiological relevance. *Immunity* **38**, 209-223, doi:10.1016/j.immuni.2013.02.003 (2013).
- 225 Pasparakis, M. & Vandenabeele, P. Necroptosis and its role in inflammation. *Nature* **517**, 311-320, doi:10.1038/nature14191 (2015).
- 226 Kang, R. *et al.* Intracellular Hmgb1 inhibits inflammatory nucleosome release and limits acute pancreatitis in mice. *Gastroenterology* **146**, 1097-1107, doi:10.1053/j.gastro.2013.12.015 (2014).
- 227 Huang, H. *et al.* Hepatocyte-specific high-mobility group box 1 deletion worsens the injury in liver ischemia/reperfusion: a role for intracellular high-mobility group box 1 in cellular protection. *Hepatology* **59**, 1984-1997, doi:10.1002/hep.26976 (2014).
- 228 Yanai, H. *et al.* Conditional ablation of HMGB1 in mice reveals its protective function against endotoxemia and bacterial infection. *Proceedings of the National Academy of Sciences of the United States of America* **110**, 20699-20704, doi:10.1073/pnas.1320808110 (2013).
- 229 Wang, S. *et al.* Murine caspase-11, an ICE-interacting protease, is essential for the activation of ICE. *Cell* **92**, 501-509 (1998).
- 230 Wang, H. *et al.* HMG-1 as a late mediator of endotoxin lethality in mice. *Science* **285**, 248-251 (1999).
- 231 Sims, G. P., Rowe, D. C., Rietdijk, S. T., Herbst, R. & Coyle, A. J. HMGB1 and RAGE in inflammation and cancer. *Annual review of immunology* **28**, 367-388, doi:10.1146/annurev.immunol.021908.132603 (2010).
- 232 Baroja-Mazo, A. *et al.* The NLRP3 inflammasome is released as a particulate danger signal that amplifies the inflammatory response. *Nature immunology* **15**, 738-748, doi:10.1038/ni.2919 (2014).
- 233 Franklin, B. S. *et al.* The adaptor ASC has extracellular and 'prionoid' activities that propagate inflammation. *Nature immunology* **15**, 727-737, doi:10.1038/ni.2913 (2014).
- 234 Willingham, S. B. *et al.* Microbial pathogen-induced necrotic cell death mediated by the inflammasome components CIA1/cryopyrin/NLRP3 and ASC. *Cell host & microbe* **2**, 147-159, doi:10.1016/j.chom.2007.07.009 (2007).
- 235 Duncan, J. A. *et al.* Neisseria gonorrhoeae activates the proteinase cathepsin B to mediate the signaling activities of the NLRP3 and ASC-containing inflammasome. *Journal of immunology* **182**, 6460-6469, doi:10.4049/jimmunol.0802696 (2009).

- 236 Masumoto, J. *et al.* ASC is an activating adaptor for NF-kappa B and caspase-8-dependent apoptosis. *Biochemical and biophysical research communications* **303**, 69-73 (2003).
- 237 Sagulenko, V. *et al.* AIM2 and NLRP3 inflammasomes activate both apoptotic and pyroptotic death pathways via ASC. *Cell death and differentiation* **20**, 1149-1160, doi:10.1038/cdd.2013.37 (2013).
- 238 Pierini, R. *et al.* AIM2/ASC triggers caspase-8-dependent apoptosis in Francisella-infected caspase-1-deficient macrophages. *Cell death and differentiation* **19**, 1709-1721, doi:10.1038/cdd.2012.51 (2012).
- 239 Gurung, P. *et al.* FADD and caspase-8 mediate priming and activation of the canonical and noncanonical Nlrp3 inflammasomes. *Journal of immunology* **192**, 1835-1846, doi:10.4049/jimmunol.1302839 (2014).
- 240 Man, S. M. *et al.* Salmonella infection induces recruitment of Caspase-8 to the inflammasome to modulate IL-1beta production. *Journal of immunology* **191**, 5239-5246, doi:10.4049/jimmunol.1301581 (2013).
- 241 Man, S. M. *et al.* Inflammasome activation causes dual recruitment of NLRC4 and NLRP3 to the same macromolecular complex. *Proceedings of the National Academy of Sciences of the United States of America* **111**, 7403-7408, doi:10.1073/pnas.1402911111 (2014).
- 242 Gringhuis, S. I. *et al.* Dectin-1 is an extracellular pathogen sensor for the induction and processing of IL-1beta via a noncanonical caspase-8 inflammasome. *Nature immunology* **13**, 246-254, doi:10.1038/ni.2222 (2012).
- 243 Antonopoulos, C., El Sanadi, C., Kaiser, W. J., Mocarski, E. S. & Dubyak, G. R. Proapoptotic chemotherapeutic drugs induce noncanonical processing and release of IL-1beta via caspase-8 in dendritic cells. *Journal of immunology* **191**, 4789-4803, doi:10.4049/jimmunol.1300645 (2013).
- 244 Bossaller, L. *et al.* Cutting edge: FAS (CD95) mediates noncanonical IL-1beta and IL-18 maturation via caspase-8 in an RIP3-independent manner. *Journal of immunology* **189**, 5508-5512, doi:10.4049/jimmunol.1202121 (2012).
- 245 Shenderov, K. *et al.* Cutting edge: Endoplasmic reticulum stress licenses macrophages to produce mature IL-1beta in response to TLR4 stimulation through a caspase-8- and TRIF-dependent pathway. *Journal of immunology* **192**, 2029-2033, doi:10.4049/jimmunol.1302549 (2014).
- 246 Puri, A. W., Broz, P., Shen, A., Monack, D. M. & Bogoy, M. Caspase-1 activity is required to bypass macrophage apoptosis upon Salmonella infection. *Nature chemical biology* **8**, 745-747, doi:10.1038/nchembio.1023 (2012).
- 247 Masumoto, J. *et al.* ASC, a novel 22-kDa protein, aggregates during apoptosis of human promyelocytic leukemia HL-60 cells. *The Journal of biological chemistry* **274**, 33835-33838 (1999).
- 248 Conway, K. E. *et al.* TMS1, a novel proapoptotic caspase recruitment domain protein, is a target of methylation-induced gene silencing in human breast cancers. *Cancer research* **60**, 6236-6242 (2000).
- 249 Cai, X. *et al.* Prion-like polymerization underlies signal transduction in antiviral immune defense and inflammasome activation. *Cell* **156**, 1207-1222, doi:10.1016/j.cell.2014.01.063 (2014).

- 250 Lu, A. *et al.* Unified polymerization mechanism for the assembly of ASC-dependent inflammasomes. *Cell* **156**, 1193-1206, doi:10.1016/j.cell.2014.02.008 (2014).
- 251 Zamboni, D. S. *et al.* The Birc1e cytosolic pattern-recognition receptor contributes to the detection and control of *Legionella pneumophila* infection. *Nature immunology* **7**, 318-325, doi:10.1038/ni1305 (2006).
- 252 Miao, E. A. *et al.* Caspase-1-induced pyroptosis is an innate immune effector mechanism against intracellular bacteria. *Nature immunology* **11**, 1136-1142, doi:10.1038/ni.1960 (2010).
- 253 Doitsh, G. *et al.* Cell death by pyroptosis drives CD4 T-cell depletion in HIV-1 infection. *Nature* **505**, 509-514, doi:10.1038/nature12940 (2014).
- 254 Monroe, K. M. *et al.* IFI16 DNA sensor is required for death of lymphoid CD4 T cells abortively infected with HIV. *Science* **343**, 428-432, doi:10.1126/science.1243640 (2014).
- 255 Broz, P. *et al.* Caspase-11 increases susceptibility to *Salmonella* infection in the absence of caspase-1. *Nature* **490**, 288-291, doi:10.1038/nature11419 (2012).
- 256 Hoffman, H. M. Hereditary immunologic disorders caused by pyrin and cryopyrin. *Current allergy and asthma reports* **7**, 323-330 (2007).
- 257 Kuemmerle-Deschner, J. B. CAPS - pathogenesis, presentation and treatment of an autoinflammatory disease. *Seminars in immunopathology* **37**, 377-385, doi:10.1007/s00281-015-0491-7 (2015).
- 258 Frew, B. C., Joag, V. R. & Mogridge, J. Proteolytic processing of Nlrp1b is required for inflammasome activity. *PLoS pathogens* **8**, e1002659, doi:10.1371/journal.ppat.1002659 (2012).
- 259 Matusiak, M., Van Opendenbosch, N. & Lamkanfi, M. CARD- and pyrin-only proteins regulating inflammasome activation and immunity. *Immunological reviews* **265**, 217-230, doi:10.1111/imr.12282 (2015).
- 260 Russo, H. M. *et al.* Active Caspase-1 Induces Plasma Membrane Pores That Precede Pyroptotic Lysis and Are Blocked by Lanthanides. *Journal of immunology* **197**, 1353-1367, doi:10.4049/jimmunol.1600699 (2016).
- 261 Kayagaki, N. *et al.* Caspase-11 cleaves gasdermin D for non-canonical inflammasome signalling. *Nature* **526**, 666-671, doi:10.1038/nature15541 (2015).
- 262 Aglietti, R. A. *et al.* GsdmD p30 elicited by caspase-11 during pyroptosis forms pores in membranes. *Proceedings of the National Academy of Sciences of the United States of America* **113**, 7858-7863, doi:10.1073/pnas.1607769113 (2016).
- 263 Ding, J. *et al.* Pore-forming activity and structural autoinhibition of the gasdermin family. *Nature* **535**, 111-116, doi:10.1038/nature18590 (2016).
- 264 Liu, X. *et al.* Inflammasome-activated gasdermin D causes pyroptosis by forming membrane pores. *Nature* **535**, 153-158, doi:10.1038/nature18629 (2016).
- 265 Sborgi, L. *et al.* GSDMD membrane pore formation constitutes the mechanism of pyroptotic cell death. *The EMBO journal* **35**, 1766-1778, doi:10.15252/embj.201694696 (2016).

- 266 Chen, X. *et al.* Pyroptosis is driven by non-selective gasdermin-D pore and its morphology is different from MLKL channel-mediated necroptosis. *Cell research* **26**, 1007-1020, doi:10.1038/cr.2016.100 (2016).
- 267 Saeki, N., Kuwahara, Y., Sasaki, H., Satoh, H. & Shiroishi, T. Gasdermin (Gsdm) localizing to mouse Chromosome 11 is predominantly expressed in upper gastrointestinal tract but significantly suppressed in human gastric cancer cells. *Mamm Genome* **11**, 718-724 (2000).
- 268 Tamura, M. *et al.* Members of a novel gene family, Gsdm, are expressed exclusively in the epithelium of the skin and gastrointestinal tract in a highly tissue-specific manner. *Genomics* **89**, 618-629, doi:10.1016/j.ygeno.2007.01.003 (2007).
- 269 Saeki, N. *et al.* Distinctive expression and function of four GSDM family genes (GSDMA-D) in normal and malignant upper gastrointestinal epithelium. *Genes Chromosomes Cancer* **48**, 261-271, doi:10.1002/gcc.20636 (2009).
- 270 Van Laer, L. *et al.* Nonsyndromic hearing impairment is associated with a mutation in DFNA5. *Nature genetics* **20**, 194-197, doi:10.1038/2503 (1998).
- 271 Wang, Y. *et al.* Chemotherapy drugs induce pyroptosis through caspase-3 cleavage of a gasdermin. *Nature* **547**, 99-103, doi:10.1038/nature22393 (2017).
- 272 Rogers, C. *et al.* Cleavage of DFNA5 by caspase-3 during apoptosis mediates progression to secondary necrotic/pyroptotic cell death. *Nature communications* **8**, 14128, doi:10.1038/ncomms14128 (2017).
- 273 Lee, B. L. *et al.* ASC- and caspase-8-dependent apoptotic pathway diverges from the NLR4 inflammasome in macrophages. *Scientific reports* **8**, 3788, doi:10.1038/s41598-018-21998-3 (2018).
- 274 Fink, S. L., Bergsbaken, T. & Cookson, B. T. Anthrax lethal toxin and Salmonella elicit the common cell death pathway of caspase-1-dependent pyroptosis via distinct mechanisms. *Proceedings of the National Academy of Sciences of the United States of America* **105**, 4312-4317, doi:10.1073/pnas.0707370105 (2008).
- 275 von Moltke, J. *et al.* Rapid induction of inflammatory lipid mediators by the inflammasome in vivo. *Nature* **490**, 107-111, doi:10.1038/nature11351 (2012).
- 276 Broz, P. & Dixit, V. M. Inflammasomes: mechanism of assembly, regulation and signalling. *Nature reviews. Immunology* **16**, 407-420, doi:10.1038/nri.2016.58 (2016).
- 277 Jorgensen, I., Zhang, Y., Krantz, B. A. & Miao, E. A. Pyroptosis triggers pore-induced intracellular traps (PITs) that capture bacteria and lead to their clearance by efferocytosis. *The Journal of experimental medicine* **213**, 2113-2128, doi:10.1084/jem.20151613 (2016).
- 278 Rauch, I. *et al.* NAIP-NLR4 Inflammasomes Coordinate Intestinal Epithelial Cell Expulsion with Eicosanoid and IL-18 Release via Activation of Caspase-1 and -8. *Immunity* **46**, 649-659, doi:10.1016/j.immuni.2017.03.016 (2017).
- 279 Van Opdenbosch, N. *et al.* Caspase-1 Engagement and TLR-Induced c-FLIP Expression Suppress ASC/Caspase-8-Dependent Apoptosis by

- Inflammasome Sensors NLRP1b and NLRC4. *Cell reports* **21**, 3427-3444, doi:10.1016/j.celrep.2017.11.088 (2017).
- 280 Johansson, A. C. *et al.* Regulation of apoptosis-associated lysosomal membrane permeabilization. *Apoptosis : an international journal on programmed cell death* **15**, 527-540, doi:10.1007/s10495-009-0452-5 (2010).
- 281 Ozdogan, H. & Ugurlu, S. Canakinumab for the treatment of familial Mediterranean fever. *Expert Rev Clin Immunol* **13**, 393-404, doi:10.1080/1744666X.2017.1313116 (2017).
- 282 Sharma, D., Sharma, B. R., Vogel, P. & Kanneganti, T. D. IL-1beta and Caspase-1 Drive Autoinflammatory Disease Independently of IL-1alpha or Caspase-8 in a Mouse Model of Familial Mediterranean Fever. *The American journal of pathology* **187**, 236-244, doi:10.1016/j.ajpath.2016.10.015 (2017).
- 283 Kanneganti, A. *et al.* GSDMD is critical for autoinflammatory pathology in a mouse model of Familial Mediterranean Fever. *The Journal of experimental medicine*, doi:10.1084/jem.20172060 (2018).

6. Acknowledgements

Nothing in this thesis could have been accomplished without the support from key people/institutions. Thus, here is my thank you:

To Gent University, for the opportunity. Thank you the jury members for reading and evaluating the thesis, with your valuable comments.

To the work of my both promotors: Mo, thank you for your guidance, support and the several opportunities you provided to develop my scientific thinking and career along the way; Andy, thank you for taking over the task of running the lab and for making these final stages of my PhD possible.

A huge acknowledgement must be given to all – past and current – members of the MoLab/Awu Unit. Lieselotte, Nina, Hanne, Dieter, Filip, Anna, Amelie, Maarten, Hanne-Honey, Pedro, Daniel, Magda, Kevin, Ona, Tomoko, Mike, Giulia, and Linyan: thank you for the great scientific support, knowledge and discussions. Most of all, thank you for the laughter, the fun bets and baby pools, movie (and moving!) making, best vib-seminar parties and lab retreats and the unforgettable good moments. You've made my days sweeter (many times in literal ways!).

To IRC and Rommelaere colleagues, for the great parties, meetings in conferences, corridor and TC talks, and the support and scientific (or reagent) exchange. A special thank you to the BioImaging core, where I spent uncountable days during these last years: your support and expertise made this work possible.

To my "Ghentian" friends, for sharing coffees, dinners, lunches and for the support in this exciting experience of living in Ghent. Thank you to my Brazilian friends for always being there for me, either by skype or on my short visits.

To my family, who deserve the biggest “thank you” of all. I imagine it must not be easy to be supportive when someone you love decides to move to an ocean of distance. But you’ve made yourselves present in my life at every moment, showing me that wherever I am, you also are. Tiago, a special thank you for sharing your dreams and life with me. Your endless support and calm were essential for me this past year.

7. Curriculum Vitae

Nathalia Moraes de Vasconcelos



Personal e-mail: nathalia.mvasc@gmail.com

Address: Ghent 9000, Belgium

Nationality: Brazil

Education and Research Experience

- 2013/10 – 2018/06 **PhD** – Health Sciences – Ghent University, Belgium
Supervisor: Prof. Dr. Mo Lamkanfi
NOD-like Receptor & Inflammasome Laboratory – Department of Internal Medicine, Ghent University; Center for Inflammation Research, VIB, Ghent
Project: Cell death at the crossroads of inflammasome activation
Defence: June, 2018
- 2012/03 - 2013/08 **MSc** – Molecular Biology – University of Brasília, Brazil
Supervisors: Prof. Dr. José R. Corrêa and Prof. Dr. Kelly G. Magalhães
Electronic Microscopy Laboratory – University of Brasília
Project: Study of the relationship between the inflammasomes and breast cancer cell death *in vitro*.
- 2007/08 - 2011/12 **BSc** – Biology – University of Brasília, Brazil
Supervisor: Dr. Anamélia L. Bocca
Applied Immunology Laboratory – University of Brasília
Project: Development of alternative treatments for *Paracoccidioides brasiliensis* systemic mycosis using nanostructured drugs. (Ribeiro *et al.*, 2013; Souza *et al.*, 2015)
International exchange program: University of Porto, Portugal (Feb/10 to July/10)

Scientific and Technical Skills

<u>Cellular Biology</u>	<p>Isolation and culture of primary bone marrow-derived macrophages; establishing, culturing and differentiation into macrophages of ER-Hoxb8-immortalized myeloid progenitors; isolation of PBMC from whole blood; culture of mammalian cell lines (THP1, Jurkat, MH-S, J774.A, KBM-7, HEK-293T, Hela, MCF-7).</p> <p>Standard techniques for protein overexpression, lentiviral transduction, establishing single cell clones, cell death analysis (Incucyte, ATP, LDH release).</p> <p><i>In vitro</i> bacterial infection with <i>Salmonella enterica</i> serovar Typhimurium, <i>Franciscella tularensis</i>, <i>Escherichia coli</i>, <i>Citrobacter rodentium</i>.</p> <p>Basic work flows for flow cytometry detecting cell death, cell cycle, proliferation and transfection efficiency.</p>
<u>Biochemistry</u>	Western blotting, cytokine measurements (ELISA, Luminex)
<u>Microscopy</u>	<p>Experimental setup, acquisition and analysis of live cell imaging assays or immunocytochemistry; confocal microscopy on ZEISS and LEICA-based platforms.</p> <p>Image analysis and quantification with ImageJ, Volocity and Imaris.</p>
<u>Molecular Biology</u>	Restriction enzyme-based cloning, genomic PCR.
<u>Others</u>	<p>Graph Pad Prism, Microsoft Word, Excel and Power Point.</p> <p>Animal training at the level of FELASA C.</p>
<u>Collaborations</u>	Mass spectrometry – Shotgun and COFRADIC analysis
<u>(my contribution</u>	(sample preparation and data analysis)
<u>between brackets)</u>	<p>Recombinant protein production (inducing bacterial expression, His-tag-based purification)</p> <p>Maintenance of mice (managing breeding)</p>
<u>Laboratory supervision</u>	One 1 st year Master student (2016)

Presentations in Conferences

2017	<p>25th Euroconference on Apoptosis – European Cell Death Organization Leuven, Belgium</p>
------	--

- 2016 Flash Talk: High-Resolution Time-Lapse Analysis of Organelle Dynamics During Pyroptosis
IMMUNO 2016, XLI Congress of the Brazilian Society of Immunology 2016
Campos do Jordão, Brazil
10 min-Express Presentation: High-Resolution Time-Lapse Analysis of Organelle Dynamics During Pyroptosis.
- 2016 10th EWCD – Death never Dies
Fiuggi, Italy
Poster: High-Resolution Time-Lapse Analysis of Subcellular Organelle Dynamics During Pyroptosis

Awards

- 2017 Best Flash Talk presentation on the 25th Euroconference on Apoptosis – European Cell Death Organization
- 2013 PhD Scholarship – CAPES, Brazil
- 2012 Masters' Scholarship – CNPq, Brazil
- 2011 Scientific Initiation Scholarship – CNPq, Brazil
- 2009 Scientific Initiation Scholarship – CNPq, Brazil
- 2008 Scientific Initiation Scholarship – CNPq, Brazil

Publications

1. de Vasconcelos, N. M., Van Opdenbosch, N., Van Gorp, H., Parthoens, E., Lamkanfi, M. Single-cell analysis of pyroptosis dynamics reveals conserved GSDMD-mediated subcellular events that precede plasma membrane rupture. *Cell Death and Differentiation*, 2018.
2. Van Opdenbosch, N., Van Gorp, H., Verdonckt, M., Saavedra, P. H. V., de Vasconcelos, N. M., Gonçalves, A., Vande Walle, L., Demon, D., Matusiak, M., Van Hauwermeiren, F., D'Hont, J., Hochepped, T., Krautwald, S., Kanneganti, T. D., Lamkanfi, M. (2017). Caspase-1 engagement and TLR-induced c-FLIP expression suppress ASC/Caspase-8-dependent apoptosis by inflammasome sensors NLRP1b and NLRC4. *Cell Reports*, 21(12), 3427–3444.
3. Van Gorp, H., Viana Saavedra, P. H., de Vasconcelos, N. M., Van Opdenbosch, N., Vande Walle, L., Matusiak, M., Prencipe, G., Insalaco, A., Van Hauwermeiren, F., Demon, D., Bogaert, D., Dullaers, M., De Baere, E., Hochepped, T., Dehoorne, J., Vermaelen, K., Haerynck, F., De Benedetti, F., Lamkanfi, M. (2016). Familial Mediterranean fever mutations lift the obligatory requirement for microtubules in Pyrin inflammasome activation. *Proceedings of The National Academy of Sciences of The United States of America*, 113(50), 14384–14389.
4. de Vasconcelos, N. M., Van Opdenbosch, N., & Lamkanfi, M. (2016). Inflammasomes as polyvalent cell death platforms. *Cellular and Molecular Life Sciences*, 73(11-12), 2335–2347.
5. Souza, A. C. O., Nascimento, A. L., de Vasconcelos, N. M., Jerônimo, M. S., Siqueira, I. M., R-Santos, L., Cintra, D. O. S., Fuscaldi, L. L., Pires Júnior, O. R., Titze-De-Almeida, R., Borin, M. F., Bão, S. N., Martins, O. P., Cardoso, V. N.,

- Fernandes, S. O., Mortari, M. R., Tedesco, A. C., Amaral, A. C., Felipe, M. S. S., Bocca, A. L., (2015). Activity and in vivo tracking of Amphotericin B loaded PLGA nanoparticles. *European Journal of Medicinal Chemistry*, (95) 267-276.
6. Ribeiro, A. M., Souza, A. C. O., Amaral, A. C., de Vasconcelos, N. M., Jerônimo, M. S., Carneiro, F. P., Faccioli, L. H., Felipe, M. S. S., Silva, C. L., Bocca, A. L., (2013). Nanobiotechnological approaches to delivery of DNA vaccine against fungal infection. *Journal of Biomedical Nanotechnology*, (9) 221-230.
 7. Neto, B. A. D., Carvalho, P. H. P. R., Santos, D. C. B. D., Gatto, C. C., Ramos, L. M., de Vasconcelos, N. M., Corrêa, J. R., Costa, M. B., de Oliveira, H. C. B., Silva, R. G., (2012). Synthesis, properties and highly selective mitochondria staining with novel, stable and superior benzothiadiazole fluorescent probes. *RSC Advances*, (4), 1524-1532.